DYNAMIC AMPLIFICATION FACTOR FOR THE DESIGN OF REINFORCEMENT IN THE TRANSVERSE DIRECTION OF DECK SLAB OF BOX GIRDER BRIDGES

FARHANA HAQUE RICH

MASTER OF SCIENCE IN CIVIL ENGINEERING (STRUCTURAL)

Department of Civil Engineering

BANGLADESH UNIVERSITY OF ENGINEERING AND TECHNOLOGY

March, 2014

DYNAMIC AMPLIFICATION FACTOR FOR THE DESIGN OF REINFORCEMENT IN THE TRANSVERSE DIRECTION OF DECK SLAB OF BOX GIRDER BRIDGES

By

FARHANA HAQUE RICH

Roll Number: 0409042366

A thesis submitted to the Department of Civil Engineering of Bangladesh University of Engineering and Technology, Dhaka, in partial fulfillment of the requirements for the degree of

MASTER OF SCIENCE IN CIVIL ENGINEERING (STRUCTURAL)

March, 2014

The thesis titled **"Dynamic Amplification Factor for the Design of Reinforcement in the Transverse Direction of Deck Slab of Box Girder Bridges"** submitted by Farhana Haque Rich, Student No. 0409042366 and Session: April 2009 has been accepted as satisfactory in partial fulfillment of the requirement for the degree of M.Sc. Engg. (Civil and Structural) on 30th March, 2014.

BOARD OF EXAMINERS

____________________________________ **Chairman**

Dr. Khan Mahmud Amanat (Supervisor)
Professor
Department of Civil Engineering, BUET, Dhaka-1000

____________________________________ **Member**

Dr. A. M. M. Taufiqul Anwar (Ex-officio)
Professor and Head
Department of Civil Engineering, BUET, Dhaka-1000

____________________________________ **Member**

Dr. Tahsin Reza Hossain
Professor
Department of Civil Engineering, BUET, Dhaka-1000

____________________________________ **Member**

Dr. Sharmin Reza Chowdhury (External)
Associate Professor
Department of Civil Engineering
Ahsanullah University of Science and Technology
141-142 Love Road, Tejgaon Industrial Area, Dhaka -1208

DECLARATION

Declared that except where specified by reference to other works, the studies embodied in thesis is the result of investigation carried out by the author. Neither the thesis nor any part has been submitted to or is being submitted elsewhere for any other purposes.

Signature of the student

Farhana Haque Rich

TABLE OF CONTENTS

Chapter 5: Conclusions

LIST OF ABBREVIATIONS

υ	Poison ratio
ϵ	Modulus of Elasticity
ρ	Mass Density
$R_{DYNAMIC_{MAX}}$	Peak Dynamic Effect
$R_{STATIC_{MAX}}$	Peak Static Effect
ω_n	Natural Frequency
k	Stiffness
m	Mass
I	Impact Factor
DAF	Dynamic Amplification Factor
AASHTO	American Association of State Highway and Transportation Officials
ASCE	American Society of Civil Engineers

ACKNOWLEDGEMENT

First, I would like to express to my deepest gratitude to almighty Allah, the benevolent and the kind, for His graciousness, unlimited kindness and divine blessings for allowing me to bring this effort to an end.

I would feel extremely privileged to work under most revered teacher Dr. Khan Mahmud Amanat, Professor, Department of Civil Engineering, Bangladesh University of Engineering and Technology (BUET) and would like to express my heartfelt gratitude and sincere thanks to him for his adept guidance and enthusiastic support throughout the progress of this thesis. I would be very thankful for his constant supervision, continuous guidance, helpful criticism, continued encouragement and suggestions, generous help and unfailing enthusiasm at all the stages of my work. His active interest in this topic and valuable advice was the source of my inspiration.

I also wish to convey my honest gratefulness to the Head of the Department of Civil Engineering, BUET and all members of the defense board for their time and patience.

I also would like to express my appreciation to all my teachers, who did spark the flame of knowledge in front of me.

I would like to pay my deepest homage to my family members, friends and colleagues who helped me with necessary advice and moral support during the course of this study.

ABSTRACT

This thesis studies the dynamic responses of moving vehicle loads. This response is measured for both transverse stresses and deformations in the cantilever slab adjacent to the main deck of concrete highway bridges. The whole analytical process regarding this investigation is based on finite element analysis. A finite element model to analyze the cantilever three-span box girder bridge has been developed using shell element. A vehicle is simulated according to the HS20-44 truck design loading contained in the AASHTO specifications and vehicle load is applied at various points on the vehicle path. A step by step full transient dynamic analysis has been performed. Parameters like vehicle speed, span length, width of the cantilever part and damping condition are included in the investigation with a systematic approach. Span length variation is done with appropriate slab thickness and deck height for being realistic practice. Dynamic amplification factors (DAF) are evaluated at various points along the middle span of the bridge. From the numerical results, it has been found that dynamic amplification factor is critical at the piers rather than mid span or other part of the span. The effects of vehicle speed, span length and cantilever slab width on dynamic amplification factor were significant. But the variation of the DAF with respect to those parameters is rather arbitrary. Again, it was also found that 0% damping caused abnormally high value, whereas, 2.5% and 5% damping gave closely similar values which was more realistic. Based on the overall findings, DAF value for vertical deflections of the cantilever part of deck slab is recommended as 1.7 near pier and 1.64 near midspan i.e. recommending 70% and 64% impact increment near pier and midspan over static results calculated for deflections. Again, for stresses in the transverse direction DAF value is suggested as 1.91 near pier and 1.78 near midspan i.e. recommending 91% and 78% impact increment near pier and midspan over static results calculated for stresses.

CHAPTER 1
INTRODUCTION

1.1 General

In modern structural design practice, dynamic effect in accordance with static effect is recognized for analysis of bridges. In recent times, it has been acknowledged from some practical observations that only static analysis is inadequate for ensuring the structural safety of bridges. So, dynamic and static both responses are essential to take into account for determining the characteristic of a bridge structure during structural analysis and design. In safety assessments of bridges, the dynamic effect caused by the vehicle is taken into consideration using equivalent loads determined by multiplying the static loads by a dynamic amplification factor (DAF). Improper exercise of DAFs leads to unsafe road conditions for vehicular movement. Consequently, the practice of inappropriate DAFs can have remarkable financial implications. Therefore, determination of the appropriate value of DAF for different stress components is essential.

1.2 Background

In modern design analysis, dynamic analysis is taken into consideration along with static analysis for defining structural behavior. At the same time, designers are bound to follow code provisions. In design of bridges, conventionally, the dynamic effect of vehicle is taken into consideration through the use of impact factor, I. Generally this impact factor is prescribed for stresses in the longitudinal direction. However, for stresses in the transverse direction no such guideline is generally available. In the design of bridges, especially in designing the deck slab, dynamic effect of live load is an important parameter for the design of transverse reinforcements.

Few years back, longitudinal cracks were observed on the deck of Bangabandhu Bridge, Bangladesh. Confusion aroused to predict the amount of impact increment for analyzing the crack. The reasons behind the formation of cracks might be high impact in the transverse direction and low amount of required reinforcement specified by the conventional theories.

Therefore, it is necessary to determine the dynamic amplification factor for stresses in the transverse direction as well as for deflections of the cantilever part of the deck slab.

Cantilever part of the deck slabs of bridges is of significant structural importance. Despite that, most of the previous studies pertinent to the dynamic amplification factor of bridges excluded the local dynamic effects in the transverse direction of the cantilever part. AASHTO (2002) and IRC (1996) codes have provided guideline to estimate the dynamic effect of vehicles in designing reinforcement in the longitudinal direction. But no guideline is provided to measure the dynamic effect of vehicle load in designing the transverse reinforcement especially in the cantilever part of box girders. It is thus understood that there are good scopes of research in studying the dynamic effect of vehicle load for the stresses in the transverse direction.

1.3 Objectives and Scopes

The major objective of this study and analysis has been to enlarge our knowledge about the influencing parameters related to responses due to static and dynamic loading conditions along with the DAF. This investigation represents the distribution of peak transient and static response by a moving standard vehicle load along the cantilever deck and along the centerline of deck slab of box girder bridge. In this thesis, analysis was performed to get DAF for both stresses in the transverse direction at the root of cantilever slab and vertical deflection at the tip of the cantilever. Recommendation was made for a feasible DAF value based on the results achieved through the investigation.

The principle scope and features of this thesis are as follows:

1. To model a box girder bridge with three continuous spans using shell elements.
2. To model the slab with different thickness at different points.
3. To apply moving vehicle loads as external forces along two vehicular path :
    i) One along the cantilever part of box.
    ii) Another along the centerline of deck slab of box.
4. To analyze the model for static and full transient dynamic analysis.

5. To get dynamic amplification factor for both stresses in the transverse direction at the root of the cantilever part and vertical deflections at the tip of cantilever for different parametric study.
6. To propose a reasonable dynamic amplification factor along with the impact increment over the static results measured through the whole analysis.

1.4 Methodology

Finite element analysis would be used for the complete analysis in this thesis. A model of three spans of box girder bridge would be developed using this software. Moving axle load would be assumed as a series of concentrated force applied along the course of the road on the path parallel to the edge of the cantilever at different positions on the deck and along centerline path of deck slab. Recommendation would be provided for the selection of a feasible DAF so that an impact increment could be suggested for the static results that would be calculated during the analysis process.

1.5 Assumptions

The investigation was effectuated based on some assumptions to avoid complications. These assumptions are as follows:

1. Materials involved in the study were elastic.
2. Analysis was performed for a single vehicle passing over the cantilever part and also along centerline of the deck of box girder bridge. The effects of lane load were ignored.
3. Vehicle loads were applied as concentrated loads. Axle loads was considered instead of wheel loads.
4. Mass of the vehicle was not taken into account.
5. Damping effect was taken into account for the study. 0%, 2.5% and 5% damping condition were considered for the analysis.
6. As the thickness of slab is different at different points, so the slab can be considered as similar to curved slab.
7. The roughness of the road surface was not included.

1.6 Organizations of Thesis

Five essential chapters are organized systematically to describe the whole thesis. Chapter 1 is the current chapter, which introduces the entire study which is performed in this thesis. Chapter 2 induces the provisions of different code specifications as well as all the recent and past publications relevant to the topic. In chapter 3, the description of the actual work regarding the finite element modeling related to the subject is given. In this chapter systematic descriptions are provided to have better understanding about parameters of the model, bridge modeling, vehicle modeling and vehicle travel simulation with proper boundary and load conditions, deflections over time which give an overall view over bridge characteristics for both static and dynamic responses. Parametric analysis is done in Chapter 4. In this chapter, influencing parameters of dynamic amplification factors are studied numerically for static and transient analyses for 0%, 2.5% and 5% damping condition to obtain the value of DAF and achieve the effects of different parameters on DAF. Finally, the summary of the organized outcomes of the thesis is provided and future research works recommendations are proposed in Chapter 5.

CHAPTER 2
BACKGROUND LITERATURE

2.1 General

This thesis is concerned with the Dynamic Amplification Factor (DAF) for stresses in the transverse direction and for deflections at the tip of the cantilever part of the box girder bridge. In this study, two different path for vehicular loading is used, one in the cantilever part and another at the centerline of the box girder bridge. This chapter presents the literature review and historical overview of the researches regarding various aspects of the dynamic behavior of bridges due to vehicular loading.

2.2 Review of Related Works

For bridge study, dynamic response due to vehicular loading has become a concerning part to engineers for more than 100 years. Significant amount of researches have been performed to investigate the behavior of bridges for transient analysis as well as static analysis. The dynamic response of bridges is complicated by a number of independent but interacting factors. As a consequence different studies have produced conflicting results and conclusions.

The dynamic amplification factors defined in codes have classically been derived from the measurement or simulation of global traffic action effects in the main structural elements of bridges. On the other hand, local dynamic effects in deck slabs have not yet been studied in detail. Apart from few approaches based on the fundamental theory of plate vibration: ASCE (1931), Gupta and Trail-Nash (1980), Agarwal and Billing (1990), Green and Cebon(1994), no references have been found dealing with deck slabs in particular.

A better understanding of dynamic behavior of deck slab under vehicle loading will lead to the definition of more appropriate dynamic amplification factor and avoid the use of values that are too conservative. Therefore, a more rational load model is needed. A detailed review literature and an extensive list of references on this topic can be found in Huang (1976), Buckland (1981), Paultre *et al.* (1992), Farfard *et al.* (1993), Lafalamme *et al.* (1995) and Nowak (1995).

2.2.1 Specification of Different Codes

Early on, the main concern of studies of bridge-vehicle interaction was on railway bridges design in the long direction of the span, where dynamic forces were generated due to the hammer-blow effect of steam locomotive drive wheels. In 1911, the American Railway Engineering Association (AREA) initiated a series of tests on railroad bridges that led to the following design provision for impact forces in railroad bridges for design in the long direction of the span:

$$I = \frac{50}{L+150}$$

In which,

I = Impact Factor not exceeding 0.30

L = Span length in feet

In 1927, a joint committee (ASCE 1931) of AREA and American Association of State Highway Officials (AASHO) adopted the following equation for both railroad and highway bridge impact:

$$I = \frac{50}{L+125}$$

A Special Committee was appointed in 1922 by the American Society of Civil Engineers. This committee was asked to search for available data on the subject of impact in highway bridges to encourage experimental work in a more systematic manner. The final report of the Committee on impact in highway bridges was published in 1929. As a basis for its recommendations, the committee considered the following facts:

- Stresses due to static loads and impact are important, in regard to the safety of the structure, only when they approach design values.
- The percentage of impact increment decreases as the loads increase and, therefore, as the unit stresses increase.
- The larger impacts observed in the tests were produced by obstructions, such as would be accidental and infrequent under actual traffic conditions.

- The actual occurrence, on a bridge, of loads having a magnitude corresponding to those used in the design of modern structures is infrequent.
- the simultaneous occurrence on a bridge floor of a maximum truck load and an accidental obstruction capable of producing high impact will be such a rare coincidence that presumably the factor of safety will usually provide safety for this condition

There was an implied discussion of the report by the society's Special Committee on the specifications for bridge design and construction in the revision of section 113 which was published in pamphlet from under date of June 27, 1929. The revised section included:
'The dynamic increment of the live load shall be added to the maximum computed live load stresses. For floor beams and stringers, the increment shall be taken as 30% and for floor beam hangers as 60%, of the live load stress. Impact shall not be added to stresses produced by longitudinal and lateral forces.'

For unusually rigid concrete floor, the committee suggested to raise the impact factor by 80% to 85 or 90% or to another value that might meet the judgment of the designer or specification writer.

In 1931, an ASCE committee (ASCE 1931) reported on 'Search for available data on the subject of impact in highway bridges'. Observations of the committee in addition to the report of 'Impact in Highway Bridges Committee' were those:

- Existing data are too meager to establish a relationship between impact and span length. Approximately the same impacts were indicated for all spans.
- Uncertainties in the distribution of the stress over the various parts of a bridge are much greater than uncertainties in impact.

The ASCE committee recommended that an impact of stress of 25% of live load stress be used in design of bridge floors and highway suspenders. For girders and trusses of highway bridges, the committee recommended an impact increment of stress as a fraction of live load determined from:

$$I = \frac{50}{L+160} \qquad \text{With, } I \text{ not greater than 25\%}$$

AASHTO (2002) suggested in article 3.8.2.1 of Standard Specification for Highway Bridges that the amount of the impact allowance or increment is expressed as a fraction of the live load stress and shall be determined by the formula:

$$I = \frac{50}{L+125}$$

In which,

I = Impact fraction (maximum 30%)

L = Length in feet of the portion of the span that is loaded to produce the maximum stress in the member

In article 3.8.2.2, loaded length, L, was defined as followed:

a) For roadway floors: the design span length
b) For transverse members, such as floor beams: the span length of member center to center of supports.
c) For computing truck load moments: the span length, or for cantilever arms the length from the moment center to center the farthermost axle.
d) For shear due to truck load moments: the length of the loaded portion of span from the point under consideration to the far reaction; except, for cantilever arms, use a 30% impact factor.
e) For continuous spans: the length of span under consideration for positive moment and the average of two adjacent loaded spans for negative moment.

The Indian Road Congress (IRC) suggested that the amount of impact increment is computed as a function of span length. However, the basis for impact factors predicted by IRC is not fully known. It has been felt by the researchers that the impact factor to a large extent depends on the weight of the vehicles, its velocity as well as the surface characteristics of the road.

1. **For IRC Class A or Class B loading**

$$I = \frac{A}{B+L}$$

In which,

$I =$ Impact Factor

A = Constant, 4.5 for RCC bridges, 9.0 for steel bridges

B = Constant, 6.0 for RCC bridges, 13.50 for steel bridges

L = Span length in meter

2. **For IRC Class AA and 70R Loading**

a) Spans < 9 meter

i. Tracked vehicle: 25% for spans up to 5 m linearly reducing to 10% for spans up to 9 m.
ii. Wheeled vehicle: 25% for spans up to 9 m.

b) Spans > 9 meter

i. Tracked vehicle: For RCC bridges, 10% for spans up to 40 m and as per graph for spans > 40 m. For steel bridges, 10% for all spans
ii. Wheeled vehicle: For RCC bridges, 25% for spans up to 12 m and in accordance with graph for spans > 12 m. For steel bridges, 25% for spans up to 23 m and as per graph (IRC 6) for spans exceeding 23 m.

Appropriate impact factors as mentioned below is needed to be considered:

- At the bottom of the bed block: 0.5
- For the top 3 m of the substructure: 0.5 – 0
- For portion of substructure > 3 m below the block: 0

From the above study, it is seen that most of the design provisions are regarding the design for in the longitudinal directions of the span. Provisions for the design in the short direction of span are unavailable. But now a day, design provision for short direction of the span is also very important for design purpose. Very few studies are seen regarding this matter. So, more studies are needed regarding this provision.

2.2.2 Overview of Past Research

Beginning in the 1950s, new investigations of the dynamic performances of bridges were conducted. But most of the studies correspond to the design of longitudinal direction of the span. These studies include those by Foster (1952), Hayes and Sbarounis (1955), Edgerton and Beecroft (1955), Biggs and Suer (1955) and Wright and Green (1959 and 1963).

In 1961, Fleming and Romualdi (1961) conducted an analytic investigation the dynamic response of single-span and three-span bridges to transient loads. It was found that for small spans (less than 13 m), the DAF was higher than that predicted by AASHTO, whereas for medium spans (greater than 13 m), the DAF was in accordance with AASHTO recommendations. The following observations were reached:

- For unsprung loads, the velocity of the load is the most important variable. Modifying the mass of the load changes the velocity at which the maximum dynamic amplification occurs.
- Large dynamic amplification can be produced in the bridge due to initial vibration of the vehicle caused by unevenness of the bridge approach.

A major experimental investigation was conducted in 1958 by AASHO (1962). The main objectives were to determine the behavior of short span highway bridges under repeated applications of overstress as well as to determine the dynamic effects of moving vehicles on these bridges. Eighteen simply-supported bridges with a span of 15 m were investigated. Test vehicles consisting two-axle trucks and three-axle tractor-trailer combinations were driven over the test bridges at varying speed. Observations from these tests included:

- Initial vertical oscillations of the test vehicle were present in practically all tests and introduced a large uncertainty in the dynamic response of the bridge.
- Spring models could be used with reasonable accuracy to represent the static load deflection characteristics of the vehicle, including the effect of frictional damping in the suspension system. Viscous damping in the tires was found to be close to 1 %.
- The largest dynamic impact factor based on displacement measurements was 0.63, although only 5% of measured values exceeded 0.40. The impact factor based on strains

were somewhat lower, the largest value was 0.41 and only 55 of the values exceeded 0.29, which was the impact value specified by AASHO provision at the time.

- The DAF increased with the number of vehicle runs during regular traffic only for bridges with permanent set and an approach profile roughness increasing with time. A decrease in the DAF was measured for bridges with a decrease in camber and smoothing of the approach profile by patching.
- The peak value of the DAF was not strongly influenced by the weight ratio (ratio of the gross weight of vehicle over the total weight of bridge).
- Reasonable agreement was observed between the experimental results and analytical results based on dynamic spring-supported vehicle models.
- The dynamic impact factor generally increased with increasing vehicle speed, which was characterized in terms of a speed parameter α,

$$\alpha = \frac{V}{2Lf}$$

In which,

$V =$ Truck speed in ft/sec

L = Span Length in ft

f = First flexural frequency of bridge in Hz

Based on the result of this research an alternative equation was developed :

$$I = 0.15 + \alpha$$

The first term of the equation is an allowance for the initial oscillation of the truck coming onto the bridge and the second term represents the effects from a smoothly rolling mass crossing the beam (Walker and Veletsos 1963).

In 1963 Wright and Green reported on a series of experimental investigations of vehicle-bridge interaction made on 52 highway bridges in Ontario from 1956 to 1957. The bridges selected for study were of different types with widely varying approach and deck conditions. For each bridge, measurements of bridge stiffness, natural frequency, damping and dynamic amplification factor (DAF) under both normal traffic conditions and test vehicles were made. DAFs up to 75% were observed, but most values were around 30%. The larger values were obtained for the bridges with observed frequencies in the range of 2 to 5 Hz (Figure 2.1). This frequency range encompasses the bounce frequencies typical for heavy commercial vehicles. The investigation also concluded that the DAF was strongly influenced by any irregularities in the bridge approaches or riding surface, including the presence of expansion joints. Some of the principal findings of this research program were:

- Theoretical studies on bridge-vehicle interaction available at the time were of little use for design purposes.
- Experimental values of the stiffness were always larger than the calculated values, because of parameters not ordinarily considered in design calculations (composite action, joint rigidity, participation of secondary elements, etc).
- Natural frequencies of simply supported spans could be predicted with reasonable accuracy, although some of the experimental values tended to be larger than the calculated values. A substantial number of forced vibrations associated with the natural frequency of test vehicles suspension systems (at about 2.5 Hz) were observed.
- Dynamic amplifications of 30% were typically observed, with peak values of up to 75%.
- The DAF was strongly affected by irregularities of the bridge approaches, by the smoothness of the riding surface (bumps, expansion joints, etc.), and by application of vehicle brakes.
- The DAF values were much larger for bridges with low stiffness.

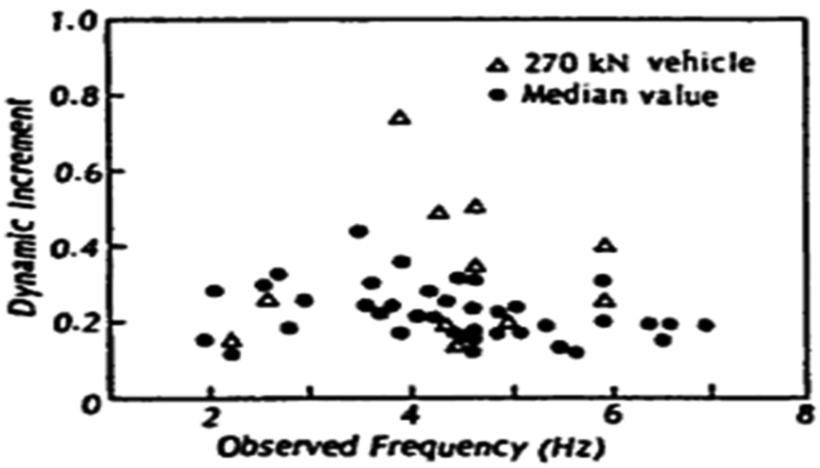

Figure 2.1: Dynamic increment vs. Observed frequency (from Billing and Green 1984)

Tung (1967) formulated the problem of highway bridge response to traffic on a probabilistic basis recognizing thereby that vehicular traffic is statistical in nature. A simple Poisson process was used to model traffic flow pattern and the response was evaluated using probability density functions and a linear damped system for the bridge.

In 1970, Veletsos developed a numerical method for computing the dynamic response of highway bridges to moving vehicular loads. Veletsos considered a linear elastic beam element with distributed flexibility and lumped masses. Loading was considered using a three-axle spring mass model.

Whitmore (1970) studied the dynamic effects of heavy vehicles moving on pavement roadway. Roadway profile irregularities (using a profilometer and a spectral density technique) and vehicle characteristics (mass distribution, suspension system, and speed) were examined. The objectives were:

- To investigate the effect of roadway profile and vehicle characteristics on the dynamic loadings.
- To isolate specific parameters influencing loads.
- To develop a technique capable of predicting the dynamic loads from the aforementioned parameters.

The following observations were made:

- In presence of step bump irregularities, higher values of the DAF were observed as well as a wide range of frequency components in the dynamic motion.
- The force at the tire-roadway interface could be measured on the vehicle or on the roadway, and was found to increase with tire pressure and suspended mass.
- Damping of the dynamic loads depended on the vehicle mass and suspension.

In 1972, Csagoly *et al.* conducted a second series of tests on bridges in Ontario in 1969 to 1971. Eleven bridges were investigated. The maximum dynamic amplification factors obtained from the tests ranged from 30% to 85% and were again obtained for bridges with measured frequencies in the 2 to 5 Hz. Dynamic amplification was found to be a function of roadway roughness and bridge deck conditions. Later these data were reanalyzed and compared to the provisions in the AASHTO design specification. They came to conclusion that DAF were higher than those in AASHTO for bridges having natural frequencies in the range of 2.5 to 4.5 Hz.

Leonard (1974) and Page (1976) reported a series of dynamic tests conducted on highway bridges by the Transport and Road Research Laboratory (TRRL) in England. The main testing program was on 30 bridges and the impact values of between 0.09 and 0.75 were reported. It was reported that the impact response vehicles travelled over smooth humps and planks.

Shepherd and Sidwell (1973) and Shepherd and Aves (1973) reported on a series of bridge tests conducted in New Zealand. Impact values were calculated from deflection measurements obtained during the passage of a standard two-axle truck over the bridge along with normal vehicular traffic. Fourteen bridges were investigated and the impact values ranging from 0.1 to 0.7 were reported. The researchers noted that 'Vehicle characteristics have a significant impact on the recorded impact.'

Campbell *et al.* (1977) carried out further studies on the test data obtained from the second series of bridge testing in Ontario. One of the objectives of this investigation was to compare the DAF values obtained from measurements with those recommended by the AASHTO design specifications. They concluded that:

- The DAF based on tests was generally higher than that of AASHTO for bridges having their natural frequencies ranging from 2.5 to 4.5 Hz.
- The beam idealization used to predict fundamental frequencies were sufficiently accurate for design purposes.
- The dynamic response was dependent on the exciting frequency of the vehicle with respect to the fundamental frequency of the bridge.

In 1980 Sweatman of the Australian Road Research Board (ARRB) measured wheel forces in a series of test vehicles driven over a variety of road conditions. Impact was found to be a function of type of vehicle and suspension system.

Australian Road Research Board (ARRB) sponsored research into the impact effects associated with vehicle braking (Gupta and Trail-Nash 1980). Single-span, multi-girder highway bridges were considered and represented by three mathematical models:

- A beam representation,
- A beam with torsional freedom,
- A uniform orthotropic plate allowing for eccentric loads to be taken into account.

A two-axle sprung mass system with frictional damping was used for the vehicle. The authors presented DAF curves and compared the absolute maximum values of the DAF for constant uniform speed and breaking effects. They showed that a non-uniform vehicle motion can considerably influence the dynamic response of a bridge. The maximum impact factors for bending moment and deflection were obtained due to the ramp and in combination with the braking of vehicle for symmetric as well as eccentric loading of the vehicle.

The effects of initial bounce were also studied by Gupta (1980), using the same mathematical models, with similar conclusions.

In 1981, the ASCE Committee on Loads and Bridges (ASCE 1981) recommended that the term ‘impact’ would be replaced by more descriptive term ‘dynamic allowance for traffic loading’.

In 1985, O’Connor and Pritchard reported on field studies carried out in 1981 and 1983 on a short span, composite steel and concrete bridge, which was instrumented to measure mid span bending moments (i.e. strains). Results from the study were used by ARRB in the preparation of new bridge design code. Values of impact varied from -0.08 to 1.32 for 170 trucks in normal traffic with weight from 27 to 44 tons. The researcher noted that higher impact value occurred with lighter vehicles and there was a slight trend of decreasing impact values with heavier trucks. Later field measurements on the same bridge (O’Connor and Chan 1988a and 1988b) supported the same general conclusions.

Palamas *et al.* (1985) presented a theoretical study of the effects of surface irregularities on the dynamic response of bridges under suspended moving loads. The paper dealt with two types of geometrical imperfections:

- Global, simulating irregularities due to permanent loads, creep or prestressed forces,
- Local, representing joints or local defects.

This study showed that in some cases, the DAF could be two to three times that recommended by current international design codes, and suggests therefore that irregularities could no longer be neglected. It: also showed that speed limitations did not always guarantee a reduction of dynamic effects.

In 1980, a third set of dynamic testing of highway bridges in Ontario was performed (Billing 1984 and Billing and Green 1984). The tests were conducted on 27 bridges of various configurations of steel, concrete and timber construction, and with spans of 5 to 122 m to obtain comprehensive data to support the Ontario Highway Bridge Design Code (OHBDC 1979). Accelerations, deflections and strain measurements were made to characterize the dynamic response of the bridges. The conclusions from this research included:

- The mean dynamic amplifications were relatively modest, even though for some tests dynamic amplifications greater than 0.5 were observed. The coefficients of variation for the amplification magnitudes were large.
- The mean dynamic amplification generally decreased with the increase in truck weight for bridge spans greater than 30 m.
- When test runs were made with two vehicles side by side, the dynamic amplifications were generally reduced.
- The largest dynamic amplifications were obtained for bridges with a fundamental flexural frequency in the range of 2 to 5 Hz.

In 1987 Inbanathan and Wieland performed an analytical investigation of the dynamic response of a simply supported box girder bridge due to a vehicle moving across the span. They considered different roughness by representing the roadway profile using a power spectrum of highway elevation variables and a steady state sinusoidal relationship between dynamic force and the pavement surface elevation. Among their conclusions were:

- The effect of vehicle mass on bridge response is more significant in high speeds.

- Maximum response does not necessarily occur simultaneously for bending moments and deflections. It is necessary to consider both forces and deflections when evaluating dynamic response. Small variations in deflections can result in large differences in the dynamic forces.
- Dynamic stresses developed by a heavy vehicle moving over a rough deck at high speeds were larger than those predicted by several bridge codes.

In 1989 Coussy *et al.* presented an analytical study of the influence of random surface irregularities on the dynamic response of bridges. The authors concluded that the DAF decreases with span length but not as strongly as given by the codes of different countries. This was explained by the coupling of bridge and vehicle motions. Results from the investigation also showed that, in the absence of significant surface irregularities, the dynamic amplification factor was independent of bridge span.

Bakht and Pinjarkar (1989) presented a comparison of different methods of calculating the DAF from test data. The authors showed that the axiomatic definition of equation 2 has been interpreted in at least eight different ways by researchers throughout the world, making it difficult to compare results from field studies. Among the factors that can lead to differences in computed values of the DAF are:

- Vehicle type: A final value of the DAF for a specific bridge should be obtained from repeated dynamic testing under normal traffic conditions.
- Vehicle weight: It has been shown that the DAF decreases with an increase of the vehicle weight. Therefore, data obtained from lightly loaded vehicles will lead to an overestimation of the DAF and should not be considered when computing this factor.
- Vehicle position: It has been observed that the DAF obtained from measurement points far from the vehicle position is higher than that for a measurement point located directly under the vehicle load. Data obtained from such measurement points should not be used to compute the DAF.
- Type of measurements: The DAF is usually computed from vertical deflection measurements. Strain measurements have also been used and it has been observed that the DAF values obtained from such measurements are usually smaller. Without bearing

restraint, the girder strains are proportional to the girder moments, and can be used directly to compute the DAF for girder moments. However, it is still unclear whether the DAF values obtained from deflections or strain measurements can be applied directly to other responses.

- Bearing restraint effects: In the presence of bearing restraint forces, girder strains are no longer proportional to girder moments and the DAF values obtained from strain measurements do not represent moment amplification. These forces also stiffen the bridge and can explain differences between calculated and measured frequencies.

The authors concluded that the DAF is not a deterministic quantity and should be evaluated by a probabilistic means and recommended a procedure for obtaining the DAF from dynamic tests.

Chan and O'Connor (1990a) presented a simple vehicle model in which each axle load consists of a constant component and a sinusoidally varying dynamic component. The amplitude of the dynamic component was chosen equal to 10% of the static axle load. This upper-bound value was calibrated by field studies (Chan and O'Connor 1990) where wheel loads were obtained from measured strains on a highway bridge. The following observations were made:

- The maximum dynamic amplification occurs when the dynamic component of the load varies at the bridge's first flexural frequency, leading to high values of the DAF.
- Large dynamic amplification occurs when the maximum response due to succeeding axle loads coincide.
- For high dynamic amplifications, the axles within a group (tandem or tri-axle) can be replaced by a single axle load at the centre of the group.
- As the vehicle weight increases, the DAF decreases and the DMR reduces even more significantly, despite the fact that the maximum response increases.
- Computed and measured dynamic amplification factors were found in excess of code values.

Hwang and Nowak (1989, 1991) and Nowak *et al.* (1990) developed procedures for calculating the statistical parameters of dynamic loads on highway bridges to be used in development of a reliability-based bridge design code. Variables considered included different vehicle characteristics (mass, suspensions and tires, axle arrangement and speed), road roughness and bridge properties (span, mass, support type, material and geometry). Dynamic load factors were found to be lower for heavier trucks. The factors were found to be lower for two side by side trucks compared to single truck. Based on the results, a uniform dynamic load factor of 0.25 was recommended for all spans greater than 6 m.

In 1995, Field measurements were conducted by Nassif and Nowak to verify the previous analytical method. Observation indicated that the dynamic load factor decreased with increasing vehicle weight and that the factors were in agreement with the analytical prediction for heavy trucks. Larger factors were obtained when calculated based on the strains in the exterior girders. Therefore, the researchers recommended that dynamic amplification factors should be based on measurements from the interior girders.

In 1992 Paultre *et al.* presented a comprehensive review of analytical and experimental findings on bridge dynamics and the evaluation of the dynamic amplification factor (DAF). The conclusions from his research included:

- The DAF is related to the fundamental frequency of the bridge.
- While the specified live loads differ in the bridge design codes that exist throughout the world, this does not justify the large differences in the treatment of dynamic load allowance s in the various codes
- Analytical models cannot reliably evaluate the DAF for a particular bridge at present time (1992). Full scale testing under traffic loading is the only economical and practical way to evaluate the DAF with reasonable confidence.
- Roadway roughness, pavement irregularities and vehicle suspension system all strongly influence DAF. Vehicle speed and axle loading can also be important parameters.
- Geometries and construction materials of typical highway bridges do not seem to influence the DAF

2.2.3 Overview of Recent Works

In 1996, Wang *et al.* studied the free vibration characteristics and the dynamic response to a multivehicle load moving across rough bridge deck of continuous and cantilever thin-walled box girder bridges. The dynamic responses of the bridges were evaluated for single truck, three, and six trucks, with different speeds and road surface roughness. The analytical results showed that, the effects of different loading models, road surface profiles, and vehicle speeds on the dynamic response for different types of bridges are quite different. The most important factor which affects the impact of cantilever bridges is the vehicle speed.

In 1997, Kim and Nowak published a paper which presented the procedure and results of field tests that were performed on two simply supported steel I-girder bridges to assess girder distribution and impact factors. The data were processed to obtain statistical parameters (mean and standard deviation) of the girder distribution and impact factors. The results were compared with the values calculated according to AASHTO methods. Measured girder distribution factors are lower than AASHTO values. Measured impact factors were well below AASHTO values.

In 1998, Fafard *et al.* presented a paper investigating the effect of dynamic loads on the dynamic amplification factors (DAFs) of an existing continuous bridge. The DAFs were computed from finite element model for three different types of measurements (displacements, strains, and reactions). The numerical results showed that, the DAFs computed with displacements are less than those estimated from strains and reactions. The researchers concluded that current design codes tend to underestimate dynamic amplification factors, especially for long-span continuous bridges.

In 1998, Chaallal and Shahawy published a report that provided a state of the art review on dynamic testing procedures for bridges, with a special emphasis on experimental evaluation of the DAF. A synthesis of previous studies on the evaluation of the DAF is also provided in terms of the following important parameters:

- Fundamental frequency and damping characteristics of the bridge,
- Roadway roughness,

- Excitation source, vehicle speed and test vehicles,
- Bridge geometry and construction materials,
- Position of the measurement points and number of instruments used,
- Wheel dynamic loading measurement.

From a review of analytical and experimental findings, the following conclusions were reached:

- The DAF is related to the fundamental frequency of the bridge. Most modern highway bridges were found to have fundamental frequencies in the range of 2 to 5 Hz, corresponding to the resonant frequencies of commercial vehicles.
- Analytical methods cannot reliably evaluate the DAF for a specific bridge, owing to the many parameters involved that are difficult to model.
- Full-scale testing under traffic loading is the only economical and practical way to evaluate the dynamic amplification factor with reasonable confidence.
- Vehicle speed is an important parameter in the evaluation of the DAF. Dynamic testing under controlled traffic should be carried out over a sufficient range of speeds to cover critical speeds.
- The peak value of the DAF is not strongly influenced by vehicle mass.
- Roadway roughness and pavement irregularities strongly influence the DAF.
- Axle spacing of vehicles affects the amplitude of the maximum static response and hence the DAF.
- Geometry and construction materials of typical highway bridges do not seem to play an influencing role on the value of the DAF.

This review clearly shows that there is a need to establish quantitative as well as qualitative test procedures and numerical signal processing standards based on international consensus. This would result in a standardization of the experimental evaluation of the dynamic amplification factor.

In 2004, Broquet *et al.* published a paper on ‘Dynamic Behavior of Deck Slabs of Concrete Road Bridges’. The paper describes a parametric study, based on the stimulation of bridge-vehicle interaction that was carried out to investigate characteristic properties of the dynamic behavior of the bridge deck slabs of concrete bridges and to deduce the distribution of dynamic amplification factors (DAFs) throughout the deck slab. The variation of DAF was analyzed for various factors i.e. vehicle speed, vehicle mass, road surface condition, bridge cross section. The dynamic amplification factor varied between 1.0 and 1.55 for the bridges and vehicles studied.

Typical simulation result reported by the researchers for the determination of DAF is shown graphically in Figure 2.2. The variation of the DAF as function vehicle speed is shown in Figure 2.3. It was found that, there is no critical speed or critical relationship between the DAF and speed.

The influence of vehicle mass is shown in Figure 2.4. It can be seen that although the static and dynamic effects increase as the vehicle load increases, the DAF decreases. The influence of the road profile on the DAF is shown in Figure 2.5. It can be seen that an increase in road roughness causes an increases in DAFs.

Although the value for the traffic action affects the deck slab and their distribution varied from bridge to bridge, no clear relationship was found between the DAF and the type of bridge or configuration of the deck slab.

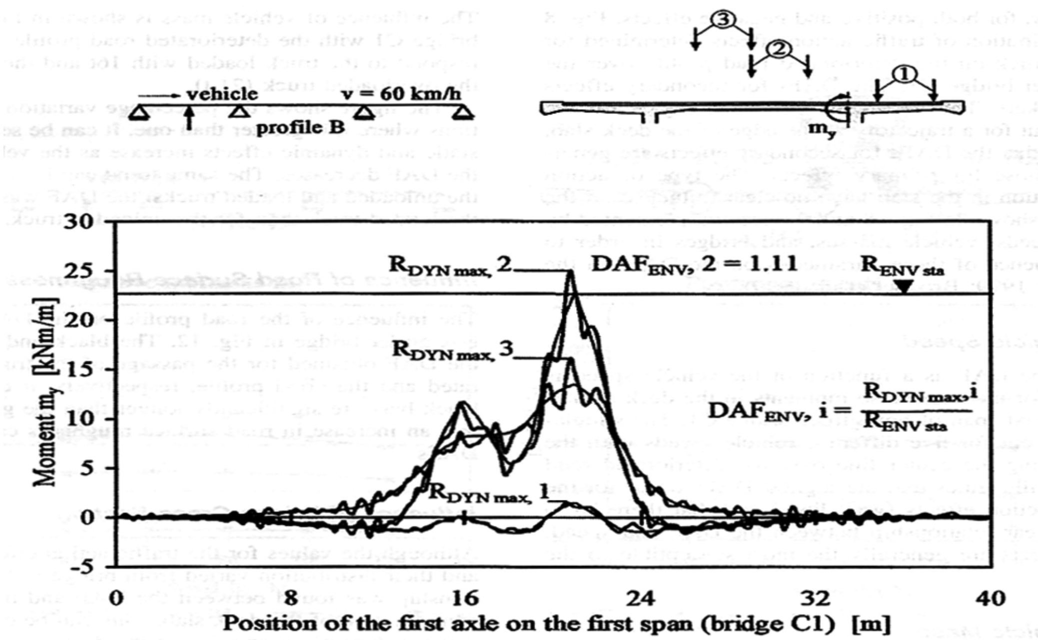

Figure 2.2: Typical simulation results of DAFs reported by Broquet et al. (2004)

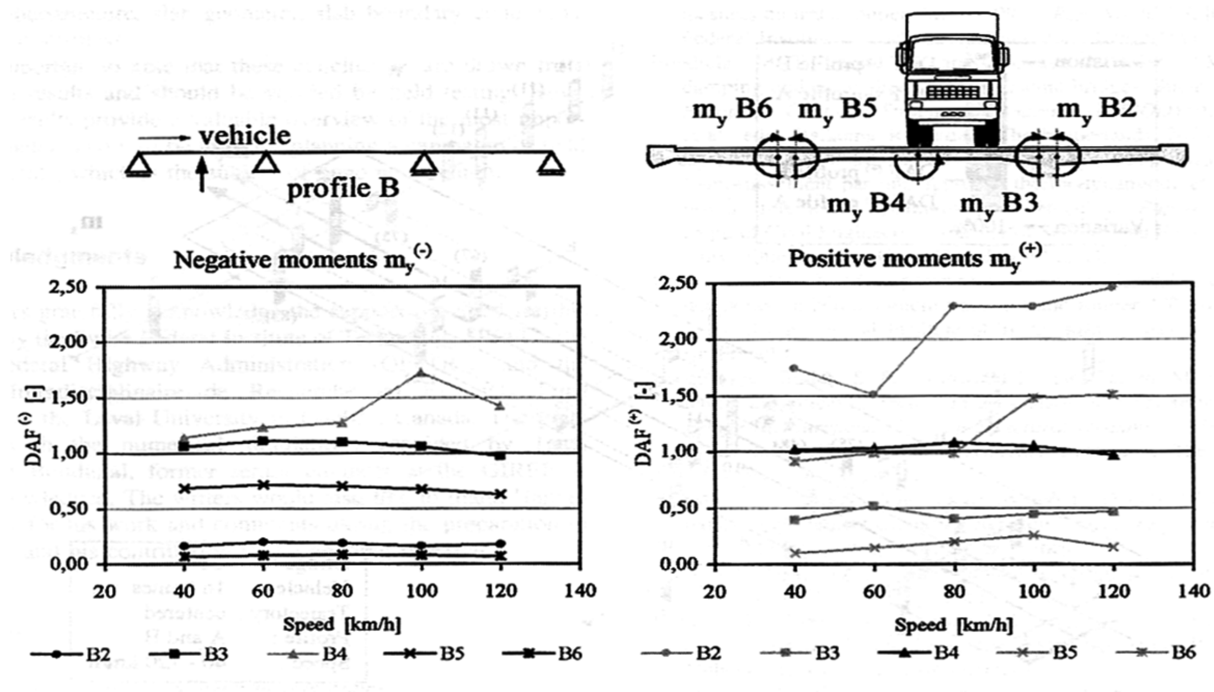

Figure 2.3: DAF as a function of vehicle speed reported by Broquet *et al.* (2004)

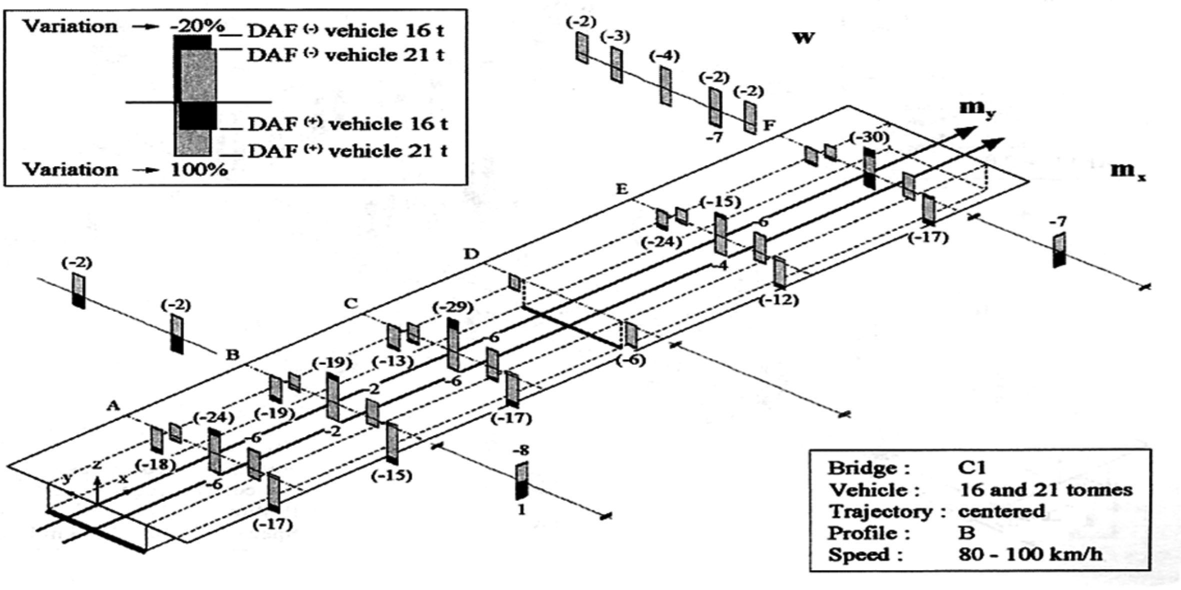

Figure 2.4: Influence of vehicle mass on DAF in deck slab reported by Broquet *et al.* (2004)

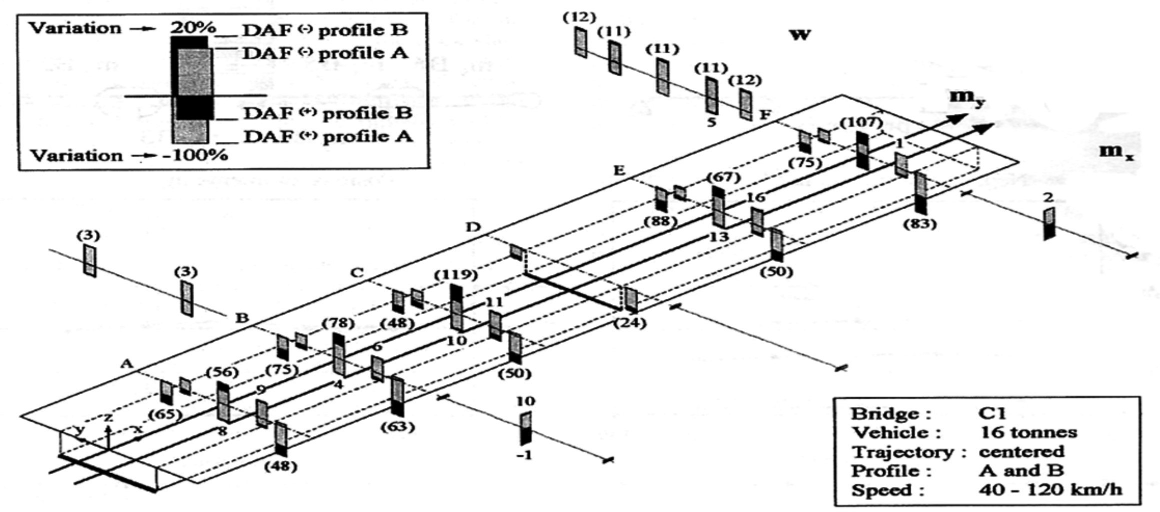

Figure 2.5: Influence of road roughness on DAF in deck slab reported by Broquet *et al.* (2004)

Broquet *et al.* (2004) came to the following conclusions with respect to DAF in road bridge deck slabs:

- DAF in deck slabs are not influenced significantly by vehicle speed.
- The static effects increase with the vehicle mass but the DAF decreases.
- The increase in road roughness leads to higher DAFs.
- DAFs do not vary significantly as a function of the type of action effect, location in a deck slab, type of superstructure, slab geometry, slab boundary conditions or slab stiffness.

In 2004, Sennah *et al.* presented a method for determining the dynamic impact factors for horizontally curved composite single or multi-cell box girder bridges under AASHTO truck loading. The key parameters considered in this study were: Number of cells, number of lanes, degree of curvature, arc span length, slope of the outer steel webs, number and area of bracing and top chord systems, and truck(s) speed and truck(s) positioning. Based on the data generated from the parametric study, expressions for dynamic impact factors for longitudinal moment, reaction, and deflection were proposed as function of the ratio of the arc span length to the radius of curvature.

In 2006, Brady *et al.* used relatively simple numerical models to investigate the effect of vehicle velocity on a bridge's dynamic amplification. A set of critical velocities were determined associated with peaks of dynamic amplification for all beams. The reasons for these large amplifications were discussed. A more complex finite element model, validated with field tests, was used to test the applicability of the conclusions obtained from the simple models to a realistic bridge/vehicle system.

In 2008, Shi *et al.* calculated the responses of vehicle induced dynamic bridge by modeling the bridge and vehicle as one coupled system. A parametric study was conducted to analyze the effects of different truck speeds and different road surface conditions. The faulting condition of the approach slab was found to cause significantly large dynamic responses in short-span slab bridges. Impact factors obtained from numerical analyses are compared with those values specified in the AASHTO codes.

In 2008, Li *et al.* performed several full-scale load tests on Florida Highway Bridge. Experimental data were compared with simplified vehicle and bridge finite-element models. It was found that the numerical analysis matched well with the experimental data and was used to successfully explain critical dynamic phenomena observed during the testing. Impact factors for this tested bridge were thoroughly investigated by using these models.

2.3 Remarks

Most of the previous researches relating the DAF in deck slabs of bridges involved with the local dynamic effect in the longitudinal direction excluding the effect in the transverse direction of the cantilever part except the work of Broquet *et al.* (2004). For certain bridge types, cantilever part of the deck slab has immense structural and functional importance. The previously performed studies did not take into account the effect of vehicular loading in the transverse direction of the cantilever part. Again there was no defined rule in AASHTO (2002) and IRC specifications to determine local dynamic effect in the transverse direction of the cantilever part of deck slabs.

Few years ago, cracks were observed along the root of cantilever part of the deck in the longitudinal direction of Bangbabandhu Bridge, Bangladesh. So, for analyzing the longitudinal crack, researchers came to predict the requirement of steel in the transverse direction. Confusion aroused to predict the amount of impact increment in the pertaining portion. Cracks might be developed in the specified portion of deck if the impact effect was found high in the transverse direction and required reinforcement determined by the conventional theory was found too low.

Therefore, researches may be carried out to find out the DAFs for stresses as well as for deflections in the transverse direction of the cantilever part of the deck slab to provide guideline for determining required reinforcement in the transverse direction.

CHAPTER 3
FINITE ELEMENT MODELING

3.1 Introduction

In modern structural design, use of sophisticated numerical tools and computer hardware technology for analysis is very advantageous. So with the advent of these types of numerical tools like the finite element method, it has become possible to model the dynamic behavior of bridge prototypes. So a finite element model regarding the cantilever part was modeled for determination of the dynamic response of the deck. In this chapter the actual work regarding the finite element modeling which was pertaining the subject has been described. Attempts are made to describe bridge modeling, vehicle modeling and vehicle speed simulation with proper boundary and loading conditions, deflection over time for both static and dynamic analysis and as a whole, total deflected shape from this investigation. The dynamic impact for repeated loading has synthesized by determining dynamic amplification factor (DAF). In this Study, dynamic response for different damping condition as well as statistical analysis is done with the help of finite element modeling to obtain DAF. In this chapter finite element modeling has described for both statistical and dynamic analysis with damping effect.

3.2 Model for Finite Element Investigation

In this thesis, a typical box girder bridge with cantilever portion was chosen as the model for finite element investigation. For analysis, the model was so chosen that it included three spans with its cantilever portion which was modeled as a sub structure assuming the box girder as a collection of natural components. Vehicle loading were supposed to move along two different paths, one along cantilever part of the box girder bridge at a distance from cantilever edge of the bridge and another along center line of the deck slab of the box girder bridge. Vehicle load was modeled as a pair of concentrated force which moved along these two paths separately.

3.2.1 Geometries of the Structure of Parametric Study

A specific and comprehensive parametric study was executed in this study for the geometries of the cantilever part. The key parameters considered were vehicle speed, width of the cantilever, wheel position, length and thickness of the slab.

The reference median geometries of these key parameters of the model were taken for width of the cantilever slab 4.0 meter, for wheel position from the root of the cantilever as 1.0 meter, for maximum and minimum thickness of cantilever slab as 500 mm and 800 mm respectively, for length of slab as 100 m and for vehicle speed as 100 km/h. Reference median geometries of the structure are illustrated in Figure 3.1A.

Practically the thickness of the deck slab is designed and fabricated as non uniform with the maximum value at the root of the cantilever gradually reducing to a minimum value at the tip. Similarly, thickness also reduces gradually and a minimum thickness is achieved at the middle point of the cross section of the deck slab which is maintained in this study and shown in Figure 3.1B.

Conceptual side elevation of the reference model is shown in Figure 3.2. Three-dimensional model of the box girder bridge is illustrated in Figure 3.3.

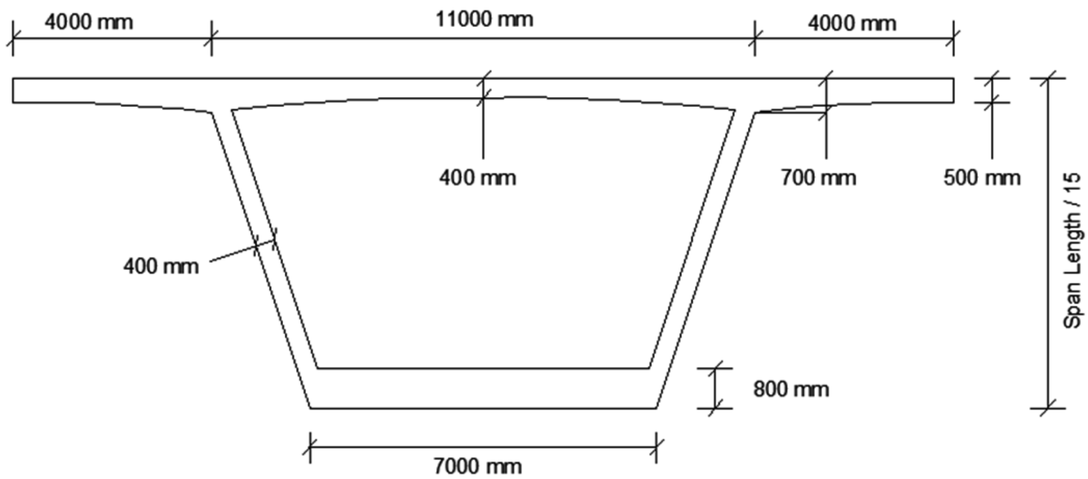

Figure 3.1A: Cross-Section at Pier of the Reference Model

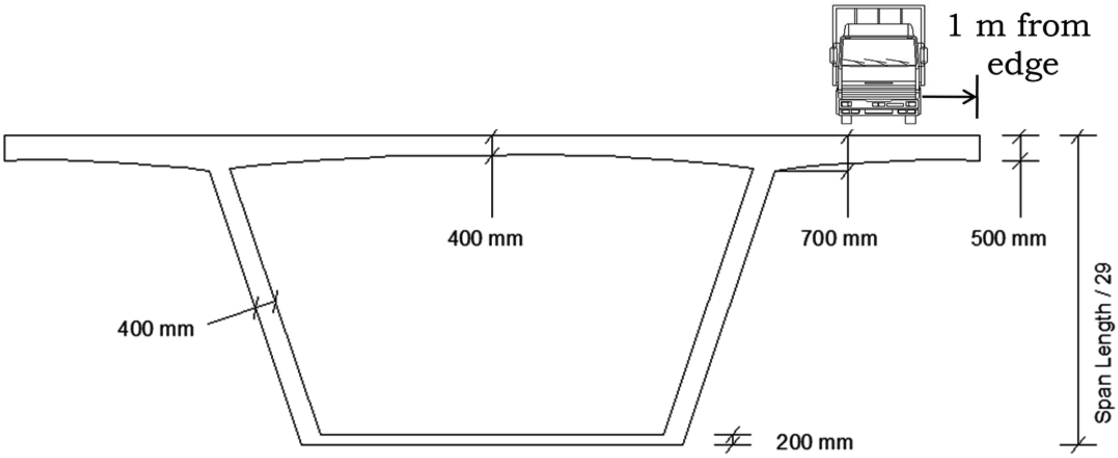

Figure 3.1B: Cross Section at Mid Span of the Reference Model

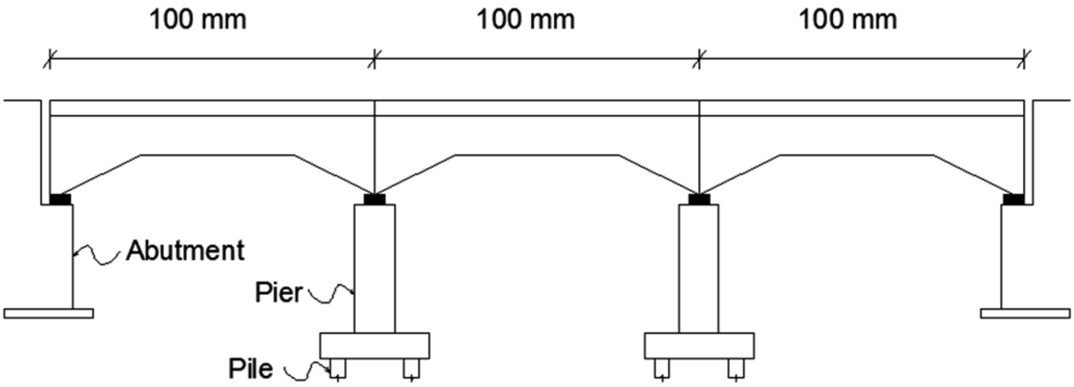

Figure 3.2: Conceptual Side Elevation of the Reference Model

Figure 3.3: Finite Element Model of Box Girder Bridge

3.2.2 Load

The highway truck loading considered in this study was HS20-44 highway standard design truck of AASHTO (2002) shown in Figure 3.4 and 3.5. Simplified AASHTO (2002) truck loading configuration is described in Figure 3.6. The vehicle was idealized as a pair of concentrated forces moving along the deck in two paths, one at centerline position and another at the cantilever part which is parallel to the centerline of the bridge at different wheel position. The vehicle was assumed to move with constant velocity.

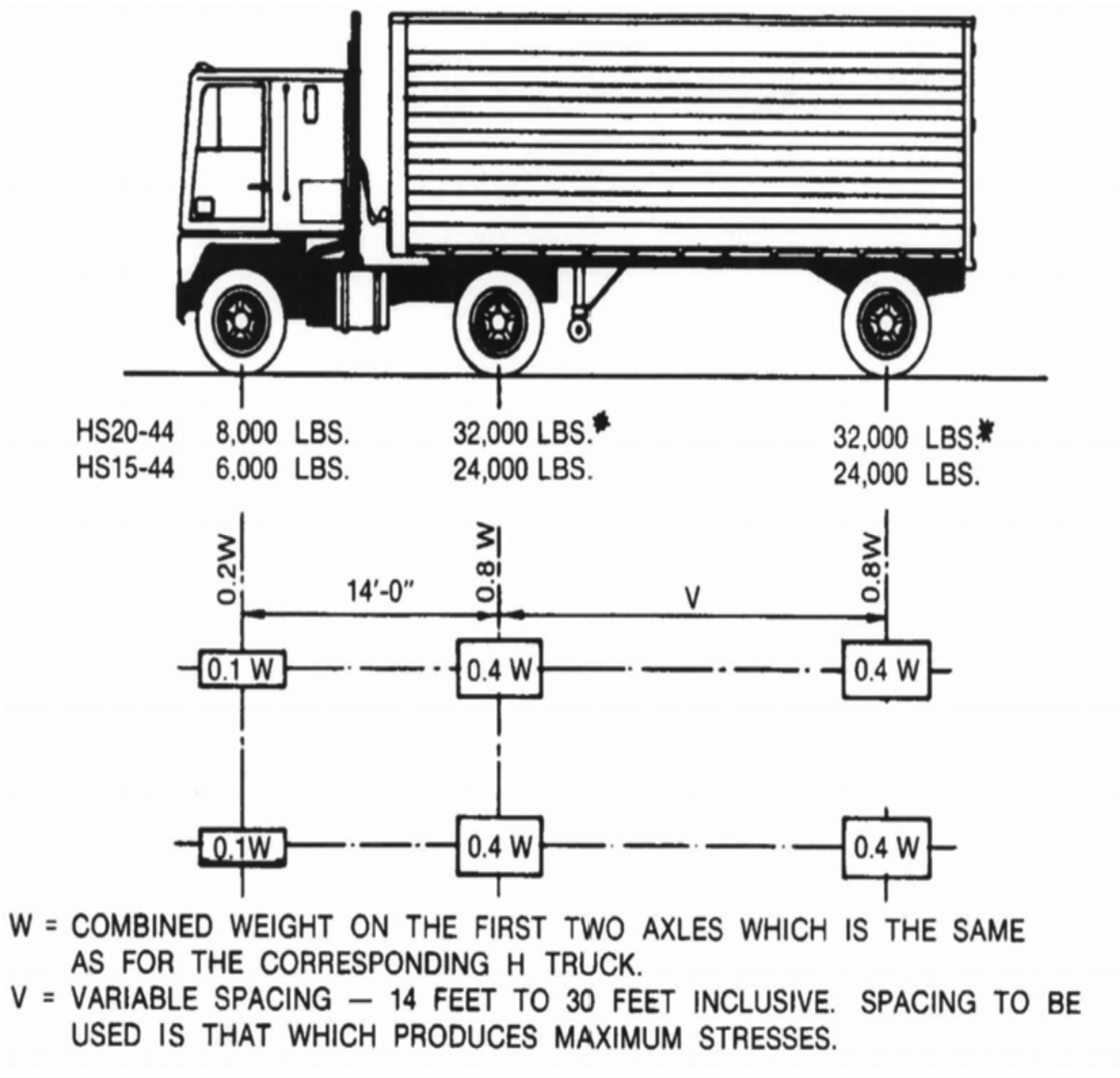

Figure 3.4: Axle Load and Wheel Load of AASHTO HS Standard Truck

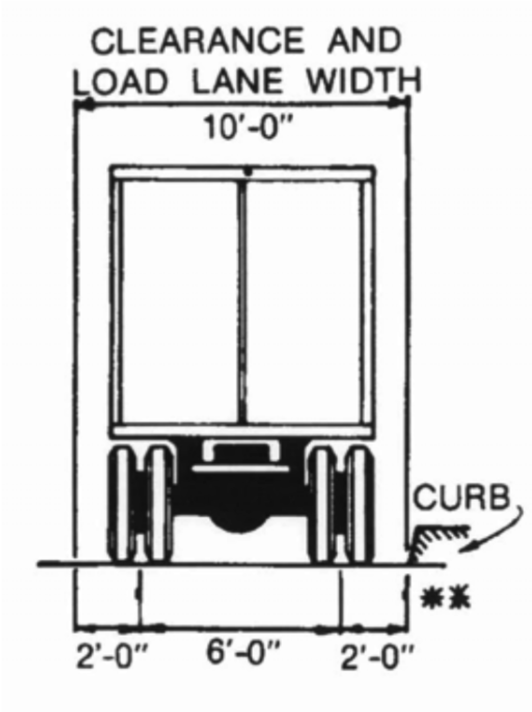

Figure 3.5: Clearances and Load Lane Width of AASHTO HS 20-44 Standard Truck

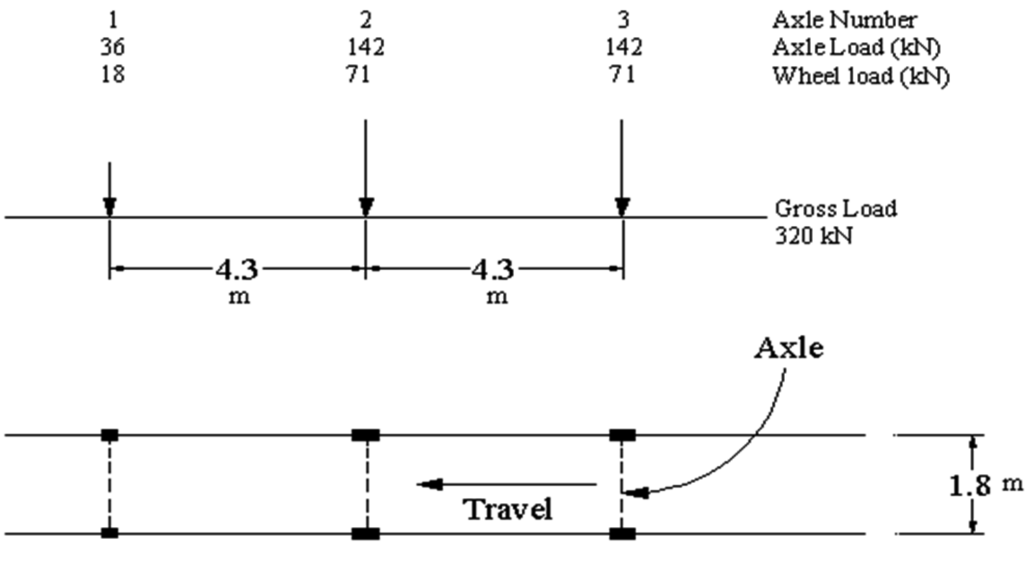

Figure 3.6: Simplified Truck Loading Configuration of AASHTO HS 20-44

3.2.3 Boundary Condition

Mathematically boundary matrices which are load and stiffness matrices are reduced from the interior points to the exterior or boundary points to model a structure. The related topic was concerned with the boundary condition of three spans as the model consists of three adjacent spans. Both end points of each span adjacent to the successive spans were kept in consideration which would be structured by applying boundary conditions at the exterior points of the each span. To represent the continuity of the modeled bridge all the end nodes of the three spans were constrained along bridge span.

In the existing problem the whole structure was simply supported. Diaphragms were provided at both external ends of the whole model to resist the vertical settlement of the bridge slab at span end which also refers to support condition. Diaphragm was also provided at interior end support of the spans.

3.2.4 Material

In this investigation, material used for the model was considered linear and isotropic. Again, cantilever part of the deck was assumed to be made of reinforced concrete. So, reinforcement in the slab was ignored. Material properties are shown in Table 3.1.

Table 3.1: Material Properties

Poison Ratio, υ	Modulus of Elasticity, ϵ	Density, ρ
	kN/m^2	kN/m^3
0.3	20×10^6	2.44×10^{-6}

3.2.5 Damping Characteristics

Effects of damping parameters for conducting the analysis are also considered in this investigation. In this analysis, 0%, 2.5% and 5% damping has considered for each parametric study to get stresses in the transverse direction and deflections at the tip of the cantilever part of the box girder bridge so as to obtain dynamic amplification factor.

3.2.6 Study Parameters

Parametric study is the most important part for analysis. It helps to identify the most important parameters which have greater influences on the concerned factor. In this thesis, for determining dynamic response of the deck slab, several parameters were chosen among numerous parameters for close investigation in a parametric study which was described in article 3.2.1 The aim was to identify the parameters which have the greatest influence the dynamic response as well as to determine the maximum DAFs. The values of each parameter that was considered in the analysis are shown in Table 3.2 and Figure 3.7 illustrates cross section of reference model showing parameters that were approximated for this study.

Table 3.2: Geometries of the Structure in Parametric Study

Parameters	Unit	Geometry
Thickness of top deck slab at middle: *TM1*, *TM2*, *TM3*,*TM4*	millimeter	400, 500, 600, 700
Thickness of top deck slab at left: *TL1*, *TL2*, *TL3*, *TL4*	millimeter	800, 700, 600, 500
Thickness of top deck slab at right: *TR1*, *TR2*, *TR3*, *TR4*	millimeter	800, 700, 600, 500

Parameters	Unit	Geometry
Thickness of inclined web: *TD*	millimeter	TD=300+(Span Length/1000)-50)/25*50 (50mm increment for 25m increment in span)
Thickness of bottom slab: i) *TBB1* (at Midspan) ii) *TBB2* (at Pier)	millimeter	i) *TBB1*=150+(Span Length/1000)-50)/25*25 (25mm increment for 25m increment in span) ii) *TBB2*=600+(Span Length/1000)-50)/25*100 (100mm increment for 25m increment in span)
Span Length	meter	50, 75, 100, 125, 150
Width of the Cantilever, *B*	meter	3, 3.5, 4, 4.5
Vehicle Speed	km/h	40, 60, 80, 100, 120, 140, 160
Wheel Position	meter	i) Centerline of deck slab of box girder bridge ii) 1 m away from edge of cantilever (at cantilever part)
Length of top deck: i) at middle part, *BM* ii) at left cantilever part, *BL* iii) at right cantilever part, *BR*	millimeter	i) *BM* = 11000 ii) *BL* = 4000 iii) *BR* = 4000

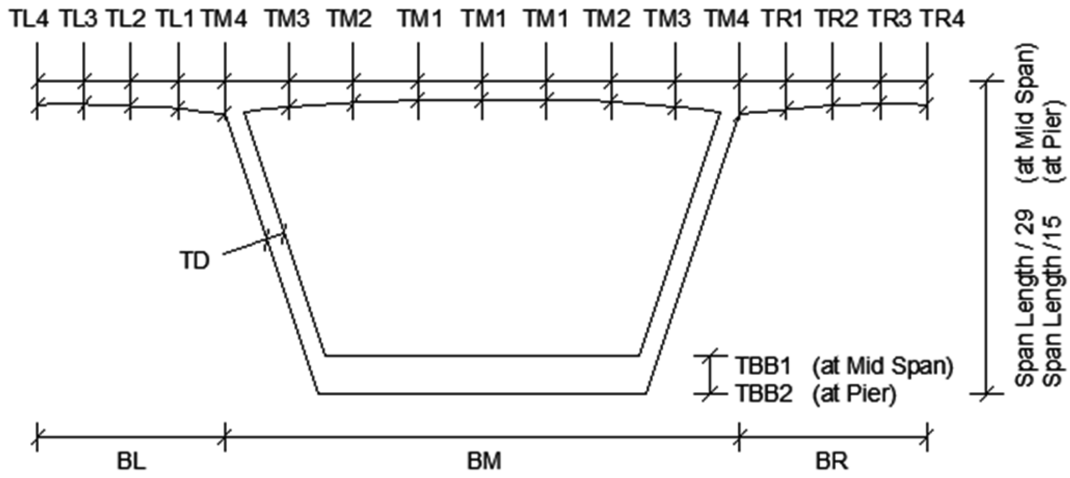

Figure 3.7: Cross Section of the Reference Model Approximated for this Study

3.3 Finite Element Modeling of Cantilever Bridge Deck

The modeling of the structure of cantilever bridge prototype was carried out in three dimensions using the finite element software ANSYS 13.0. A four node shell element Shell63 with six degrees of freedom at each node was used to model the cantilever box girder bridge of concrete deck. In the following article the element type is described.

3.3.1 Shell63: Elastic Shell

SHELL63 has both bending and membrane capabilities. Both in-plane and normal loads are permitted. The element has six degrees of freedom at each node: translations in the nodal *x*, *y*, and *z* directions and rotations about the nodal *x*, *y*, and *z*-axes. Stress stiffening and large deflection capabilities are included. A consistent tangent stiffness matrix option is available for use in large deflection (finite rotation) analyses.

The geometry, node locations, and the coordinate system for this element are shown in Figure 3.8A. The element is defined by four nodes, four thicknesses, elastic foundation stiffness, and the orthotropic material properties. Orthotropic material directions correspond to the element coordinate directions.

Several items are illustrated in Figure 3.8B. Printout includes the moments about the *x* face (*MX*), the moments about the *y* face (*MY*), and the twisting moment (*MXY*). The moments are calculated per unit length in the element coordinate system. The element stress directions are parallel to the element coordinate system.

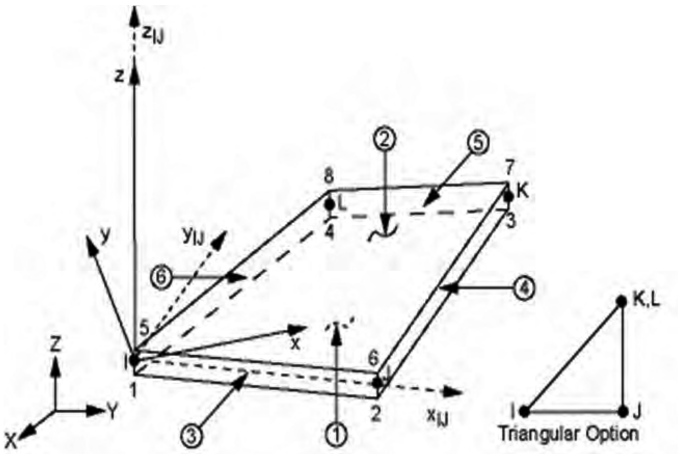

Figure 3.8A: SHELL63 Geometry

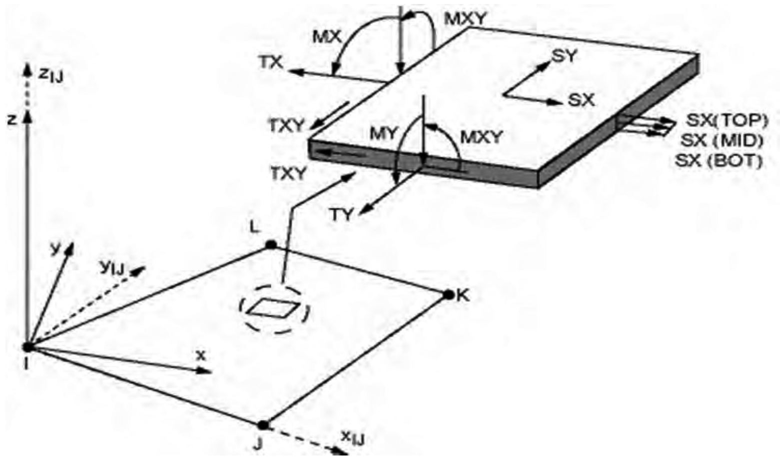

Figure 3.8B: SHELL63 Stress Output

3.3.2 Boundary Condition

In this investigation, there were three successive spans. The whole model was acted as a simply supported model. Hinge support condition was applied at the external end (which had no successive span in the model) of the first span i.e. three degrees of freedom (UX, UY, UZ) at two external end points were kept fixed. Only one degree of freedom (UY) at internal end points (which had successive span in the model) of the spans was kept fixed. Diaphragms were provided at both external ends of the whole model and also at internal ends to resist the vertical settlement of the bridge slab at span end which also refers to support condition. 3D view of the model with boundary condition, side view of structure with boundary condition and boundary Condition at the external end and internal end is illustrated in Figure 3.9A, 3.9B, 3.9C and 3.9D.

Figure 3.9A: Boundary Condition (3D View)

Figure 3.9B: Boundary Condition (Side View)

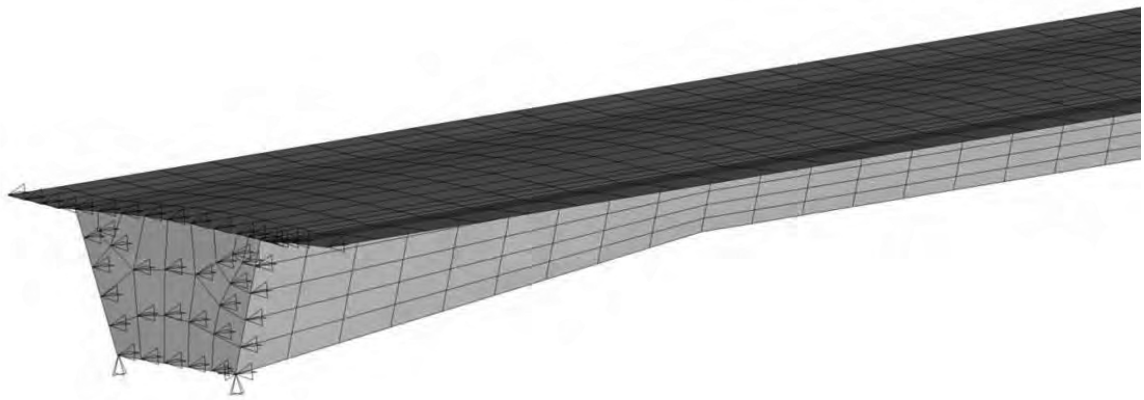

Figure 3.9C: Boundary Condition (At the External End)

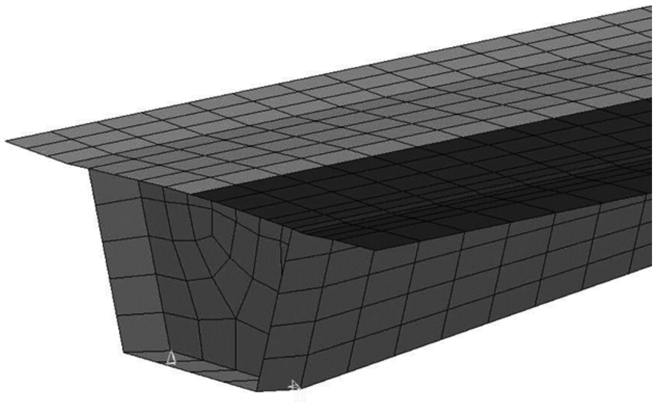

Figure 3.9D: Boundary Condition (At the Internal Edge)

3.3.3 Meshing

The cantilever deck was meshed in both longitudinal and lateral direction as shown in figure of above article and in Figure 3.10 meshed models with thickness is shown. Meshing along the width was done as an approximate basis. Meshing along the length was designed in such a way that, the length between the wheels 4.3 meters was a multiplier of number of divisions and division size along its length i.e.

Number of divisions between wheel × division size = 4.3 meters

This type of meshing was chosen for parametric study for positioning the vehicle at any location of the cantilever of the deck.

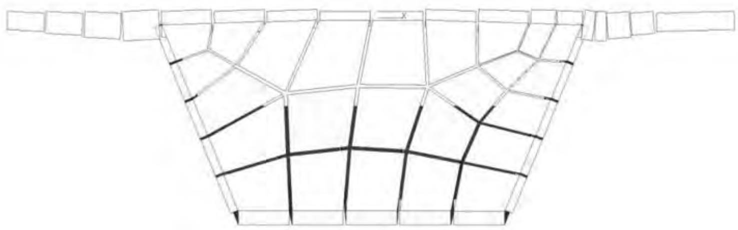

Figure 3.10: Finite Element Model of the Structure (Front View)

3.3.4 Damping Properties

Damping is a process by which free vibration steadily diminishes in amplitude i.e. the energy of the vibrating system is dissipated by various mechanisms. So, for determining the damping properties of a structure for dynamic responses, it can be computed by modal analysis. It is impractical to determine the coefficients of the damping matrix directly from the structural dimensions, structural member sizes and the damping properties of the structural materials used. Therefore, damping is generally specified by numerical values for the modal damping ratios and these are sufficient for analysis of linear systems. In this study, modal analysis is done with Ansys software for 5 different span lengths and 4 different cantilever widths for 2.5% and 5% damping. For each variation modal analysis is done and frequency is got for it. This frequency is used in the main dynamic analysis for different span length and cantilever width variation.

3.4 Vehicle Modeling

3.4.1 Vehicle Load Simulation

The vehicle was idealized as pairs of concentrated forces moving along the bridge in two paths, one at cantilever part of box girder bridge which is parallel to the centerline of the bridge and another at the centerline of the box girder bridge at different wheel position. The vehicle was assumed to move with constant velocity.

Finite element modeling of the structure including vehicle loads for vehicle at cantilever part is shown in Figure 3.11A.

Figure 3.11A: Finite Element Model Including Vehicle Load at Cantilever Part

Finite element modeling of structure including vehicle load at centerline of box is shown in Figure 3.11B. In these two cases, vehicle load was simulated as pairs of concentrated force and HS20-44 highway standard design truck of AASHTO (2002) was used.

Figure 3.11B: Finite Element Model Including Vehicle Load at Centerline of Box

3.4.2 Vehicle Travel Simulation

For a certain velocity, vehicle travel was simulated in such a way that forces coming from vehicle loads were applied on each consecutive node for a time period, 2Δt where Δt was the time in which vehicle had to pass the half of the division size along its length i.e.

$$2\Delta t = \frac{\text{dimention of the mesh along the vehicle path}}{\text{vehicle speed}}$$

After each time period 2Δt, vehicle had to pass the next series of nodes consecutively. Stepped type loading was considered on pertaining node for a time period 2Δt instead of ramped load. Each of the following figures demonstrates application of step loading on nodes of which vehicle loads are applied for a time period 2Δt.

The dynamic equilibrium equation at time (t+2Δt) was solved by adopting Newmark integration formulae consecutively with help of ANSYS software by default. Stepped loading on node and vehicle travel simulation are shown in Figure 3.12, 3.13 respectively.

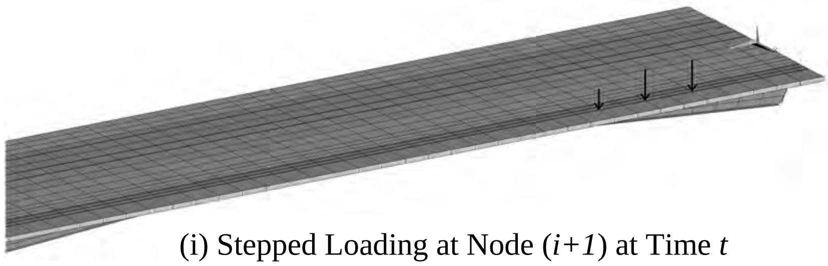

(i) Stepped Loading at Node (*i+1*) at Time *t*

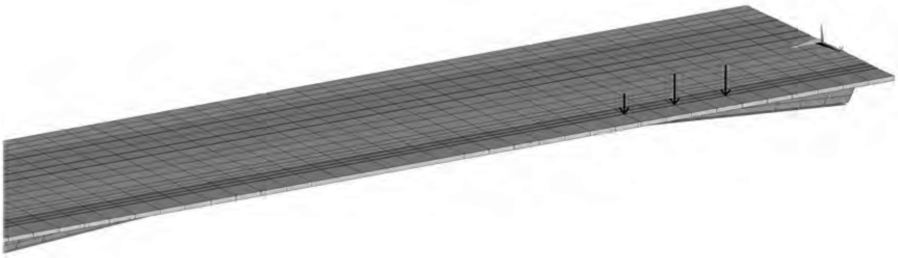

(ii) Stepped Loading at Node (*i+2*) at Time (*t* + *2Δt)*

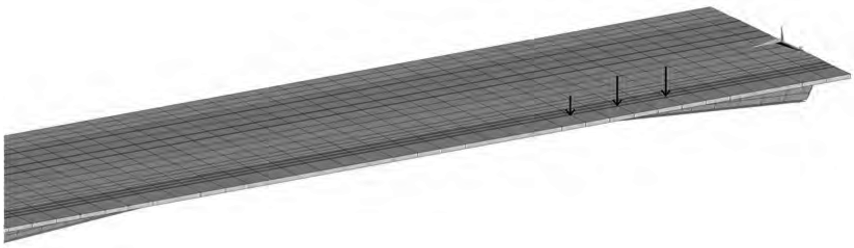

(iii) Stepped Loading at Node (*i+3*) at Time (*t* + *4Δt)*

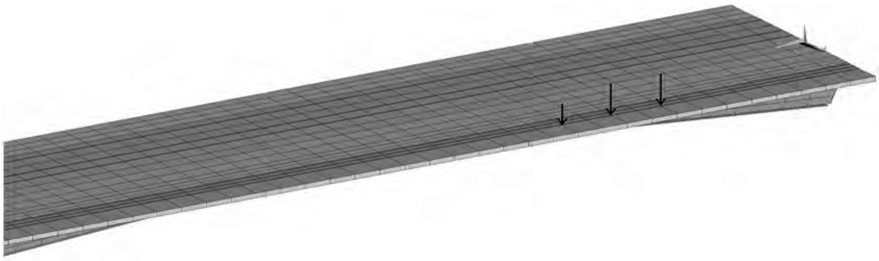

(iv) Stepped Loading at Node (*i+4*) at Time (*t +6Δt)*

Figure 3.12: Stepped Loading on Nodes

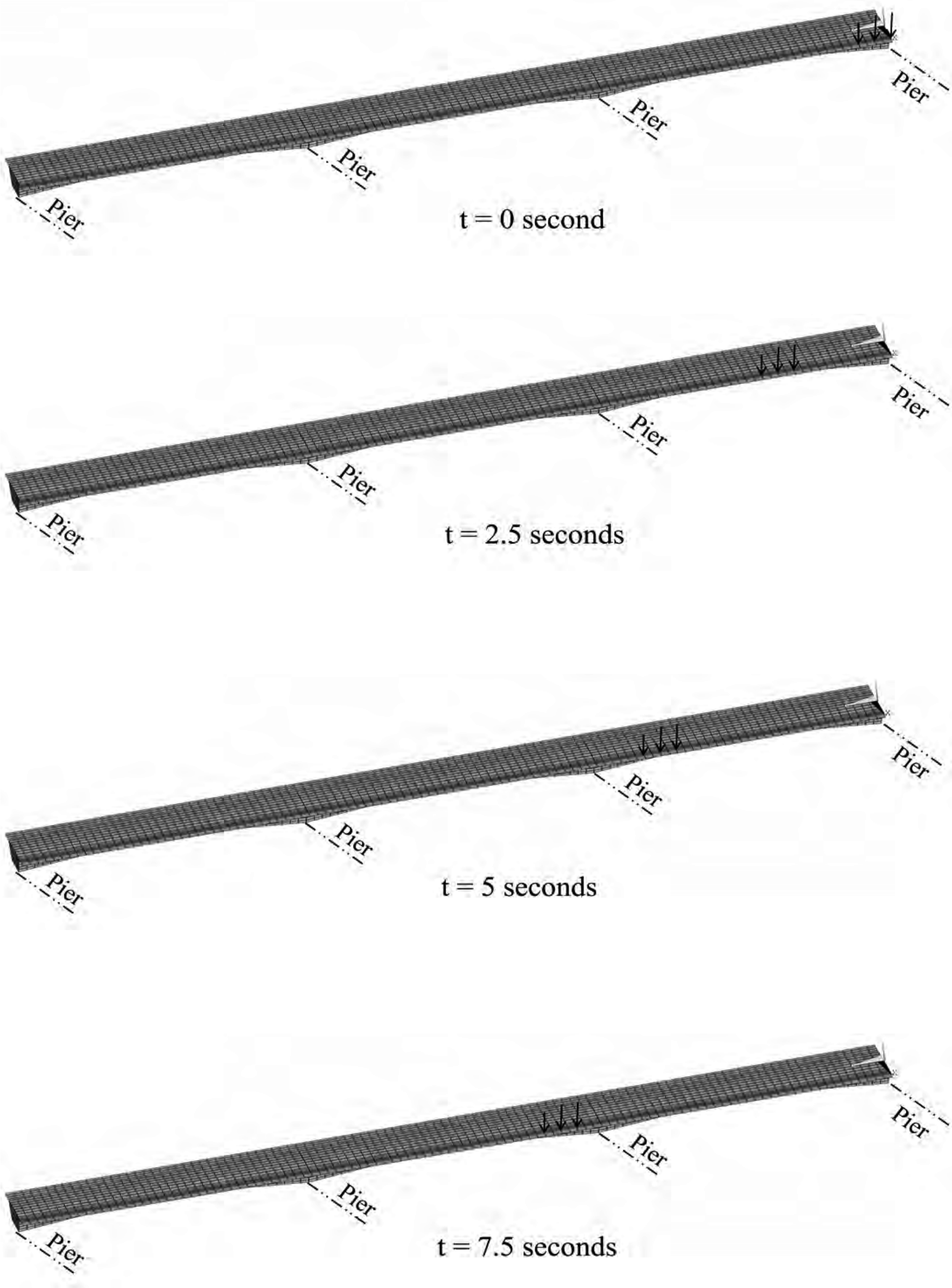

Figure 3.13: Vehicle Travel Simulation (for Span = 100 m and Velocity = 40 km/hr)

3.5 Deflection over Time for Static and Dynamic Analysis

3.5.1 Vehicle Position along Cantilever Part of Box Girder Bridge

Deflection over time in static analyses and animated deflection over time in full transient dynamic analyses for 0% damping are shown in this investigation where vehicle was assumed to move along cantilever part of the box girder bridge.

Deflection over time in static analyses and in deflection analyses for 0% damping at t = 0 sec and vehicle speed 40 km/h are shown in Figure 3.14A and Figure 3.14B respectively for vehicle path along cantilever part of box girder bridge.

Deflection over time in static analyses and for 0% damping, deflection over time in full transient dynamic analyses are shown in Figure 3.15A and Figure 3.15B respectively for t = 5 sec at vehicle speed 40 km/h for vehicle path along cantilever part of box girder bridge.

For static, deflection over time is illustrated in Figure 3.16A and for full transient dynamic analyses; deflection over time for 0% damping is shown in Figure 3.16B. This investigation of static and dynamic analysis was done for t = 10 sec at vehicle speed 40 km/h for vehicle position along cantilever part of the box girder bridge.

Deflection over time in static analysis is shown in Figure 3.17A and for full transient dynamic analyses; deflection over time for 0% damping is shown in Figure 3.17B. In both cases analysis was done for t = 15 sec at vehicle speed 40 km/h for vehicle position along cantilever part of box girder bridge.

For static, deflection over time is illustrated in Figure 3.18A and for full transient dynamic analyses; deflection over time for 0% damping is shown in Figure 3.18B. This investigation of static and dynamic analysis was done for t = 20 sec at vehicle speed 40 km/h for vehicle position along cantilever part of the box girder bridge.

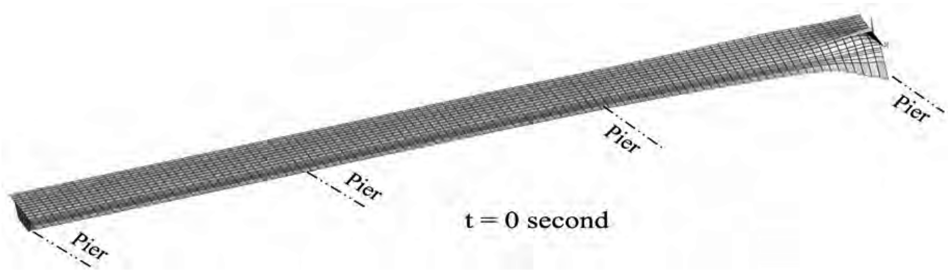

Figure 3.14A: Static Deflection for Vehicle at Cantilever Part (for t = 0 sec, V = 40 km/h)

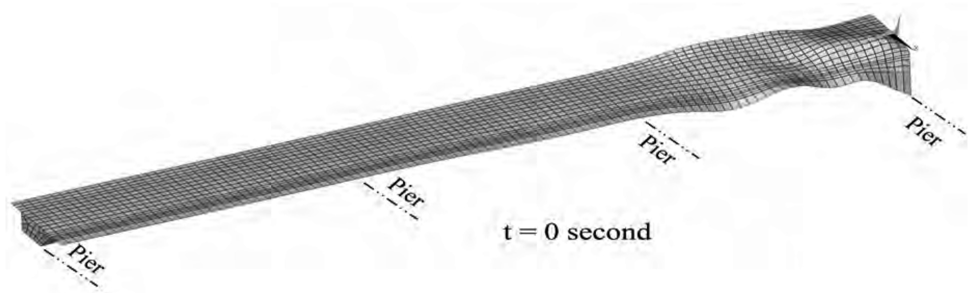

Figure 3.14B: Dynamic Deflection for Vehicle at Cantilever Part at 0% Damping (for t = 0 sec and V = 40 km/h)

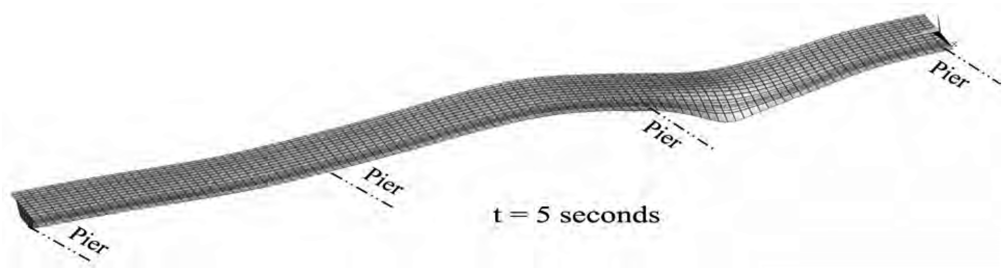

Figure 3.15A: Static Deflection for Vehicle at Cantilever Part (for t = 5 sec, V = 40 km/h)

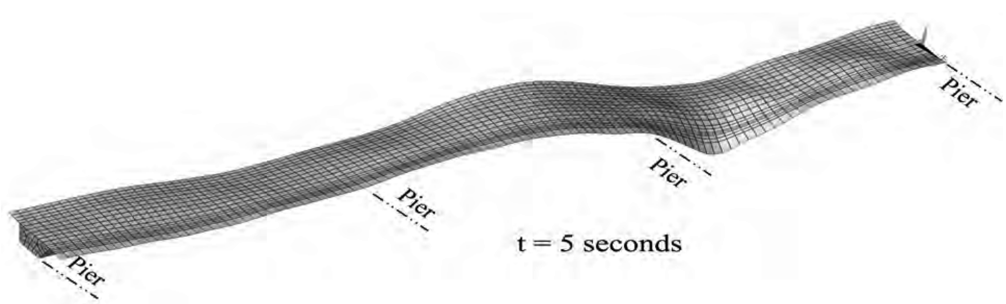

Figure 3.15B: Dynamic Deflection for Vehicle at Cantilever part at 0% Damping (for t = 5 sec and V = 40 km/h)

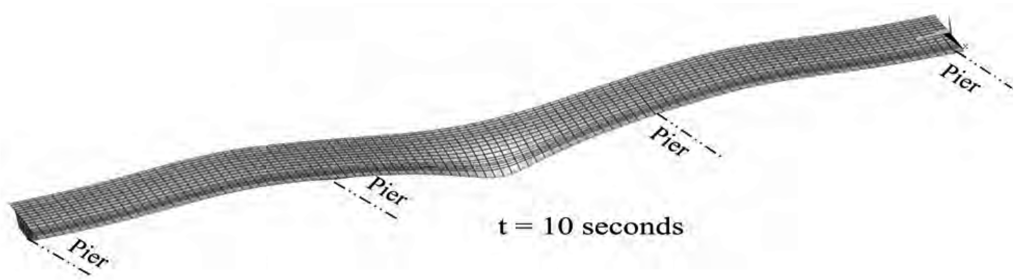

Figure 3.16A: Static Deflection for Vehicle at Cantilever Part (for t =10 sec, V = 40 km/h)

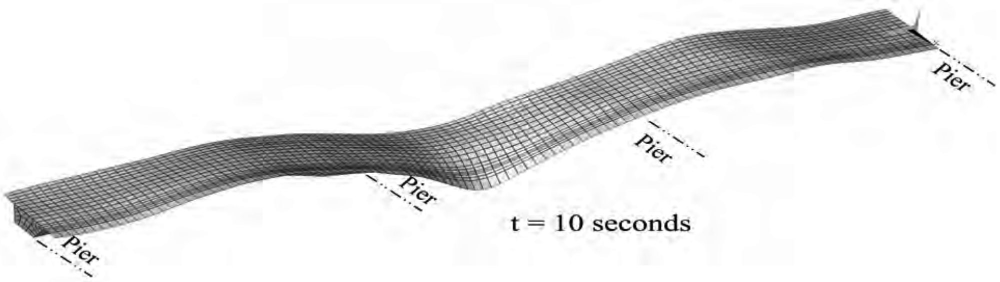

Figure 3.16B: Dynamic Deflection for Vehicle at Cantilever Part at 0% Damping

(for t = 10 sec and V = 40 km/h)

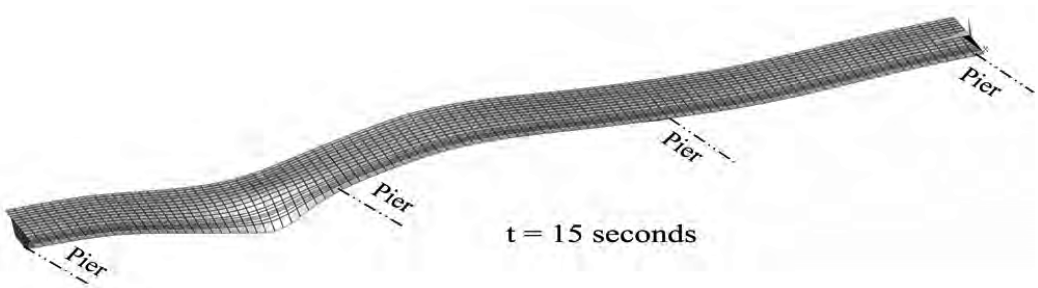

Figure 3.17A: Static Deflection for Vehicle at Cantilever Part (for t =15 sec, V = 40 km/h)

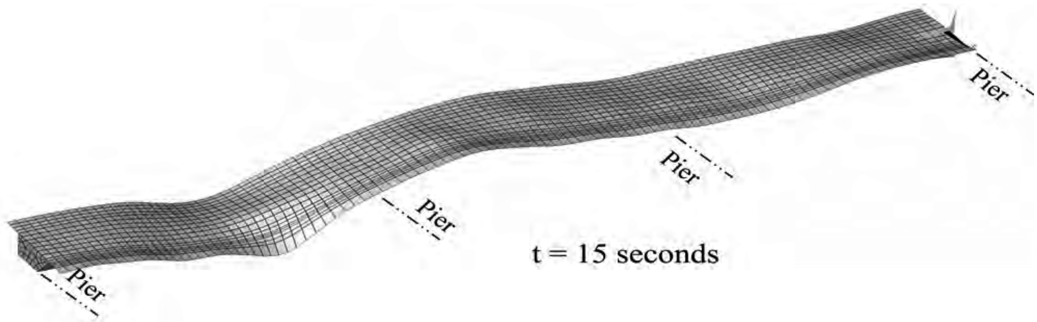

Figure 3.17B: Dynamic Deflection for Vehicle at Cantilever Part at 0% Damping

(for t = 15 sec and V = 40 km/h)

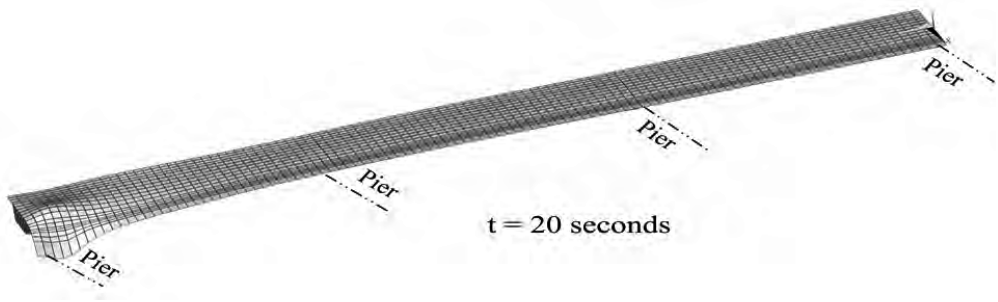

Figure 3.18A: Static Deflection for Vehicle at Cantilever Part (for t = 20 sec, V=40 km/h)

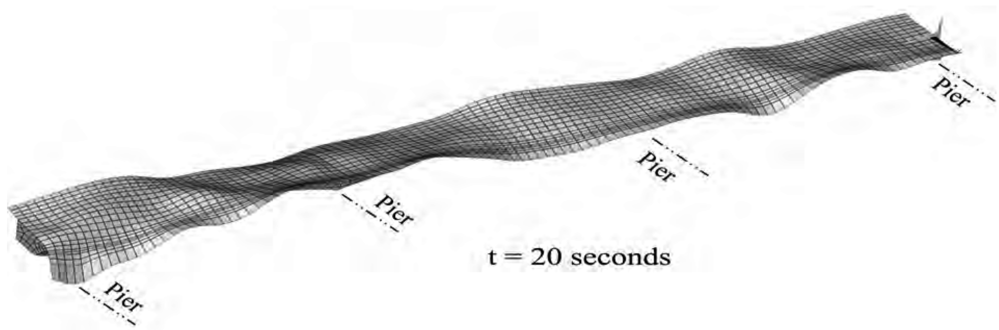

Figure 3.18B: Dynamic Deflection for Vehicle at Cantilever Part at 0% Damping (for t = 20 sec and V = 40 km/h)

3.5.2 Vehicle Position along Centerline of Box Girder Bridge

Deflection over time in static analyses and for 0% damping, deflection over time in full transient dynamic analyses are shown in Figure 3.19A and Figure 3.19B respectively for t = 0 sec at vehicle speed 40 km/h for vehicle path along centerline of box girder bridge.

Deflection over time in static and full transient dynamic analyses for 0% damping are shown in Figure 3.20A and Figure 3.20B respectively for t = 5 sec at vehicle speed 40 km/h for vehicle position along centerline part of box girder bridge.

Deflection over time in static and full transient dynamic analyses for 0% damping are shown in Figure 3.21A and Figure 3.21B respectively for t = 10 sec at vehicle speed 40 km/h for vehicle position along centerline part of box girder bridge.

Deflection over time in static and full transient dynamic analyses for 0% damping are shown in Figure 3.22A and Figure 3.22B respectively for *t* = 15 sec at vehicle speed 40 km/h for vehicle potion along centerline part of box girder bridge.

Deflection over time in static and full transient dynamic analyses for 0% damping are shown in Figure 3.23A and Figure 3.23B respectively for *t* = 20 sec at vehicle speed 40 km/h for vehicle position along centerline part of box girder bridge.

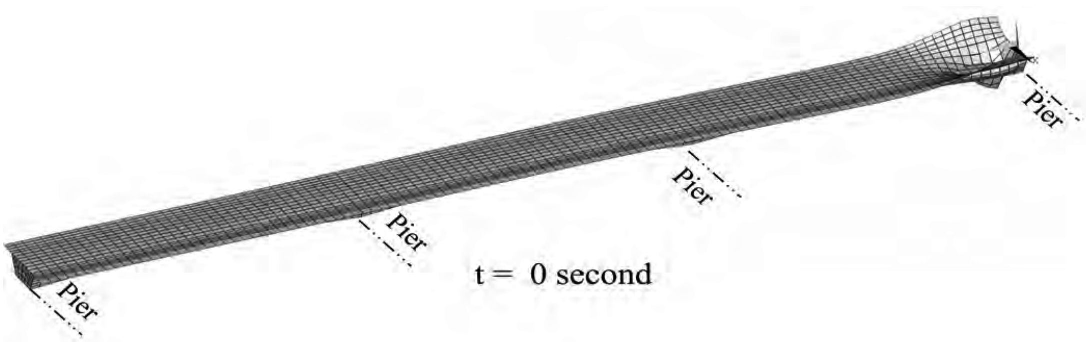

Figure 3.19A: Static Deflection for Vehicle at Centerline (for t=0 sec and V = 40 km/h)

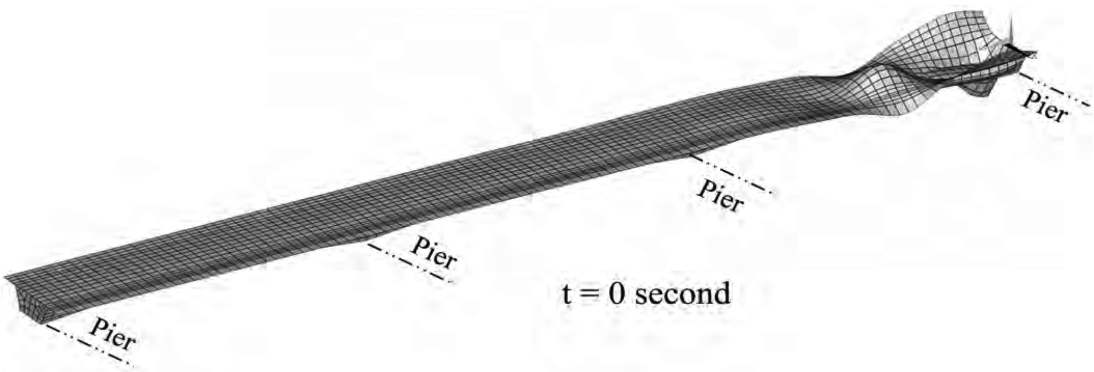

Figure 3.19B: Dynamic Deflection for Vehicle at Centerline at 0% Damping
(for t = 0 sec and V = 40 km/h)

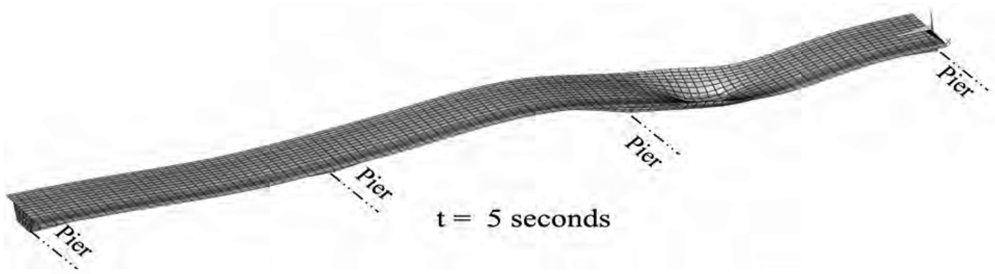

Figure 3.20A: Static Deflection for Vehicle at Centerline (for t=5 sec and V=40 km/h)

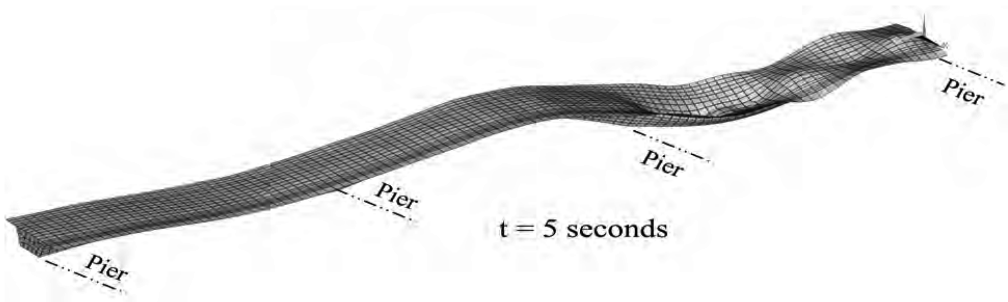

Figure 3.20B: Dynamic Deflection for Vehicle at Centerline at 0% Damping

(for t = 5 sec and V = 40 km/h)

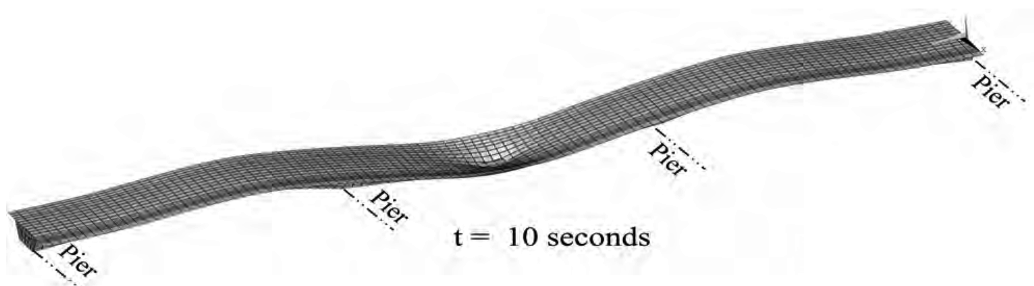

Figure 3.21A: Static Deflection for Vehicle at Centerline (for t=10 sec and V=40 km/h)

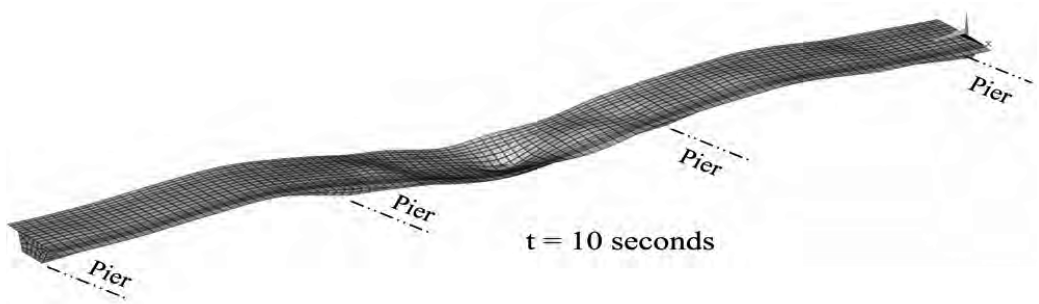

Figure 3.21B: Dynamic Deflection for Vehicle at Centerline at 0% Damping

(for t =10 sec and V = 40 km/h)

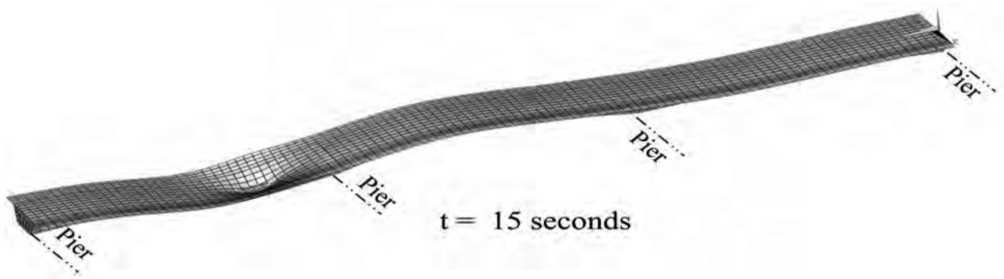

Figure 3.22A: Static Deflection for Vehicle at Centerline (for t=15 sec and V=40 km/h)

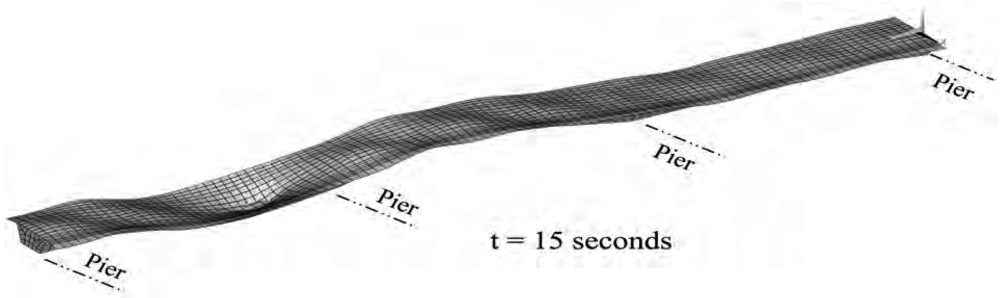

Figure 3.22B: Dynamic Deflection for Vehicle at Centerline at 0% Damping
(for t = 15 sec and V = 40 km/h)

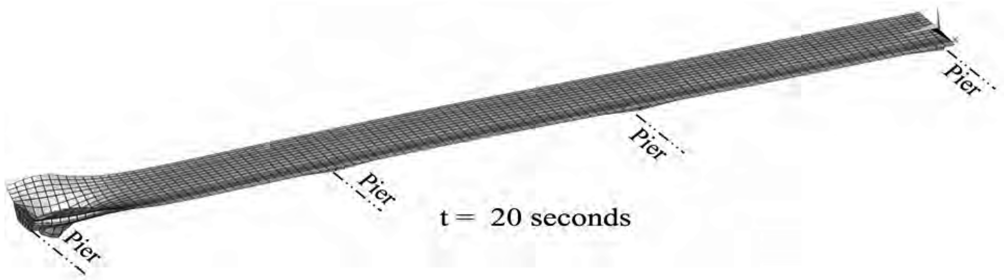

Figure 3.23A: Static Deflection for Vehicle at Centerline (for t=20 sec and V=40 km/h)

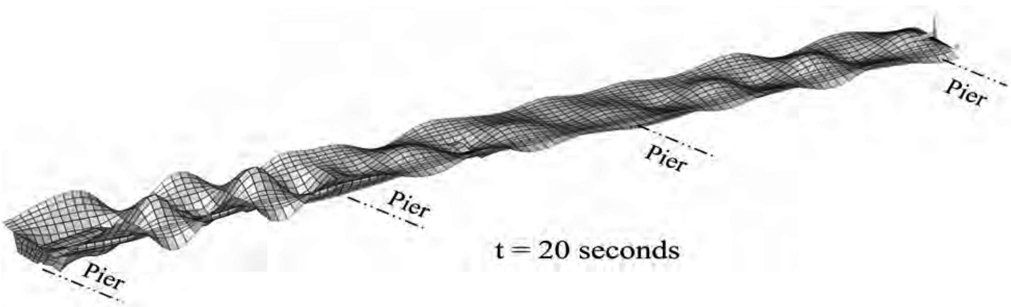

Figure 3.23B: Dynamic Deflection for Vehicle at Centerline at 0% Damping
(for t = 20 sec and V = 40 km/h)

The curves of these figures show that, static vibration is moving over time, while dynamic vibration increases with time and occurs throughout the whole the span. Again, damping effect is also vulnerable for dynamic deflection.

3.6 Total Deflected Shape of Span for Static and Dynamic Analysis

3.6.1 Vehicle Position along Cantilever Part of Box Girder Bridge

The total deflected shape of span for static and for full transient analyses for 75 m span and all the velocities with 0% and 2.5% damping condition is shown in this investigation, when the vehicle is at mid span. In this investigation vehicle load was assumed to move along cantilever part of the box girder bridge. Here, deflection at 1st pier and at middle of mid span of the box girder bridge for both static analysis and dynamic analysis at 0% damping and 2.5% damping are illustrated in this investigation. This study illustrates that deflection for dynamic analysis is more critical than static analysis.

Total deformed shape at the first pier of the middle span for 75 m span and all the velocities are illustrated in Figure 3.24, Figure 3.25A and Figure 3.25B for static and full transient dynamic analyses at 0% and 2.5% damping condition respectively.

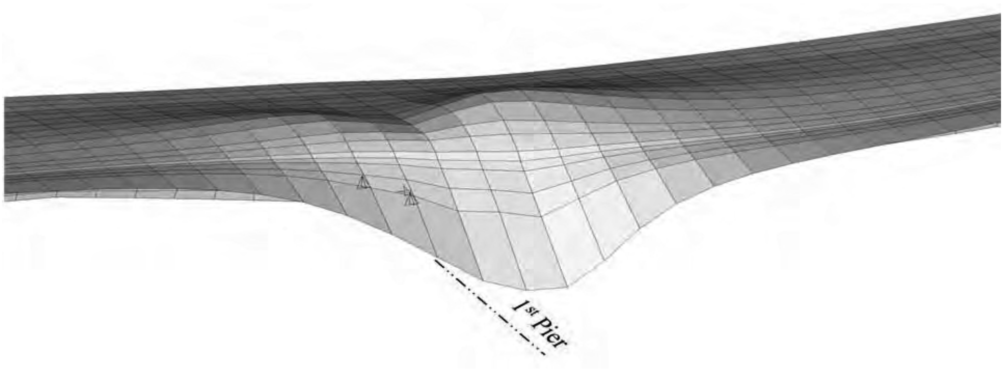

Figure 3.24: Deformed Shape at the First Pier of the Middle Span for Vehicle along cantilever Part of Box Girder Bridge for Static Analysis

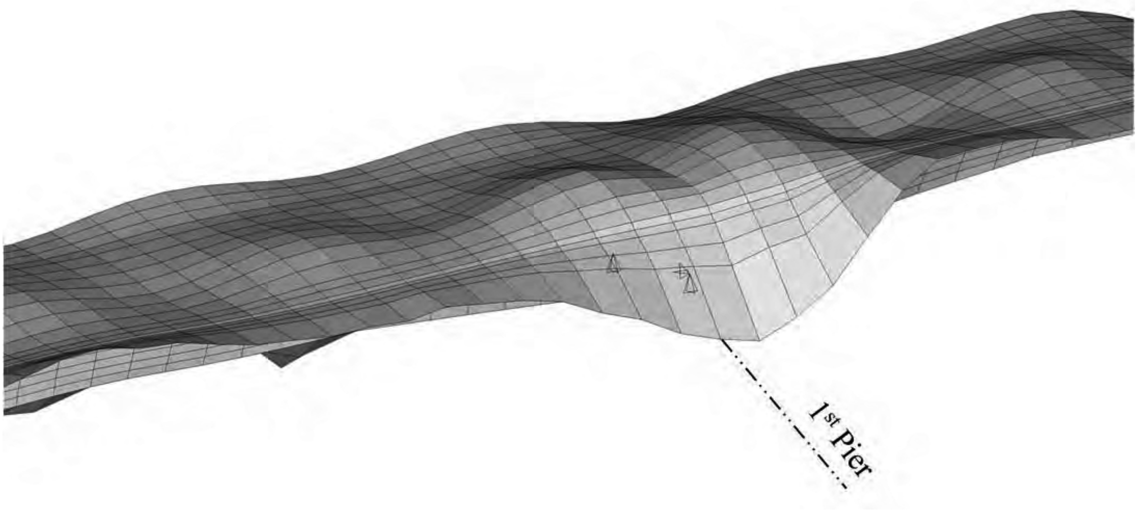

Figure 3.25A: Deformed Shape at the First Pier of the Middle Span for Dynamic Analysis for Vehicle at Cantilever Part of Box Girder Bridge at 0% Damping

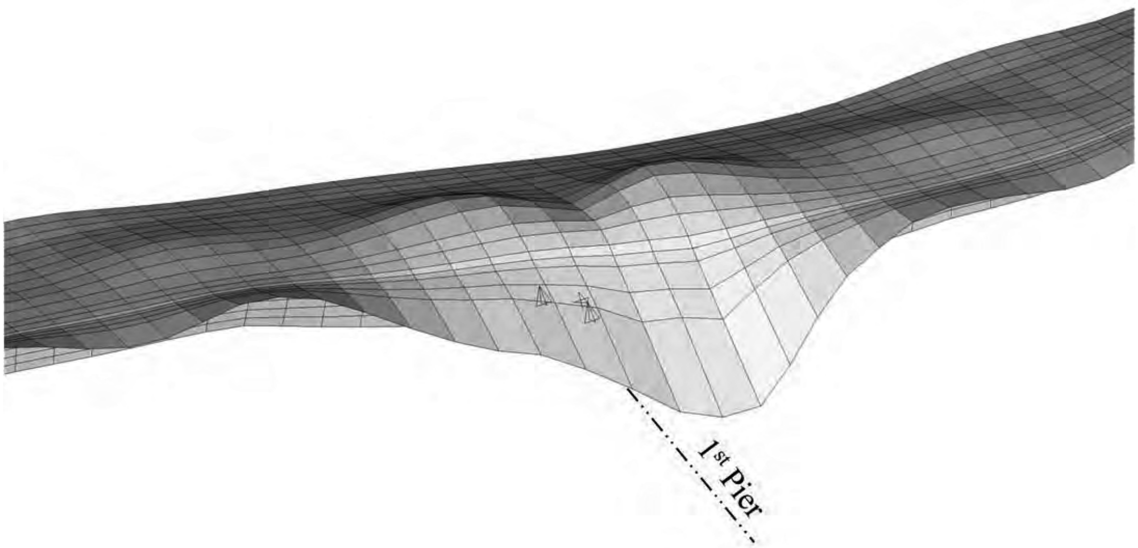

Figure 3.25B: Deformed Shape at the First Pier of the Middle Span for Dynamic Analysis for Vehicle at Cantilever Part of Box Girder Bridge at 2.5% Damping

Deformed shape at midspan of the middle span are illustrated in Figure 3.26, Figure 3.27A and Figure 3.27B for static and full transient dynamic analyses at 0% damping and 2.5% damping condition respectively.

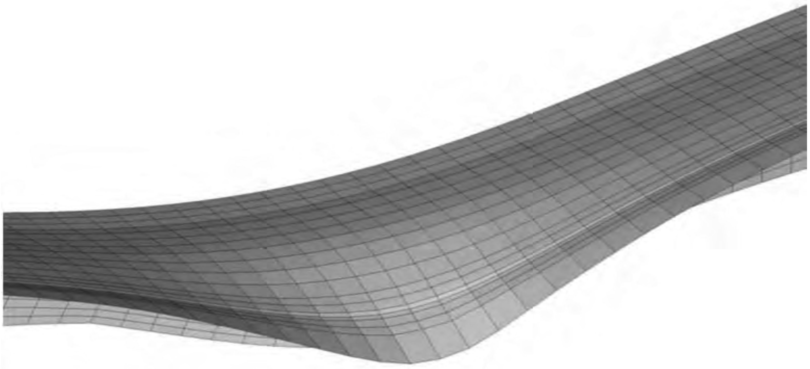

Figure 3.26: Deformed Shape at the Midspan of the Middle Span for Static Analysis for Vehicle at Cantilever Part of Box Girder Bridge

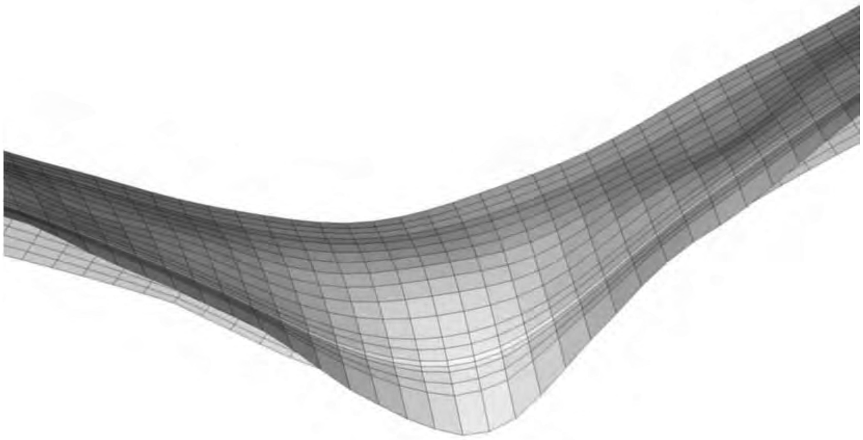

Figure 3.27A: Deformed Shape at the Midspan of the Middle Span for Dynamic Analysis for Vehicle at Cantilever Part of Box Girder Bridge at 0% Damping

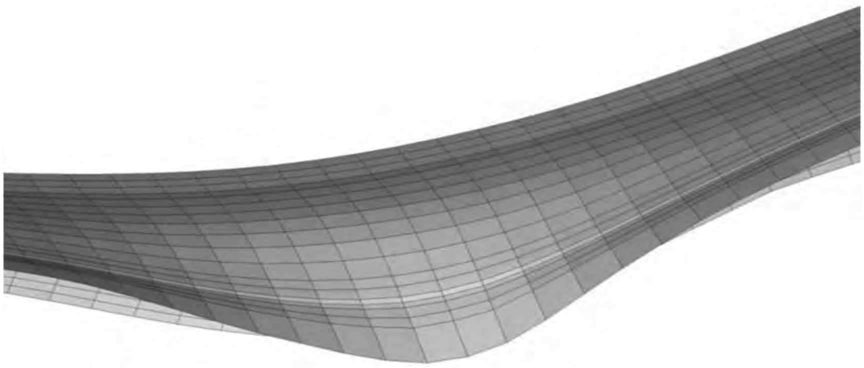

Figure 3.27B: Deformed Shape at the Midspan of the Middle Span for Dynamic Analysis for Vehicle at Cantilever Part of Box Girder Bridge at 2.5% Damping

3.6.2 Vehicle Position along Centerline of Box Girder Bridge

Total deflected shape of span for static and full transient analyses for 75 m span and all the velocities at 0% and 2.5% damping condition are shown in this study when the vehicle is at mid span of centerline of deck slab of box girder bridge. These figures illustrates that deflection for dynamic analysis is more critical than static analysis.

Deformed shape at the first pier of the middle span are illustrated in Figure 3.28 and Figure 3.29A. Figure 3.29B for static and full transient dynamic analyses at 0% and 2.5% damping for vehicle at centerline of deck slab of box girder bridge respectively.

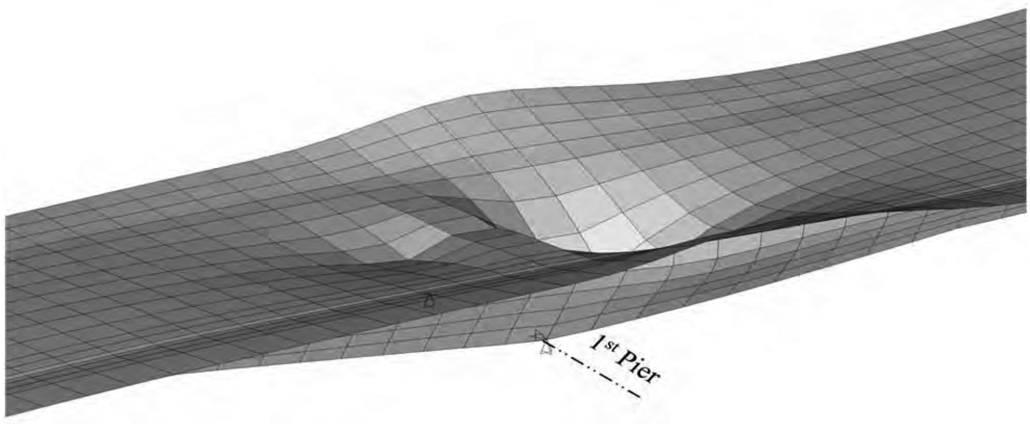

Figure 3.28: Deformed Shape at the First Pier of the Middle Span for Vehicle along cantilever Part of Box Girder Bridge for Static Analysis

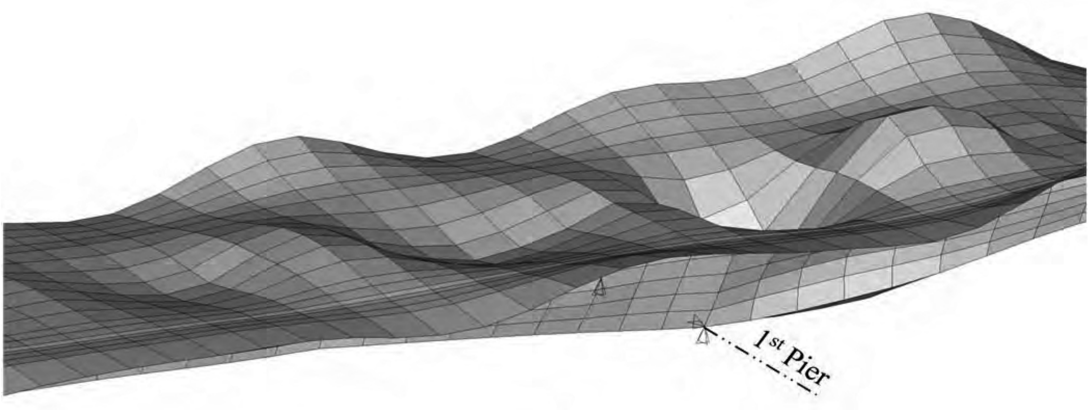

Figure 3.29A: Deformed Shape at the First Pier of the Middle Span for Dynamic Analysis for Vehicle at Cantilever Part of Box Girder Bridge at 0% Damping

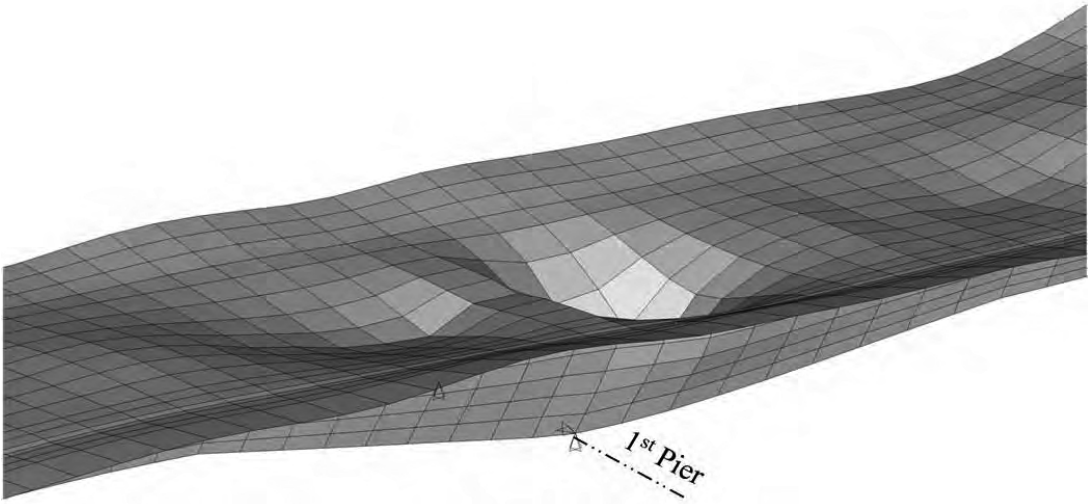

Figure 3.29B: Deformed Shape at the First Pier of the Middle Span for Dynamic Analysis for Vehicle at Cantilever Part of Box Girder Bridge at 2.5% Damping

Deformed shape at midspan of the middle span are illustrated in Figure 3.30 and Figure 3.31A, Figure 3.31B for static and full transient dynamic analyses at 0% and 2.5% damping respectively.

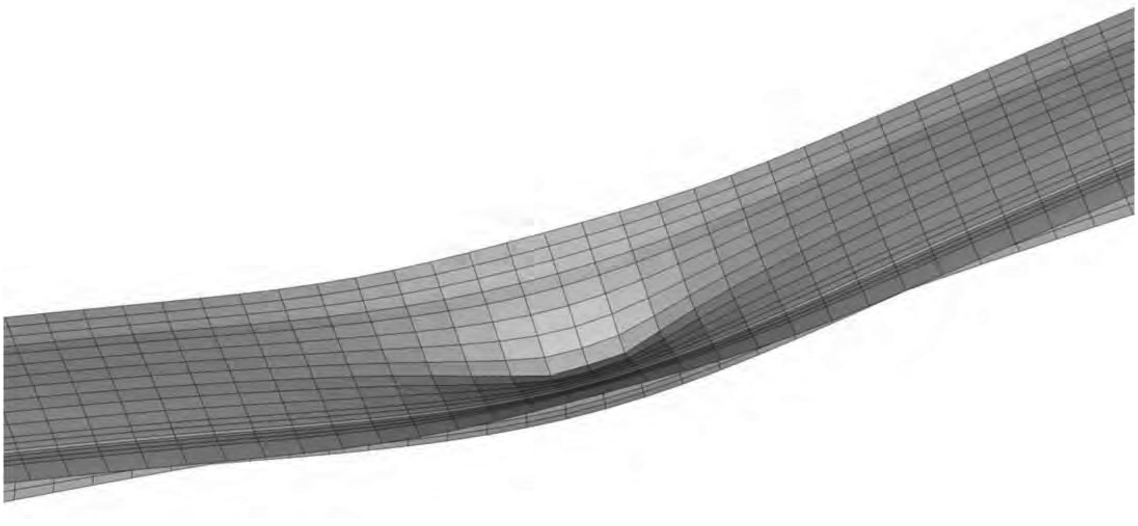

Figure 3.30: Deformed Shape at the Midspan of the Middle Span for Static Analysis for Vehicle at Cantilever Part of Box Girder Bridge

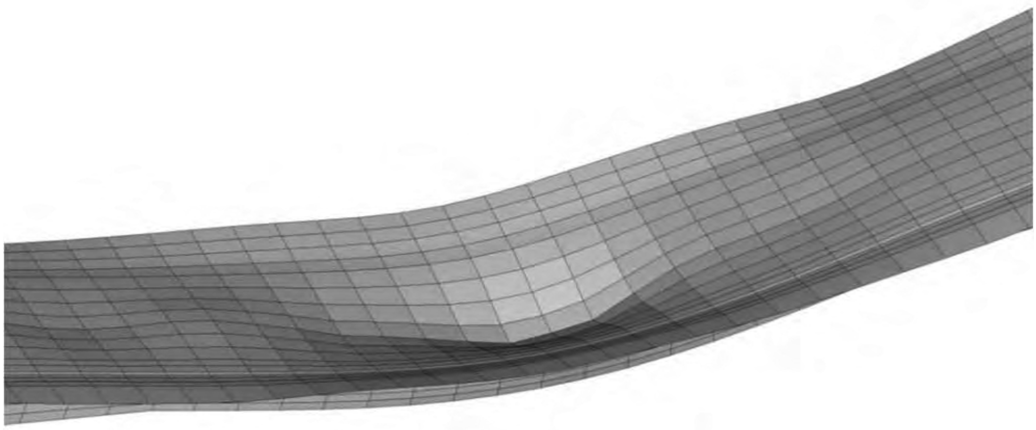

Figure 3.31A: Deformed Shape at the Midspan of the Middle Span for Dynamic Analysis for Vehicle at Cantilever Part of Box Girder Bridge at 0% Damping

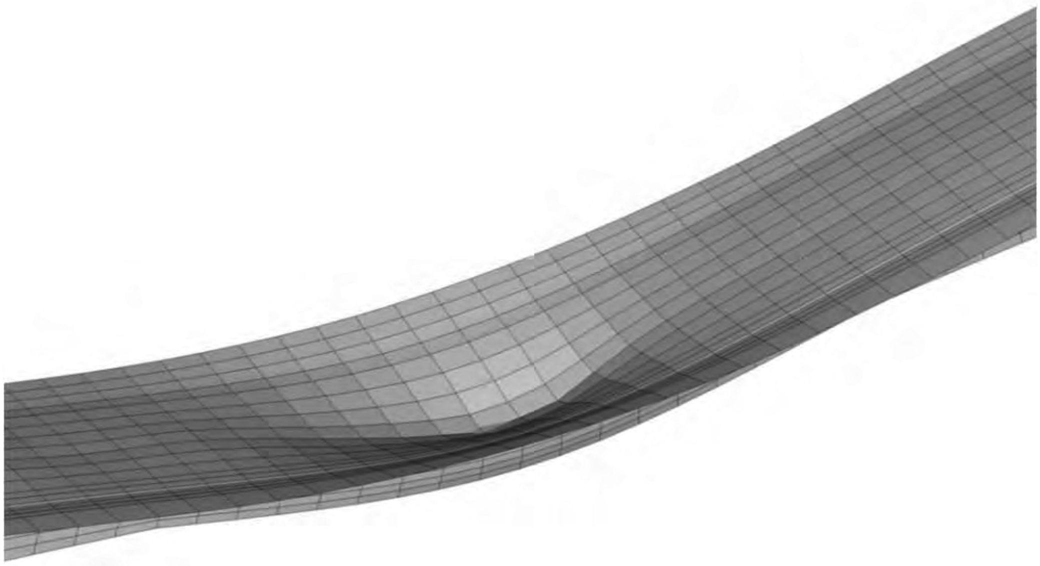

Figure 3.31B: Deformed Shape at the Midspan of the Middle Span for Dynamic Analysis for Vehicle at Cantilever Part of Box Girder Bridge at 2.5% Damping

From these figures of article 3.6, it is observed that, i.e., with damping properties, values show difference from static results. Again, greater damping condition for dynamic analysis shows more similarity to static condition for deflection. 0% damping shows greater difference than 2.5% damping condition from static results and 2.5% damping shows closely similar situation to static condition.

3.7 Calculation of Dynamic Amplification Factor

3.7.1 Calculation of Dynamic Amplification Factor for Stresses

Stresses were measured at some definite nodes (node '*l*' shown in Figure 3.32) a little far from the root of the cantilever. For a particular vehicle speed, vehicle loads were applied at a path parallel to the edge of the cantilever as explained in Article 3.4.1 and stresses were measured for both static and full transient analyses at each of the specific nodes defined for stress measurement. For each position of the vehicle, ratio of dynamic stress to static stress at a particular node was measured. The absolute maximum ratio was taken as the DAF for that particular node.

To avoid fictitious errors, lower values of stresses were ignored for static loading. Only stresses having a magnitude greater than one-fourth of the maximum stress at a node were considered for static loading condition. Otherwise, the ratio of two insignificant small values might be too high and consequently the value of DAF might be found too large.

3.7.2 Calculation of Dynamic Amplification Factor for Deflections

Deflections were measure at some definite points along the tip of the cantilever of the middle span. The deflected shape is shown in Figure 3.32.

i, j and *k* nodes were subjected to deformation of magnitude U_1, U_2 and U_3 respectively. The deformation U_3 consisted of two components: Rigid Body Movement U_4 and Deflection δ.

Geometrically,

$$U_4 = (U_2 - U_1)\frac{L+B}{B} + U_1 \quad \text{……………} \quad (3.1)$$

$$\delta = U_3 - U_4 \quad \text{……………} \quad (3.2)$$

For a particular vehicle speed, vehicle loads were applied at a path parallel to centerline of the bridge in the cantilever part and at centerline of the bridge as explained in Article 3.4.1 and displacements were measured for both static and full transient analyses at each of the specific nodes defined for displacement measurement. By using equation (3.1) and (3.2), the magnitudes of Deflections were obtained at definite nodes at the edge of the cantilever. For each position of the vehicle, ratio of dynamic deflection to static deflection at a particular node was measured by using equation (3.3). The absolute maximum ratio was taken the DAF for that particular node.

$$DAF = \frac{\delta_{DYN}}{\delta_{STATIC}} \qquad \text{……..……… (3.3)}$$

Here, $\delta_{DYN} =$ Deflection for dynamic analysis

and $\delta_{STATIC} =$ Deflection for static analysis

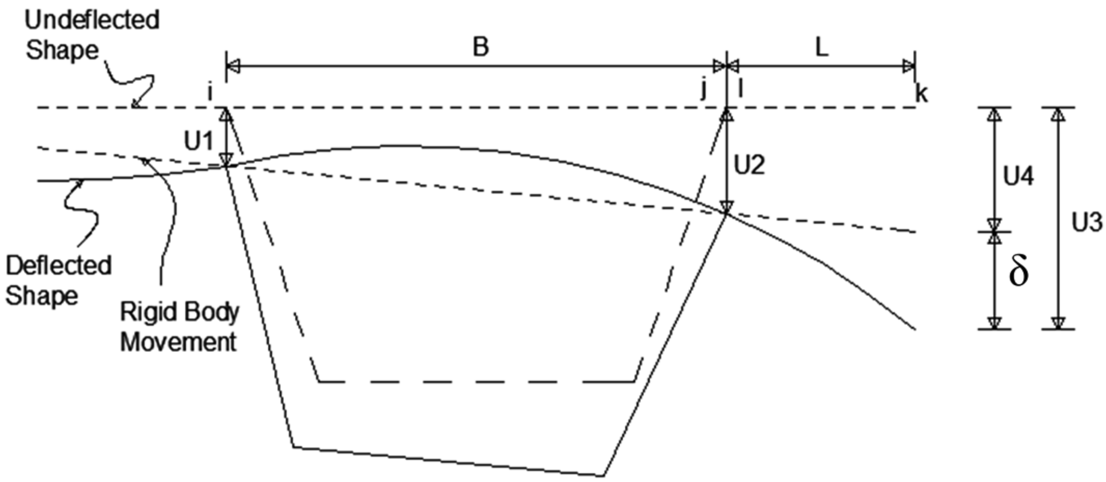

Figure 3.32: Deflected Shape (Cross Section)

To avoid fictitious errors, lower values of deflections were ignored for static loading. Only deflections having a magnitude greater than one-fourth of the maximum deflection at a node were considered for static loading condition. Otherwise, the ratio of two insignificant small values might be too high and consequently the value of DAF might be found too large.

CHAPTER 4

ANALYSIS AND RESULT OF FINITE ELEMENT MODEL

4.1 Introduction

In this chapter, different influencing parameters are investigated numerically for both static and dynamic analyses in order to obtain DAF and have a clear understanding of the effect of different parameters on DAF, based on simulation of bridge vehicle interaction. This analysis was performed to observe the characteristic properties of the dynamic responses for cantilever part of the deck slab and also for centerline of concrete box girder bridge. Purpose of this study is also to analyze the distribution of DAFs for transverse direction throughout the pertaining portion for stress and deflection analysis.

4.2 Development Methodology

Many studies have done for dynamic amplification factor and many definitions of the dynamic amplification factor are used in experimental and numerical studies. Most frequently, the DAF is defined as the ratio of maximum dynamic response to maximum static response. The definition suggested in this study is more appropriate for deck slabs and to determine DAF as peak dynamic effect, $R_{DYN_{MAX}}$ for a given vehicle path divided by the peak static effect, $R_{STATIC_{MAX}}$ from the envelope for all vehicle paths i.e.

$$DAF = \frac{R_{DYN_{MAX}}}{R_{STATIC_{MAX}}}$$

Here, static and dynamic responses were measured for stress at transverse and deflection at vertical direction at nodes throughout the middle span for all vehicle paths to get DAF.

4.3 Numerical Analysis

4.3.1 Static Analysis

Static analysis is carried out to identify the effects in cantilever part of deck slab due to static traffic loading for 3 different velocities. Vertical deflection was measured at the tip of cantilever at mid span of bridge and transverse stress was measured at a particular location at mid span of cantilever for 80, 120 and 160 km/hr velocity. Figure 4.1 and 4.2 illustrate static response for deflection at the tip and for stresses in the transverse direction at 1m from the root of cantilever for 160 km/hr respectively. Static response for deflection and stress for 80 and 120 km/hr are summarized in Appendix A (Fig A1, A2, A5, A6).

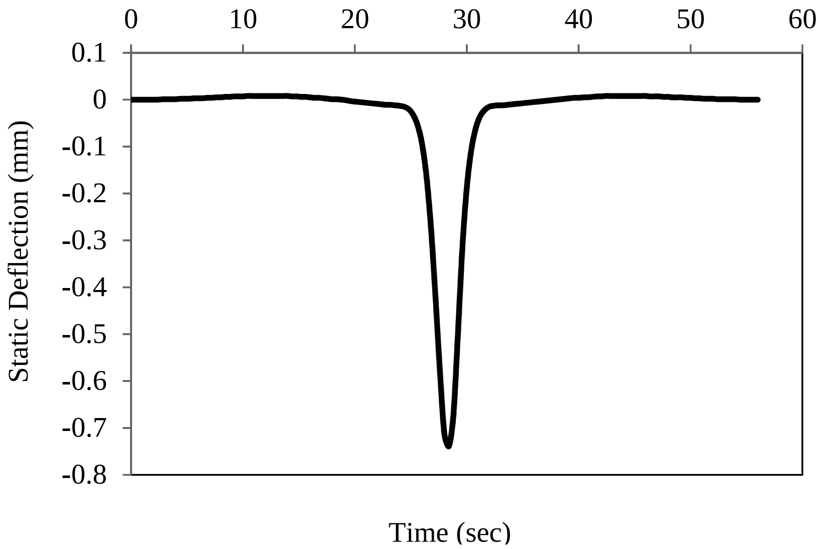

Figure 4.1: Static Response of Vertical Deflection at the Tip of the Cantilever of Mid Span at Vehicle Speed 160 km/h

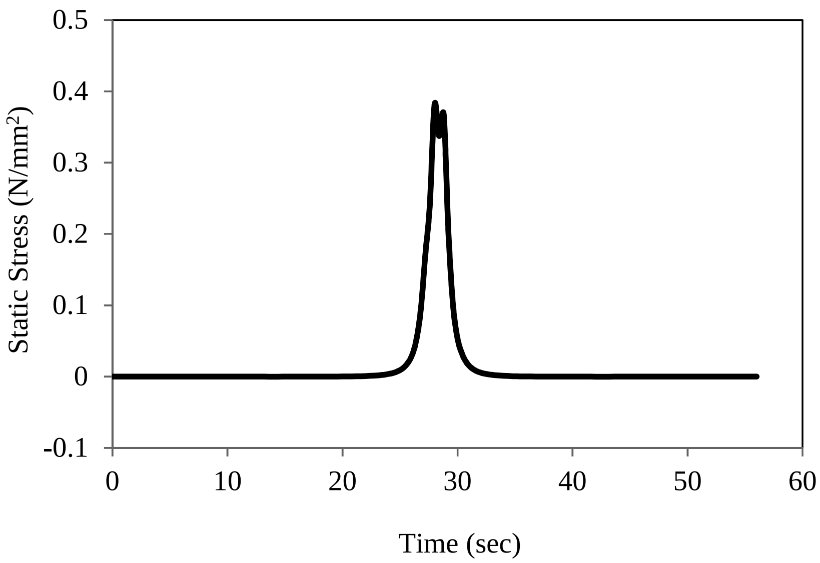

Figure 4.2: Static Response of Transverse Stress at the Root of the Cantilever of Mid Span at Vehicle Speed 160 km/h

4.3.2 Full Transient Dynamic Analysis

Full transient dynamic analysis was carried out to identify the effects in the box girder bridge due to forced vibration. The vertical deflection was measured at the tip of the cantilever in the mid span of the bridge and the transverse stress was measured at a particular location in the mid span of the cantilever part for 3 different vehicular speeds.

Vehicle wheel load was applied as point loads at every node of its path for a particular time. At each step the dynamic equilibrium between the vehicle and the bridge was solved. Forced vibration was analyzed for 141 load steps with each load step divided into 20 sub steps. Figure 4.3 and 4.4 illustrate the time history dynamic responses for the deflection at the tip and the time history dynamic responses for stresses in the transverse direction at a particular point a little far from the root of the cantilever for 160 km/hr respectively. Time history dynamic responses for deflections and stresses for 80 km/hr and 120 km/hr are summarized in Appendix A (Fig A3, A4, A7, A8).

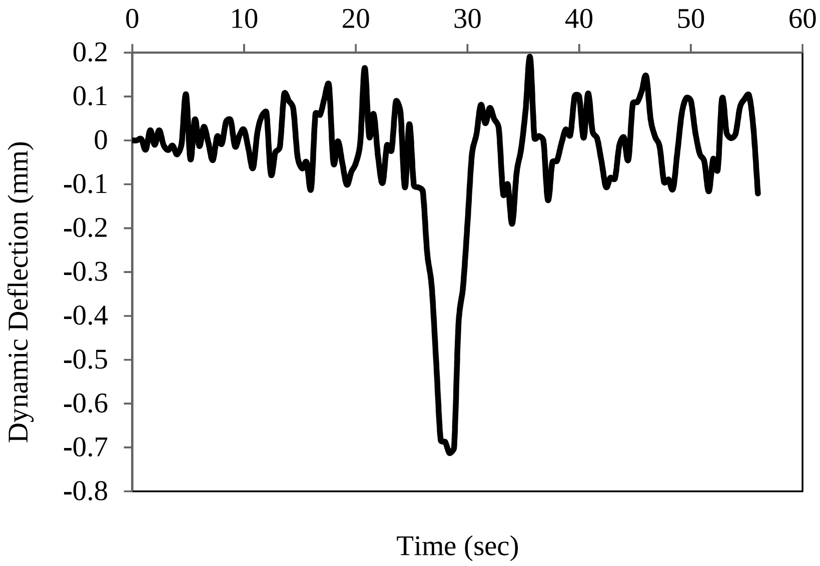

Figure 4.3: Dynamic Response of Vertical Deflection at the Tip of the Cantilever of Mid Span at Vehicle Speed 160 km/h

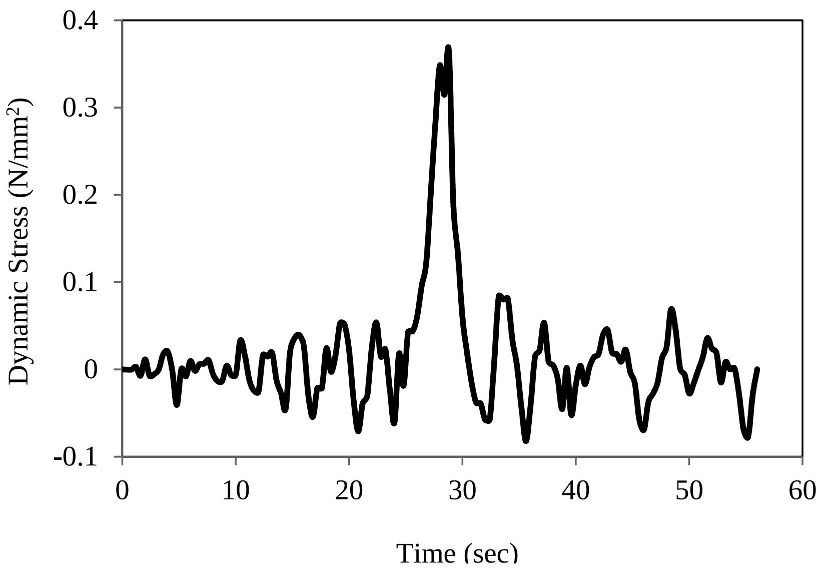

Figure 4.4: Dynamic Response of Transverse Stress at the Root of the Cantilever of Mid Span at Vehicle Speed 160 km/h

In figure 4.1 and 4.2 of previous article 4.3.1, it is shown that for static responses, stress and deflection values at mid section of mid span of three span bridge are zero at times when vehicle moves along another portion rather than mid section of mid span. But when the vehicle is at mid section, then the graph shows some value for stress and deflection.

Again, in figure 4.3 and 4.4 of article 4.3.2, it is observed that for dynamic responses, stress and deflection values at mid section of mid span of three span bridge are zero at times when the vehicle moves along another portion rather than mid section of mid span. But it shows some vibration through the graph though the values are zero as vibration occurs in the bridge span for dynamic effect. Again, when the vehicle is at mid section, then the graph shows some value for stress and deflection along with vibration.

4.4 Parametric Analysis

Parameters involved in the study of the cantilever part and centerline part of any kind of bridges are span length, slab thickness, deck height, slab width and of course vehicle speed. Investigation was done for a particular parameter considering that other parameters are constant i.e. median value. Thus a thorough parametric study was carried out for determining dynamic amplification factor. In the next article numerical results of dynamic amplification factor and parametric influence will be described.

4.5 Parametric Results

A postprocessor has been developed to aid the analysis of the simulation results graphically for two different vehicle positions along the box girder bridge. Results were picked at various nodes along the middle span of the bridge for three different damping conditions, i.e. 0%, 2.5% and 5% damping.

4.5.1 Variation along the Length of Middle Span for Different Span Length

This study has been done for two different vehicle positions along the box girder bridge. One path of vehicle wheel is along the cantilever part of the box girder bridge which is at a fixed distance from the edge of cantilever part of the bridge. Another path of vehicle wheel load is along the centerline of the box girder bridge. Three damping conditions, i.e. 0% damping, 2.5% damping and 5% damping conditions are also considered for both wheel positions along the cantilever part of the bridge and centerline of the bridge. The simulations were carried out for 7 different vehicular speeds for 5 different span lengths. Maximum DAF was obtained for each span length at a particular vehicle speed within the 7 different vehicular speeds. Graphical representations of the maximum DAF for both deflections and stresses for each span length at particular vehicular speed are shown in figure 4.5 through 4.19. Similar graphs of other vehicular speed are represented in Appendix B.

4.5.1.1 Variation along the Length of Middle Span for Wheel Position along Cantilever Part of Box Girder Bridge

4.5.1.1.1 Variation along the Length of Middle Span for Vertical Deflections

The variations of DAF, for vertical deflections at the tip of the cantilever at different points along the middle span for wheel position along the cantilever part of the box girder bridge for 0%, 2.5% and 5% damping conditions are shown in Figure 4.5 through Figure 4.9.

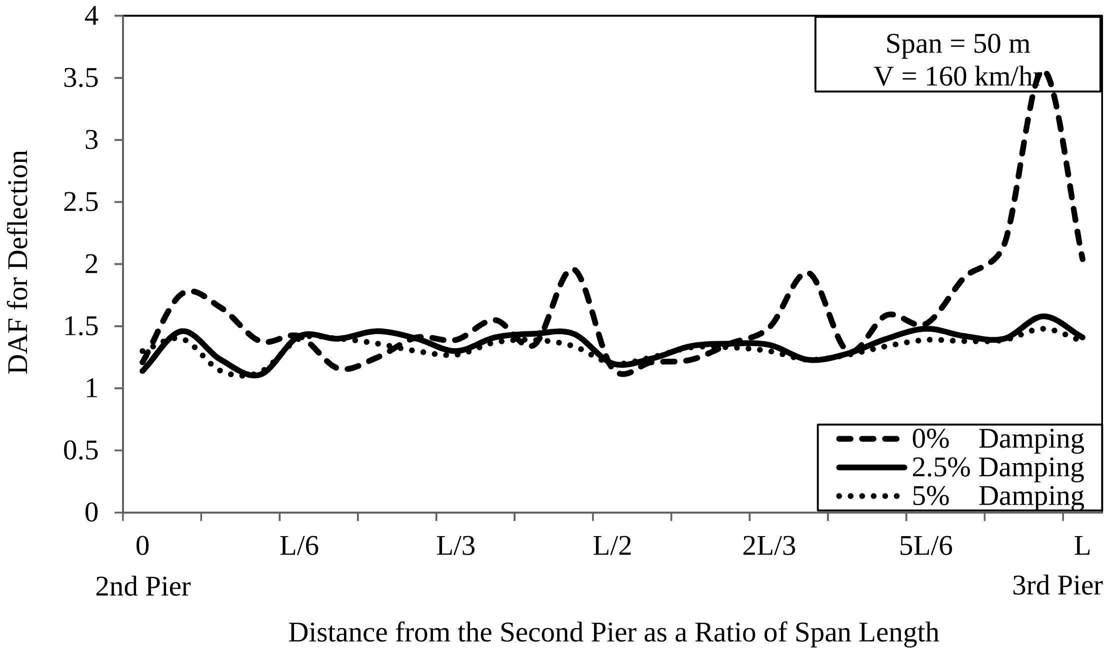

Figure 4.5: Variation of Dynamic Amplification Factor for Deflections along the Length of the Middle Span at Vehicle Speed = 160 km/h and for Span Length = 50 m

Figure 4.5 illustrates the variation of DAF for deflections along the length of middle span among three spans of the box girder bridge for 50 m span length and vehicle speed 160 km/h. Minimum DAF was found to appear at a distance 5L/24 and L/2 from 2nd pier for 0% damping and that was at a distance L/8 from 2nd pier for 2.5% and 5% damping; whereas maximum DAF occurred at a distance 23L/24 from 2nd pier for three damping conditions. The range varied from 1.16~3.56, 1.11~1.58 and 1.13~1.48 for 0%, 2.5% and 5% damping respectively. So, the overall range for DAF is 1.11~3.56. However, if we exclude 0% damping from our consideration, then the range is 1.11~1.58 for 2.55 and 5% damping.

Figure 4.6 illustrates the variation of DAF, for deflections for 75 m span length and vehicle speed 100 km/h. Minimum DAF was found to appear at a distance 35L/36, 17L/18 from 2nd pier for 0% and 2.5% damping respectively and that was at several distances from 2nd pier for 5% damping. Maximum DAF occurred at a distance 11L/12, 8L/9 and L/18 from 2nd pier for 0%, 2.5% and 5% damping respectively. The range varied from 0.81~3.09, 1.01~1.52 and 1.02~1.34 for 0%, 2.5% and 5% damping respectively. So, the overall range for DAF is 0.81~3.09. However, if we exclude 0% damping from our consideration, then the range is 1.01~1.52 for 2.5% and 5% damping.

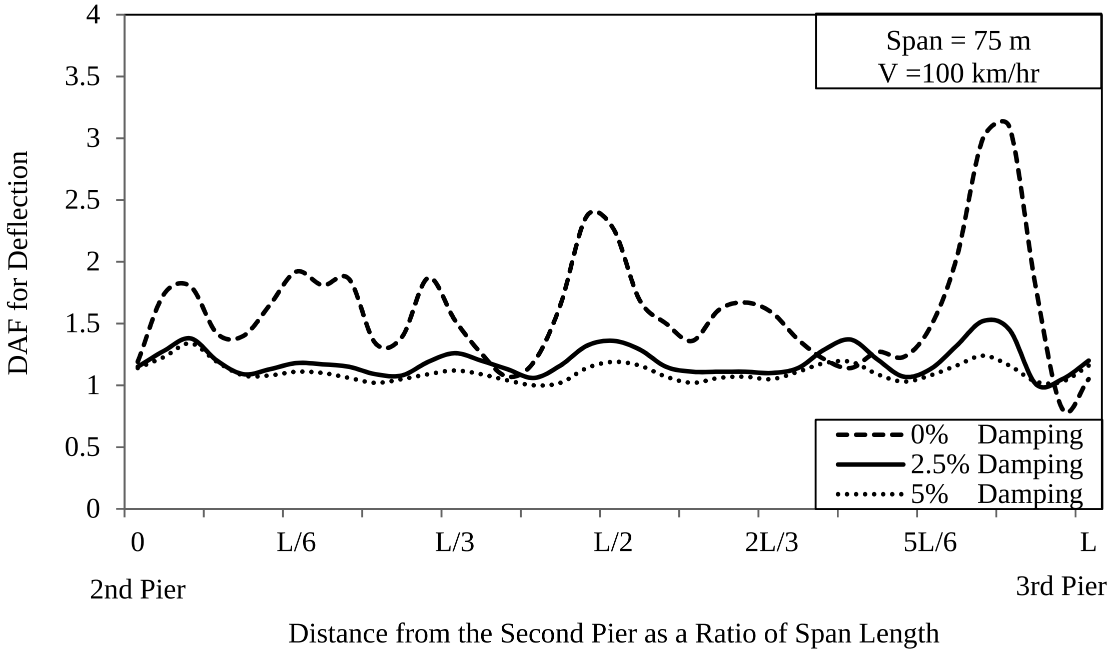

Figure 4.6: Variation of Dynamic Amplification Factor for Deflections along the Length of the Middle Span at Vehicle Speed = 100 km/h and for Span Length = 75 m

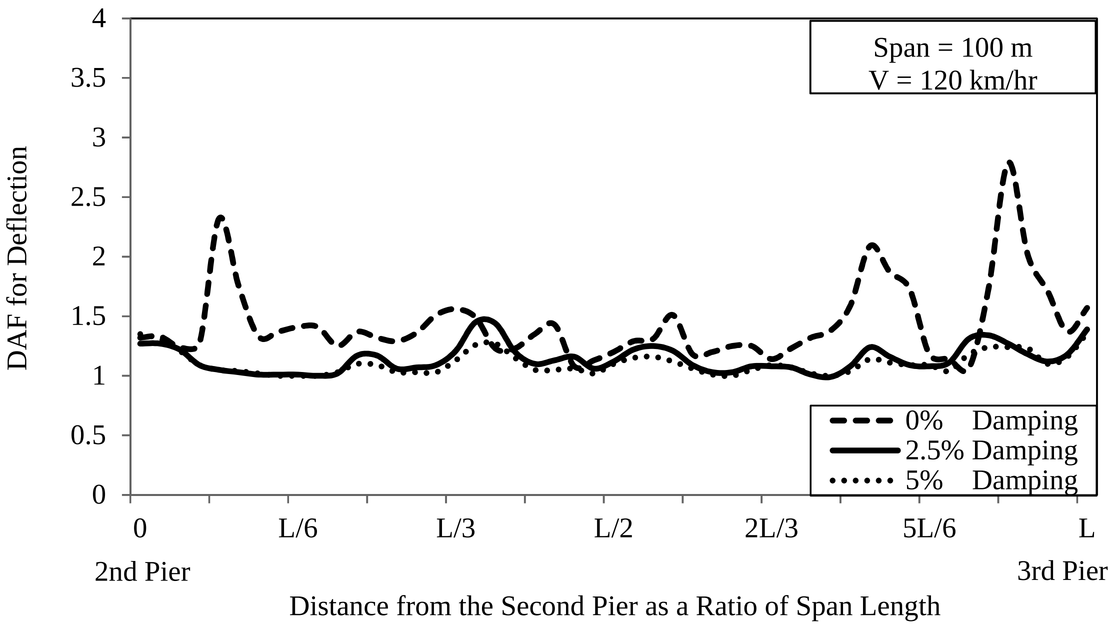

Figure 4.7: Variation of Dynamic Amplification Factor in terms of Deflections along the Length of the Middle Span at Vehicle Speed = 120 km/h and for Span Length = 100 m

Figure 4.7 illustrates the variation of DAF for deflections for 100 m span length and vehicle speed 120 km/h. Minimum DAF was found to appear at a distance 7L/8 and 35L/48 from 2nd pier for 0% and 2.5% damping respectively and that was at several distances from 2nd pier for 5% damping; whereas maximum DAF occurred at a distance 11L/12, 17L/48 from 2nd pier and at 3rd pier for 0%, 2.5% and 5% damping respectively. The range varied from 1.06~2.79, 0.99~1.45 and 1.00~1.36 for 0%, 2.5% and 5% damping respectively. So, the overall range for DAF is 0.99~2.79. However, if we exclude 0% damping from our consideration, then the range is 0.99~1.45 for 2.5% and 5% damping.

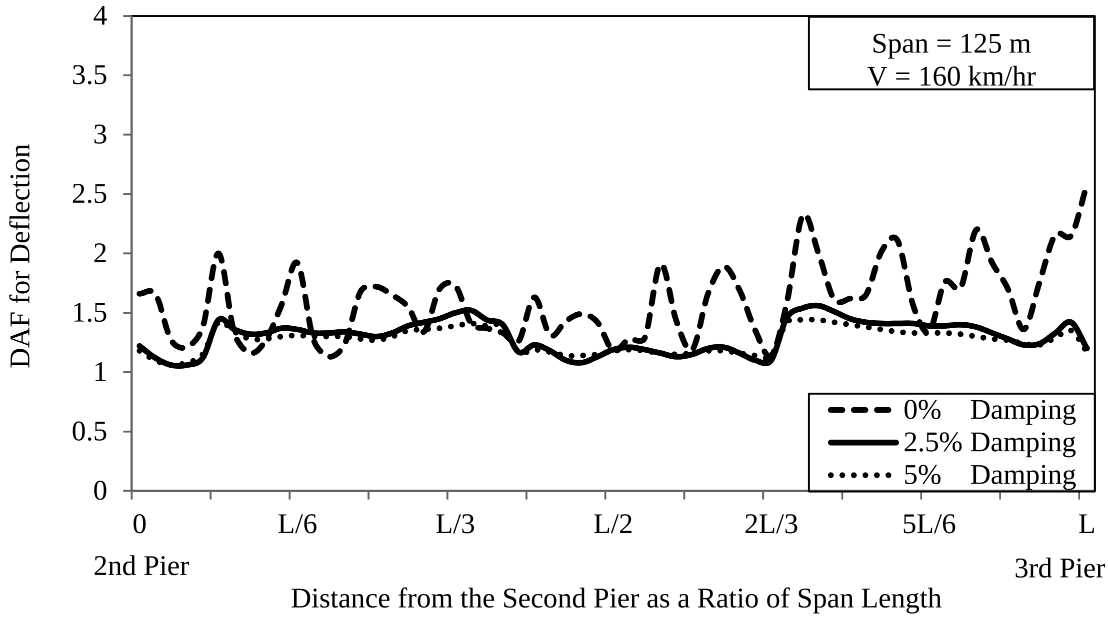

Figure 4.8: Variation of Dynamic Amplification Factor for Deflections along the Length of the Middle Span at Vehicle Speed = 160 km/h and for Span Length = 125 m

Figure 4.8 illustrates the variation of DAF for deflections, along the length of middle span among the three spans of the box girder bridge for 125 m span length and vehicle speed 160 km/h. Minimum DAF was found to appear at a distance L/5 from 2nd pier for 0% damping, L/30 and L/20 from 2nd pier for 2.5% damping and L/30 from 2nd pier for 5% damping; whereas maximum DAF occurred at 3rd pier and at a distance 43L/60 from 2nd pier for 0% and 2.5% damping respectively and that was at a distance 7L/10 and 43L/60 from 2nd pier for 5% damping. The range varied from 1.13~2.58, 1.06~1.56 and 1.06~1.44 for 0%, 2.5% and 5% damping respectively. So, the overall range for DAF is 1.06~2.58.

However, if we exclude 0% damping from our consideration, then the range is 1.06~1.56 for 2.5% and 5% damping.

Figure 4.9 illustrates the variation of DAF for deflections for 150 m span length and vehicle speed 160 km/h. Minimum DAF was found to appear at a distance 13L/36 and L/24 from 2nd pier for 0% and 2.5% damping respectively and that was at L/36 and L/24 from 2nd pier for 5% damping; whereas maximum DAF occurred at a distance L/3 from 2nd pier for 0% damping and that was at a distance 25L/72 from 2nd pier for both 2.5% and 5% damping. The range varied from 1.03~2.34, 1.03~1.55 and 1.05~1.44 for 0%, 2.5% and 5% damping respectively. So, the overall range for DAF is 1.03~2.34. However, for 2.5% and 5% damping excluding 0% damping, then the range is 1.03~1.55.

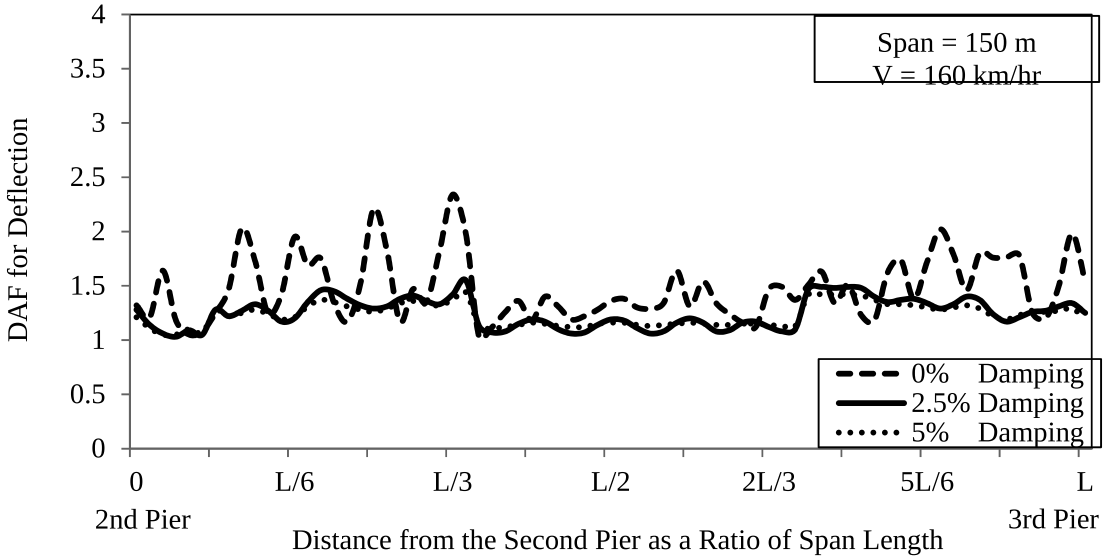

Figure 4.9: Variation of Dynamic Amplification Factor for Deflections along the Length of the Middle Span at Vehicle Speed = 160 km/h and for Span Length = 150 m

Hence, there were little similarities observed in the shape of the curves. In most of the points, the values of the DAF for deflections were greater than unity unlike that measured in terms of stresses. Arbitrary variations were observed along the length of the middle span for all vehicle speeds. Therefore, as a whole DAF for deflections, ranged from 0.81~3.56 for 0%, 2.5% and 5% damping consideration and 0.99~1.58 for 2.5% and 5% damping excluding 0% damping for vehicle speed and span length variation analysis with respect to results at different nodes along the middle span and for wheel position along the cantilever part of the box girder bridge.

4.5.1.1.2 Variation along the Length of Middle Span for Stresses

The variations of the DAF for stresses at some distances from the edge of the cantilever at different points along the middle span among the three spans and for wheel position along the cantilever part of the box girder bridge for 0%, 2.5% and 5% damping conditions are shown in Figure 4.10 through Figure 4.14.

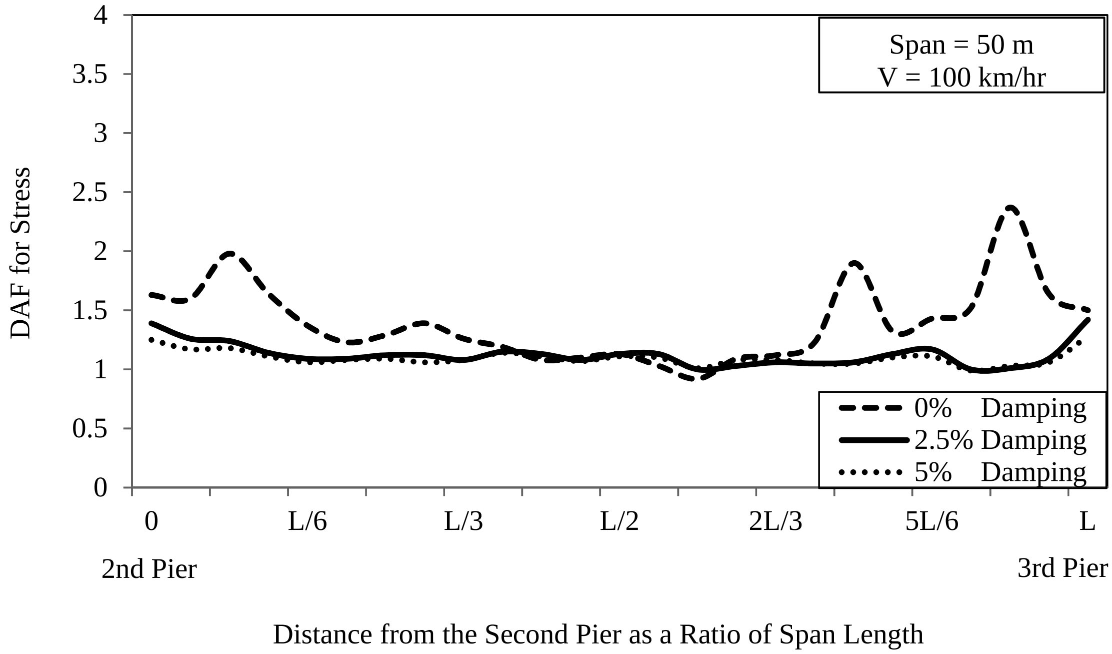

Figure 4.10: Variation of Dynamic Amplification Factor for Stresses along the Length of the Middle Span at Vehicle Speed = 100 km/h and for Span Length = 50 m

Figure 4.10 illustrates the variation of DAF, for stresses at some distances from the edge of the cantilever along the length the middle span for 50 m span length and vehicle speed 100 km/h. Minimum DAF was found to appear at a distance 7L/12 from 2nd pier for the three damping conditions and for 2.5% damping, that was also found at a distance 7L/8 from 2nd pier; whereas maximum DAF occurred at a distance 11L/12 from 2nd pier for 0% damping and that was at 3rd pier for both 2.5% and 5% damping. The range varied from 0.92~2.37, 1.00~1.42 and 1.01~1.28 for 0%, 2.5% and 5% damping respectively. So, the overall range for DAF is 0.92~2.37. However, if we exclude 0% damping from our consideration, then the range is 1.00~1.42 for 2.5% and 5% damping.

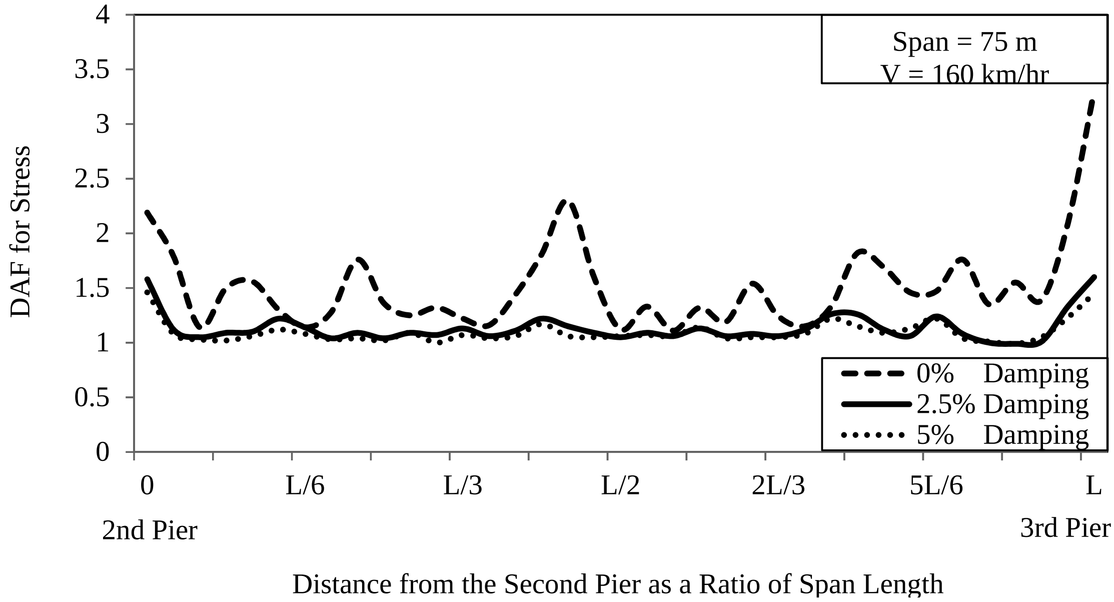

Figure 4.11: Variation of Dynamic Amplification Factor for Stresses along the Length of the Middle Span at Vehicle Speed = 160 km/h and for Span Length = 75 m

Figure 4.11 illustrates variation of DAF for stresses at some distances from the edge of cantilever along the length of middle span for 75 m span length and vehicle speed 160 km/h. Minimum DAF was found to appear at a distance 5L/9 from 2nd pier for 0% damping and that was at a distance 11L/12 from 2nd pier for 2.5% and 5% damping; whereas maximum DAF occurred at 3rd pier for 0% and 2.5% damping and at 2nd for 5% damping. The range varied from 1.11~3.3, 0.99~1.6 and 0.99~1.46 for 0%, 2.5% and 5% damping respectively. So, overall range for DAF is 0.99~3.3. However, if we exclude 0% damping from consideration, then the range is 0.99~1.6 for 2.5% and 5% damping.

Figure 4.12 illustrates the variation of DAF, for stresses at some distances from the edge of the cantilever along the length the middle span for 100 m span length and vehicle speed 160 km/h. Minimum DAF was found to appear at a distance 7L/8 from 2nd pier for 0% damping and that was found at a distance L/12 from 2nd pier for 2.5% and 5% damping; whereas maximum DAF occurred at a distance 47L/48 from 2nd pier for the three damping conditions. The range varied from 0.95~2.00, 0.97~1.3 and 0.99~1.21 for 0%, 2.5% and

5% damping respectively. So, the overall range for DAF is 0.95~2.00. However, for 2.5% and 5% damping excluding 0% damping, the range is 0.97~1.3.

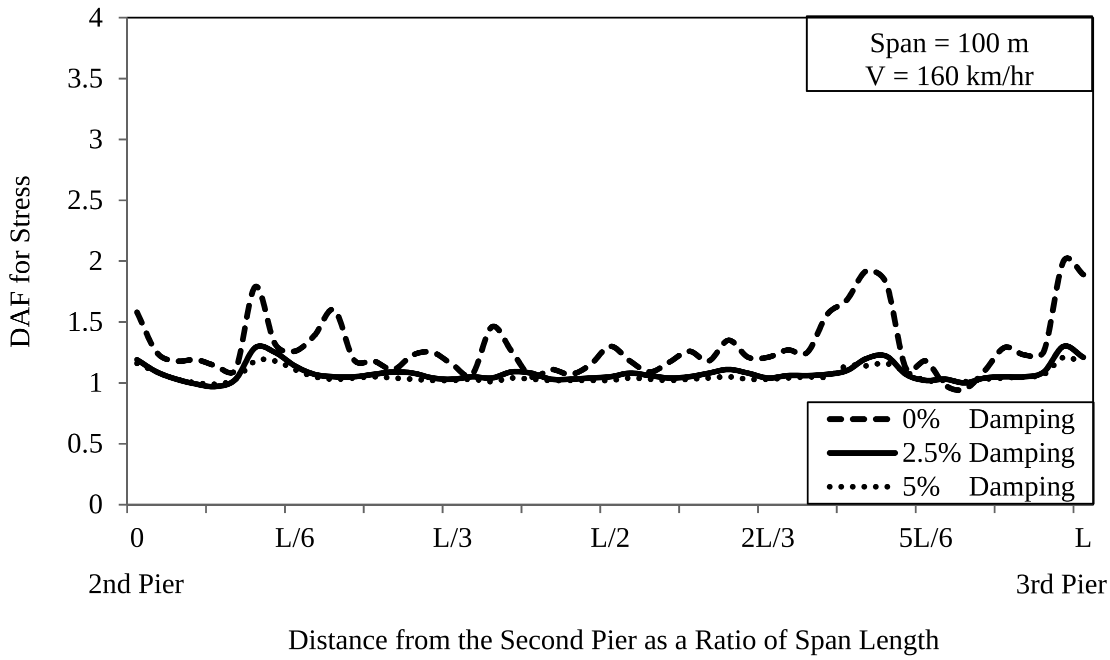

Figure 4.12: Variation of Dynamic Amplification Factor for Stresses along the Length of the Middle Span at Vehicle Speed = 160 km/h and for Span Length = 100 m

Figure 4.13 illustrates the variation of DAF, for stresses at some distances from the edge of the cantilever along the length the middle span for 125 m span length and vehicle speed 160 km/h. Minimum DAF was found to appear at a distance L/15 from 2nd pier for 0% damping and that was occurred at a distance 19L/60 from 2nd pier for 2.5% and 5% damping; whereas maximum DAF occurred at 3rd pier for 0% damping and that was at a distance 59L/60 from 2nd pier for both 2.5% and 5% damping. The range varied from 0.95~2.68, 1.01~1.25 and 1.01~1.21 for 0%, 2.5% and 5% damping respectively. So, the overall range for DAF is 0.95~2.68. However, for 2.5% and 5% damping excluding 0% damping, the range is 1.01~1.25.

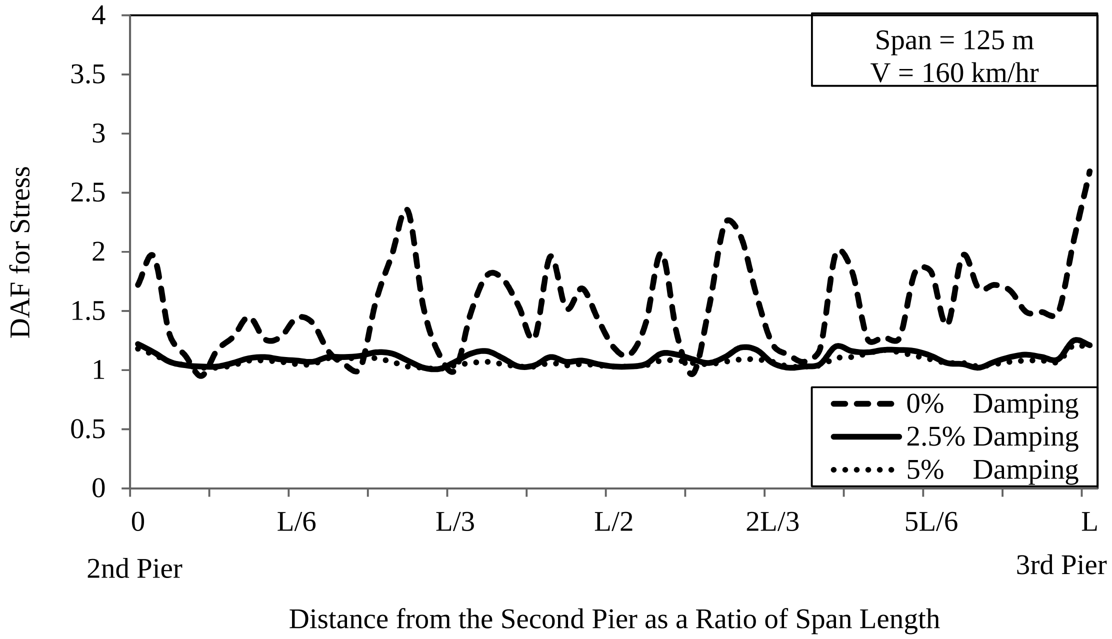

Figure 4.13: Variation of Dynamic Amplification Factor in terms of Stresses along the Length of the Middle Span at Vehicle Speed = 160 km/h and for Span Length = 125 m

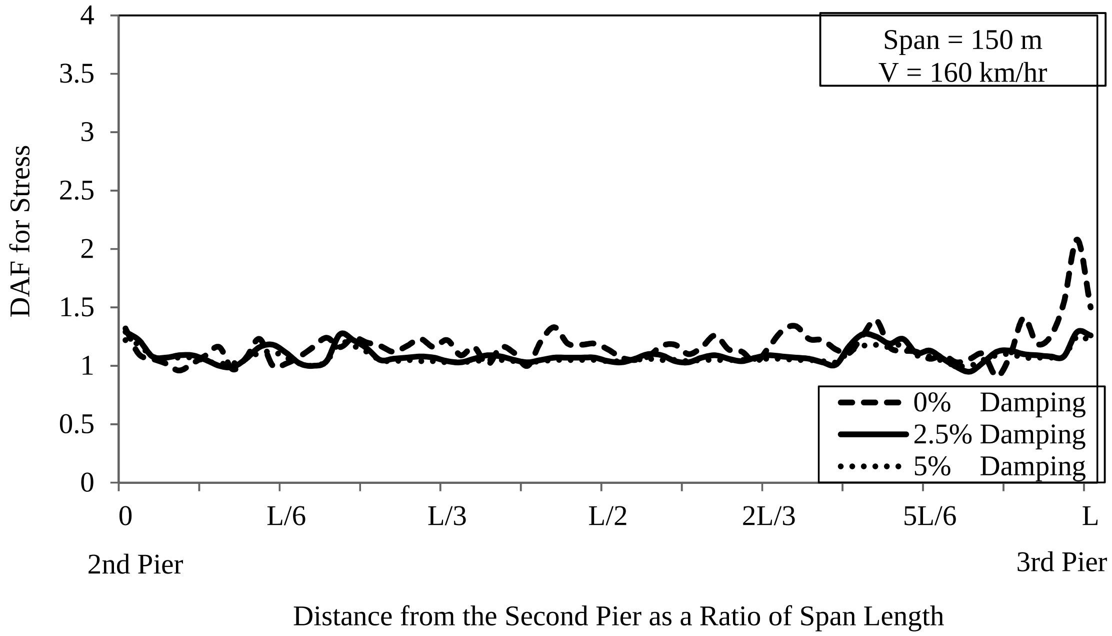

Figure 4.14: Variation of Dynamic Amplification Factor for Stresses along the Length of the Middle Span at Vehicle Speed = 160 km/h and for Span Length = 150 m

Figure 4.14 illustrates variation of DAF for at some distances from the edge of cantilever along the length the middle span for 150 m span length and vehicle speed 160 km/h.

Minimum DAF was found to appear at a distance 65L/72 and 7L/8 from 2nd pier for 0% and 2.5% damping and for 5% damping, that was found at several distances; whereas maximum DAF occurred at a distance 71L/72 from 2nd pier for the three damping conditions. The range varied from 0.91~2.08, 0.95~1.29 and 1.00~1.25 for 0%, 2.5% and 5% damping respectively. So, the overall range for DAF is 0.91~2.08. However, for 2.5% and 5% damping excluding 0% damping, the range is 0.95~1.29.

Therefore, as a whole the DAF, for stresses, ranged from 0.91~3.3 for 0%, 2.5% and 5% damping consideration and 0.95~1.6 for 2.5% and 5% damping excluding 0% damping for vehicle speed and span length variation analysis with respect to results at different nodes along the middle span and for wheel position along the cantilever part of the box girder bridge. There were little similarities observed in the shape of the curves. Higher values of the DAF were obtained near the piers for some vehicle speeds. Arbitrary variations were observed along the length of the middle span for all vehicle speeds.

From above analyses, it can be observed that, for wheel position along the cantilever part of the box girder bridge, DAF is critical for deflections rather than stresses, as the DAF obtained at maximum nodes were high. None of the curves showed any particular relation of the DAF with the distance along the span. So, maximum DAF is 3.56 for deflections for 0%, 2.5% and 5% damping consideration. But if we exclude 0% damping, then maximum value of DAF is 1.6 for 2.5% and 5% damping which was caused for stress.

4.5.1.2 Variation along Middle Span Length for Wheel Position along Centerline of Box Girder Bridge

When vehicle moves along the centerline of box girder bridge, deflections along different points at the cantilever edge for vehicular load are negligible. So, only stresses for vehicular movement along the centerline of the box girder bridge are studied in this investigation.

4.5.1.2.1 Variation along the Length of Middle Span for Stresses

The variations of the DAF, for stresses at some distances from the edge of the cantilever part at different points along the middle span among the three spans and for wheel position along the centerline of the Box Girder Bridge for 0%, 2.5% and 5% damping conditions are shown in Figure 4.15 through Figure 4.19.

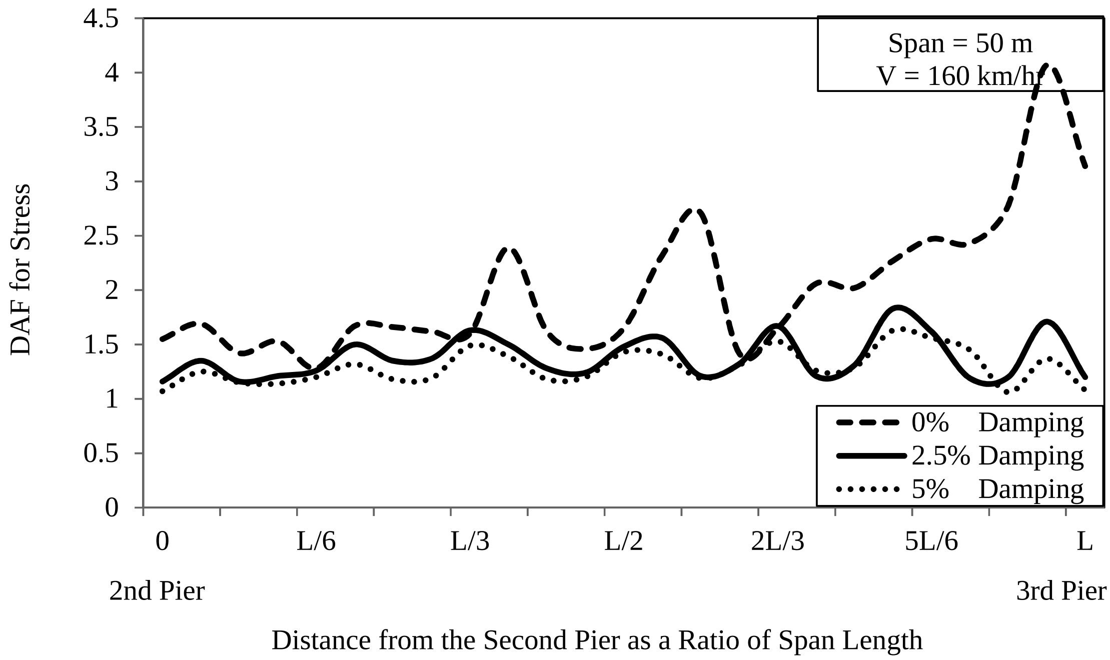

Figure 4.15: Variation of Dynamic Amplification Factor for Stresses along the Length of the Middle Span at Vehicle Speed = 160 km/h and for Span Length = 50 m

Figure 4.15 illustrates the variation of DAF for stresses at some distances from the edge of the cantilever along the length the middle span for 50 m span length and vehicle speed 160 km/h. Minimum DAF was found to appear at a distance L/6 and 11L/12 from 2nd pier for 0% and 5% damping and that was found at 2nd pier and at a distance L/12 from 2nd pier for 2.5% damping; whereas maximum DAF occurred at a distance 23L/24 from 2nd pier for 0% damping and 19L/24 from 2nd pier for both 2.5% and 5% damping. The range varied from 1.28~4.07, 1.16~1.83 and 1.06~1.63 for 0%, 2.5% and 5% damping respectively. So, the overall range for DAF is 1.06~4.07. However, for 2.5% and 5% damping excluding 0% damping, the range is 1.06~1.83.

Figure 4.16 illustrates the variation of DAF for transverse stresses at some distances from the edge of the cantilever along the length the middle span of three spans of the box girder bridge for 75 m span length and vehicle speed 100 km/h. Minimum DAF was found to appear at a distance L/36 from 2nd pier for 0% damping, 2.5% damping and 5% damping conditions; whereas maximum DAF occurred at a distance 13L/18 from 2nd pier for 0% damping, L/12 from 2nd pier for 2.5% and 5% damping and that was also found at a distance 35L/36 from 2nd pier for 5% damping conditions. The range of DAF varied from 0.37~2.84, 0.69~1.46 and 0.87~1.27 for 0% damping, 2.5% damping and 5% damping respectively. So, the overall range for DAF for stresses for this condition is 0.37~2.84. However, for 2.5% and 5% damping excluding 0% damping, the range is 0.69~1.46.

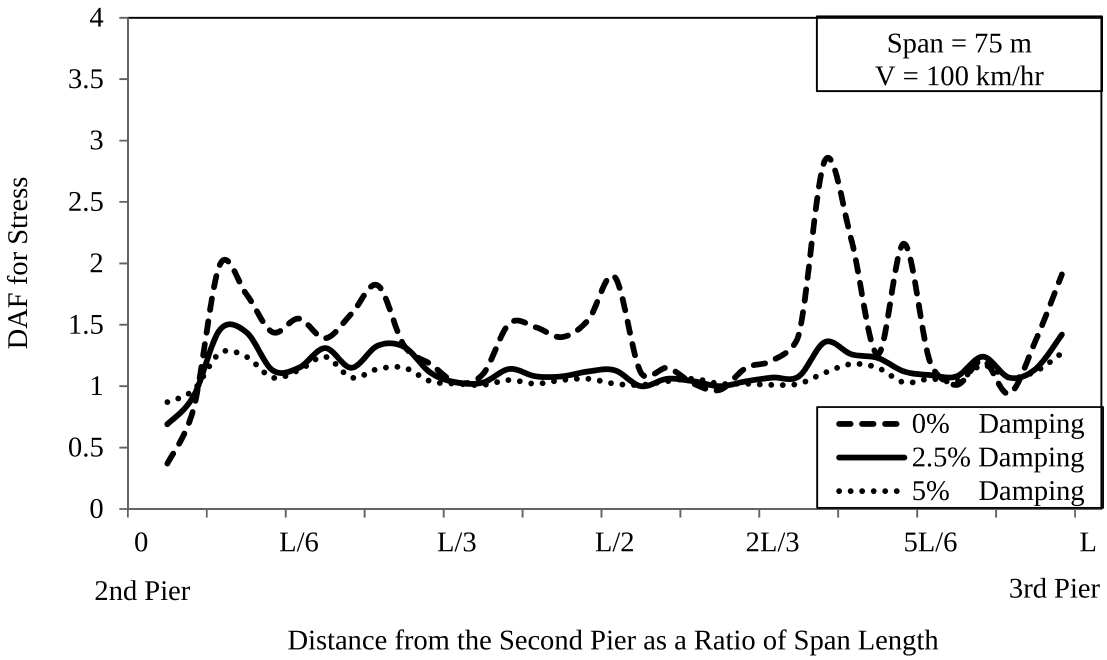

Figure 4.16: Variation of Dynamic Amplification Factor for Stresses along the Length of the Middle Span at Vehicle Speed = 100 km/h and for Span Length = 75 m

Figure 4.17 illustrates variation of DAF for stresses along the length of middle span of three spans of box girder bridge for 100 m span length and vehicle speed 160 km/h. Minimum DAF was found to appear at a distance 47L/48 from 2nd pier for 0% damping and L/48 from 2nd pier for 2.5% damping and 5% damping; whereas maximum DAF occurred at a distance 5L/6 from 2nd pier for 0% and 2.5% damping and that was found at a distance L/3 from 2nd pier for 5% damping. The range of DAF varied from 0.96~4.04, 0.76~1.63 and 0.7~1.41 for 0% damping, 2.5% damping and 5% damping respectively. So, overall range for DAF is 0.7~4.04. However, if we exclude 0% damping from our consideration, then the range is 0.7~1.63 for 2.5% and 5% damping.

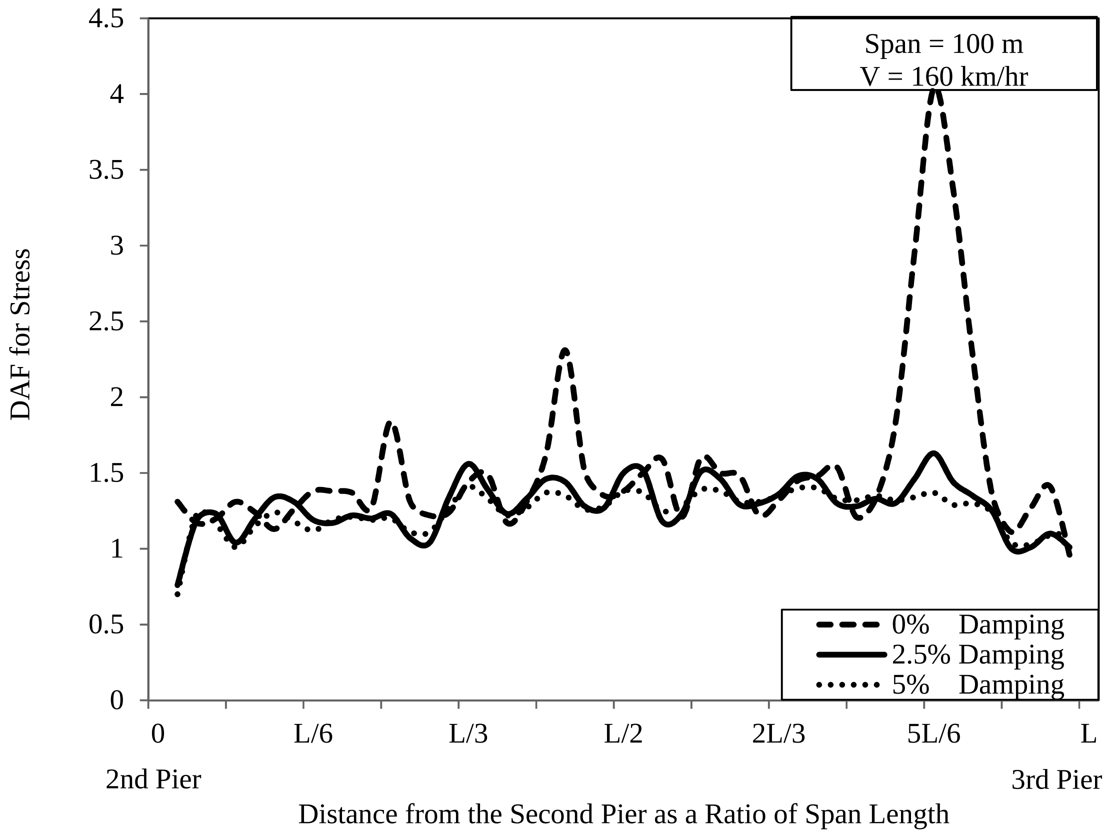

Figure 4.17: Variation of Dynamic Amplification Factor for Stresses along the Length of the Middle Span at Vehicle Speed = 160 km/h and for Span Length = 100 m

Figure 4.18 illustrates variation of DAF for stresses for 125 m span length and vehicle speed 140 km/h. Minimum DAF was found to appear at a distance L/6 from 2nd pier for 0% damping and L/60 from 2nd pier for 2.5% and 5% damping; whereas maximum DAF occurred at a distance 9L/20 from 2nd pier for 0% damping and that was found at a distance L/20 from 2nd pier for 2.5% and 5% damping. The range varied from 0.93~2.76, 0.8~1.6 and 0.72~1.48 for 0%, 2.5% and 5% damping respectively. So, overall range is 0.72~2.76. However, for 2.5% and 5% damping excluding 0% damping, the range is 0.72~1.6.

Figure 4.19 illustrates the variation of DAF for stresses for 150 m span length and vehicle speed 140 km/h. Minimum DAF was found to appear at a distance 25L/72 from 2nd pier for 0% damping and L/72 from 2nd pier for 2.5% and 5% damping. Maximum DAF occurred at a distance L/24 from 2nd pier for three damping conditions. The range varied from 1.02~3.35, 0.61~1.85 and 0.71~1.61 for three damping respectively. So, overall range is 0.61~3.35. However, for 2.5% and 5% damping, the range is 0.61~1.85.

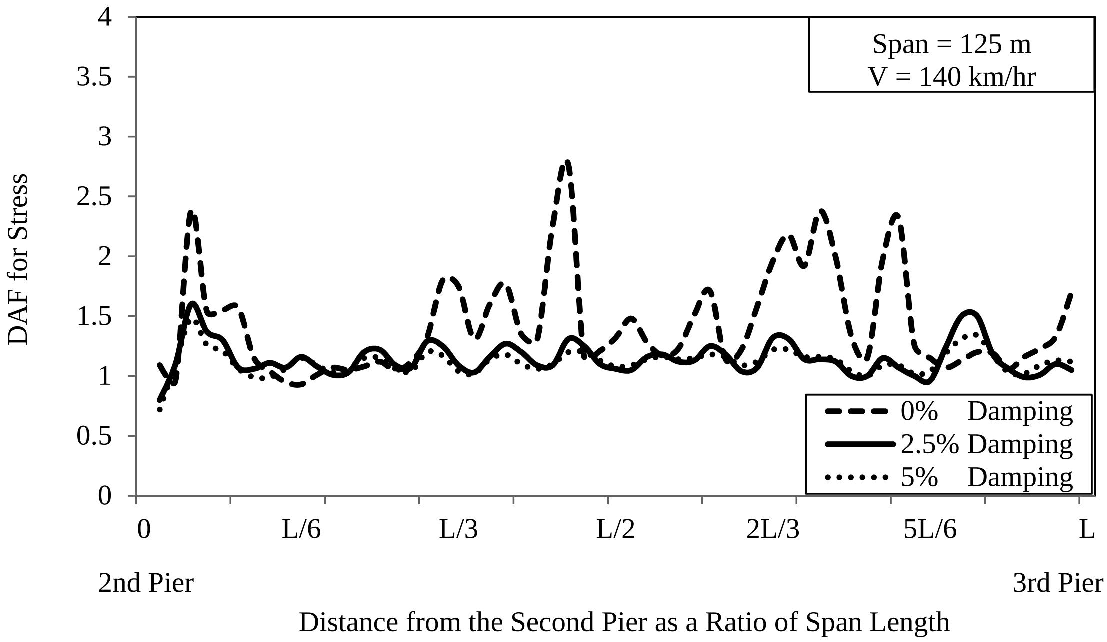

Figure 4.18: Variation of Dynamic Amplification Factor for Stresses along the Length of the Middle Span at Vehicle Speed = 140 km/h and for Span Length = 125 m

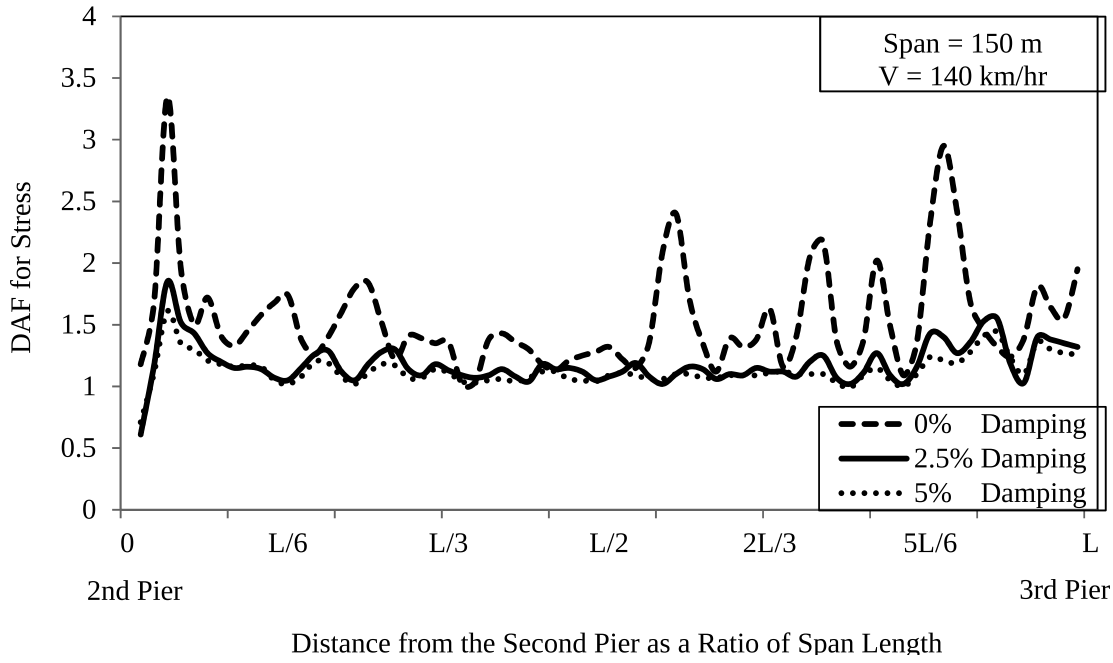

Figure 4.19: Variation of Dynamic Amplification Factor for Stresses along the Length of the Middle Span at Vehicle Speed = 140 km/h and for Span Length = 150 m

So, there were little similarities observed in the shape of the curves. Higher values of the DAF were obtained near the piers for some vehicle speeds. Arbitrary variations were observed along the length of the middle span for all vehicle speeds. Therefore, as a whole the DAF for stresses, ranged from 0.37~4.04 with 0%, 2.5% and 5% damping and 0.61~1.85 for 2.5% and 5% damping consideration for vehicle speed and span length variation analysis with respect to results at different nodes along the middle span and for wheel position along the centerline of the box girder bridge.

From the above analyses, it can be observed that, , DAF is critical for stresses for wheel position along the centerline of the box girder bridge rather than stresses and deflections for wheel position along cantilever part of the bridge, as the DAFs range is high. DAF range of stresses for wheel position along the centerline was 0.37~4.07 with 0%, 2.5% and 5% damping and 0.61~1.85 for 2.5% and 5% damping consideration and for wheel position along cantilever part, DAF range for stress was 0.91~3.3 for 0%, 2.5% and 5% damping consideration and 0.95~1.6 for 2.5% and 5% damping and for deflection was 0.81~3.56 with 0% damping and 0.99~1.58 for 2.5% and 5% damping consideration.

4.5.2 Variation along the Length of Middle Span for Different Cantilever Width

This study has been done only for vehicle position along cantilever part of box girder bridge as DAF for cantilever width variation for vehicle wheel position along centerline of box girder bridge is negligible. Three damping conditions, i.e. 0%, 2.5% and 5% damping conditions are considered for this investigation. The simulations were carried out for 7 different vehicle speeds for 4 different cantilever widths. Among the 7 vehicular speeds, one obtains the maximum DAF for each cantilever width. Graphical representations of maximum DAF for deflection and stress for each cantilever width are shown in figure 4.20 to 4.27. Similar graphs of other vehicular speed are represented in Appendix C.

4.5.2.1 Variation along the Length of Middle Span for Vertical Deflections

Parametric analysis for maximum DAF for deflections at the tip of cantilever at different points along the length of middle span among the three spans of box girder bridge w.r.to cantilever width is represented in this investigation. Four different cantilever width is studied here. This study was done for vehicle position along the cantilever part of box girder bridge. Graphs for vehicular speed in which maximum DAF is obtained are shown in figure 4.20 to 4.23.

Figure 4.20 illustrates variation of DAF for deflections at the tip of cantilever along the length of middle span among the three spans of box girder bridge for 3 m cantilever width and vehicle speed 80 km/h. Minimum DAF was found to appear at a distance 5L/16 from 2nd pier for 0% and 9L/16 from 2nd pier for 2.5% and 5% damping, that was also found at a distance 13L/24 from 2nd pier for 2.5% damping. Maximum DAF occurred at a distance 31L/48 from 2nd pier for three damping conditions. The range varied from 0.24~5.8, 0.84~1.64 and 0.89~1.32 for 0%, 2.5% and 5% damping respectively. So, the overall range for DAF is 0.24~5.8. However, for 2.5% and 5% damping, range is 0.84~1.64.

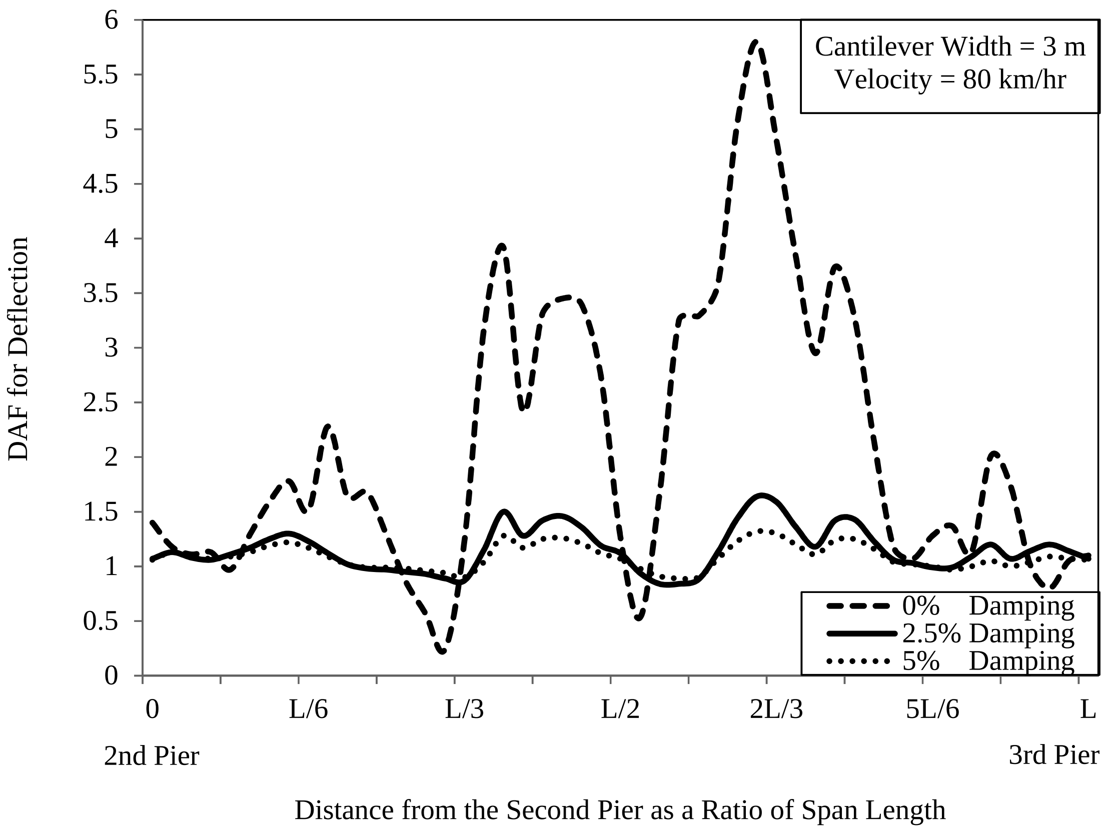

Figure 4.20: Variation of Dynamic Amplification Factor for Deflections along the Length of the Middle Span at Vehicle Speed = 80 km/h and for Cantilever Width = 3 m

Figure 4.21 illustrates variation of DAF for deflections for 3.5 m cantilever width and vehicle speed 140 km/h. Minimum DAF was found to appear at a distance 23L/24, 37L/48, 5L/12 from 2nd pier for 0%, 2.5% and 5% damping. Maximum DAF occurred at a distance 17L/24 from 2nd pier for 0% damping, that was found at a distance L/48 from 2nd pier for both 2.5%, 5% damping. Range varied from 1.01~3.43, 0.99~1.54 and 0.99~1.43 for 0%, 2.5% and 5% damping respectively. So, overall range for DAF is 0.99~3.43. However, for 2.5% and 5% damping excluding 0% damping, the range is 0.99~1.54.

Figure 4.22 illustrates variation of DAF for deflections at the tip of cantilever part along the length of middle span among the three spans of box girder bridge for 4 m cantilever width and vehicle speed 120 km/h. Minimum DAF was found to appear at a distance 7L/8, 35L/48 from 2nd pier for 0% and 2.5% damping, that was found at several distances for 5% damping. Maximum DAF occurred at a distance 11L/12 and 17L/48 from 2nd pier for 0% and 2.5% damping, that was found at 3rd pier for 5% damping. Range varied from 1.06~2.79, 0.99~1.45 and 1.00~1.36 for 0%, 2.5% and 5% damping respectively. So, overall range is 0.99~2.79. However, for 2.5% and 5% damping, range is 0.99~1.45.

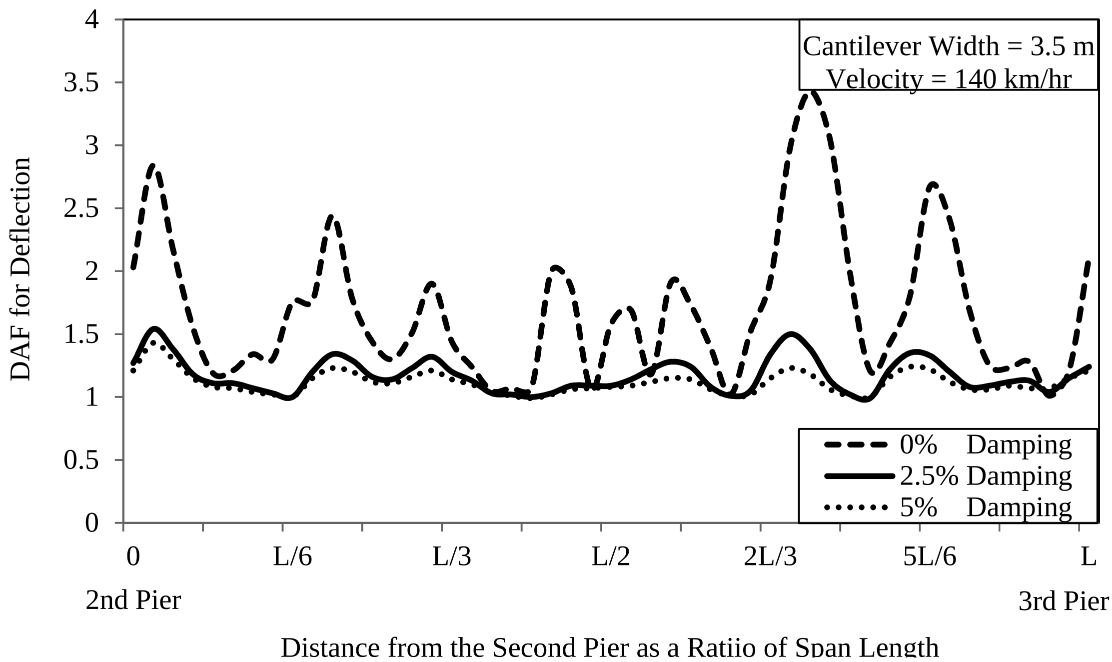

Figure 4.21: Variation of Dynamic Amplification Factor for Deflections along the Length of the Middle Span at Vehicle Speed = 140 km/h and for Cantilever Width = 3.5 m

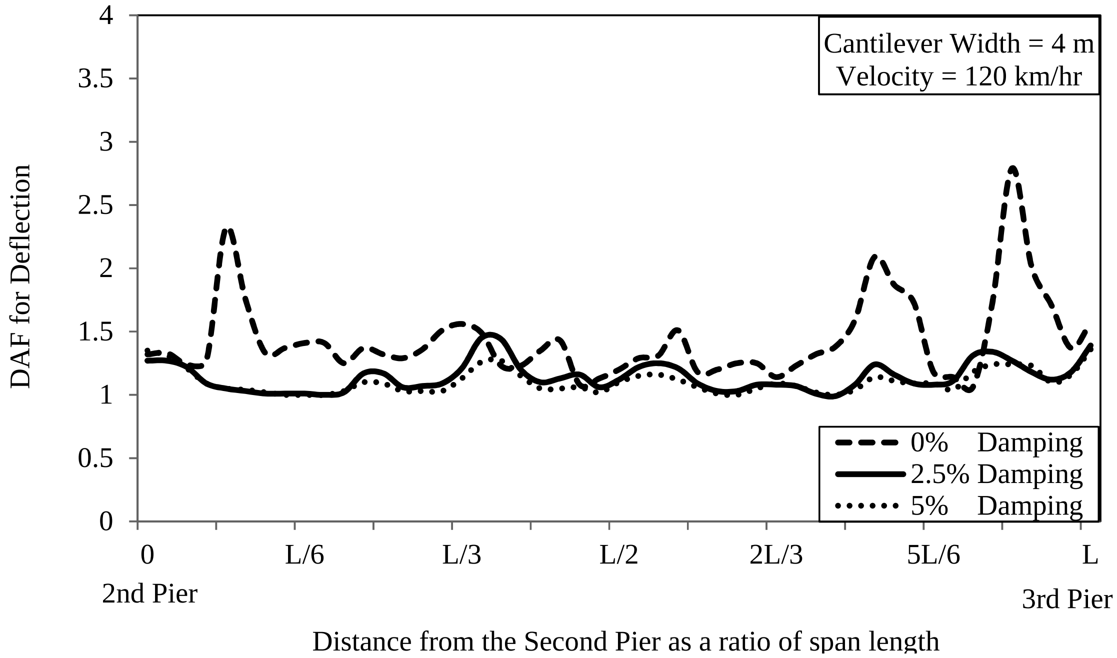

Figure 4.22: Variation of Dynamic Amplification Factor for Deflections along the Length of the Middle Span at Vehicle Speed = 120 km/h and for Cantilever Width = 4 m

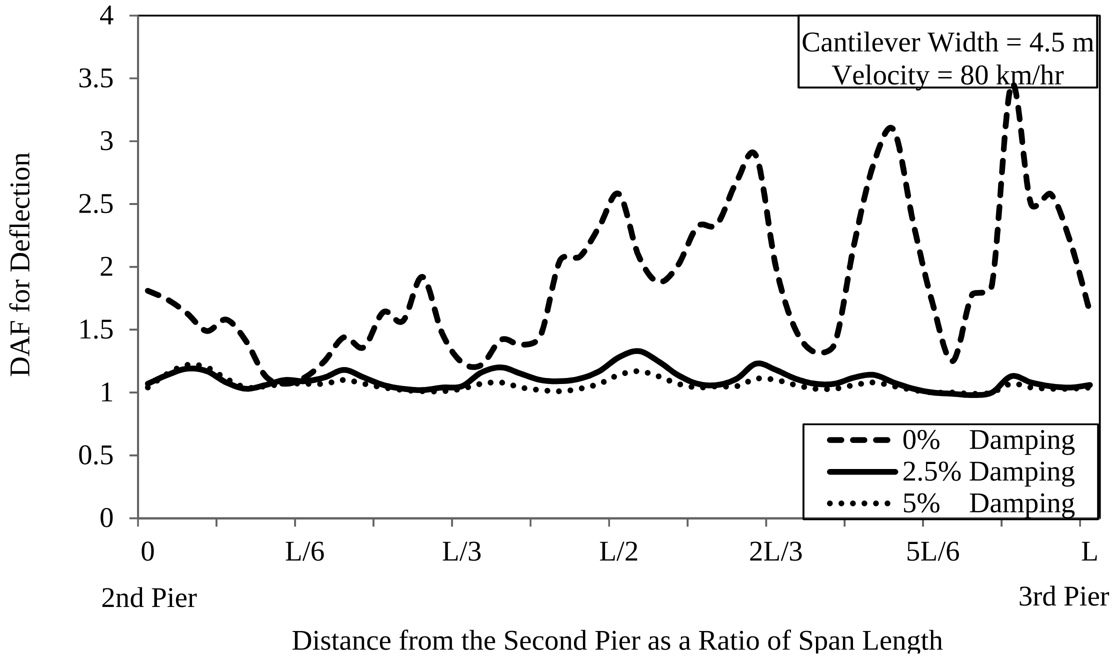

Figure 4.23: Variation of Dynamic Amplification Factor for Deflections along the Length of the Middle Span at Vehicle Speed = 80 km/h and for Cantilever Width = 4.5 m

Figure 4.23 illustrates variation of DAF for deflections at the tip of cantilever part along the length of middle span among the three spans of box girder bridge for 4.5 m cantilever width and vehicle speed 80 km/h. Minimum DAF was found to appear at a distance 7L/48 from 2nd pier for 0% damping, that was found at a distance 7L/8 from 2nd pier for 2.5% and 5% damping. Maximum DAF occurred at a distance 11L/12, 25L/48, L/24 from 2nd pier for 0%, 2.5% and 5% damping respectively. The range varied from 1.07~3.45, 0.98~1.33 and 0.99~1.22 for 0%, 2.5% and 5% damping respectively. So, the overall range for DAF is 0.98~3.45. However, for 2.5% and 5% damping, range is 0.98~1.33.

So, there were little similarities observed in the shape of the curves. Arbitrary variations were observed along the length of the middle span for all vehicle speeds. Therefore, as a whole the DAF for deflections, ranged from 0.24~5.8 for 0%, 2.5% and 5% damping consideration and 0.84~1.64 for 2.5% and 5% damping consideration for vehicle speed and cantilever slab width variation analysis with respect to results at different nodes along the middle span and for wheel position along the cantilever part of the box girder bridge.

4.5.2.2 Variation along the Length of Middle Span for Stresses

Parametric analysis of maximum DAF for stress at some distances from edge of cantilever at different points along the length of middle span among three spans of box girder bridge w.r.to cantilever width is represented in this investigation. Four different cantilever width is studied here. This study was done for vehicle position along the cantilever par. Graphs for vehicular speed in which maximum DAF is obtained are shown in figure 4.24 to 4.27.

Figure 4.24 illustrates variation of DAF for stresses at some distances from the edge of cantilever along length of the middle span among three spans of box girder bridge for 3 m cantilever width and vehicle speed 80 km/h. Minimum DAF was found to appear at a distance L/3 and 13L/24 from 2nd pier for 0% and 2.5% damping respectively and that was found at several distances for 5% damping. Maximum DAF occurred at a distance 2L/3 from 2nd pier for 0% damping and that was found at 2nd and 3rd pier for both 2.5% and 5% damping. Range varied from 0.71~2.13, 0.96~1.14 and 0.98~1.1 for 0%, 2.5% and 5% damping respectively. So, overall range for DAF is 0.71~2.13. However, range is 0.96~1.14 for 2.5% and 5% damping excluding 0% damping.

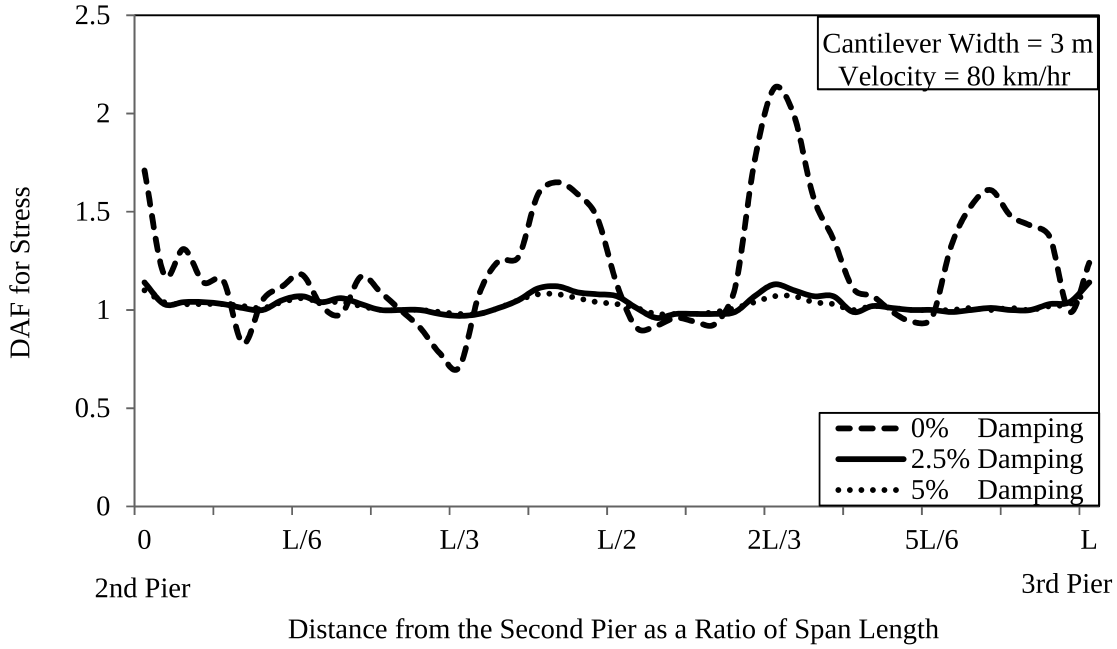

Figure 4.24: Variation of Dynamic Amplification Factor for Stresses along the Length of the Middle Span at Vehicle Speed = 80 km/h and for Cantilever Width = 3 m

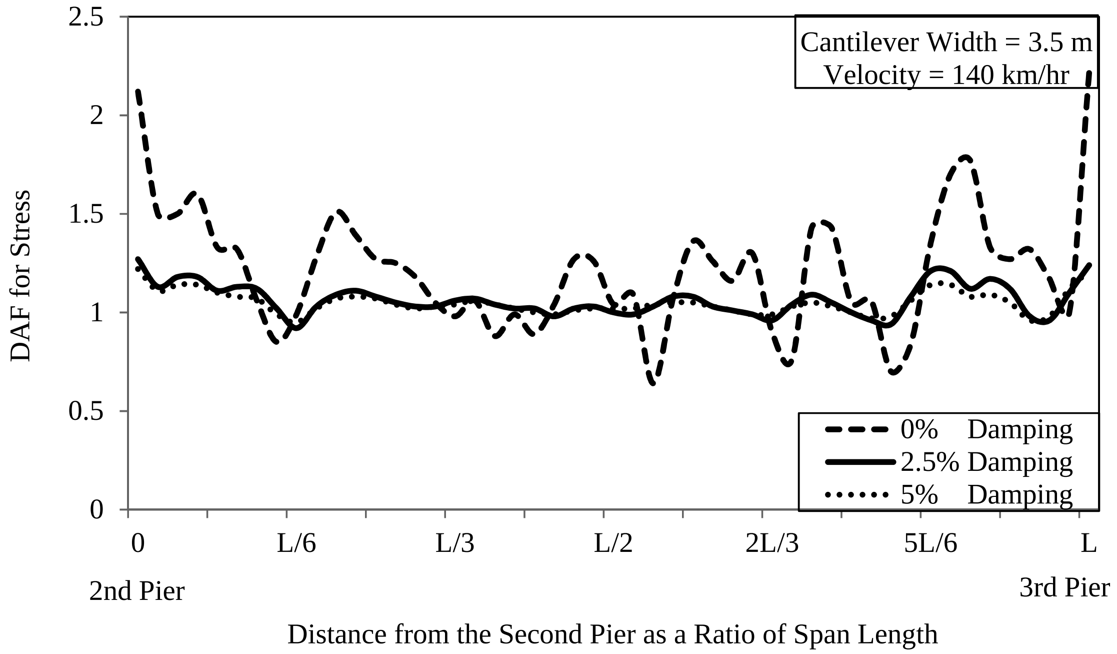

Figure 4.25: Variation of Dynamic Amplification Factor for Stresses along the Length of the Middle Span at Vehicle Speed = 140 km/h and for Cantilever Width = 3.5 m

Figure 4.25 illustrates the variation of DAF for transverse stresses at some distances from the edge of the cantilever along the length of the middle span among the three spans of the box girder bridge for 3.5 m cantilever width and vehicle speed 140 km/h. Minimum DAF was found to appear at a distance 13L/24 from 2nd pier for 0% damping and that was found at a distance L/6 from 2nd pier for both 2.5% and 5% damping. Maximum DAF occurred at 3rd pier for 0% damping and at 2nd pier for both 2.5% and 5% damping. The range varied from 0.64~2.22, 0.92~1.27 and 0.95~1.22 for 0%, 2.5% and 5% damping respectively. So, the overall range for DAF is 0.64~2.22. However, if we exclude 0% damping from our consideration, then the range is 0.92~1.27 for 2.5% and 5% damping.

Figure 4.26 illustrates the variation of DAF for stresses at some distances from the edge of the cantilever along the length of the middle span for 4 m cantilever width and vehicle speed 160 km/h. Minimum DAF was found to appear at a distance 7L/8 from 2nd pier for 0% damping and that was found at a distance L/12 from 2nd pier for both 2.5% and 5% damping. Maximum DAF occurred at a distance 47L/48 from 2nd pier for the three damping conditions. The range varied from 0.95~2.0, 0.97~1.3 and 0.99~1.21 for 0%, 2.5% and 5% damping respectively. So, the overall range for DAF is 0.95~2.0. However, neglecting 0% damping, the range is 0.97~1.3 for 2.5% and 5% damping.

Figure 4.27 illustrates the variation of DAF for stresses for 4.5 m cantilever width and vehicle speed 120 km/h. Minimum DAF was found to appear at a distance 9L/16, 7L/16 and L/8 from 2nd pier for 0%, 2.5% and 5% damping respectively. Maximum DAF occurred at a distance 5L/24 from 2nd pier for 0% damping and that was found at 3rd pier for both 2.5% and 5% damping condition. The range varied from 1.08~2.21, 0.99~1.43 and 0.98~1.32 for 0%, 2.5% and 5% damping respectively. So, the overall range for DAF is 0.98~2.21. However, if we exclude 0% damping from our consideration, then the range is 0.98~1.43 for 2.5% and 5% damping.

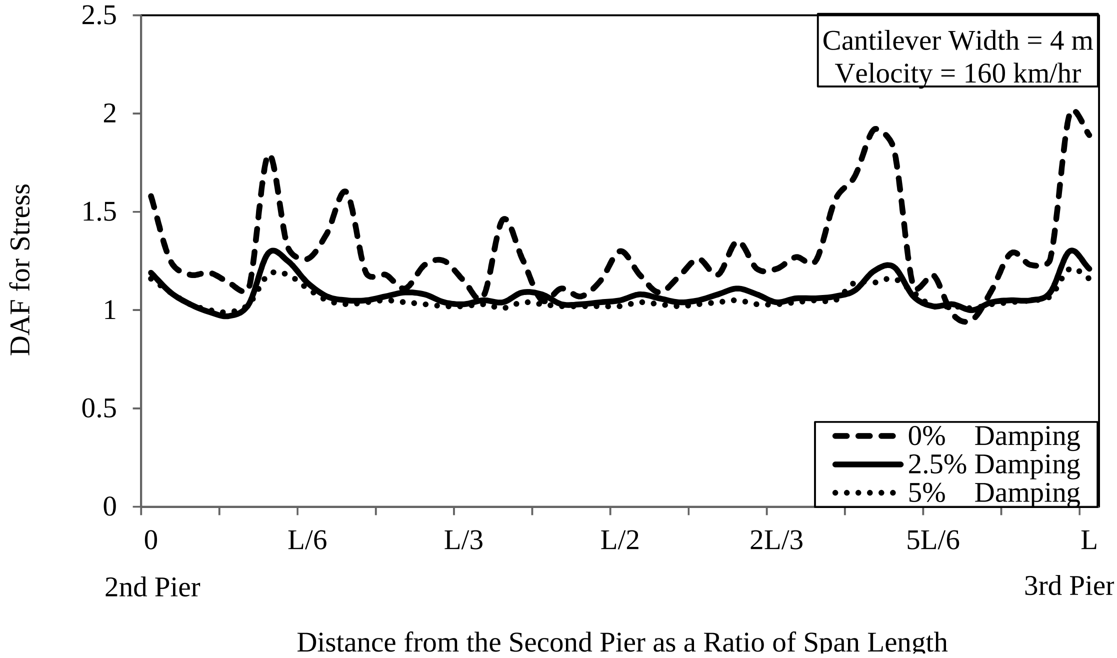

Figure 4.26: Variation of Dynamic Amplification Factor for Stresses along the Length of the Middle Span at Vehicle Speed = 160 km/h and for Cantilever Width = 4 m

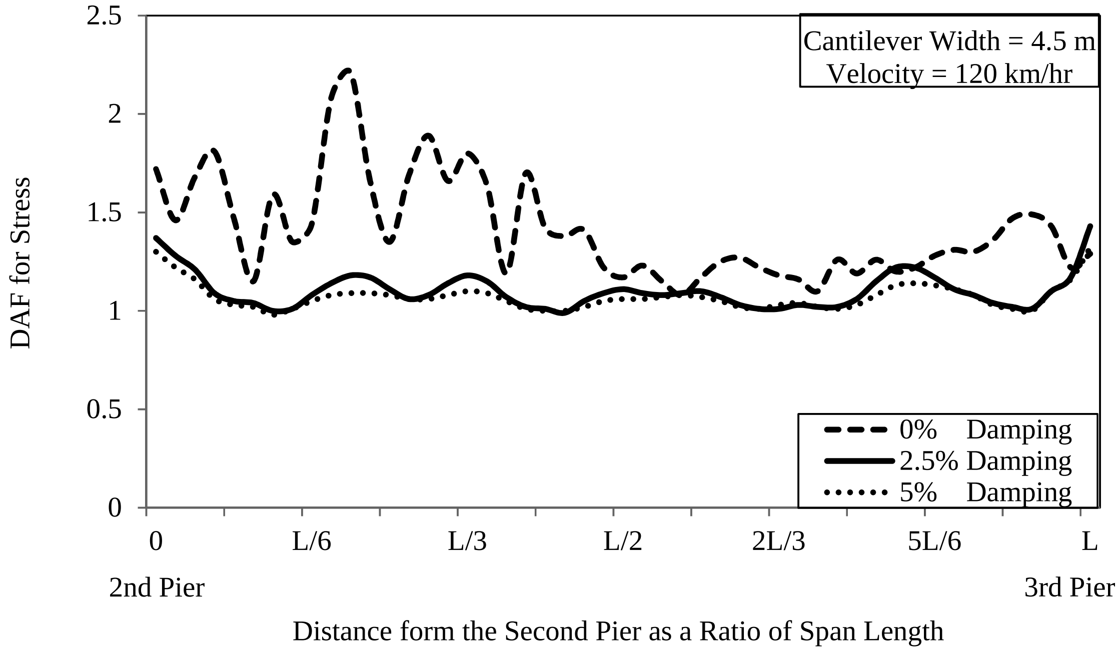

Figure 4.27: Variation of Dynamic Amplification Factor for Stresses along the Length of the Middle Span at Vehicle Speed = 120 km/h and for Cantilever Width = 4.5 m

Hence, there were little similarities observed in the shape of the curves. Arbitrary variations were observed along the length of the middle span for all vehicle speeds. Therefore, as a whole the DAF for stresses, ranged from 0.64~2.22 for 0%, 2.5% and 5% damping consideration and 0.92~1.43 for 2.5% and 5% damping for vehicle speed and cantilever slab width variation analysis with respect to results at different nodes along the middle span and for wheel position along the centerline of the box girder bridge.

From the above analyses, it can be observed that, for wheel position along the cantilever part of the box girder bridge, DAF is critical for deflections rather than stresses, as the DAFs obtained at maximum nodes were high. Again, none of the curves showed any particular relation of the DAF with the distance along the span. Maximum DAF, which is 5.8 for 0%, 2.5% and 5% damping condition and 1.64 for 2.5% and 5% damping consideration, was also noticed to occur for deflections.

4.5.3 Influence of Vehicle Speed

The variation of the DAF as a function of the vehicle speed is shown in figure 4.28 through figure 4.35 for vertical deflections at the tip of the cantilever and for transverse stresses at some distances from the edge of the cantilever for two different vehicle wheel positions. One path of vehicle wheel is along the cantilever part of the box girder bridge which is at a fixed distance from the edge of cantilever part of the bridge. Another path of vehicle wheel load is along the centerline of the box girder bridge. Three damping conditions, i.e. 0%, 2.5% and 5% damping conditions are also considered for both wheel positions. This parametric study has been done for the value of DAF at mid span and for the maximum value of DAF taken among 2nd pier and 3rd pier of the box girder bridge. The simulations were carried out for 7 different vehicle speeds.

4.5.3.1 Variation of DAF for Wheel Position along Cantilever part of Box Girder Bridge

This investigation contains the study regarding variation of the DAF as a function of the vehicle speed for vertical deflections at the tip of the cantilever and transverse stresses at some distances from the edge of the cantilever for vehicle trajectory along the cantilever part of the box girder bridge for 0%, 2.5% and 5% damping conditions. The simulations were carried out for 7 different vehicle speeds.

Figure 4.28 illustrates variation of DAF for Deflections at 3rd pier. Between 2nd pier and 3rd pier, maximum value of DAF was found at 3rd pier. So, this investigation represents the effect of vehicle speed on DAF for deflections at 3rd pier which is the maxima. Maximum DAF occurs at velocity 160 km/hr for 0% damping and at velocity 120 km/hr for both 2.5% and 5% damping; whereas minimum DAF occurs at velocity 40 km/hr for 0% damping and at 60 km/hr for both 2.5% and 5% damping conditions. From this figure, it can be seen that three graphs for three damping conditions are closely symmetrical. DAF range varied from 1.04~1.78, 1.07~1.39 and 1.05~1.36 for 0%, 2.5% and 5% damping respectively. So, total DAF ranged from 1.04~1.78. However, if we exclude 0% damping from our consideration, then the range is 1.05~1.39 for 2.5% and 5% damping.

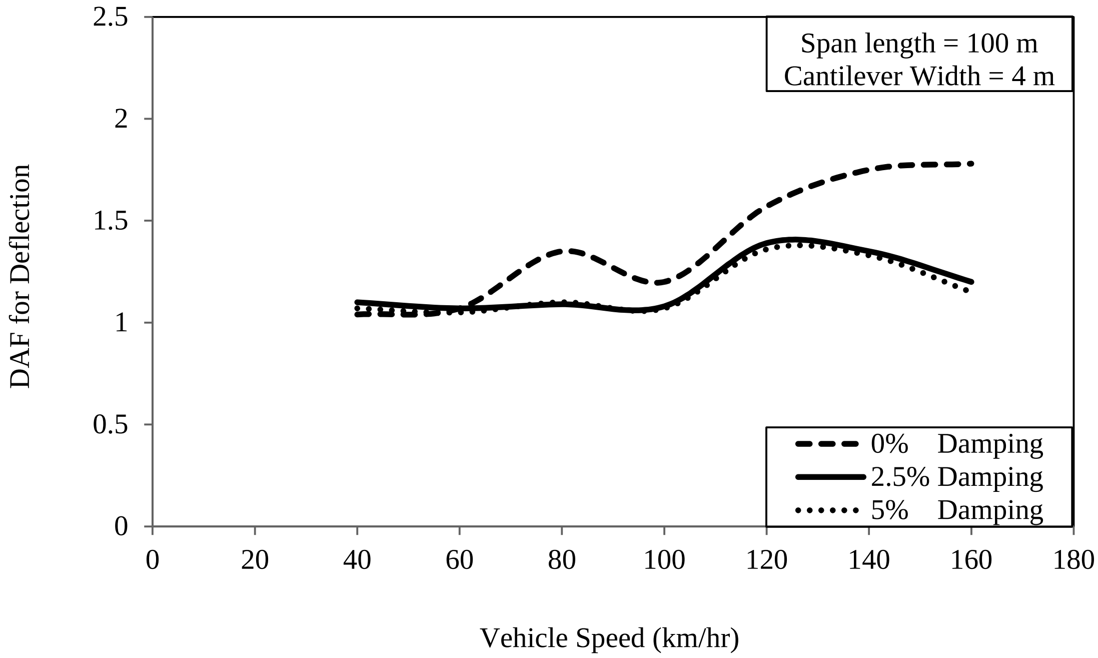

Figure 4.28: Variation of Dynamic Amplification Factor for Deflections at 3rd Pier as a Function of Vehicle Speed for Span Length = 100 m and Cantilever Width = 4 m

Figure 4.29 illustrates variation of DAF for Deflections at a distance L/4 from 2^{nd} pier. In this investigation, DAF for deflections at a distance L/4 from 2^{nd} pier and 3L/4 from 2^{nd} pier was studied and maximum value of DAF between these two points is represented in figure 4.29. So, this investigation represents the effect of vehicle speed on DAF for deflections at a distance L/4 from 2^{nd} pier which is the maxima. Maximum DAF occurs at velocity 140 km/hr for 0% damping and at velocity 160 km/hr for both 2.5% and 5% damping; whereas minimum DAF occurs at velocity 160 km/hr and 60 km/hr for 0% and 2.5% damping respectively and at several velocity for 5% damping conditions. DAF range varied from 1.14~2.02, 1.05~1.35 and 1.05~1.31 for 0%, 2.5% and 5% damping respectively. So, total DAF ranged from 1.05~2.02. However, if we exclude 0% damping from our consideration, then the range is 1.05~1.35 for 2.5% and 5% damping.

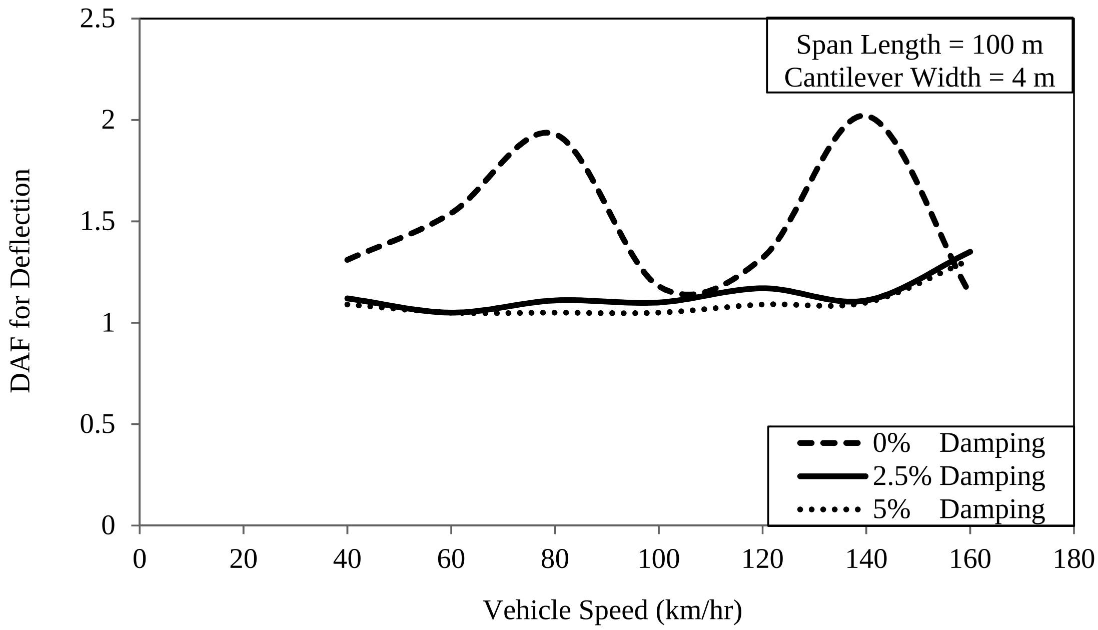

Figure 4.29: Variation of Dynamic Amplification Factor for Deflections at a Distance $L/4$ from 2^{nd} Pier as a Function of Vehicle Speed for Span Length = 100 m and Cantilever Width = 4m

Figure 4.30 illustrates variation of DAF for Deflections at mid span. Maximum DAF occurs at velocity 40 km/hr for 0% damping and at velocity 160 km/hr for both 2.5% and 5% damping; whereas minimum DAF occurs at velocity 60 km/hr for three damping conditions. DAF range varied from 0.9~1.37, 0.99~1.22 and 1.02~1.2 for 0%, 2.5% and

5% damping respectively. So, total DAF ranged from 0.9~1.37. However, for 2.5% and 5% damping excluding 0% damping, the range is 0.99~1.22.

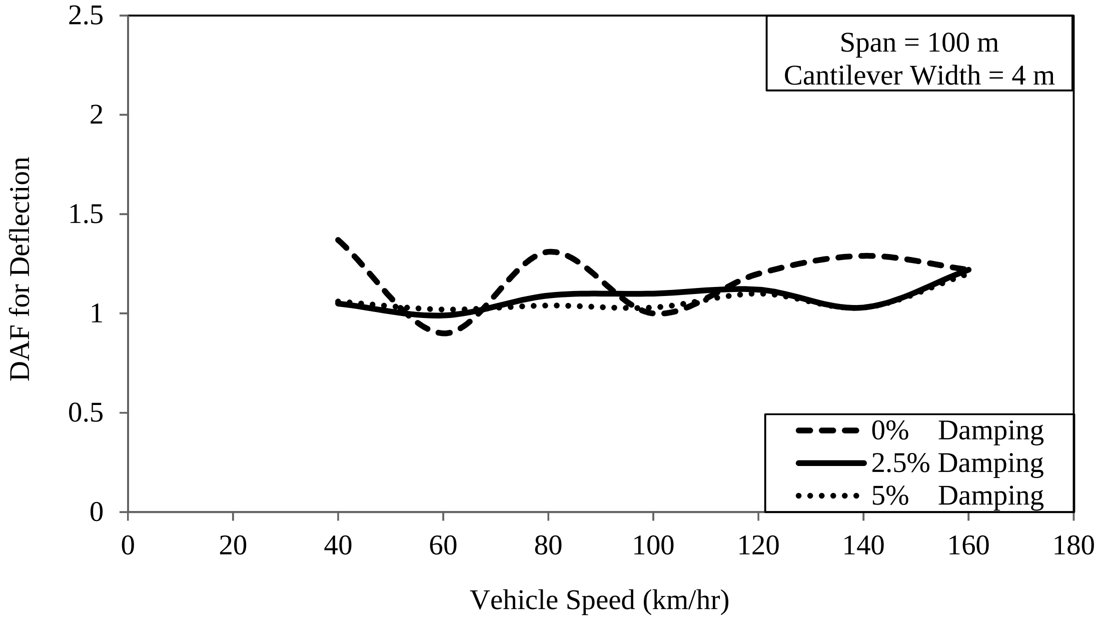

Figure 4.30: Variation of Dynamic Amplification Factor for Deflections at Mid Span as a Function of Vehicle Speed for Span Length = 100 m and Cantilever Width = 4 m

This investigation was done for maximum DAFs for deflections between values at 2nd pier and 3rd pier; at a distance L/4 and 3L/4 from 2nd pier; at mid span and for wheel position along cantilever part of the box girder bridge. The maximum DAF is found at a distance L/4 from 2nd pier. From Figure 4.28 through 4.30, arbitrary variation of the DAF with velocity was witnessed. But no distinct relationship could be developed between the DAF and velocity. Therefore, overall range from the above study for the DAF for deflections, is 0.9~2.02 for 0%, 2.5% and 5% damping and 0.99~1.39 for 2.5% and 5% damping consideration for vehicle speed variation analysis with respect to results at different nodes along the middle span.

Figure 4.31 illustrates variation of DAF for stresses at 2nd pier. Between 2nd pier and 3rd pier, maximum value of DAF was found at 2nd pier. So, this investigation represents the effect of vehicle speed on DAF for stresses at 2nd pier which is the maxima. Maximum DAF occurs at velocity 140 km/hr for 0% and 2.5% damping and at velocity 120 km/hr for 5% damping; whereas minimum DAF occurs at velocity 60 km/hr for 0% damping and at 100 km/hr for both 2.5% and 5% damping conditions. DAF range varied from 1.08~1.93, 1.05~1.45 and 1.05~1.4 for 0%, 2.5% and 5% damping respectively. So, total DAF ranged from 1.05~1.93. However, if we exclude 0% damping from our consideration, then the range is 1.05~1.45 for 2.5% and 5% damping.

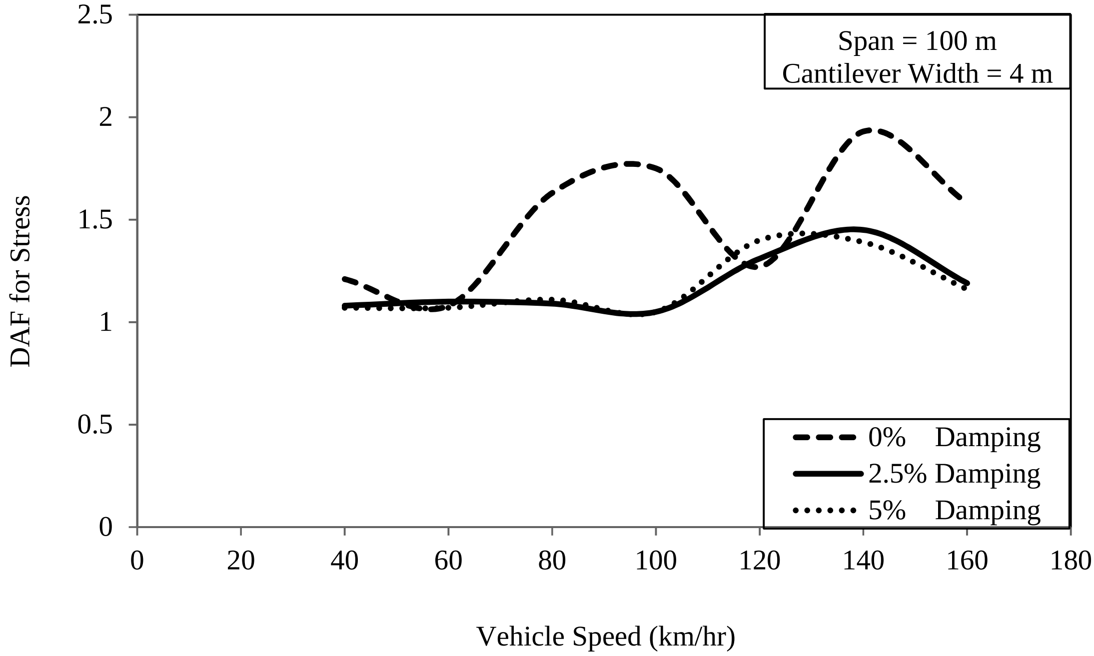

Figure 4.31: Variation of Dynamic Amplification Factor for Stresses at 2nd Pier as a Function of Vehicle Speed for Span Length = 100 m and Cantilever Width = 4 m

Figure 4.32 illustrates variation of DAF for stresses at a distance 3L/4 from 2nd pier. In this investigation, DAF for stresses at a distance L/4 from 2nd pier and 3L/4 from 2nd pier was studied and maximum value of DAF between these two points is represented in figure 4.29. So, this investigation represents the effect of vehicle speed on DAF for stresses at a distance 3L/4 from 2nd pier which is the maxima. Maximum DAF occurs at velocity 160 km/hr for 0% and 5% damping and at velocity 80 km/hr for 2.5% damping; whereas minimum DAF occurs at velocity 40 km/hr for 0% damping and at velocity 60 km/hr for both 2.5% and 5% damping conditions.DAF range varied from 0.95~1.68, 1.00~1.13 and 0.99~1.14 for 0%, 2.5% and 5% damping respectively. So, total DAF ranged from 0.95~1.68. However, if we exclude 0% damping from our consideration, then the range is 0.99~1.14 for 2.5% and 5% damping.

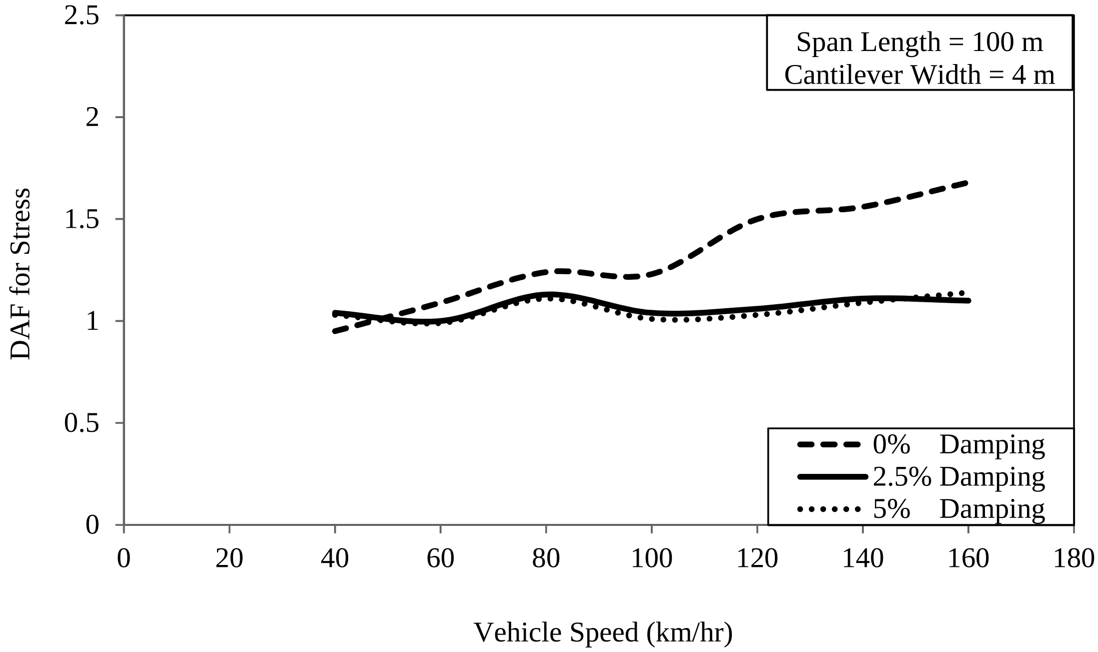

Figure 4.32: Variation of Dynamic Amplification Factor for Stresses at a Distance $3L/4$ from 2nd Pier as a Function of Vehicle Speed for Span Length = 100 m and Cantilever Width = 4m

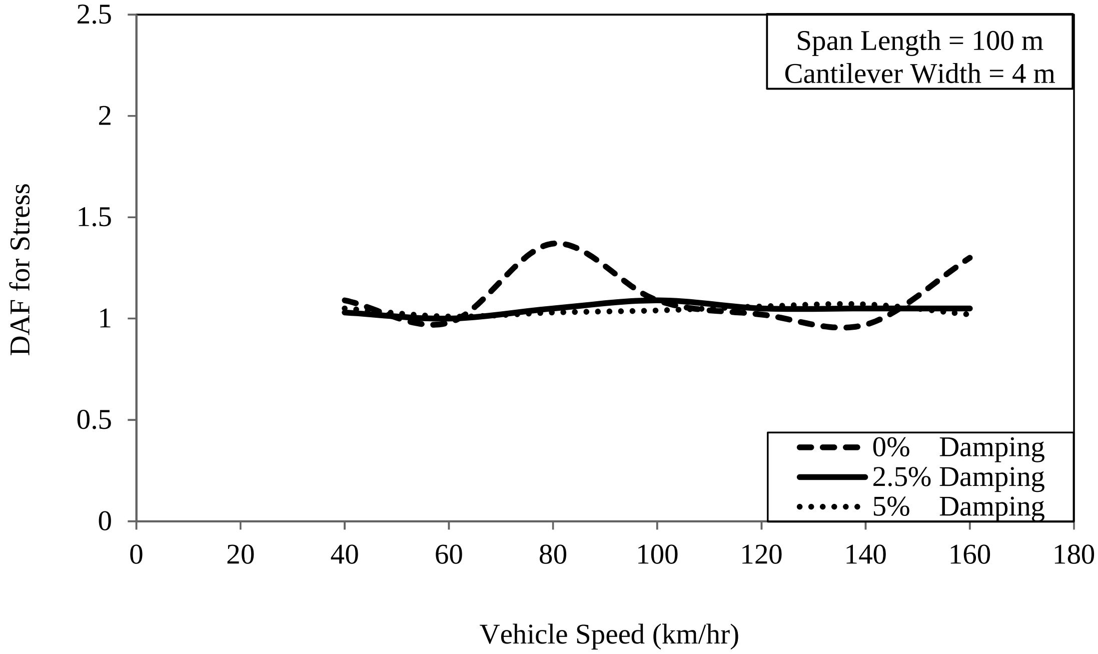

Figure 4.33: Variation of Dynamic Amplification Factor for Stresses at Mid Span as a Function of Vehicle Speed for Span Length = 100 m and Cantilever Width = 4 m

Figure 4.33 illustrates variation of DAF for stresses at some distances from the edge of the cantilever along the length of the middle span among the three spans of the box girder bridge at mid span. Maximum DAF occurs at velocity 80 km/hr, 100 km/hr and 140 km/hr for 0%, 2.5% and 5% damping respectively; whereas minimum DAF occurs at velocity 140 km/hr for 0% damping and at velocity 60 km/hr for both 2.5% damping and 5% damping conditions. DAF range varied from 0.97~1.37, 1.00~1.09 and 1.01~1.07 for 0% damping, 2.5% damping and 5% damping respectively. So, total DAF ranged from 0.97~1.37. However, if we exclude 0% damping from our consideration, then the range is 1.00~1.09 for 2.5% and 5% damping.

This investigation was done for maximum DAFs for stresses between values at 2nd pier and 3rd pier; at a distance L/4 and 3L/4 from 2nd pier; at mid span and vehicle trajectory along cantilever part of the box girder bridge. The maximum DAF is found at 2nd pier. From Figure 4.31 through 4.33, arbitrary variation of the DAF with velocity was witnessed. But no distinct relationship could be developed between the DAF and velocity. Therefore, as a whole the DAF for deflections is critical rather than the DAF for stresses for Wheel position along cantilever part of the box girder bridge, as the DAF obtained for deflection for vehicle speed variation is maximum almost for all cases. Therefore, overall range from the above study for the DAF for stresses, is 0.95~1.93 for 0%, 2.5% and 5% damping and 0.99~1.45 for 2.5% and 5% damping consideration for vehicle speed variation analysis with respect to results at different nodes along the middle span among the three spans of the bridge.

4.5.3.2 Variation of DAF for Wheel Position along Centerline of Box Girder Bridge

This investigation contains the study regarding variation of the DAF as a function of the vehicle speed for transverse stresses at some distances from the edge of the cantilever for vehicle trajectory along the centerline of the box girder bridge for 0%, 2.5% and 5% damping conditions. This study includes only the variation of DAF for stresses because values of deflections are negligible for vehicle path along centerline. Again values of stress at 2nd pier and 3rd pier are zero for wheel position along centerline. So, this study is regarding only two investigations. One is for maximum value between DAF at a distance

L/4 from 2nd pier and 3L/4 from 2nd pier. Another is for DAF for stresses at mid span. The simulations were carried out for 7 different vehicle speeds.

Figure 4.34 illustrates variation of DAF for stresses at a distance 3L/4 from 2nd pier. In this investigation, DAF for stresses at a distance L/4 from 2nd pier and 3L/4 from 2nd pier was studied and maximum value of DAF between these two points is represented in figure 4.29. So, this investigation represents the effect of vehicle speed on DAF for stresses at a distance 3L/4 from 2nd pier which is the maxima. Maximum DAF occurs at velocity 120 km/hr for 0% and at velocity 160 km/hr for both 2.5% and 5% damping; whereas minimum DAF occurs at velocity 160 km/hr for 0% damping and at velocity 80 km/hr for both 2.5% and 5% damping conditions. DAF range varied from 1.21~2.68, 1.02~1.28 and 1.01~1.32 for 0%, 2.5% and 5% damping respectively. So, total DAF ranged from 1.01~2.68. However, if we exclude 0% damping from our consideration, then the range is 1.01~1.32 for 2.5% and 5% damping.

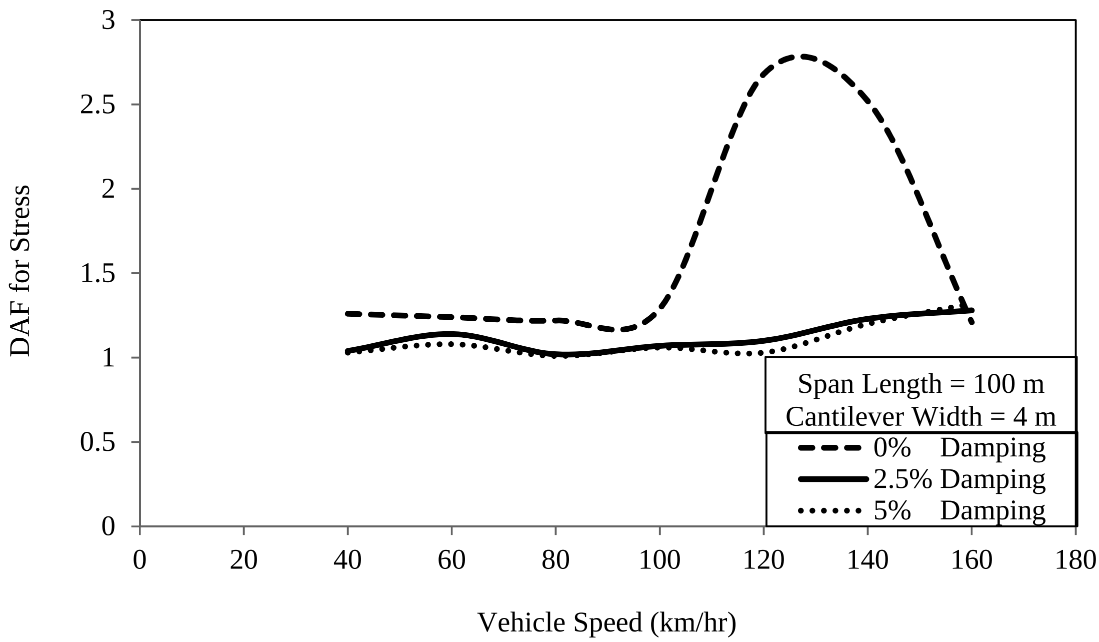

Figure 4.34: Variation of Dynamic Amplification Factor for Stresses at a Distance $3L/4$ from 2nd Pier as a Function of Vehicle Speed for Span Length = 100 m and Cantilever Width = 4m

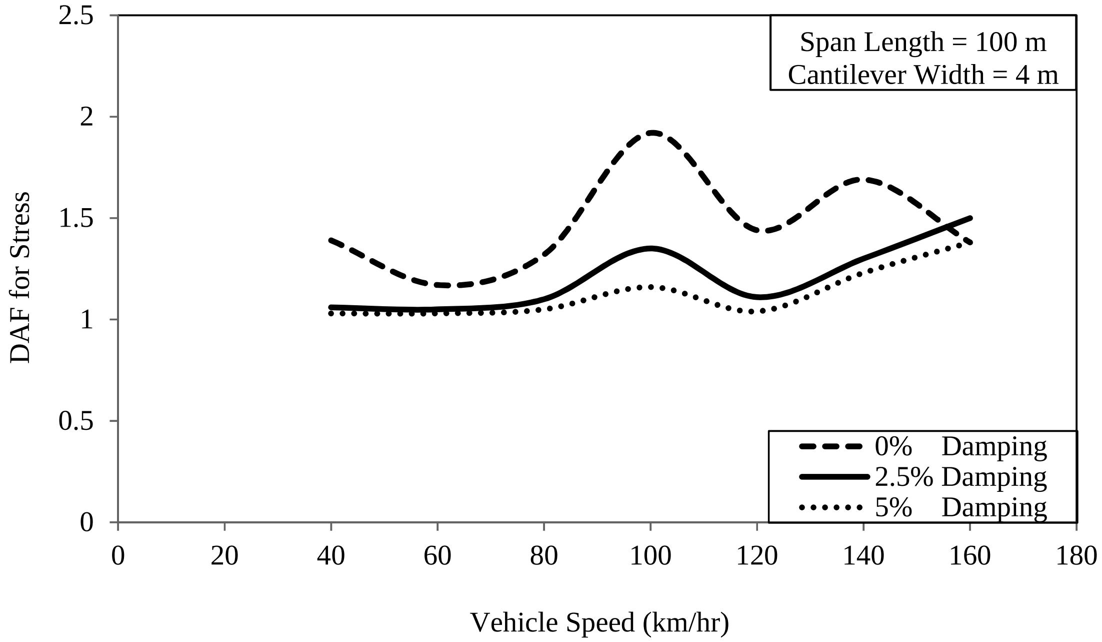

Figure 4.35: Variation of Dynamic Amplification Factor for Stresses at Mid Span as a Function of Vehicle Speed for Span Length = 100 m and Cantilever Width = 4 m

Figure 4.35 illustrates variation of DAF for stresses at mid span. Maximum DAF occurs at velocity 100 km/hr for 0% damping and at velocity 160 km/hr for both 2.5% and 5% damping; whereas minimum DAF occurs at velocity 60 km/hr for three damping conditions and minimum value for 5% damping was also found at velocity 40 km/hr. DAF range varied from 1.17~1.92, 1.05~1.5 and 1.03~1.38 for 0%, 2.5% and 5% damping respectively. So, total DAF ranged from 1.03~1.92. However, if we exclude 0% damping from our consideration, then the range is 1.03~1.5 for 2.5% and 5% damping.

This investigation was done for maximum DAFs for stresses between values at 2nd pier and 3rd pier; at a distance L/4 and 3L/4 from 2nd pier; at mid span and vehicle path along centerline of box girder bridge. Therefore, as a whole DAF for stresses for wheel position along centerline of the box girder bridge, is critical rather than the DAF for stresses and deflections for wheel position along cantilever part of the box girder bridge, as the DAF obtained for stresses for vehicle speed variation is maximum, which is 2.68. Therefore, overall range from the above study for the DAF for stresses, is 1.01~2.68 for 0%, 2.5%

and 5% damping and 1.01~1.50 for 2.5% and 5% damping consideration for vehicle speed variation analysis with respect to results at different nodes along the middle span.

4.6 Some Other Studies

4.6.1 Influence of Different Span Length and Velocity on Dynamic Amplification Factor

4.6.1.1 Influence of Different Span Length and Velocity for Wheel Position along Cantilever part of Box Girder Bridge

The variation of maximum DAFs for vertical deflections as a function of span length at 7 different vehicular speeds are shown in Figure 4.36, Figure 4.37 and Figure 4.38 and variation of maximum DAFs for transverse stresses are shown in Figure 4.39, Figure 4.40 and Figure 4.41 for 0%, 2.5% and 5% damping respectively. The simulation was carried out for 5 different span lengths which were varied with approximate slab thickness with simultaneous change in deck height which was discussed in chapter 3.

Figure 4.36 shows relationship between maximum DAF for deflections and span length for different vehicular speed at 0% damping condition. This figure also illustrates that, for different span length maximum DAF is obtained at different velocity. Maximum DAF ranges from 2.04 ~3.56 which possess in the span range of 50~150 m. So, the band width is wide enough. Again, the overall range for DAF obtained is 1.45~3.56.

Figure 4.37 shows relationship between maximum DAF for deflections and span length for different vehicle speed at 2.5% damping. This figure also illustrates that, maximum DAF is obtained almost at same span length at different velocity. Maximum DAF occurs at 50 m span length for velocity 40~140 km/hr and that was occurred at 100 m span length for 160 km/hr. The band width is almost same for any combination. Maximum DAF ranges from 1.34~1.7. Again, the overall range for DAF obtained is 1.2~1.7.

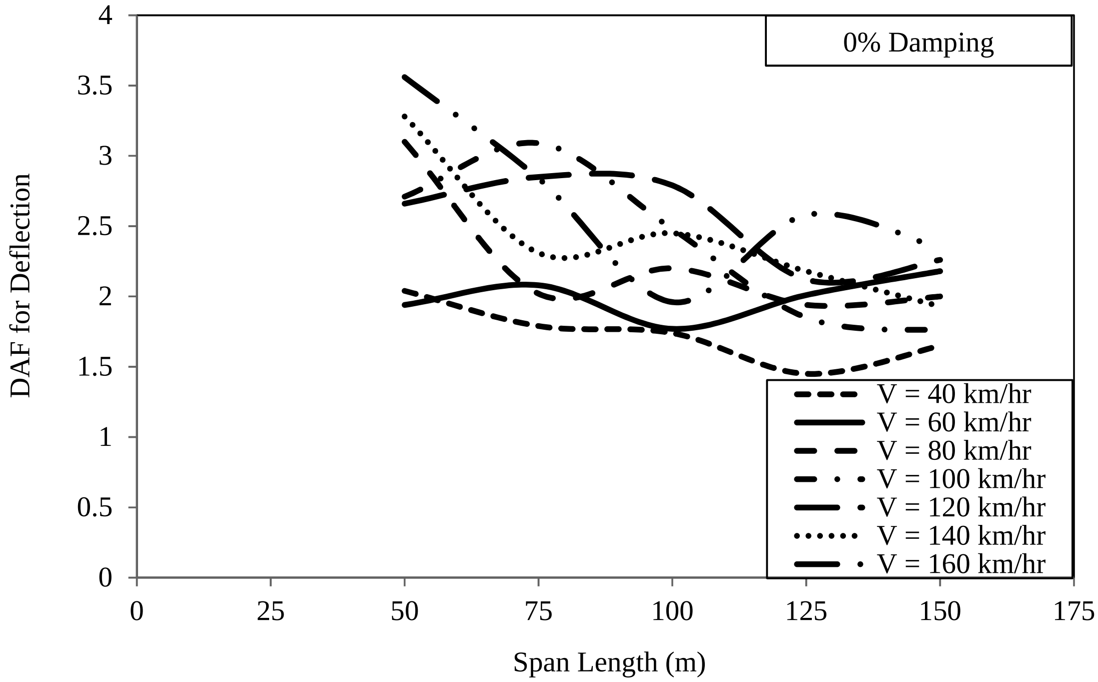

Figure 4.36: Variation of Maximum Dynamic Amplification Factor for Deflections as a Function of Span Length at Different Vehicular Speed for 0% Damping

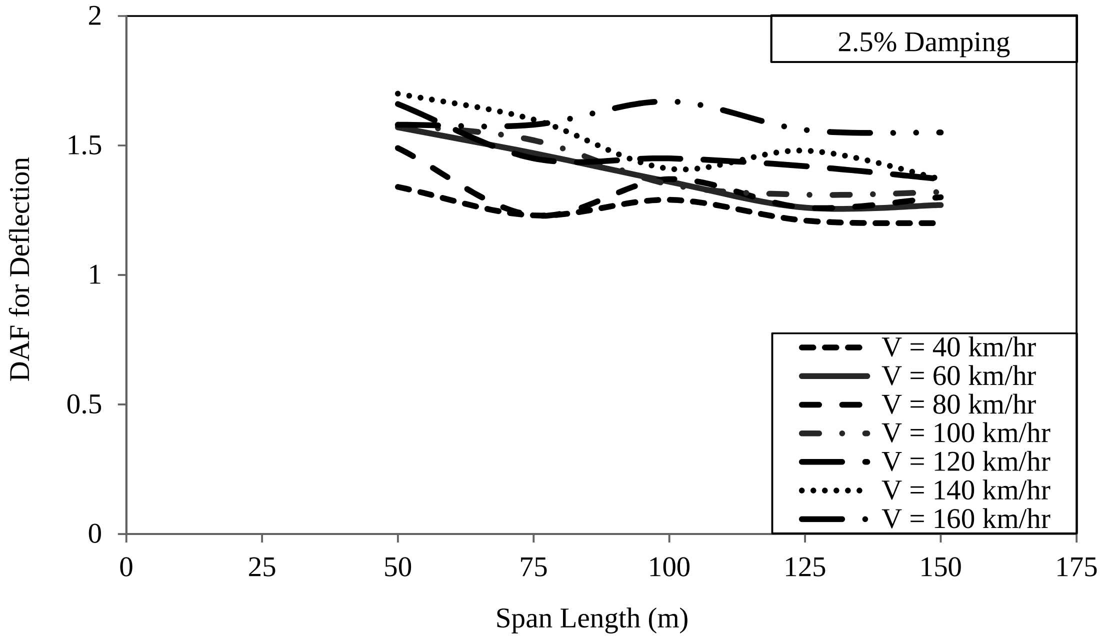

Figure 4.37: Variation of Maximum Dynamic Amplification Factor for Deflections as a Function of Span Length at Different Vehicular Speed for 2.5% Damping

Figure 4.38 shows relationship between maximum DAF for deflection and span length for different vehicle speed at 5% damping. This figure also illustrates that, maximum DAF is obtained almost at same span length at different velocity. Maximum DAF occurs at 50 m span length for velocity 40~140 km/hr and that was occurred at 100 m span length for 160 km/hr which was same as 2.5% damping. The band width is almost same for any combination. Maximum DAF ranges from 1.25~1.55. So, Overall range is 1.14~1.55.

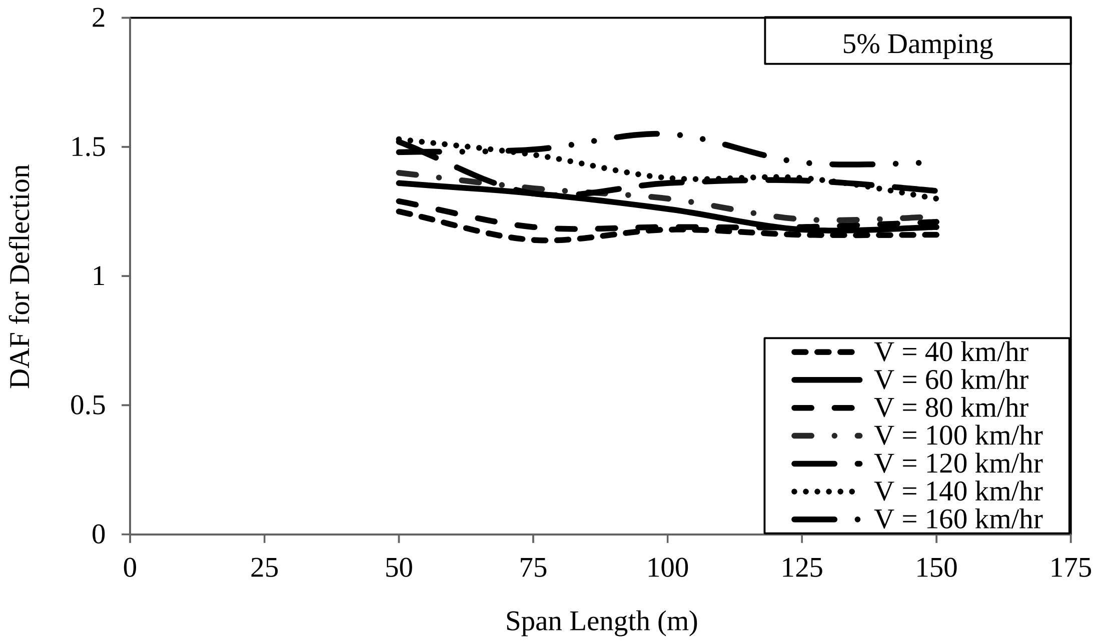

Figure 4.38: Variation of Maximum Dynamic Amplification Factor for Deflections as a Function of Span Length at Different Vehicular Speed for 5% Damping

So, total range of DAF for deflections for span length and vehicle speed variation is 1.14~3.56 for 0%, 2.5% and 5% damping and 1.14~ 1.7 for 2.5% and 5% damping for vehicle wheel position along cantilever part of the box girder bridge.

Figure 4.39 shows relationship between maximum DAF for stress at some distances from the edge of cantilever along the length of middle span and span length for different vehicular speed at 0% damping. This figure also illustrates that, for different span length maximum DAF is obtained at different velocity. Maximum DAF ranges from 1.64~3.3 which possess in the span range of 50~125 m. So, the band width is wide enough. Again, the overall range for DAF obtained is 1.23~3.3.

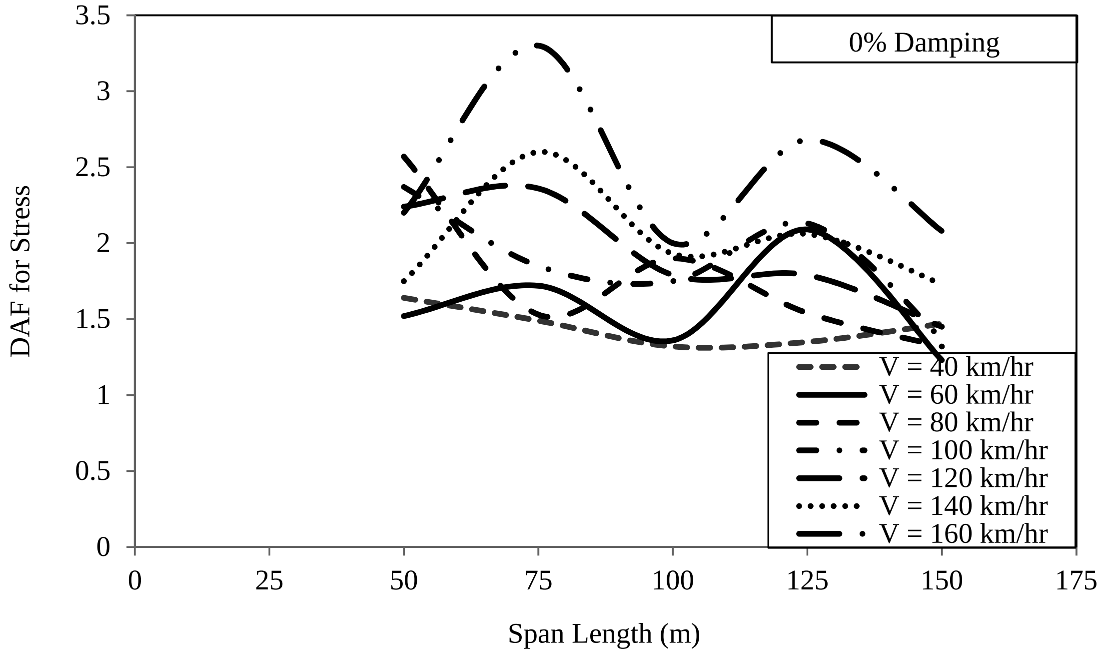

Figure 4.39: Variation of Maximum Dynamic Amplification Factor for Stresses as a Function of Span Length at Different Vehicular Speed for 0% Damping

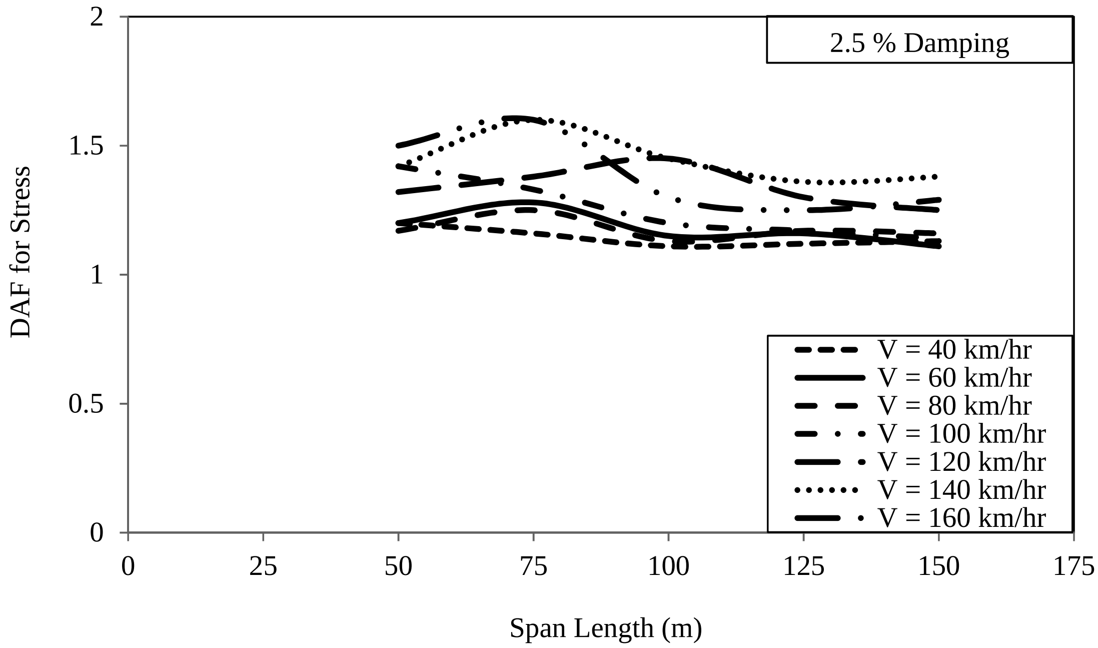

Figure 4.40: Variation of Maximum Dynamic Amplification Factor for Stresses as a Function of Span Length at Different Vehicular Speed for 2.5% Damping

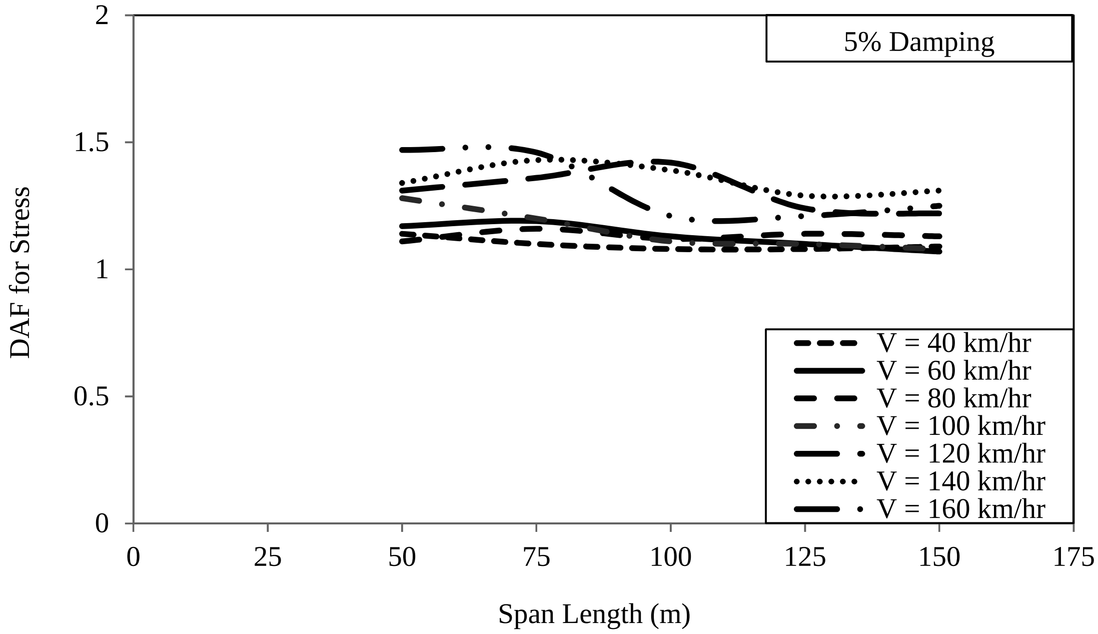

Figure 4.41: Variation of Maximum Dynamic Amplification Factor for Stresses as a Function of Span Length at Different Vehicular Speed for 5% damping

Figure 4.40 shows relationship between maximum DAF for stresses at some distances from the edge of the cantilever along the length of the middle span among the three spans of the box girder bridge and span length for different vehicular speed at 2.5% damping. Here it is also observed that, for different span length maximum DAF is obtained at different velocity. Maximum DAF ranges from 1.2~1.6 which possess in the span range of 50~100 m. So, the band width is almost same for any combination. Again, the overall range for DAF obtained is 1.11~1.6.

Figure 4.41 shows relationship between maximum DAF for stress and span length for different vehicular speed at 5% damping. It is also observed that, for different span length, it is obtained at different velocity which is same as study of relation between DAF for stresses and span length for different vehicle speed at 0% and 2.5% damping. Here, maximum DAF ranges from 1.14~1.47 which possess in the span range of 50~100 m. So, the band width is almost same for any combination. Again, overall range is 1.07~1.47.

So, total range of DAF for stresses for span length and vehicle speed variation is 1.07~3.3 for 0%, 2.5% and 5% damping and 1.07~1.60 for 2.5% and 5% damping for vehicle wheel position along the cantilever part of the box girder bridge.

So, as a whole, deflection is very critical rather than stress because maximum DAF occurs for it. Overall range for DAF variation is 1.14~3.56 for 0%, 2.5% and 5% damping and 1.14~ 1.7 for 2.5% and 5% damping for this parametric study for deflection. Again, range for DAF is 1.07~3.3 for 0%, 2.5% and 5% damping and 1.07~ 1.60 for 2.5% and 5% damping for stresses.

4.6.1.2 Influence of Span Length and Velocity for Wheel Position along Centerline of Box Girder Bridge

The variation of maximum DAFs for transverse stresses at some distances from the edge of cantilever along the length of middle span among the three spans as a function of span length at 7 different vehicular speeds are shown in Figure 4.42, 4.43 and 4.44 for 0%, 2.5% and 5% damping respectively. As wheel position was along centerline of box, effects of deflection at tip of cantilever part on DAF were negligible. So, only effects of transverse stresses are only considered in this study. The simulation was carried out for 5 different span lengths which were varied with approximate slab thickness with simultaneous change in deck height which was described in chapter 3.

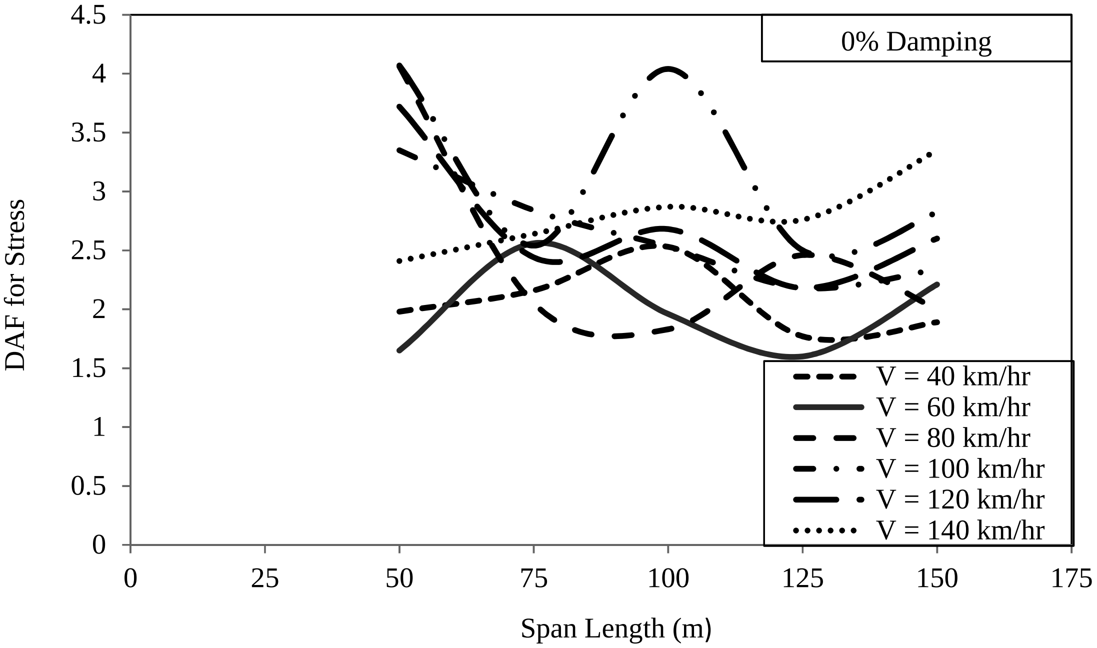

Figure 4.42: Variation of Maximum Dynamic Amplification Factor for Stresses as a Function of Span Length at Different Vehicular Speed for 0% Damping

Figure 4.42 shows relationship between maximum DAF for transverse stresses and span length for different vehicular speed at 0% damping. This figure also illustrates that, for different span length maximum DAF is obtained at different velocity. Maximum DAF ranges from 2.53~4.07 which possess in the span range of 50~150 m. So, the band width is wide enough. Again, the overall range for DAF obtained is 1.6~4.07.

Figure 4.43 shows relationship between maximum DAF for stress and span length for different vehicle speed at 2.5% damping. It also illustrates, maximum DAF is obtained almost at same span length at different velocity. Maximum DAF occurs at 50 m span for velocity 80~160 km/hr and that was occurred at 75 m span length for 40~60 km/hr. So, the band width is almost same for any combination. Maximum DAF ranges from 1.32~1.91. Again, overall range for DAF is 1.16~1.91.

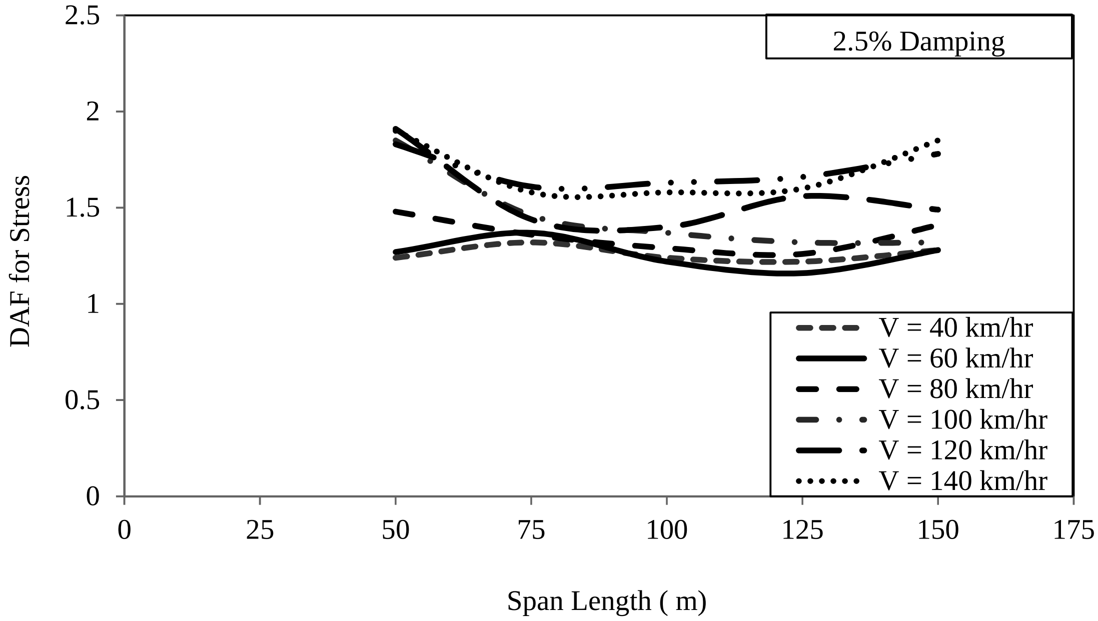

Figure 4.43: Variation of Maximum Dynamic Amplification Factor for Stresses as a Function of Span Length at Different Vehicular Speed for 2.5% Damping

Figure 4.44 shows relationship between maximum DAF for stresses and span length for different vehicular speed at 5% damping. It also illustrates that for different span length maximum DAF is obtained at different velocity. Maximum DAF ranges from 1.21~1.68

which possess in the span range of 50~150 m. So, the band width is wide enough. Again, the overall range for DAF obtained is 1.14~1.68.

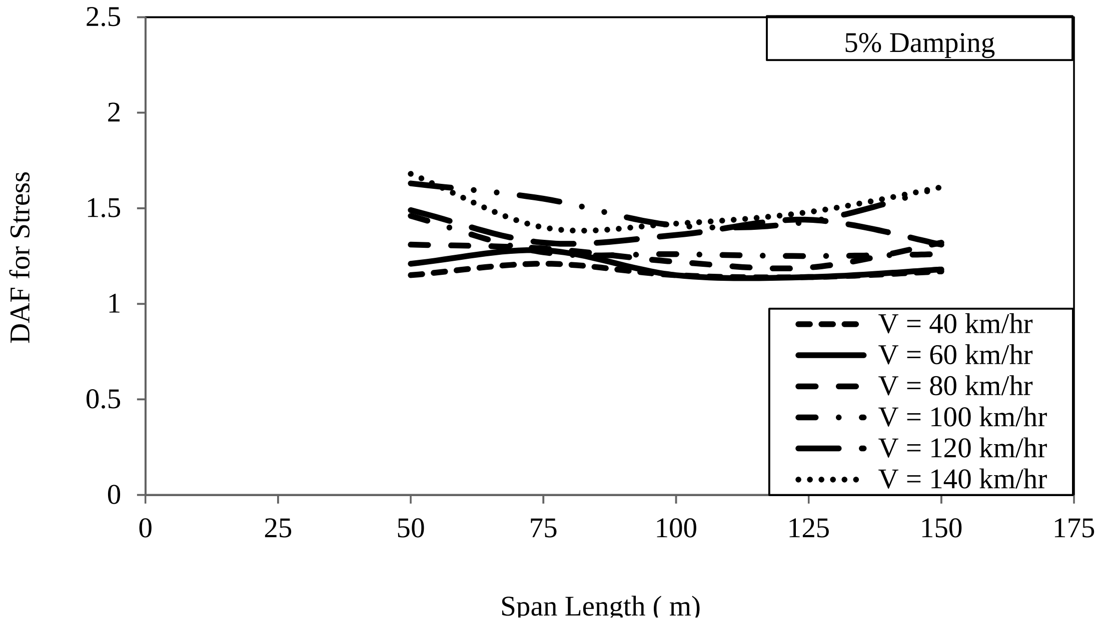

Figure 4.44: Variation of Maximum Dynamic Amplification Factor for Stresses as a Function of Span Length at Different Vehicular Speed for 5% Damping

So, total range of DAF for span length and vehicle speed variation is 1.14~4.07 for vehicle wheel position along the centerline of the box girder bridge. However, for 2.5% and 5% damping excluding 0% damping, DAF range is 1.14~1.91.

Therefore, as a whole DAF for stresses for wheel position along centerline of the box, is critical rather than DAF for stresses and deflections for wheel position along cantilever of bridge for this parametric study, as DAF obtained for stresses for this study is maximum, which is 4.07 for 0%, 2.5% and 5% damping and 1.91 for 2.5% and 5% damping.

4.6.2 Influence of Different Slab Width and Velocity on Dynamic Amplification Factor

The variation of the maximum DAF as a function of both the slab width and vehicle speed simultaneously, are shown in figure 4.45, 4.46 and 4.47 for vertical deflections at the tip of cantilever of the bridge and in figure 4.48, 4.49 and 4.50 for transverse stresses at a distance from the cantilever edge for 0%, 2.5% and 5% damping condition respectively.

Here, effects of slab width on DAF for vehicle path along centerline of the box are negligible. So, only vehicle path along cantilever of the bridge is considered in this study. The simulations were carried out for 7 different vehicle speeds and 4 different slab widths with the vehicle passing along the path always keeping a margin of 1m from the free end of cantilever.

Figure 4.45 shows relationship between maximum DAF for vertical deflections and slab width for different vehicular speed at 0% damping. This figure also illustrates that, for different span length maximum DAF is obtained at different velocity. Maximum DAF ranges from 1.88~5.8 which possess in the slab width range of 3~4 m. So, the band width is wide enough. Again, the overall range for DAF obtained is 1.51~5.8.

Figure 4.46 shows relationship between maximum DAF for vertical deflections and slab width for different vehicular speed at 2.5% damping. This figure also illustrates that, for different span length maximum DAF is obtained at different velocity as like figure 4.45. Maximum DAF ranges from 1.29~1.67 which possess in the slab width range of 3~4.5 m. So, the band width is wide enough. Again, the overall range for DAF obtained is 1.16~1.67.

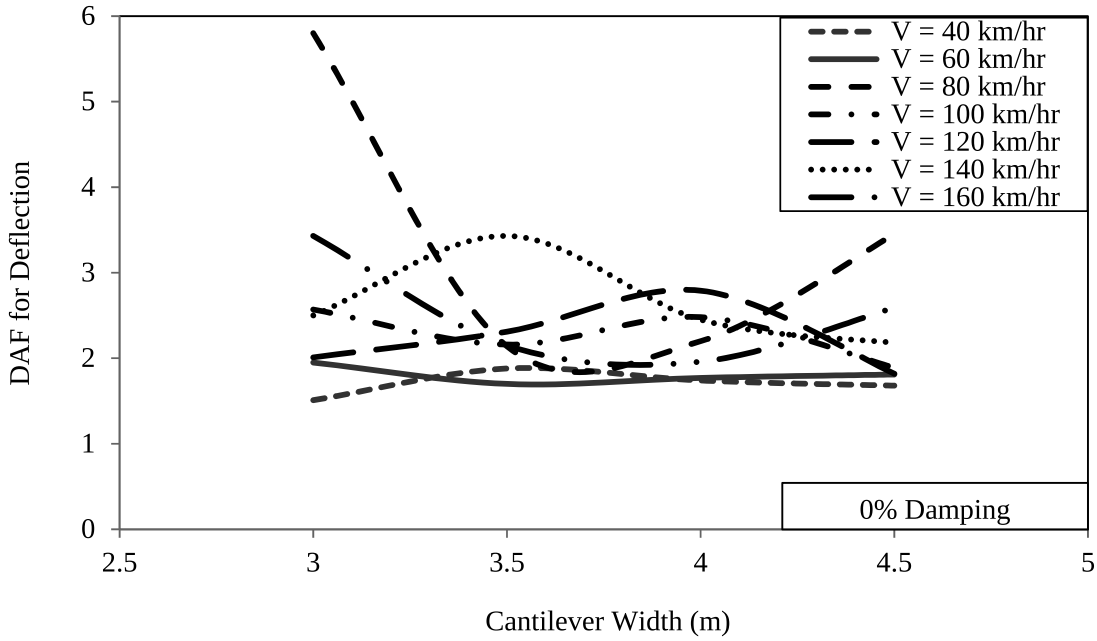

Figure 4.45: Variation of Maximum Dynamic Amplification Factor for Deflections as a Function of Cantilever Width at Different Vehicular Speed for 0% Damping

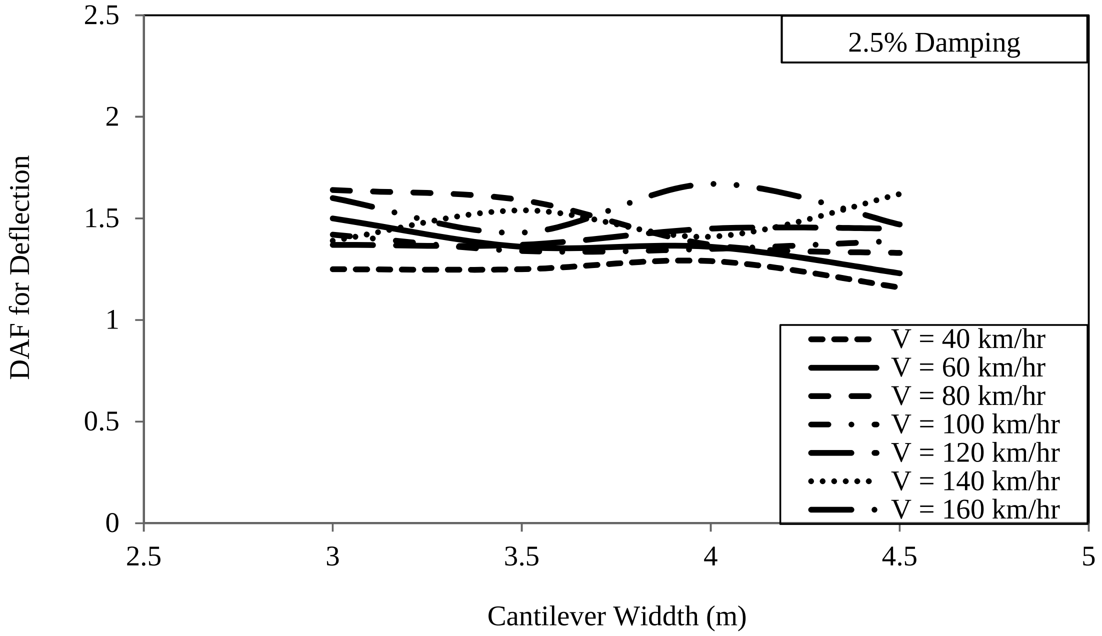

Figure 4.46: Variation of Maximum Dynamic Amplification Factor for Deflections as a Function of Cantilever Width at Different Vehicular Speed for 2.5% Damping

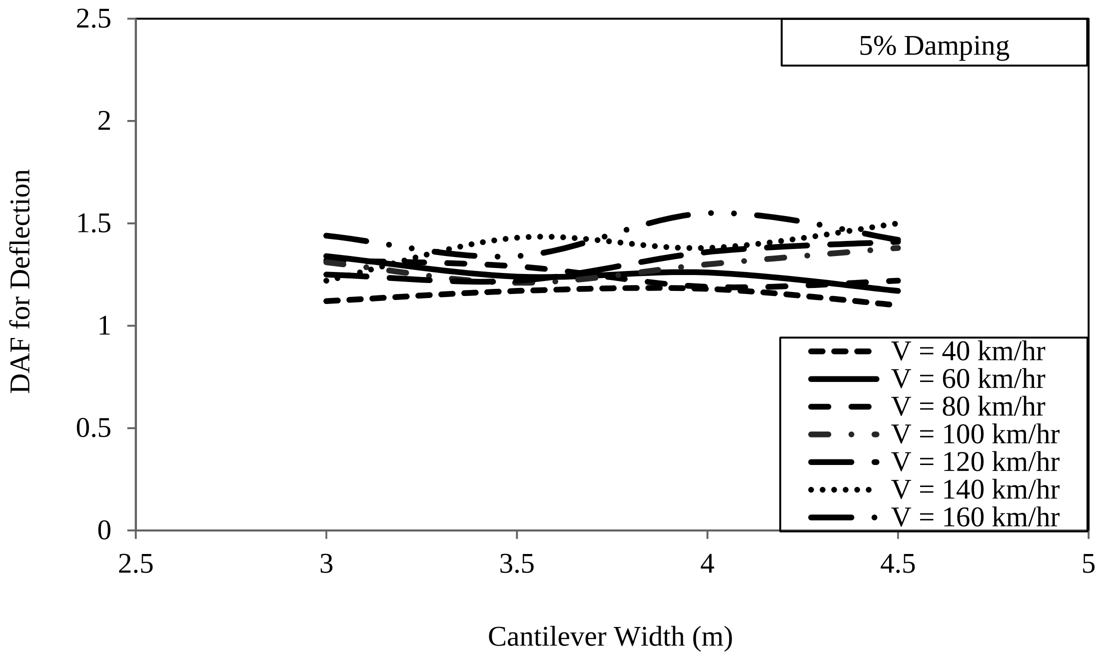

Figure 4.47: Variation of Maximum Dynamic Amplification Factor for Deflections as a Function of Cantilever Width at Different Vehicular Speed for 5% Damping

Figure 4.47 shows relationship between maximum DAF for deflections at the tip of cantilever at different points along the middle span among the three spans of bridge and slab width for different vehicular speed at 5% damping. This figure also illustrates that, for different span length maximum DAF is obtained at different velocity as like the study of relation between DAF of deflections and Slab width for different vehicular speed at 0% and 2.5% damping. Maximum DAF for deflections ranges from 1.18~1.55 which possess in the slab width range of 3~4.5 m. So, band width is wide enough. Again, overall range for DAF for deflection at the tip of cantilever for this parametric condition is 1.1~1.55.

So, the total range of Dynamic amplification factor, DAF for vertical deflections at the tip of cantilever of the bridge at different points along the middle span length among the three spans of the bridge for both cantilever width and vehicle speed variation is 1.1~5.8 with 0% damping for vehicle wheel position along the cantilever of the bridge. However, for 2.5% and 5% damping excluding 0% damping, DAF range is 1.1~1.67 for deflections.

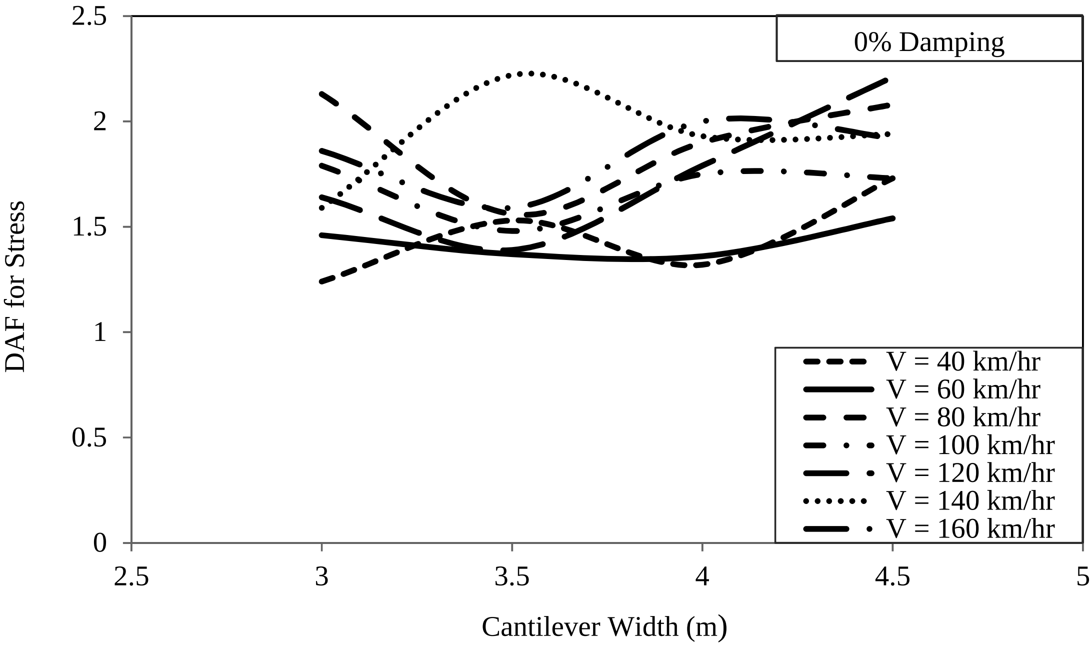

Figure 4.48: Variation of Maximum Dynamic Amplification Factor for Stresses as a Function of Cantilever Width at Different Vehicular Speed for 0% Damping

Figure 4.48 shows relationship between maximum DAF for stress at some distances from the edge of cantilever along the length of middle span and slab width for different vehicular speed at 0% damping. It also illustrates that for different span length, maximum DAF is obtained at different velocity as like the study of relation between DAF of deflections and Slab width for different vehicular speed at 0%, 2.5% and 5% damping. Maximum DAF ranges from 1.54~2.22 which possess in the slab width range of 3~4.5 m. So, band width is wide enough. Again, the overall range for DAF obtained is 1.24~2.22.

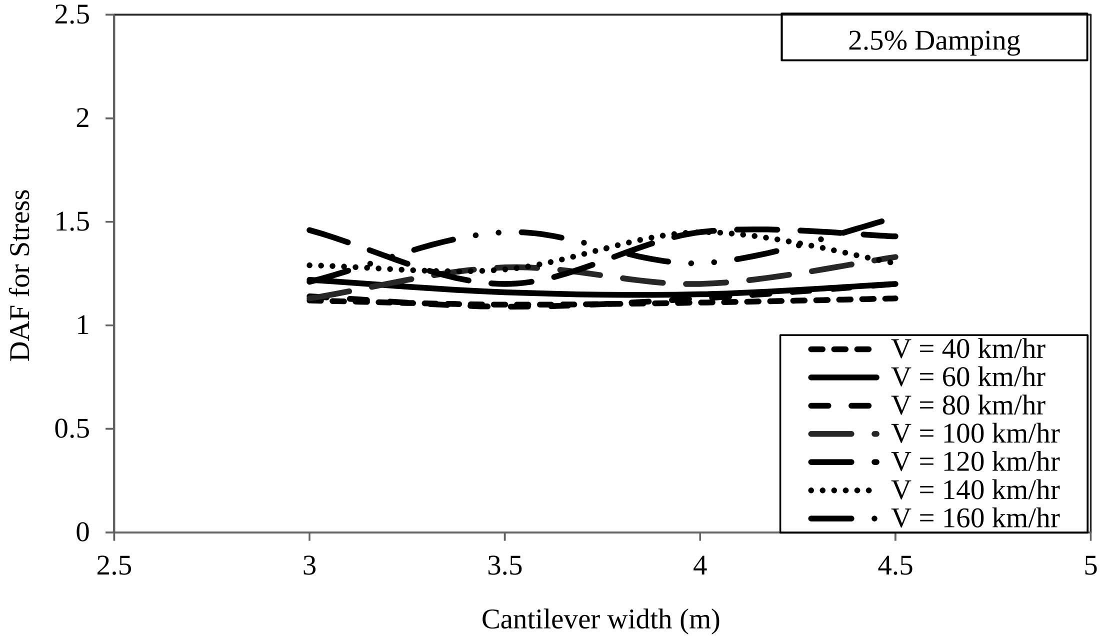

Figure 4.49: Variation of Maximum Dynamic Amplification Factor for Stresses as a Function of Cantilever Width at Different Vehicular Speed for 2.5% Damping

Figure 4.49 shows relationship between maximum DAF for stresses and slab width for different vehicular speed at 2.5% damping. This figure also illustrates that, for different span length maximum DAF is obtained at different velocity as like similar study for DAF for deflections at three damping and also for stresses at 0% damping. Maximum DAF ranges from 1.13~1.52 which possess in the slab width range of 3~4.5 m. So, the band width is wide enough. Again, the overall range for DAF obtained is 1.09~1.52.

Figure 4.50: shows relationship between maximum DAF for transverse stresses and slab width for different vehicular speed at 5% damping. This figure also illustrates that, for different span length maximum DAF is obtained at different velocity as like similar study for DAF for deflections at three damping and also for stresses at 0% and 2.5% damping.

Maximum DAF ranges from 1.1~1.46 which possess in the slab width range of 3~4.5 m. So, the band width is wide enough. Again, the overall range for DAF obtained is 1.06~1.46.

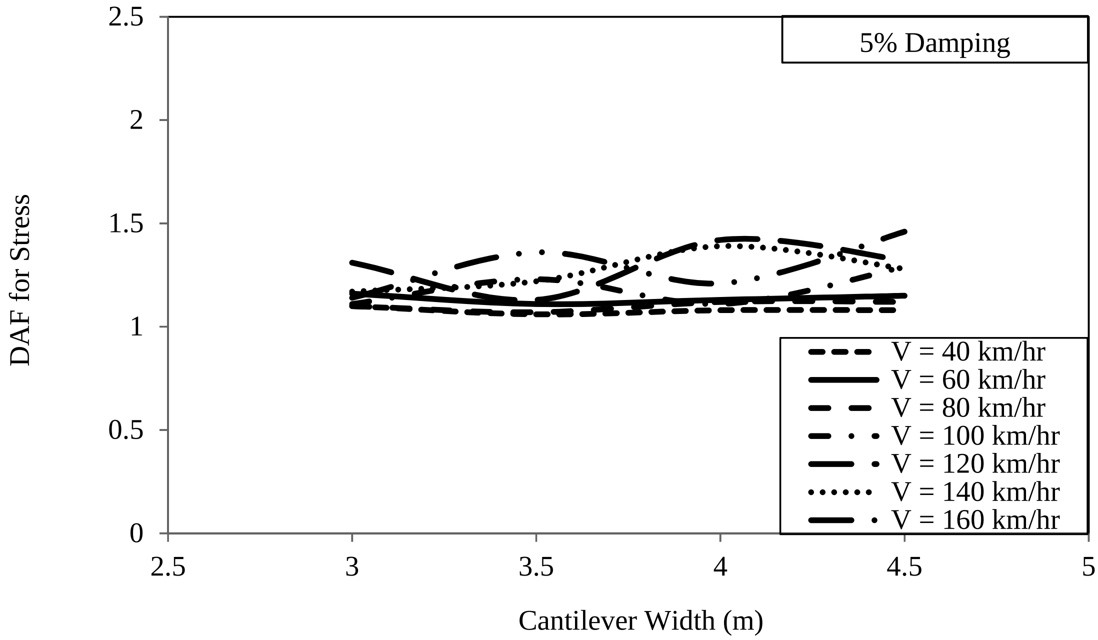

Figure 4.50: Variation of Maximum Dynamic Amplification Factor for Stresses as a Function of Cantilever Width at Different Vehicular Speed for 5% Damping

So, total range of DAF for stresses for cantilever width and vehicle speed variation is 1.06~2.22 for 0%, 2.5% and 5% damping for vehicle wheel position along the cantilever part of the box girder bridge. However, if we exclude 0% damping from our study, DAF range is 1.06~1.52 for deflections for 2.5% and 5% damping.

So, as a whole, condition for deflection is very critical because maximum DAF occurs for it as maximum DAF for this parametric study is 5.81 for 0%, 2.5% and 5% damping and 1.67 for 2.5% and 5% damping excluding 0% damping which caused for deflection rather than stress.

It can be concluded that, span length variation as well as cantilever slab width variation with different vehicle speed is very important parameter for DAF variation.

4.7 Recommendation

DAFs overviewed from our parametric study evaluate the effects of mass inertia of the deck, moment arm of wheel loads and time step required to stay on a node by the vehicle.

From the above investigation, it can be notified that for 0% damping results are very high compared to the results for 2.5% and 5% damping condition and results are almost similar for 2.5% and 5% damping for any parametric study. Again, most of the practical cases do not associated with 0% damping. So, the study offers to take a standard dynamic amplification factor for 2.5% and 5% damping rather than for 0% damping condition which is feasible for practical condition. Therefore, DAF for vertical deflections of the cantilever part of deck slab and for transverse stresses is suggested as 1.7 and 1.6 respectively for vehicle path along cantilever path of box girder bridge i.e. recommending 70% and 60% impact increment over static results calculated for deflections and stresses respectively. Again, DAF for stress for vehicle along centerline of deck of box girder bridge is recommended as 1.91 i.e. recommending 91% impact increment over static results calculated for stresses.

CHAPTER 5

CONCLUSIONS

5.1 Overview

The major purpose of this investigation and analysis was to expand our knowledge about different parameters that influence the amplitude and distribution of peak static and transient response by a moving vehicle along the cantilever part and also along centerline of the deck of the box girder bridge. The objective was also to recommend a feasible DAF value for stresses in the transverse direction at a particular distance from the edge of the cantilever and for vertical deflections at the tip of the cantilever of the box girder bridge based on the results achieved through the whole investigation. In order to do so, analysis was carried out for a 3 span box girder bridge which was modeled with different thickness at different points of the slab. Deck height was assumed variable with the span length. Results were taken at various points along the middle span. Both static and full transient dynamic analysis has been performed for different vehicle position on the span. Analysis was performed for different vehicle speeds up to 160 km/hr and different span lengths. As higher velocity is normally taken as design criteria, velocity limit was taken up to 160 km/hr in this study for academic purpose. Effects of other parameters like structural damping ratio, width of the cantilever part of the box were also being studied. By comparing the values of dynamic and static responses for stresses in the transverse direction and for vertical deflections at the tip of the cantilever at a number of points along the length of the middle span, dynamic amplification factors are determined. The dynamic amplification factor was investigated as a function of the parameters, i.e., vehicle speed, span length and cantilever slab width on the pertaining portion of the deck. Span length variation was done along with slab thickness and deck height variation to make it more practical.

5.2 Findings

On the basis of numerical analysis within the parameters that were considered, some important findings were observed. It was also found that 0% damping condition caused abnormally high values, whereas, 2.5% and 5% damping showed more practical and almost similar value. Moreover, almost all the structures have damping effect in practical. Generally 5% damping is preferred in code provision. Therefore, values for 0% damping are not considered in the following findings because of not being feasible for practical condition. So, the following conclusions can be reached with respect to the dynamic amplification factors for reinforcement design in the transverse direction of box girder bridge:

1. The variation of the DAF for vertical deflections along the span does not maintain any regularity. For most vehicle speeds, a relatively high DAF is obtained at or near 3rd pier of the bridge for most cases and most of the values stay above unity. Again, 2.5% and 5% damping condition show almost similar values of DAF which make the curves almost similar. Only vehicle along cantilever path is considered for vertical deflections, as for centerline path, vertical deflection at the tip of cantilever is negligible. Maximum DAF decreases with increment in span length. Maximum impact of 170% and 153% were obtained near pier, 152% and 145% were found near midspan for 2.5% and 5% damping respectively. So, overall findings were maximum impact of 170% near pier and 152% near midspan for vertical deflection.

2. The DAF for stresses varies along the span in a fluctuating manner for vehicle path along cantilever part and also along centerline of deck of box girder bridge. For both the vehicle path, high DAFs are obtained at or near the piers and the DAFs at the intermediate points along the spans are somewhat smaller for most of the cases. But it was found that DAF for stresses for vehicle along centerline is more critical than that of vehicle along cantilever part. Maximum impact of 160% and 147% were obtained near pier, 124% and 117% were found near midspan for 2.5% and 5% damping respectively for vehicle at cantilever part. Again, maximum impact of 191% and 168% were obtained near pier, 178% and 159% were found near midspan for 2.5% and 5% damping respectively for vehicle at centerline part. So, overall finding were maximum impact of 160% near pier, 124% near midspan for stress for vehicle at cantilever part and maximum impact of 191% near pier, 178% near midspan for stress for vehicle at centerline of box.

3. Cantilever slab width variation cannot influence the DAF variation to show proportionate changes with it. The investigation proposed to take a standard dynamic amplification factor 1.52 and 1.46 near pier, 1.31 and 1.25 near midspan for stresses in the transverse direction of the cantilever part of deck slabs for 2.5% and 5% damping respectively i.e. recommending 52% and 46% stress increment near pier and 31% and 25% stress increment near midspan respectively. Again, for deflection at the tip of cantilever, maximum DAF was found 1.67 and 1.55 near pier, 1.64 and 1.45 near midspan for 2.5% and 5% damping respectively i.e. recommending 67% and 55% deflection increment near pier and 64% and 45% deflection increment near midspan respectively. So, overall findings recommended 52% stress increment near pier and 31% stress increment near midspan, 67% deflection increment near pier and 64% deflection increment near midspan.

4. DAF for deflections does not vary proportionately or in a regular manner with the vehicle speed but it can be said from analysis that DAF increase with increment in vehicle speed. DAFs at piers are higher than that of other points or midspan. The maximum DAFs for deflection at midspan and near pier occur for 160 km/h vehicle speed. Overall output recommended taking the maximum dynamic amplification factor 1.42 and 1.38 for 2.5% and 5% damping respectively for vertical deflections at the tip of the cantilever for vehicle at cantilever part which occurs at a distance 3L/4 from 2^{nd} pier i.e. recommending 42% and 38% deflection increment near pier respectively. Again, DAF for deflection at midspan was found 1.22 and 1.2 for 2.5% and 5% damping respectively i.e. recommending 22% and 2% deflection increment correspondingly. So, overall findings recommended considering 42% deflection increment near pier and 22% deflection increment at midspan.

5. The DAF for stresses does not vary proportionately or in a regular manner with the vehicle speed either but it can be said that DAF increase with increment in vehicle speed. DAFs at piers are higher than that of other points or midspan. Conditions are more critical for stresses for vehicle at centerline than that of stresses and deflections for vehicle at cantilever part as DAF is higher in this case. So, the investigation recommended taking the standard

dynamic amplification factor 1.45, 1.42 at pier and 1.09, 1.07 at midspan for stresses in the transverse direction for 2.5% and 5% damping respectively for vehicle path along cantilever i.e. recommending 45% and 42% stress increment near pier, 9% and 7% stress increment near midspan correspondingly. Again, for vehicle at centerline path, maximum DAF was found 1.28 and 1.32 at 3L/2 distance from 2nd pier and 1.5 and 1.38 at midspan for stress for 2.5% and 5% damping respectively and for 160 km/h vehicle speed which recommends 28%, 32% increment in stress near pier and 50%, 38% stress increment near midspan. So, overall findings suggested that 45% and 9% stress increment near pier and midspan respectively for vehicle at cantilever part and 32% and 50% stress increment near pier and midspan for vehicle at centerline of the box.

6. Dynamic response is also influenced by span length variation with different vehicle speed. It can be observed that for almost all the velocities, DAF value decreases with increment in span length. It was seen that condition for stress for vehicle at centerline path is more critical. For vehicle along cantilever part of box girder bridge, maximum DAF for deflection recommends value of 1.7 and 1.55 and for stress recommends value of 1.6 and 1.47 for 2.5% and 5% damping respectively. For vehicle along centerline part, maximum in terms of stress recommends value of 1.91 and 1.68 for 2.5% and 5% damping respectively.

7. Cantilever slab width variation with different vehicle speed also influence DAF variation. Overall output recommended taking a standard dynamic amplification factor 1.52 and 1.46 for stresses in the transverse direction of the cantilever part of deck slabs for 2.5% and 5% damping respectively i.e. recommending 52% and 46% stress increment correspondingly. For deflection at the tip of cantilever, maximum DAF was found 1.67 and 1.55 for 2.5% and 5% damping respectively i.e. recommending 67% and 55% deflection increment correspondingly.

From all the findings, it can be seen that in most cases DAF value is higher near pier. Flexibility is less and rigidity is higher near pier. So, a bumping effect acts here. For this reason DAF value is higher near pier than any part of bridge for most cases.

5.3 Recommendations

From the findings of above article 5.2, it can be recommended to take a standard dynamic amplification factor for 2.5% and 5% damping rather than for 0% damping condition. Hence, DAF value for vertical deflections of the cantilever part of deck slab is recommended as 1.7 near pier and 1.64 near midspan i.e. recommending 70% and 64% impact increment near pier and midspan over static results calculated for deflections. Again, DAF for stresses is recommended as 1.91 near pier and 1.78 near midspan i.e. recommending 91% impact increment near pier and 78% near midspan over static results calculated for stresses.

5.4 Scope of Future Study

The exposition provides an enhanced approach to evaluate the dynamic amplification factor for various parameters. However, some more issues are required to be studied in order to advance towards a more accurate result. Some of these issues pertinent to the evaluation of the dynamic amplification factor are described below:

- Lump mass system including axles, wheels, shafts, brakes can be introduced to describe the application of external loads as a component and thus improve the vehicle model.
- Simulation can be carried out for different road surface roughness conditions.
- Influence of vehicle mass may be investigated in the parametric study.
- Non-linear analysis can be performed.
- The simulation results may be verified with actual numerical results derived from field tests.
- A series of trucks or lane loads can be considered instead of a single truck.
- Investigations may be done for various vehicle wheel positions along the deck slab and cantilever part of box girder bridge.
- Further investigations may be carried out for prestressing effects on the dynamic amplification factor.

REFERENCES

Amanat, K.M., Amin, A.F.M.S., Hossain, T.R., Kabir, A., Rouf, M.A., "Cracks in the Box Girders of Bongobondhu Jamuna Multipurpose Bridge – Identification of Causes Based on FE Analysis", Advances in Bridge Engineering – *II*, IABSE-JSCE Joint Conference, Dhaka, Bangladesh, 8-10 August, 2010.

Agarwal, A.C. and Billing, J.R. (1990), *Dynamic testing of the St.-Vincent Street Bridge*, Proceeding of the Annual Conference of the Canadian Society for Civil Engineering, May 16-18, Hamilton, Ont., Vol. IV, pp. 163-181.

American Society of Civil Engineers (ASCE) (1931), *Impact on Highway Bridges*, Final Report of the Special Committee on the Impact in Highway Bridges, ASCE Transaction, pp. 1089-1117.mmj

American Society of Civil Engineers (ASCE) (1981), *Recommended Design Loads for Bridges*, Committee on Loads and forces on Bridges, Journal of the Structural Division, ASCE, 107(7), pp. 1161-1213.

Indian Road Congress (IRC) (1996), *Standard Specifications & Code of Practice for Road Bridges Section II*, IRC 6, New Delhi, Clause 211.

American Association of State Highway and Transportation Officials (AASHTO) (2002), *Standard Specifications for Highway Bridges*, AASHTO, and Washington, D.C. Article 3.7.6 and Figure 3.7.7A.

American Association of State Highway and Transportation Officials (AASHTO) (2002), *Standard Specifications for Highway Bridges*, AASHTO, and Washington, D.C. Article 3.8.1 and Article 3.8.2.

American Association of State Highway Officials (AASHO) (1962), *The AASHO Road Test*, National Academy of Sciences – National Research Council, Washington D.C.

Bakht, B. and Pinjarkar, S.G. (1989), *Review of Dynamic Testing of Highway Bridges*, Structural Research Report SRR 89-01, Ministry of Transportation of Ontario, Downsview, Ontario.

Bakht, B. and Pinjarkar, S.G. (1989), *Dynamic Testing of Highway Bridges – A Review*, Transportation Research Report 1223, Transportation Research Board, National Research Council, Washington, D.C., pp. 93-100.

Biggs, J.M. and Suer, H.S. (1955), *Vibration Measurements of Simple Span Bridges*, Highway Research board, Bulletin 124, Washington D.C.

Billing, J.R. (1984), *Dynamic Loading and Testing of Bridges in Ontario*, Canadian Journal of Civil Engineering, 11, pp. 833-843.

Billing, J.R. and Green, R. (1984), *Design Provisions for Dynamic Loading of Highway Bridges*, Transportation Research Board, Washington, D.C. pp. 94-103.

Brady, S. P., O'Brien, E. J. and Žnidarič, A. (2006), *Effect of Vehicle Velocity on the Dynamic Amplification of a Vehicle Crossing a Simply Supported Bridge*, Journal of Bridge Engineering, Volume 11, Issue 2, pp. 241-249, March/April, 2006, © ASCE, ISSN 1084-0702(2006)11:2(241).

Broquet, C., Baily, S. F., Fafard, M. and Brühwiler, E. (2004), *Dynamic Behavior of Deck Slabs of Concrete Road Bridges*, Journal of Bridge Engineering, Volume 9, Issue 2, pp. 137-146, March/April, 2004, © ASCE, ISSN 1084-0702(2004)9:2(137).

Buckland, P. G. (1981), *Recommended Design Loads for Bridges, Journal of Structural Engineering, ASCE,* 107(7), pp. 1161-1213.

Campbell, T.I., Csagoly, P.F. and Agarwal, A.C. (1977), *Frequency Matching in Continuous Post-Tensioned Concrete Highway Bridges*, ACI Special Publication SP60-7 on Vibrations of Concrete Structures, pp. 139-154

Chaallal, O. and Sahawy, M. (1998), *Experimental Evaluation of the Dynamic Amplification Factor for Evaluation of Bridge Performance*, Department of Construction Engineering, university of Quebec, Technical Report No. ETS.DRSR.98.1

Chan, T.H.T. and O'Connor, C. (1990a), *Wheel Loads from Highway Bridge Strain*: Field Studies, Journal of Structural Engineering, ASCE, 116(7), pp. 1751–1771.

Chan, T.H.T. and O'Connor, C. (1990b), *Vehicle model for highway bridge impact*, Journal of Structural Engineering, ASCE, 116(7), pp. 1772–1793.

Chopra, A.K. (2002), *Dynamics of Structures*, 2nd Edition, Prentice Hall of India, New Delhi, 2002, Chapter 3, Chapter 4.

Coussy, O., Said, M. and Van Hoore, J.P. (1989), *The Influence of Random Surface Irregularities on the Dynamic Response of Bridges under Suspended Moving Loads*, Journal of Sound and Vibration, 130(2), pp. 313-320.

Csagoly, P.F., Campbell, T.I. and Agarwal, A.C. (1977), *Bridge Vibration Study*, Research Report 181, Ministry of Transportation of Ontario, Downview, Ontario

Deeba, Farah (January 2008), *Dynamic Amplification Factor in the Cantilever Part of the Box Girder Bridge for Transverse Reinforcement*, B.U.E.T., Dhaka

Edgerton, R.C. and Beecroft, G.W. (1955), *Dynamic Studies of Two Continuous Plate Girder Bridge*, Highway Research Board, Bulletin 124, Washington D.C., pp. 33-46.

Fafard, M., Laflamme, M., Savard, M., Bennur, M (1998), *Dynamic Analysis of Existing Continuous Bridge*, Journal of Bridge Engineering, Volume 3, Issue 1, pp. 28-37, February, 1998, © ASCE, ISSN 1084-0702(1998)3:1(28).

Fleming, F.J. and Romualdi, J.P. (1961), *Dynamic Response of Highway Bridges*, Journal of the Structural Division, ASCE, 87, (7), pp. 31-60.

Foster,G.M. and Oehler, L.T. (1955), *Vibration and Deflection of Rolled Beam and Plate Girder Bridges*, Highway Research Board, Bulletin 124, Washington D.C., pp. 79-110.

Green, M.F. and Cebon, D. (1992), *Dynamic tests on two highway bridges, in: Heavy Vehicles and Roads: Technology*, Safety and Policies, London, 1992, pp. 138-145.

Gupta, R. K. and Traill-Nash, R. W. (1980), *Vehicle breaking on highway bridges*, *Journal of the Engineering Mechanics Division*, 106(4), pp. 641-658.

Hayes, J. M. and Sbarounis, J. A. (1956), *Vibration study of three-span continuous I-beam bridge*, Highway Research Board, Bulletin 124, Washington D.C., pp. 47-78.

Huang, T. (1976), *Vibration of bridges, Shock Vtbr. Dig.* 8, pp. 61-76

Hwang, E.S. and Nowak, A.S. (1991), *Simulation of Dynamic Load for bridges*, Journal of Structural Engineering, Structural Division, ASCE, 117(5), pp. 1413-1434.

Hossain, Kazi Ashfaq (October, 2009), *Dynamic Amplification Factor for the Design of Transverse Reinforcement in the Deck of Box Girder Bridge*, B.U.E.T., Dhaka

Inbanathan, M.J. and Wieland, M. (1987), *Bridge Vibrations Due to Vehicle Moving Over Rough Surface*, Journal of Structural Engineering, Structural Division, ASCE, 113(9), pp. 1994-2008.

Jagadeesh, T. R. and Jayram, M. A. (2004), *Finite Element Procedures*, Prentice Hall of India, New Delhi, 2004, pp.803-806

Jagadeesh, T. R. and Jayram, M. A. (2000), *Design of Bridge Structures*, Prentice Hall of India, New Delhi, 2004, pp.82-83.

Kim, S., Nowak, A. S., (1997), *Load Distribution and Impact Factors for I-Girder Bridges*, Journal of Bridge Engineering, Volume 2, Issue 3, pp. 97-104, August, 1997, © ASCE, ISSN 1084-0702(1997)2:3(97).

Klaus-Jürgen Bathe, (2004), *Finite Element Procedures*, Prentice Hall of India, New Delhi, 2004, pp.803-806

Leonard, D.R. (1974), *Dynamic Tests on Highway Bridges, Test Procedures and Equipment*, TRRL Laboratory Report 654, Transport and Research Laboratory, Crowthorne, United Kingdom.

Li, H., Wekezer and J., Kwasniewski, L., (2008), *Dynamic Response of a Highway Bridge Subjected to Moving Vehicles*, Journal of Bridge Engineering, Volume 13, Issue 5, pp. 439-448, September/October, 2008, © ASCE, ISSN 1084-0702(2008)13:5(439).

Manual of ANSYS v.13, Elan Computer Group, Inc., USA, 1997

Mclean, D. I., Lee Marsh, M. (1996), *Dynamic Impact Factors for Bridges*, National Cooperative Highway Research Program, National Research Council (U.S.). Transportation, 1996, pp.12-15

Nassif, H.H. and Nowak, A.S. (1995), *Dynamic Load Spectra for Girder Bridges*, Transportation Research Board, Annual Meeting, 1995, pp. 69-83.

Nowak A. S. (1995), *Calibration of LRFD bridge code, Journal of Structural Engineering,* 121(8), pp. 1245-1251.

Nowak, A.S., Hong, Y. and Hwang, E. (1991), *Modeling Live Load and Dynamic Load for Bridges*, Transportation Research Record 1290, Transportation Research Board, National Research Council, Washington, D.C., pp. 110-118.

O'Connor, C. and Chan, T.H.T. (1988a), *Dynamic Wheel Loads from Bridge Strains*, Journal of Structural Engineering, ASCE, 114 (8), p1703-1723

O'Connor, C. and Chan, T.H.T. (1988b), *Dynamic Wheel Loads from Bridge Strains: Laboratory Studies*, Journal of Structural Engineering ASCE, 114 (8), p1724-1740

O'Connor, C. and Pritchard, R.W. (1985), *Impact Studies on Small Composite Girdr Bridge*, Journal of Structural Engineering, ASCE, Vol. 111, No. 3, pp. 641-653.

OHBDC (1979), Ontario Highway Bridge Design Code, MTC, Highway Engineering, Downsview, Ontario

Page, J. (1976), *Dynamic wheel load measurements on motorway bridges*, TRRL Laboratory Report 722, Transport and Road Research Laboratory, Crowthorne, United Kingdom.

Palamas, J., Cousy, O. and Bamberger, Y. (1985), *Effects of Surface Irregularities upon The Dynamic Response of Bridges under Suspended Moving Loads*, Journal of Sound and Vibration, 99(2), pp. 235-245.

Paultre, P., Challal, U., and Proulx, J. (1992), *Bridge dynamics and dynamic amplification factors — A review of analytical and experimental findings*, Canadian Journal of Civil Engineering, 19(2), pp. 260–278.

Rich, Farhana Haque (March, 2009), *Dynamic Amplification Factor for the Design of Transverse Reinforcement in the Cantilever Part of the Box Girder Bridge*, B.U.E.T., Dhaka

Samaan, M., Kennedy and J. B., Sennah, K. (2007), *Impact Factors for Curved Continuous Composite Multiple-Box Girder Bridges*, Journal of Bridge Engineering, Volume 12, Issue 1, pp. 80-88, January/February, 2007, ©ASCE, ISSN 1084-0702(2007)12:1(80).

Sennah, K. M., Zhang, X. and Kennedy, J. B. (2004), *Impact Factors for Horizontally Curved Composite Box Girder Bridges*, Journal of Bridge Engineering, Volume 9, Issue 6, pp. 512-520, November/December 2004, ©ASCE, ISSN (ASCE) 1084-0702(2004)9:6(512).

Shepherd, R and Aves R.J. (1973), *Impact Factor for Simple Bridges*, Auckland University, Wanaganui City Council, ICE Proceedings, Vol. 55, Issue No. 1, pp. 191-210.

Shepherd, R. and Sidwell, G.K. (1977), *Investigations of the Dynamic Properties of Five Concrete Bridges*, Fourth Australian Conference on the Mechanics of Structures and Materials, university of Queensland, Brisbane, Australia, August 20-22, pp. 261-268

Shi, X., Cai, C. S. and Chen, S. (2008), *Vehicle Induced Dynamic Behavior of Short-Span Slab Bridges Considering Effect of Approach Slab Condition*, Journal of Bridge Engineering, Volume 13, Issue 1, pp. 83-92, January/February, 2008, © ASCE, ISSN 1084-0702(2008)13:1(83).

Sweatman, P.F. (1983), *Effect of Heavy Vehicle Suspensions on Dynamic Road Loading*, Research Report ARR no. 16, Vermont South, Victoria, Australia: Australian Road Research Board (ARRB).

Tung, C.C. (1967), *Random Response of Highway Bridges to Vehicle Loads*, Journal of the Engineering Mechanics Division, ASCE, 93(5), pp. 79-94.

Veletsos, A.S. (1970), *Analysis of Dynamic Response of Highway Bridges*, Journal of the Engineering Mechanics Division, ASCE, 96(5), pp. 593-620.

Walker, W.H. and Veletsos, A.S. (1963), *Response of Simple-Span Highway Bridges to Moving Vehicles*, Research and Development Studies, Report 0289, U.S. Department of Commerce, Bureau of Public Roads.

Wang, T.L., Huang, D. and Sahawy, M. (1996), *Dynamic Behavior of Continuous and Cantilever Thin-Walled Box Girder Bridges*. Journal of Bridge Engineering, Volume 1, Issue 2, pp. 67-75, May 1996, © ASCE, ISSN 1084-0702(1996)1:2(67).

Whitmore, A.P. (1970), *Dynamic Pavement Loads of Heavy Highway Vehicles*, National Cooperative Highway Research Program, Report 105, Sponsored by AASHTO.

Wright, D.T. and Green, R. (1959), *Highway Bridge Vibrations Part I, A Review of Previous Studies*, Department of Civil Engineering, Queen's University, Report 4, Kingston, Ontario.

Wright, D.T. and Green, R. (1963), *Highway Bridge Vibrations Part II, A Review of Previous Studies*, Department of Civil Engineering, Queen's University, Report 5, Kingston, Ontario.

Appendix A

A. Time History Responses

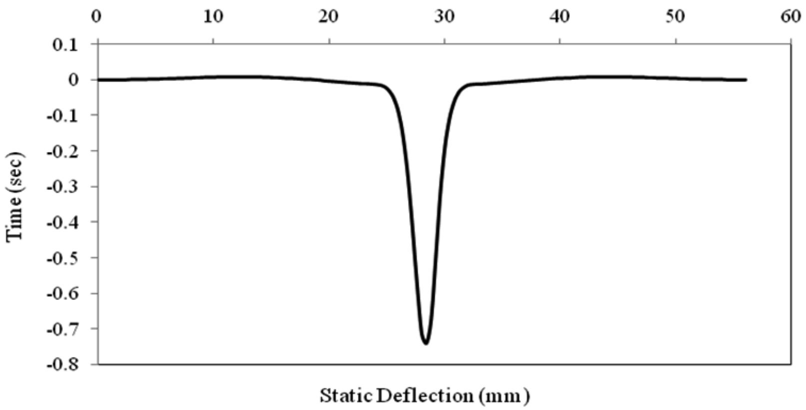

Fig A1 : Time Response for Static Deflection for V = 80 km/hr

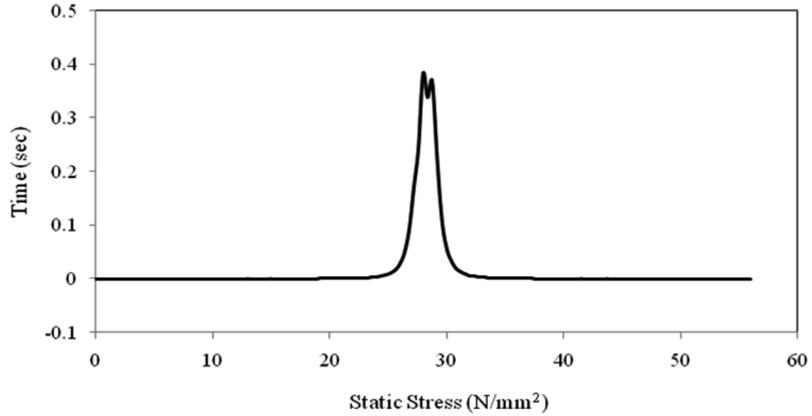

Fig A2: Time Response for Static Stress for V = 80 Km/hr

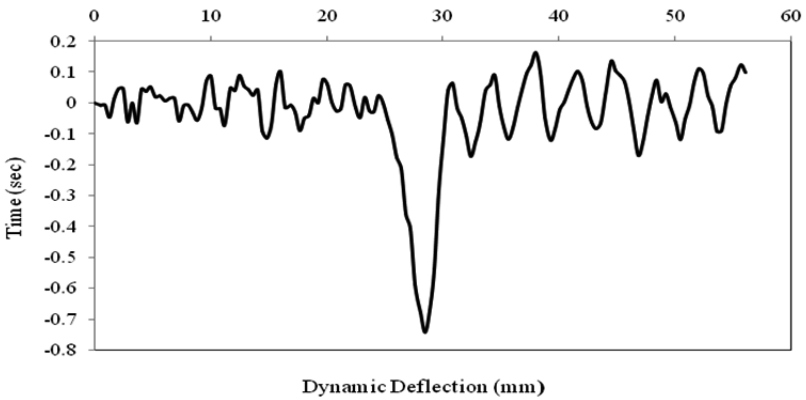

Fig A3 : Time Response for Dynamic Deflection for V = 80 km/hr

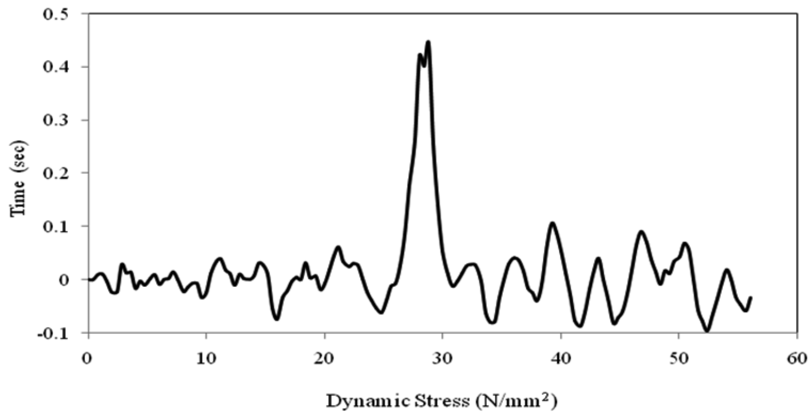

Fig A4 : Time Response for Dynamic Stress for V = 80 km/hr

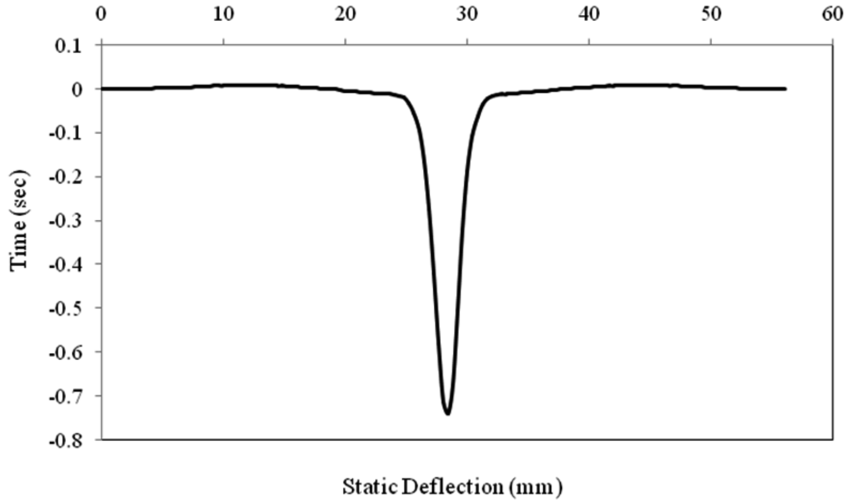

Fig A5 : Time Response for Static Deflection for V = 120 km/hr

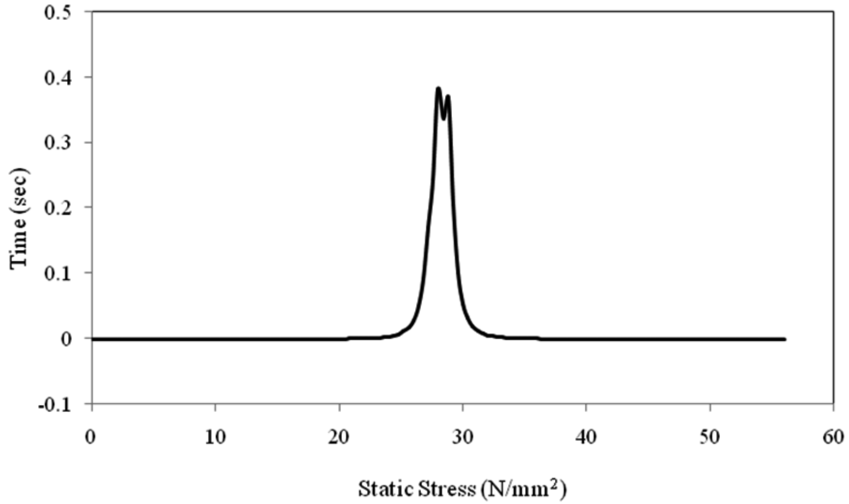

Fig A6 : Time Response for Static Stress for V = 120 Km/hr

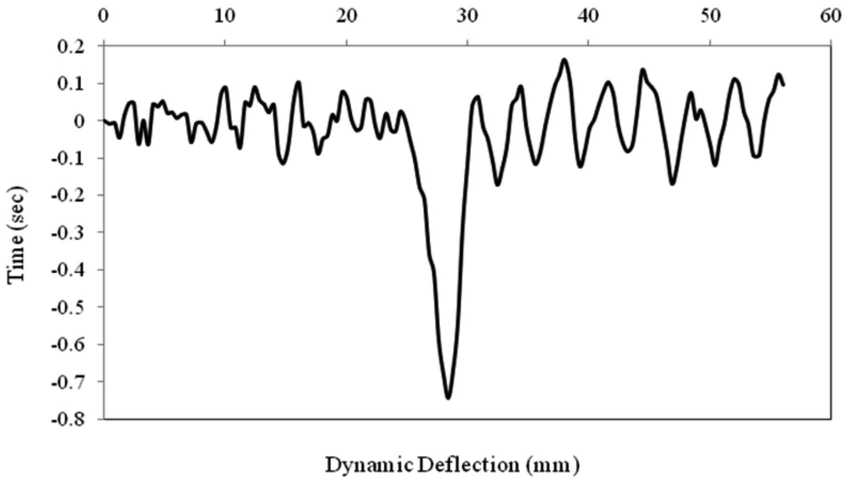

Fig A7 : Time Response for Dynamic Deflection for V = 120 km/hr

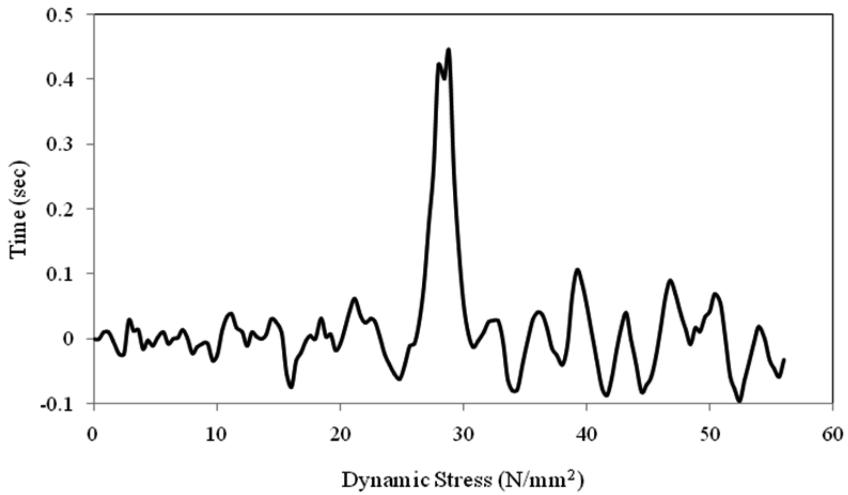

Fig A8: Time Response for Dynamic Stress for V = 120 km/hr

Appendix B

B.1 DAF Variation along the Length of the Middle Span for Different Span Length for Vehicle Position along Cantilever Part of Box Girder Bridge

B.1.1 Variation along the Length of the Middle Span in Terms of Vertical Deflections

B.1.1.1 Variation for Span Length = 50 m

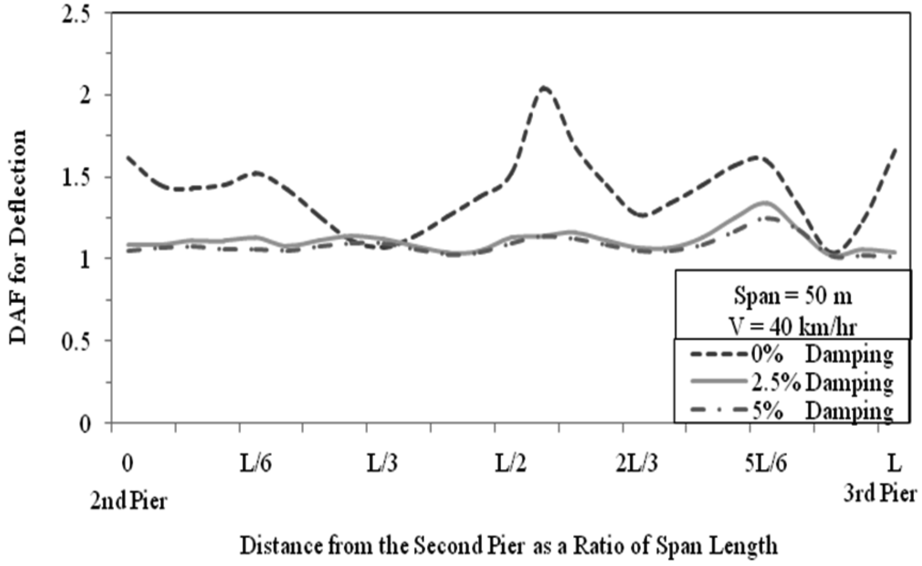

Fig B1.1 : DAF for Deflection for 50 m Span Length and V = 40 km/hr

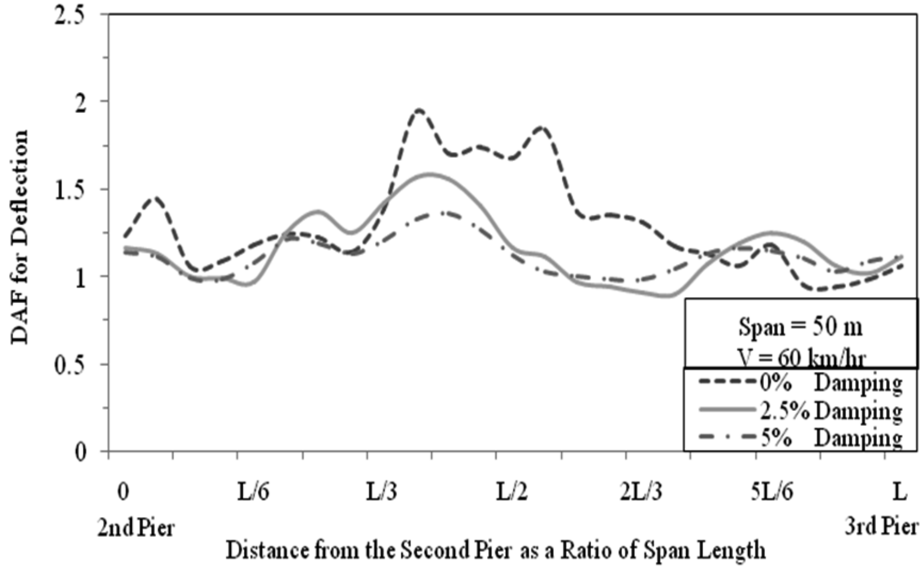

Fig B1.2 : DAF for Deflection for 50 m Span Length and V = 60 km/hr

Fig B1.3 : DAF for Deflection for 50 m Span Length and V = 80 km/hr

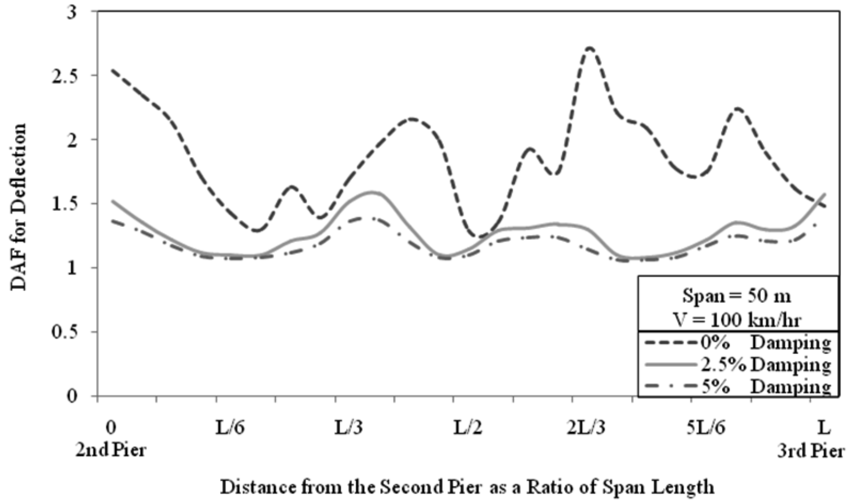

Fig B1.4 : DAF for Deflection for 50 m Span Length and V = 100 km/hr

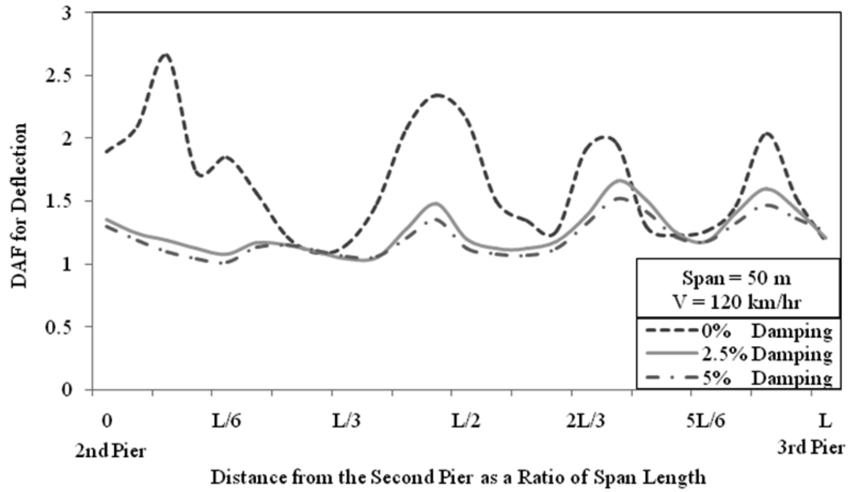

Fig B1.5 : DAF for Deflection for 50 m Span Length and V = 120 km/hr

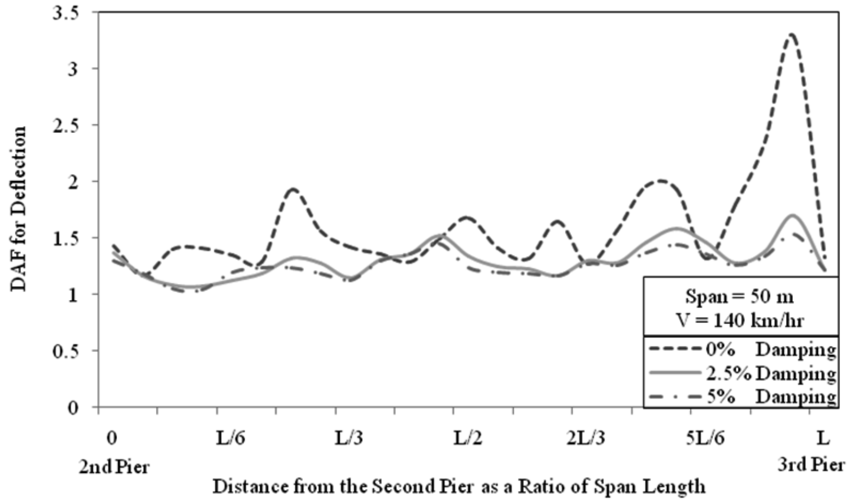

Fig B1.6 : DAF for Deflection for 50 m Span Length and V = 140 km/hr

B.1.1.2 Variation for Span Length = 75 m

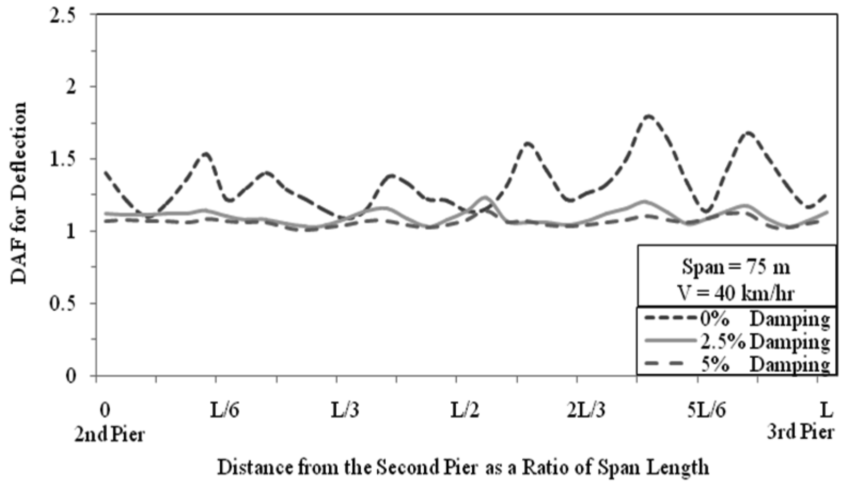

Fig B1.7 : DAF for Deflection for 75 m Span Length and V = 40 km/hr

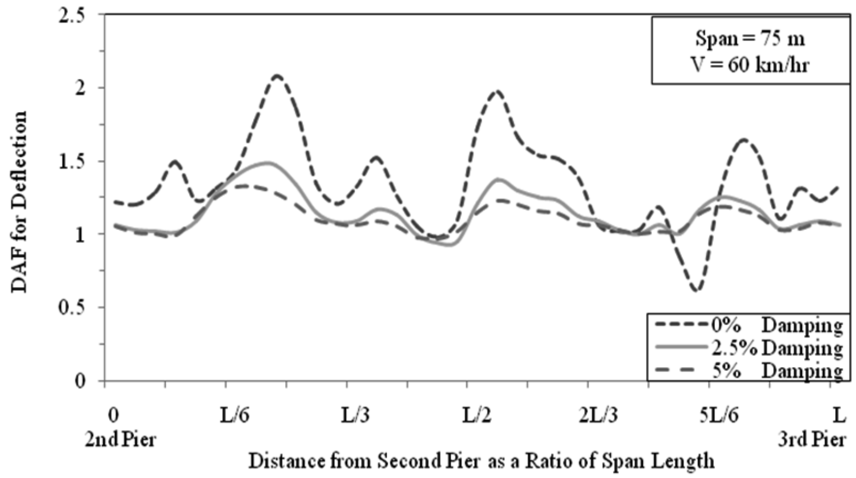

Fig B1.8 : DAF for Deflection for 75 m Span Length and V = 60 km/hr

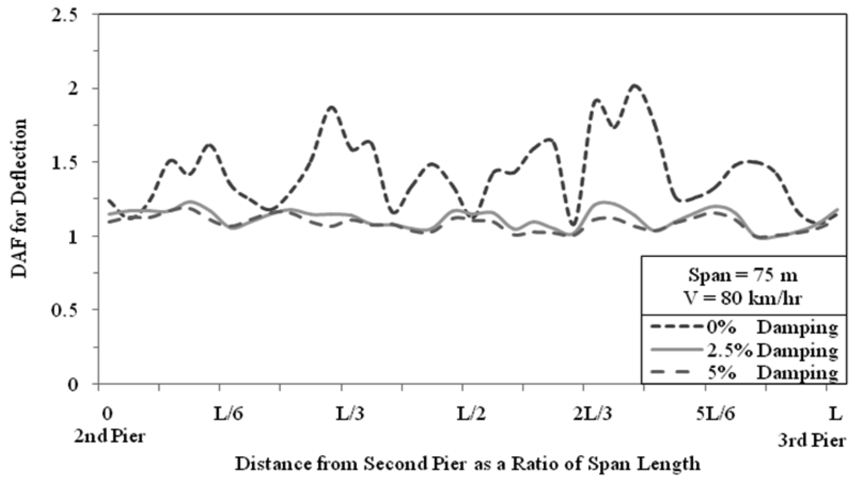

Fig B1.9 : DAF for Deflection for 75 m Span Length and V = 80 km/hr

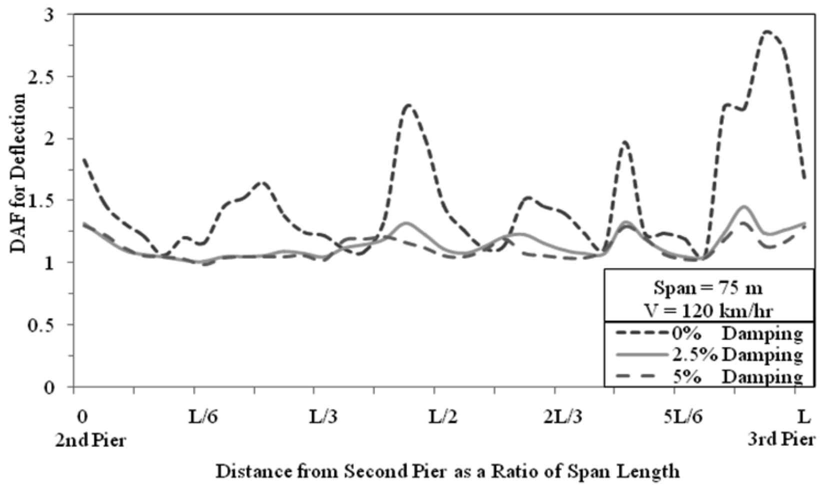

Fig B1.10 : DAF for Deflection for 75 m Span and V = 120 km/hr

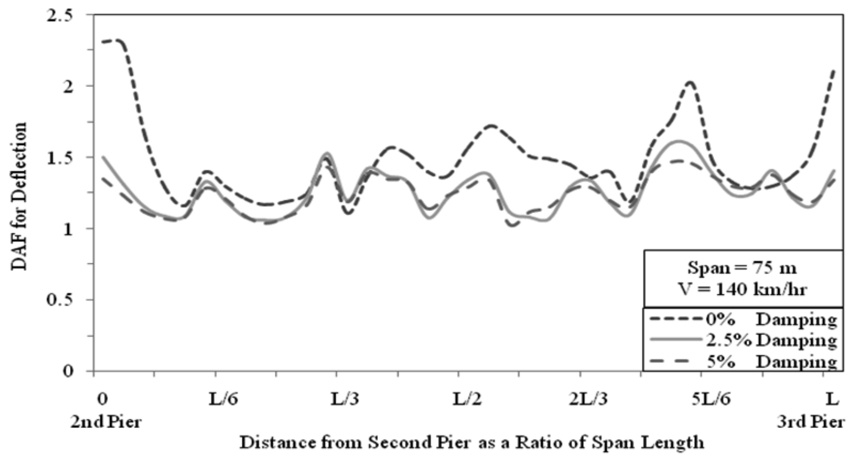

Fig B1.11 : DAF for Deflection for 75 m Span and V = 140 km/hr

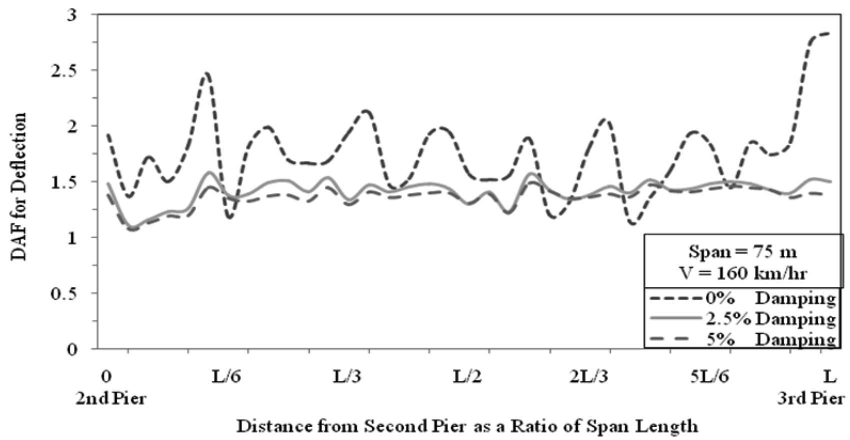

Fig B1.12 : DAF for Deflection for 75 m Span Length and V = 160 km/hr

B.1.1.3 Variation for Span Length = 100 m

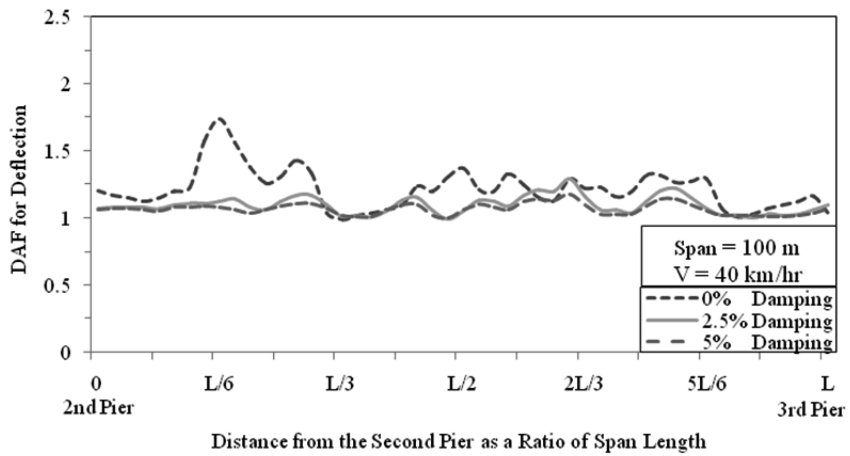

Fig B1.13 : DAF for Deflection for 100 m Span Length and V = 40 km/hr

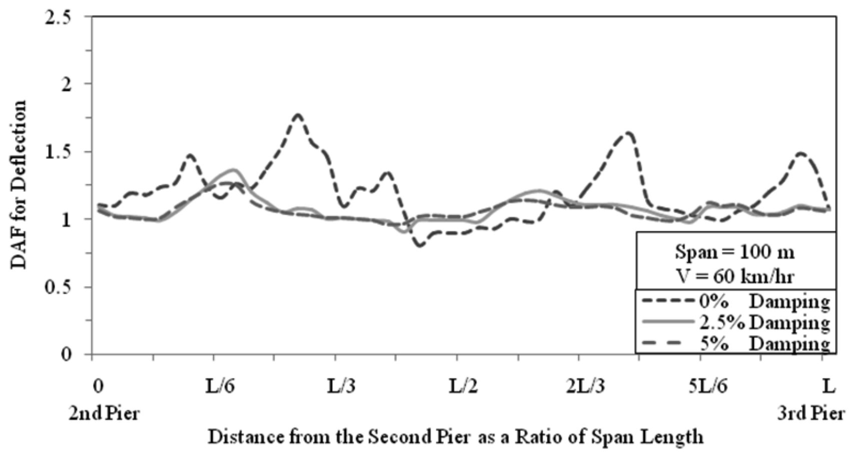

Fig B1.14 : DAF for Deflection for 100 m Span Length and V = 60 km/hr

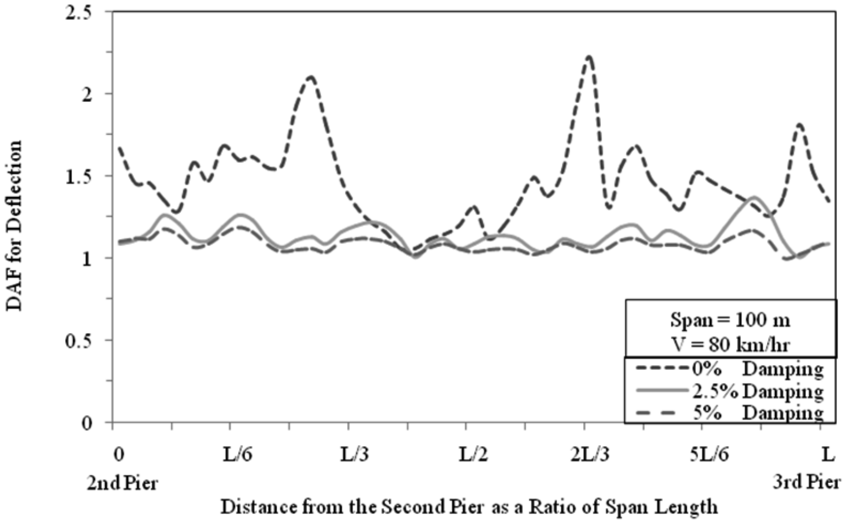

Fig B1.15 : DAF for Deflection for 100 m Span Length and V = 80 km/hr

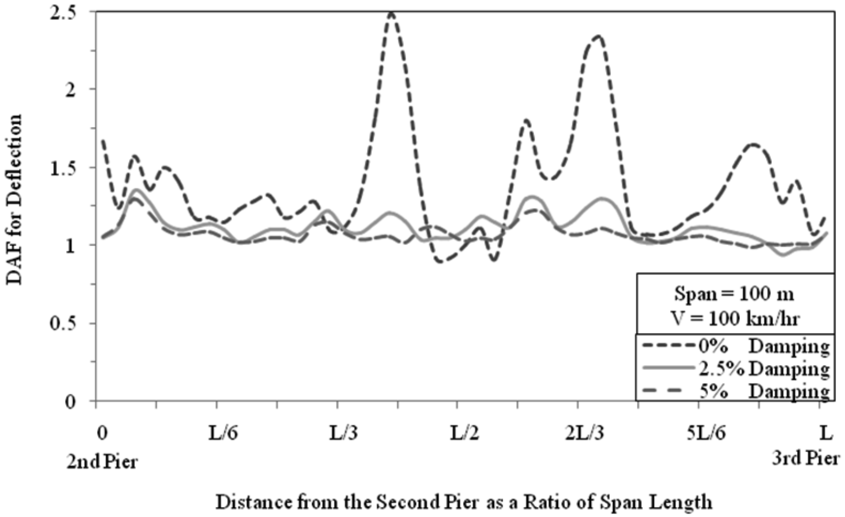

Fig B1.16: DAF for Deflection for 100 m Span Length and V = 100 km/hr

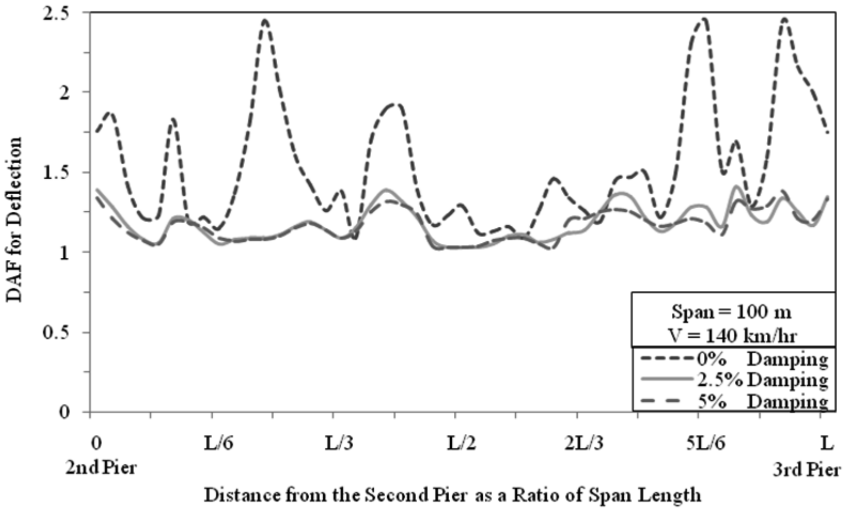

Fig B1.17 : DAF for Deflection for 100 m Span Length and V = 140 km/hr

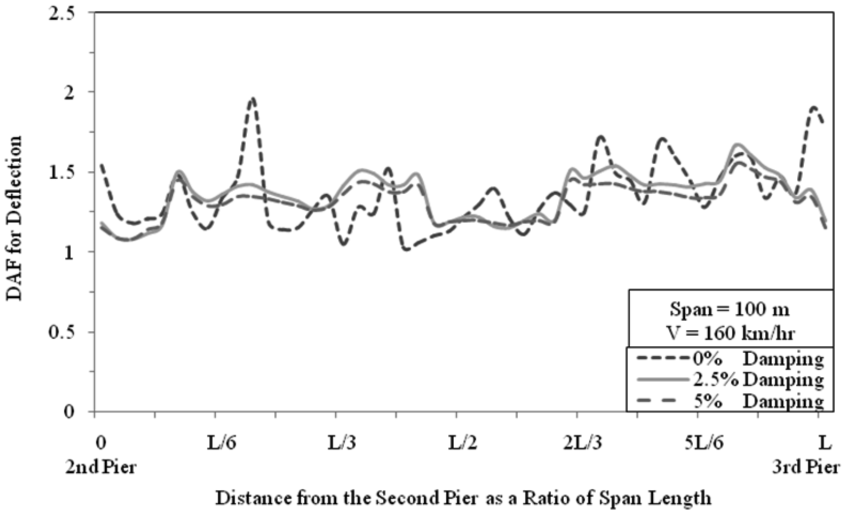

Fig B1.18 : DAF for Deflection for 100 m Span Length and V = 160 km/hr

B.1.1.4 Variation for Span Length = 125 m

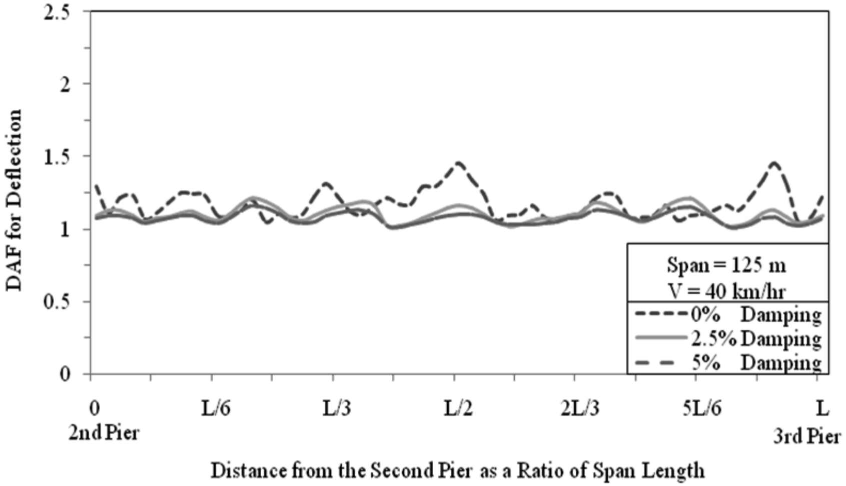

Fig B1.19 : DAF for Deflection for 125 m Span Length and V = 40 km/hr

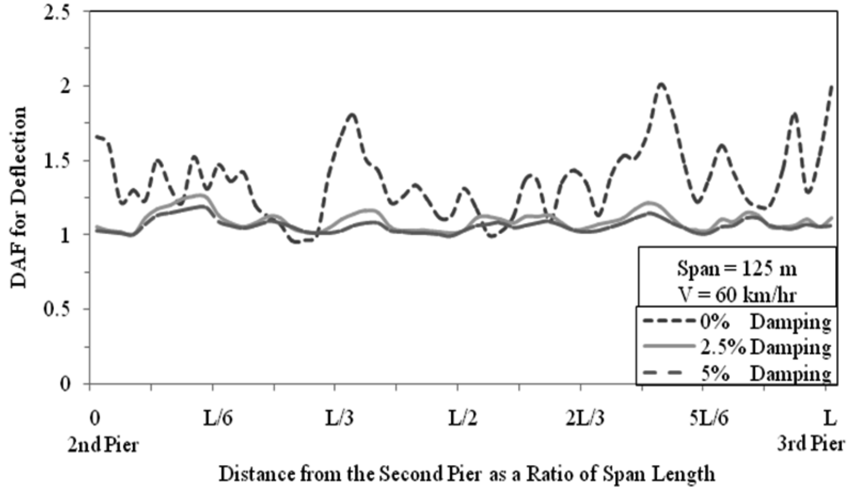

Fig B1.20 : DAF for Deflection for 125 m Span Length and V = 60 km/hr

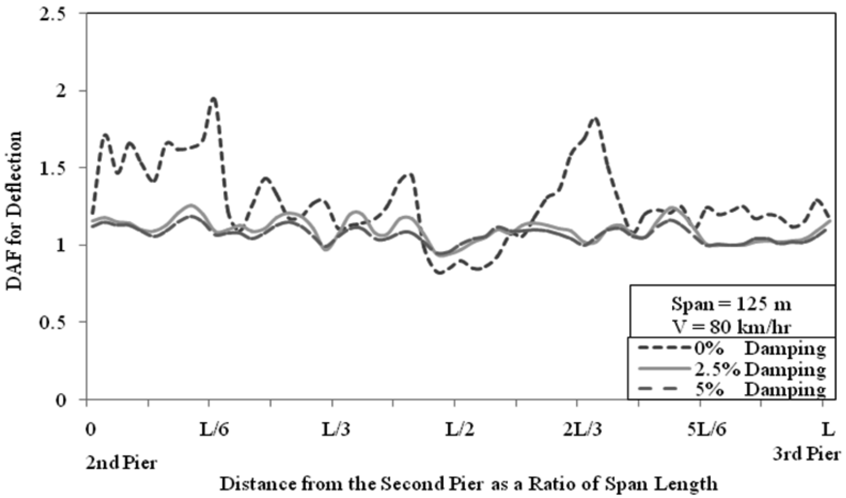

Fig B1.21 : DAF for Deflection for 125 m Span Length and V = 80 km/hr

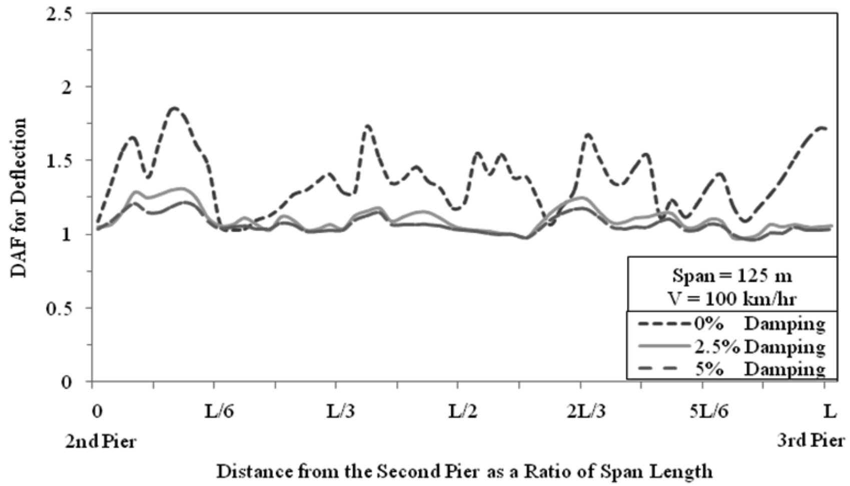

Fig B1.22 : DAF for Deflection for 125 m Span Length and V = 100 km/hr

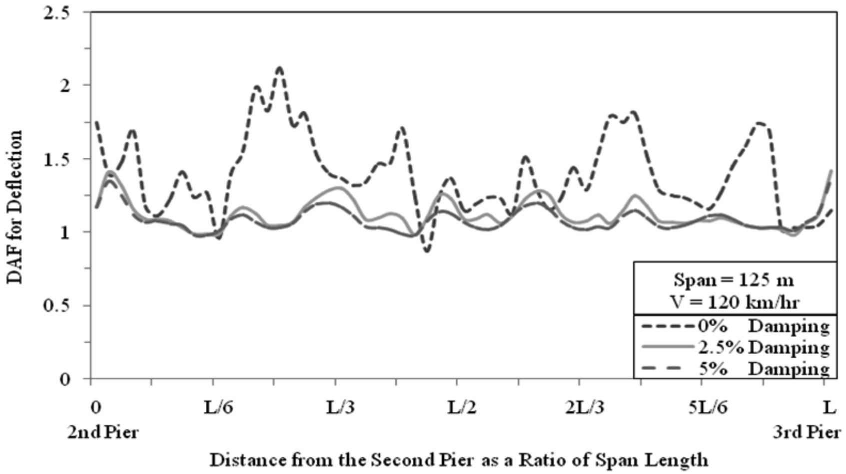

Fig B1.23 : DAF for Deflection for 125 m Span Length and V = 120 km/hr

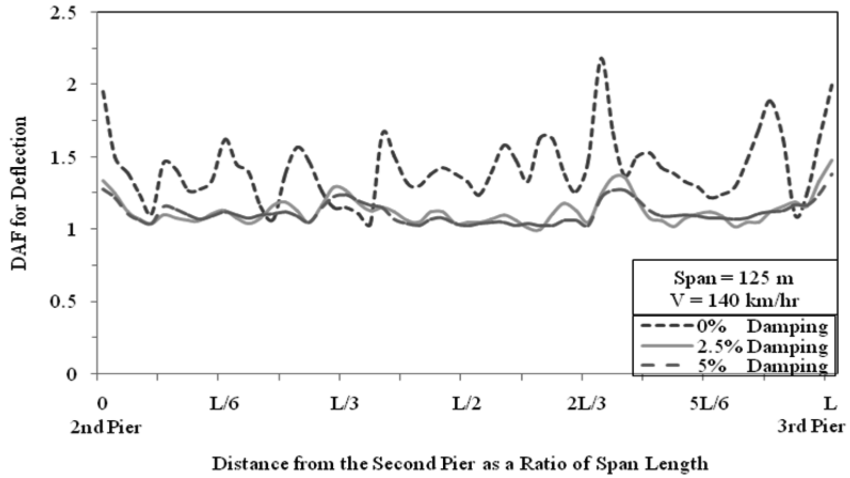

Fig B1.24 : DAF for Deflection for 125 m Span Length and V = 140 km/hr

B.1.1.5 Variation for Span Length = 150 m

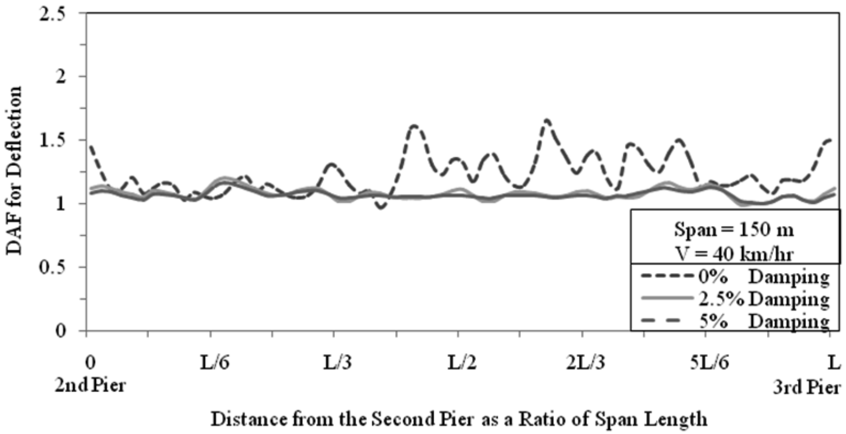

Fig B1.25 : DAF for Deflection for 150 m Span Length and V = 40 km/hr

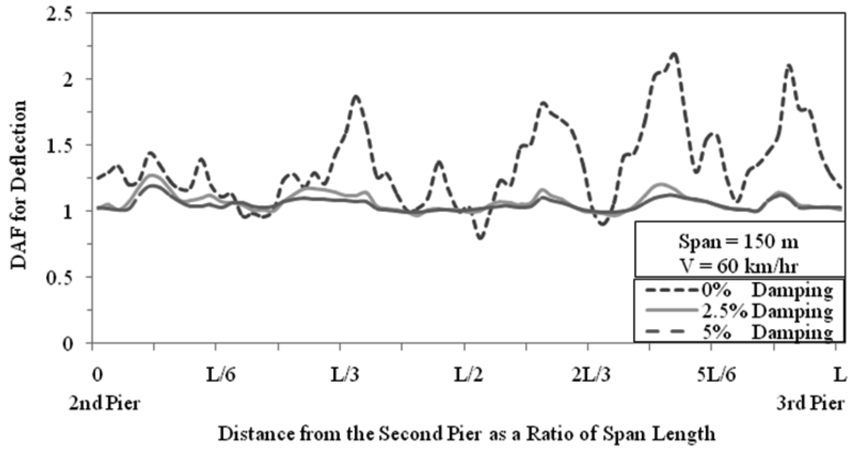

Fig B1.26: DAF for Deflection for 150 m Span Length and V = 60 km/hr

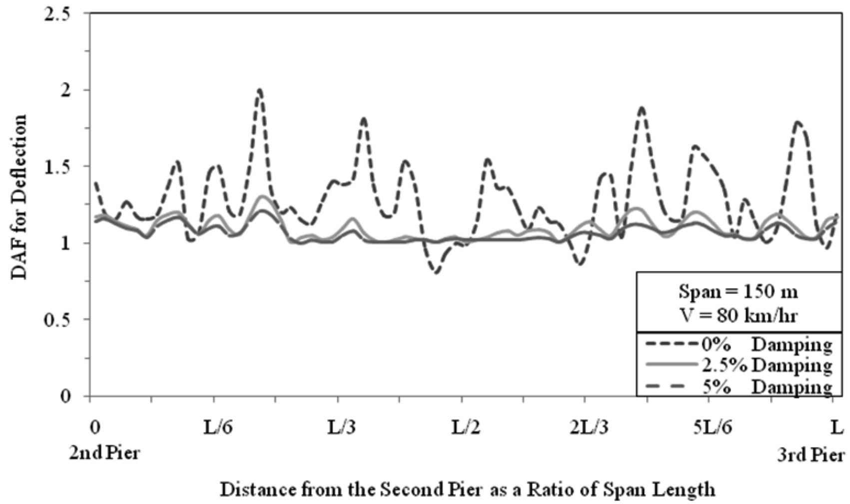

Fig B1.27 : DAF for Deflection for 150 m Span Length and V = 80 km/hr

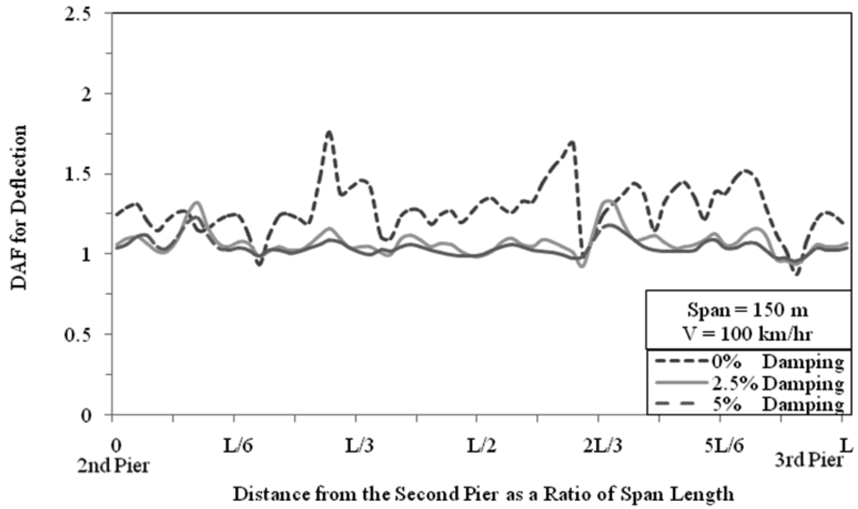

Fig B1.28 : DAF for Deflection for 150 m Span Length and V = 100 km/hr

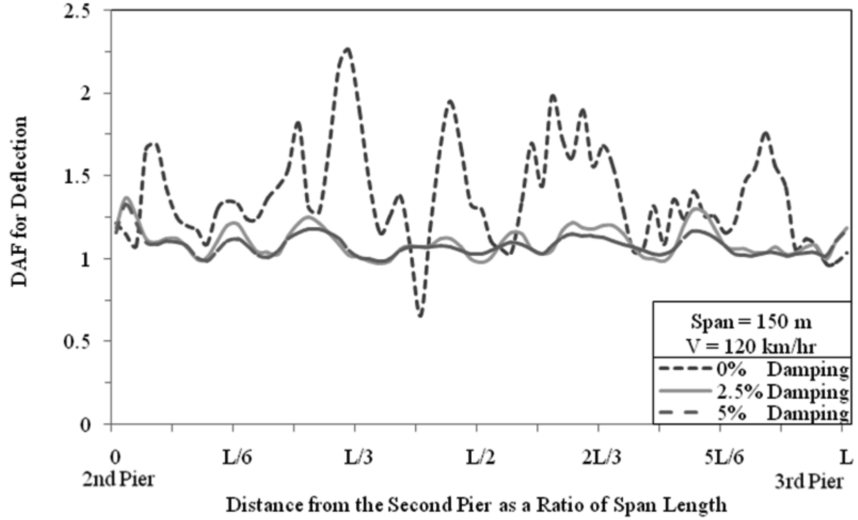

Fig B1.29 : DAF for Deflection for 150 m Span Length and V = 120 km/hr

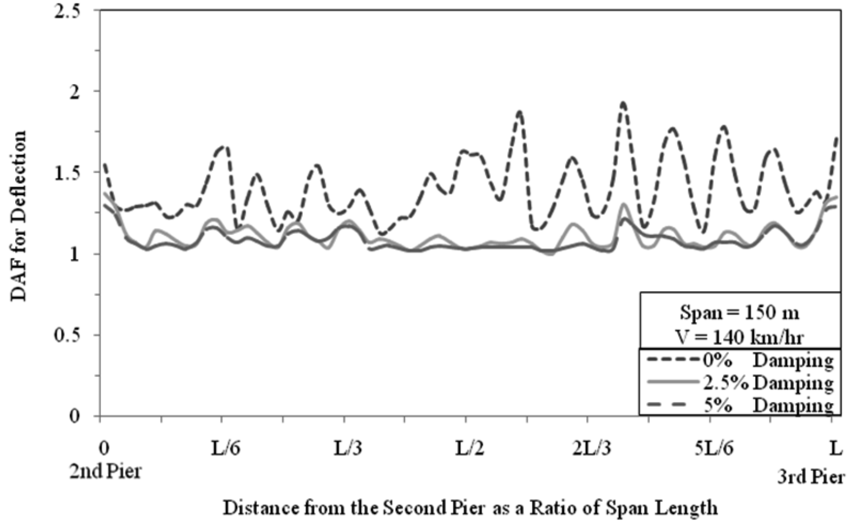

Fig B1.30 : DAF for Deflection for 150 m Span Length and V = 140 km/hr

B.1.2 Variation along the Length of the Middle Span in Terms of Stress

B.1.2.1 Variation for Span Length = 50 m

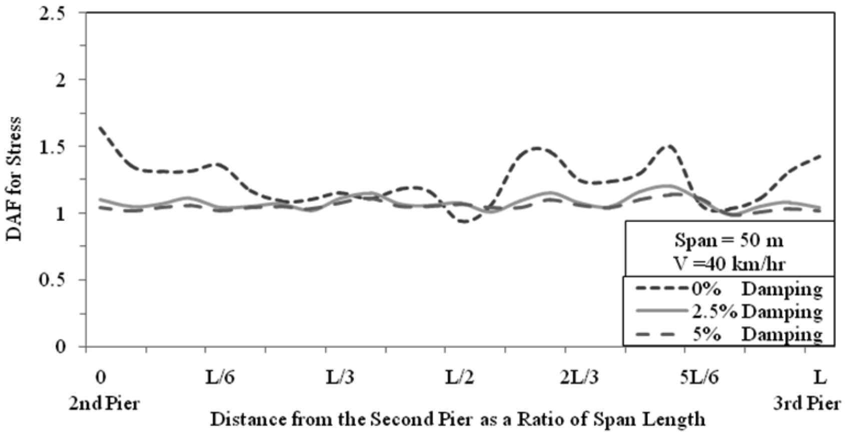

Fig B1.31 : DAF for Stress for 50 m Span Length and V = 40 km/hr

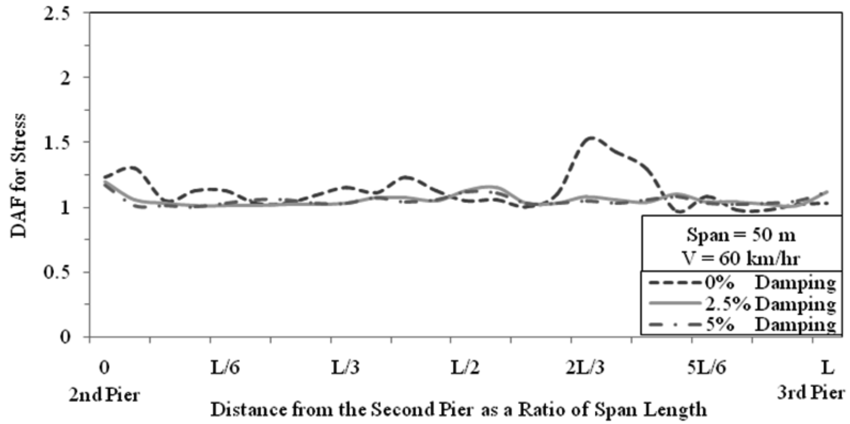

Fig B1.32 : DAF for Stress for 50 m Span Length and V = 60 km/hr

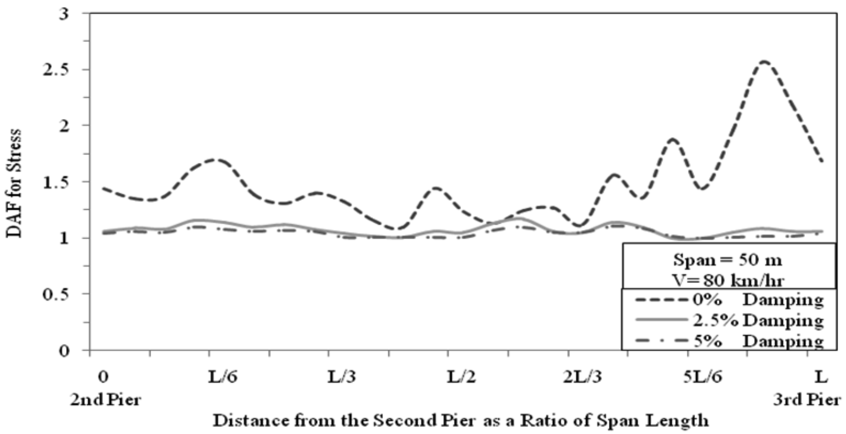

Fig B1.33 : DAF for Stress for 50 m Span Length and V = 80 km/hr

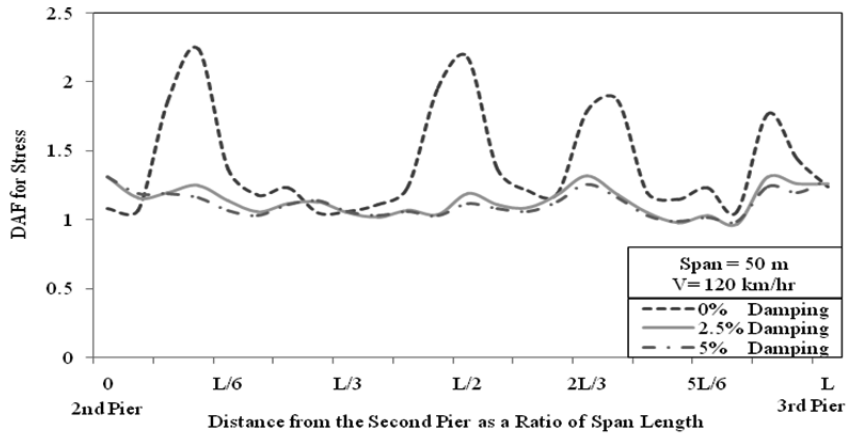

Fig B1.34 : DAF for Stress for 50 m Span Length and V = 120 km/hr

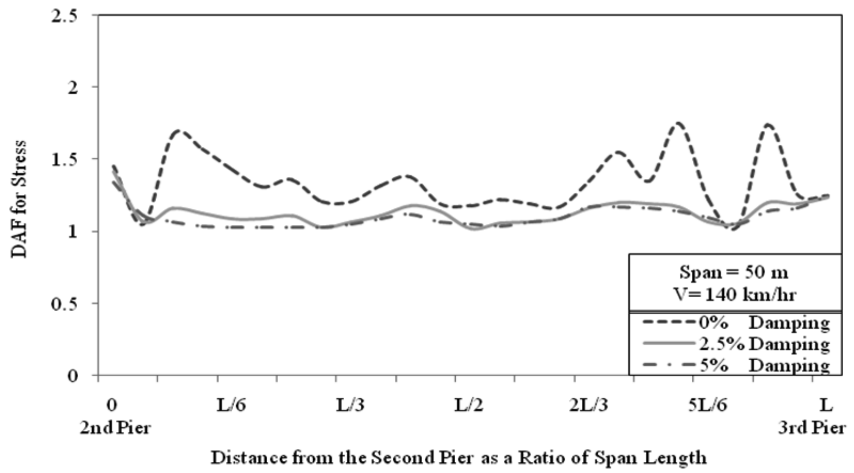

Fig B1.35 : DAF for Stress for 50 m Span Length and V = 140 km/hr

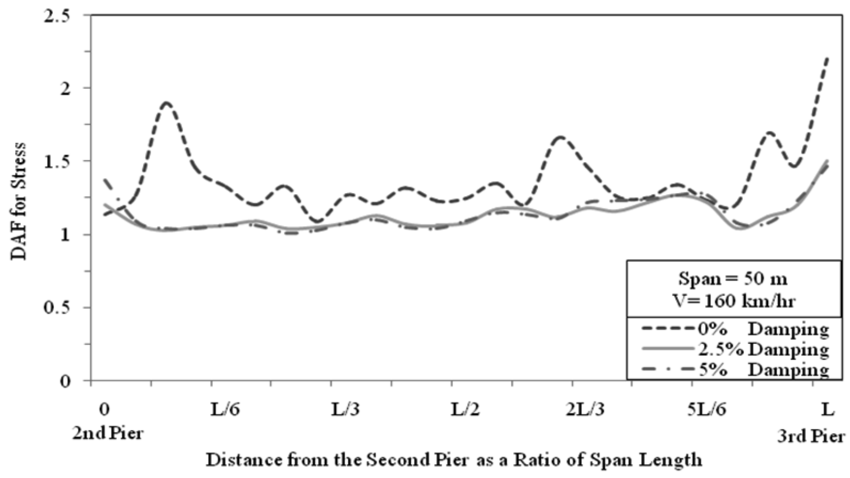

Fig B1.36 : DAF for Stress for 50 m Span Length and V = 160 km/hr

B.1.2.2 Variation for Span Length = 75 m

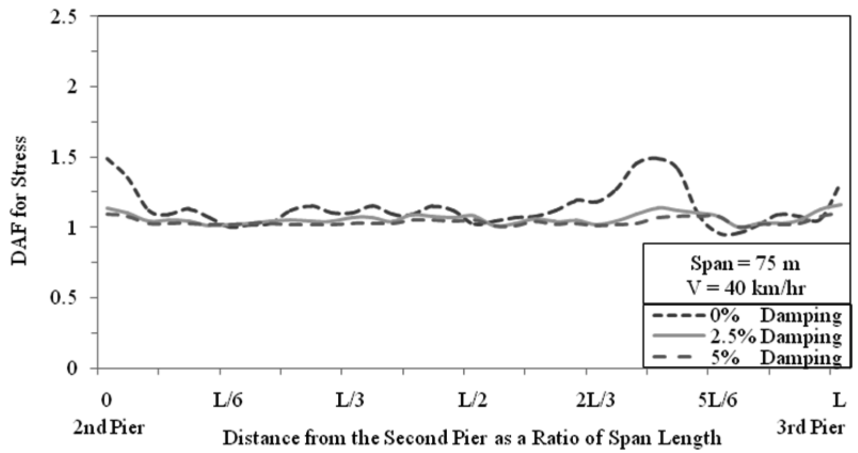

Fig B1.37: DAF for Stress for 75 m Span Length and V = 40 km/hr

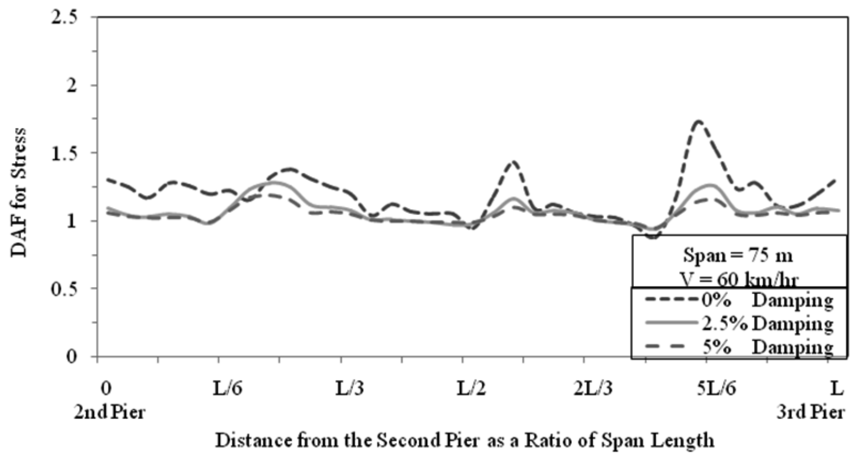

Fig B1.38 : DAF for Stress for 75 m Span Length and V = 60 km/hr

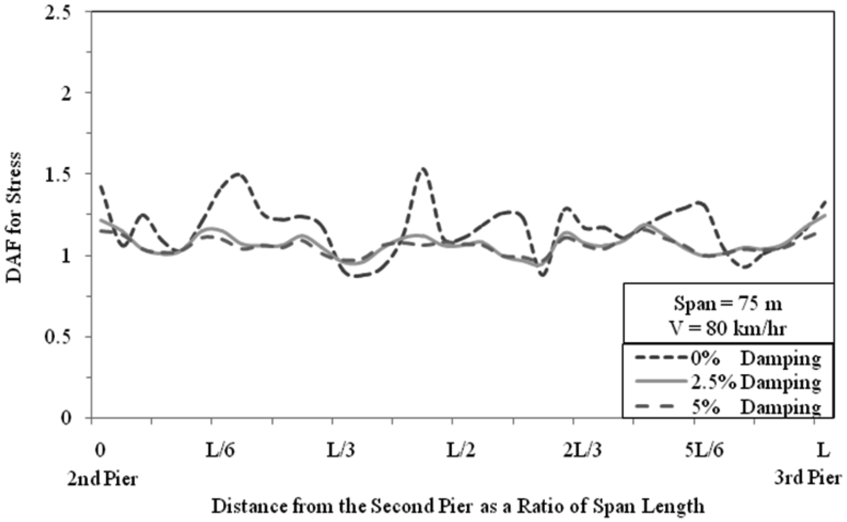

Fig B1.39 : DAF for Stress for 75 m Span Length and V = 80 km/hr

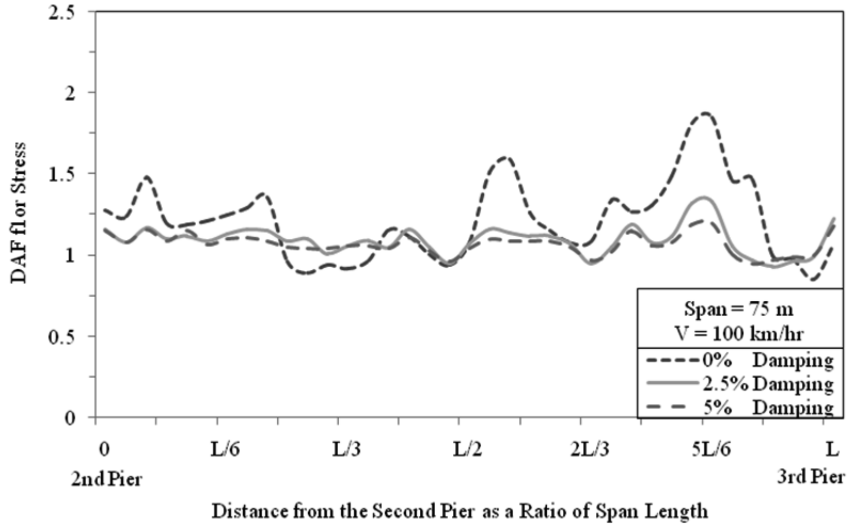

Fig B1.40 : DAF for Stress for 75 m Span and V = 100 km/hr

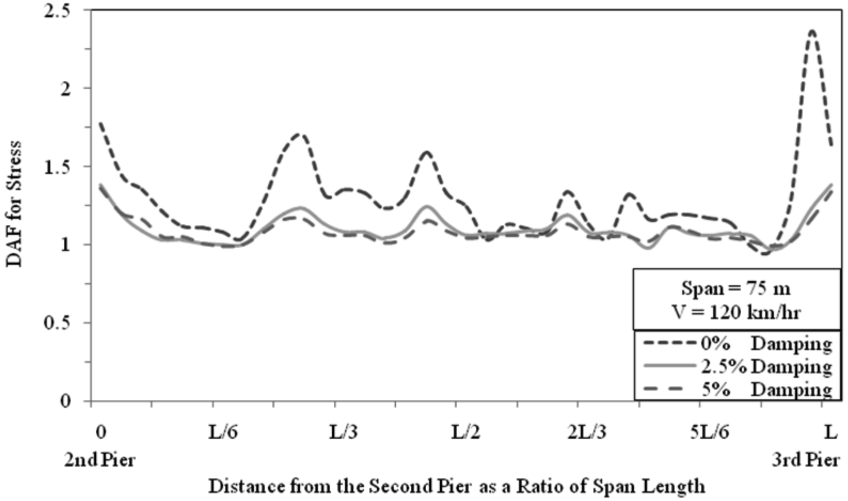

Fig B1.41 : DAF for Stress for 75 m Span and V = 120 km/hr

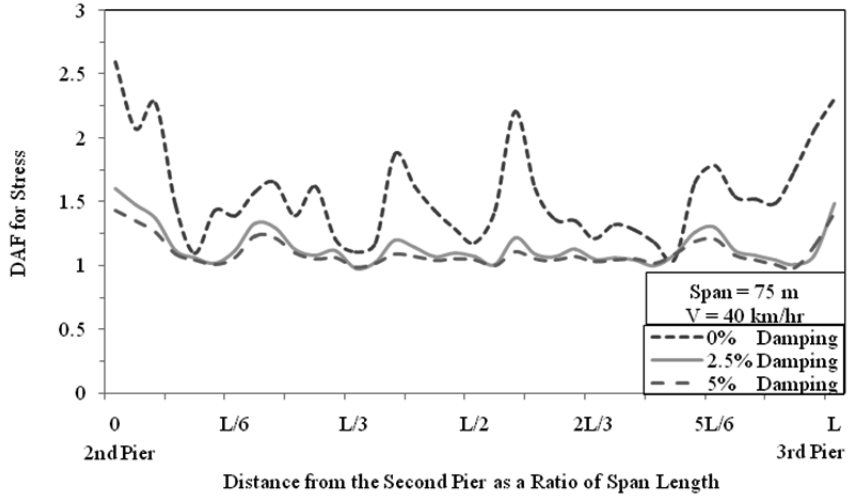

Fig B1.42: DAF for Stress for 75 m Span and V = 140 km/hr

B.1.2.3 Variation for Span Length = 100 m

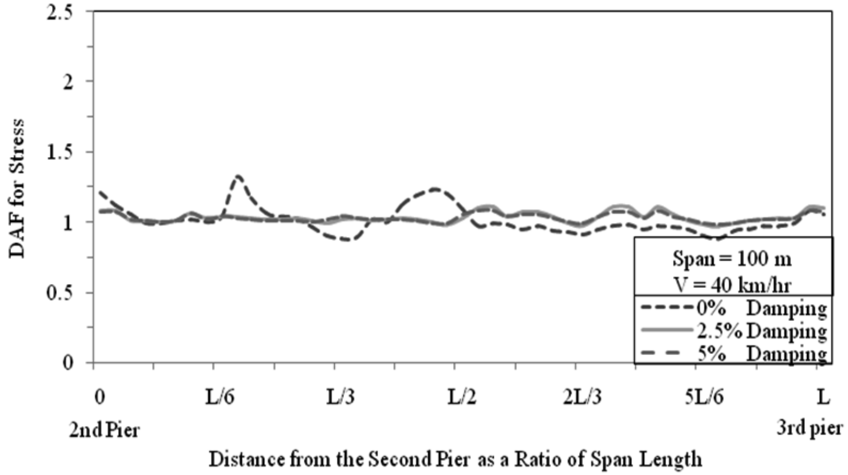

Fig B1.43 : DAF for Stress for 100 m Span Length and V = 40 km/hr

Fig B1.44 : DAF for Stress for 100 m Span Length and V = 60 km/hr

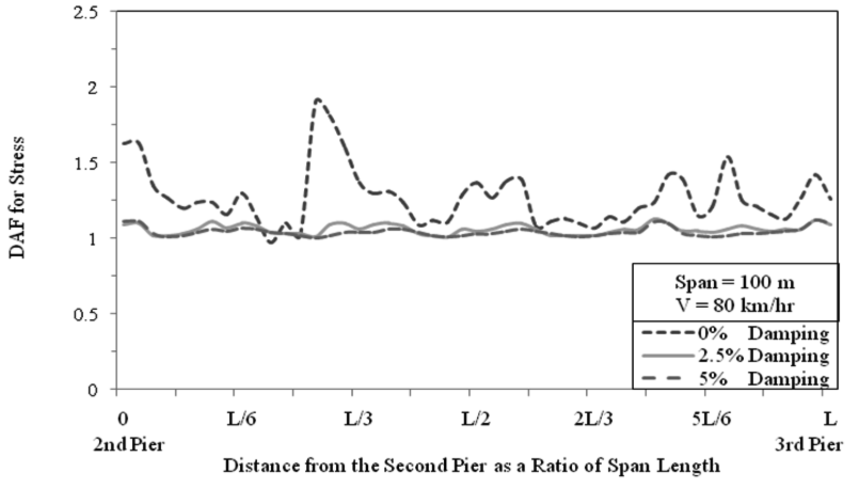

Fig B1.45 : DAF for Stress for 100 m Span Length and V = 80 km/hr

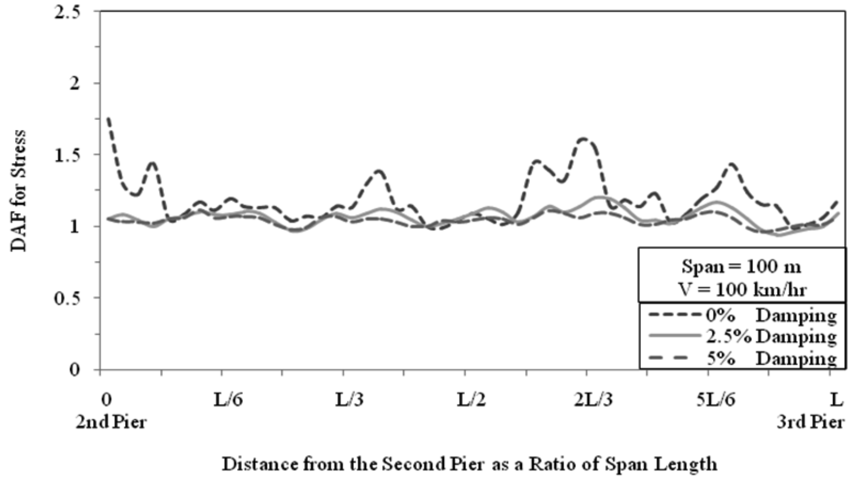

Fig B1.46: DAF for Stress for 100 m Span Length and V = 100 km/hr

Fig B1.47 : DAF for Stress for 100 m Span Length and V = 120 km/hr

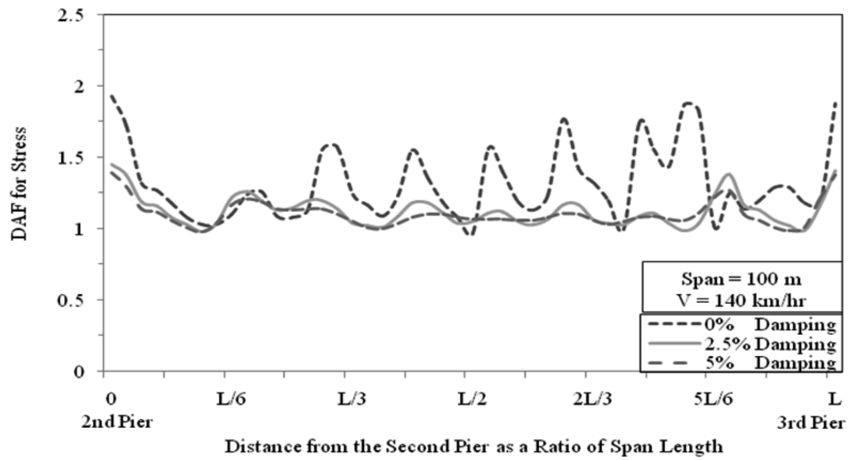

Fig B1.48 : DAF for Stress for 100 m Span Length and V = 140 km/hr

B.1.2.4 Variation for Span Length = 125 m

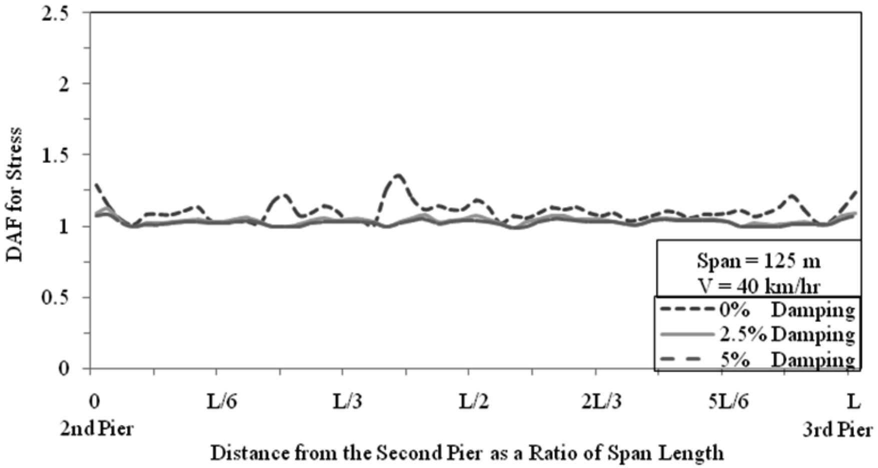

Fig B1.49: DAF for Stress for 125 m Span Length and V = 40 km/hr

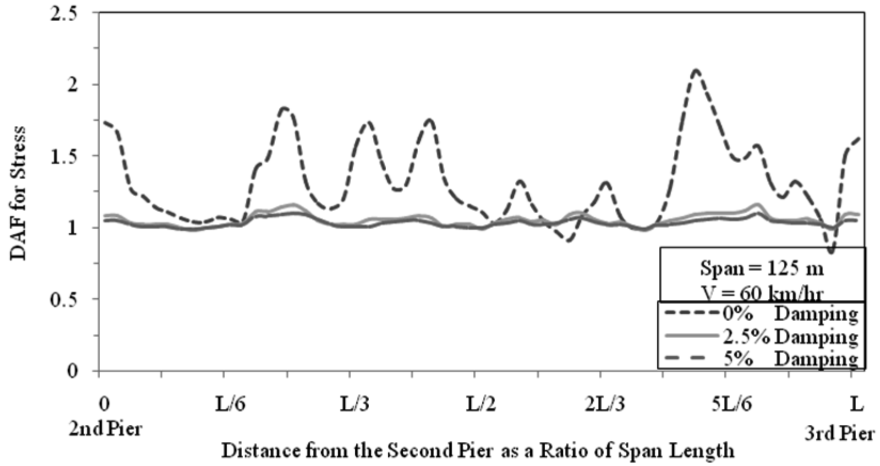

Fig B1.50 : DAF for Stress for 125 m Span Length and V = 60 km/hr

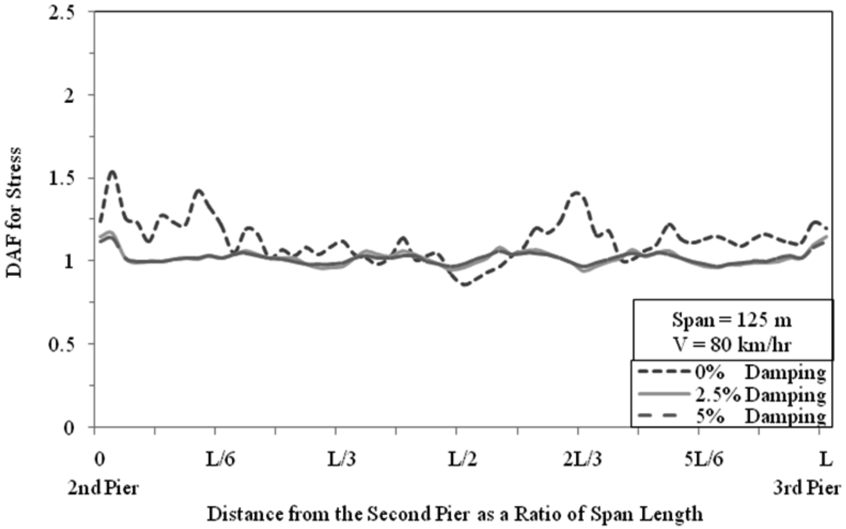

Fig B1.51 : DAF for Stress for 125 m Span Length and V = 80 km/hr

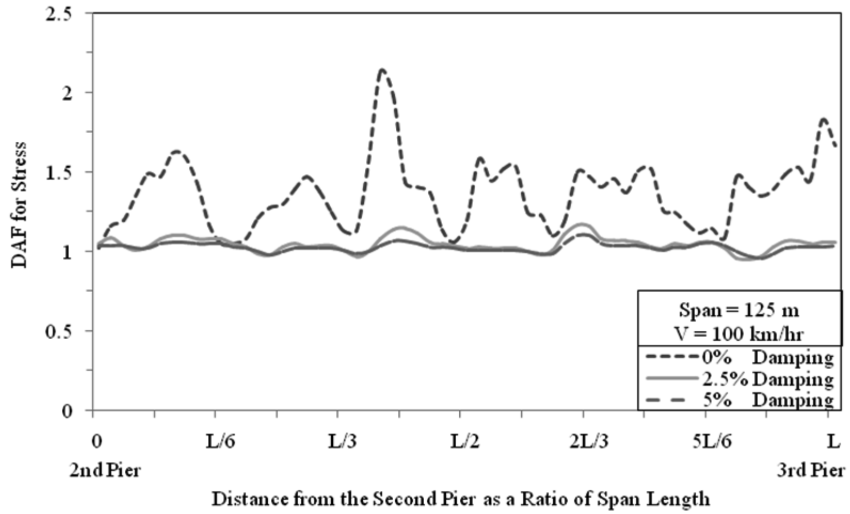

Fig B1.52 : DAF f1or Stress for 125 m Span Length and V = 100 km/hr

Fig B1.53 : DAF for Stress for 125 m Span Length and V = 120 km/hr

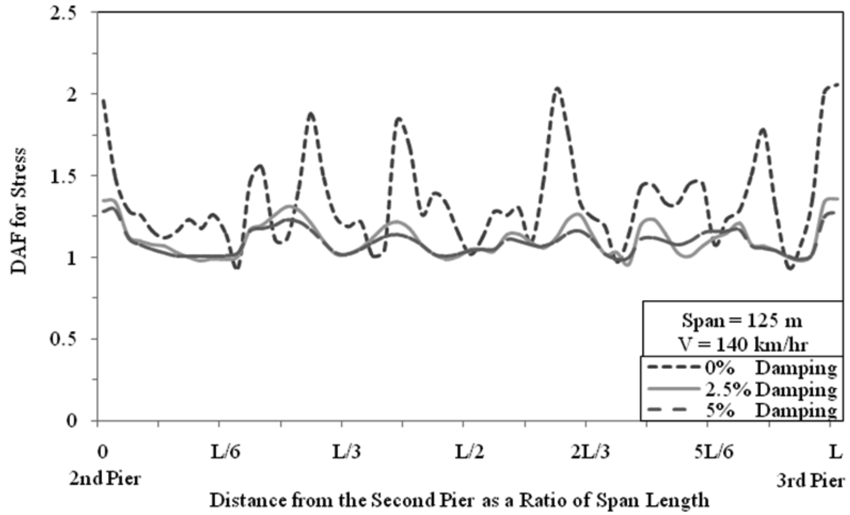

Fig B1.54 : DAF for Stress for 125 m Span Length and V = 140 km/hr

B.1.2.5 Variation for Span Length = 150 m

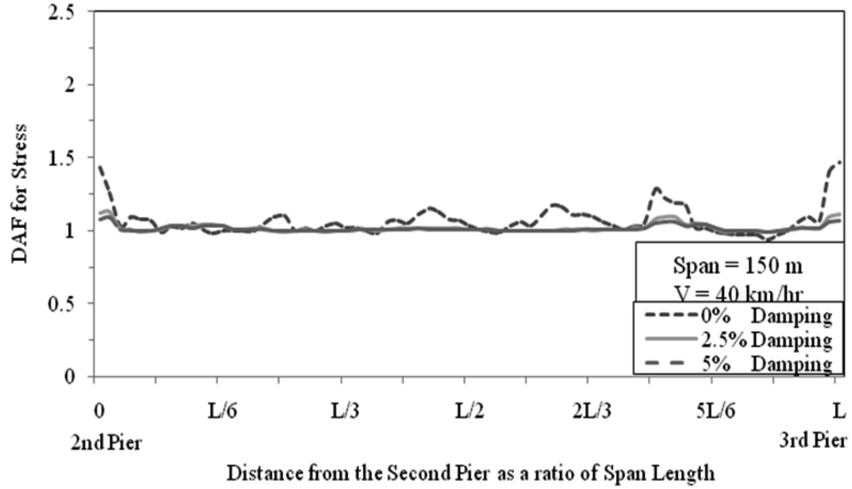

Fig B1.55 : DAF for Stress for 150 m Span Length and V = 40 km/hr

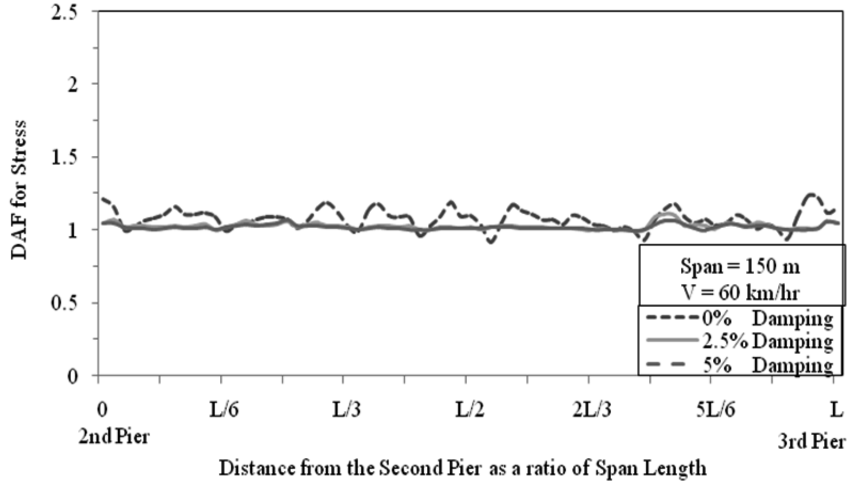

Fig B1.56 : DAF for Stress for 150 m Span Length and V = 60 km/hr

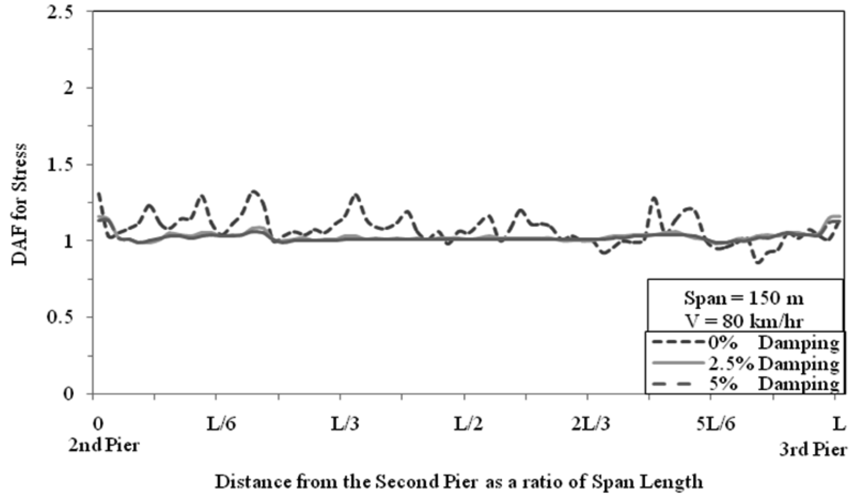

Fig B1.57 : DAF for Stress for 150 m Span Length and V = 80 km/hr

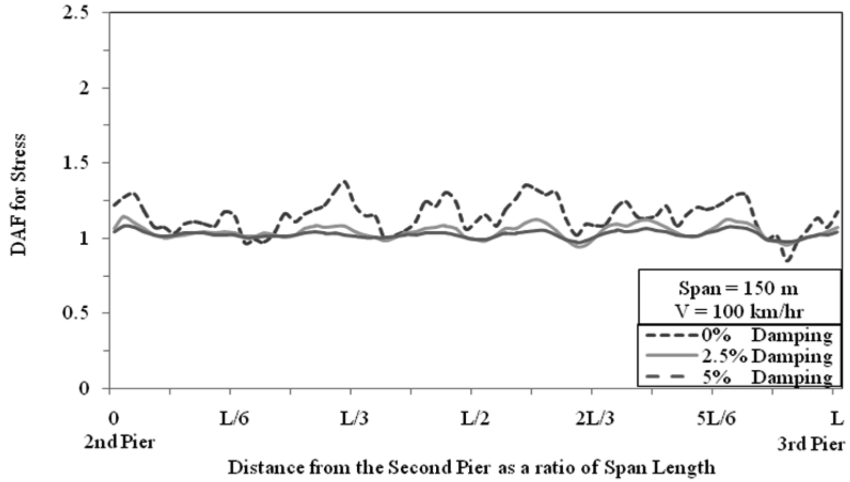

Fig B1.58 : DAF for Stress for 150 m Span Length and V = 100 km/hr

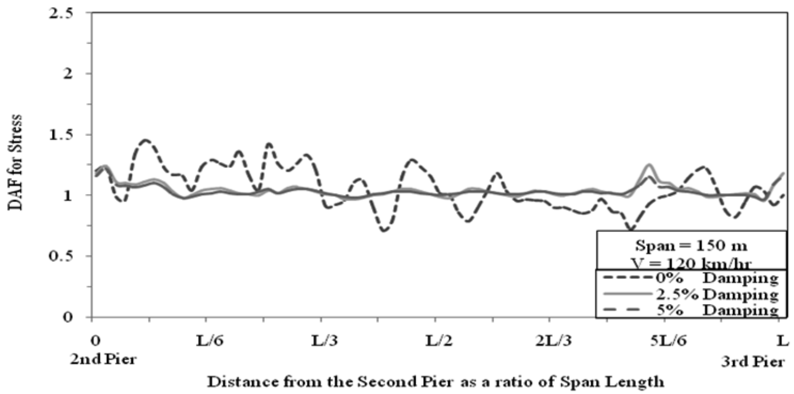

Fig B1.59 : DAF for Stress for 150 m Span Length and V = 120 km/hr

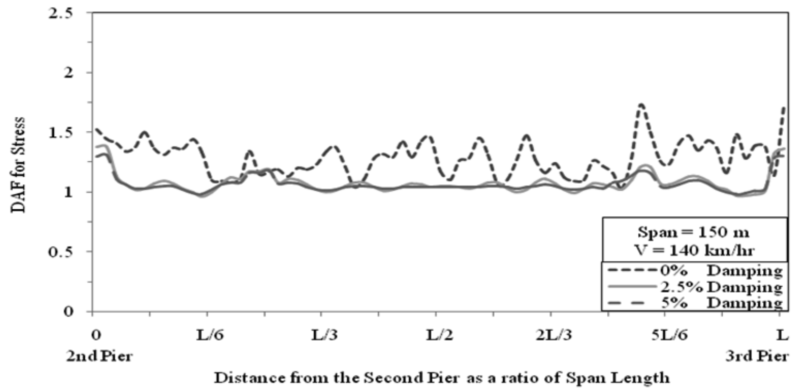

Fig B1.60 : DAF for Stress for 150 m Span Length and V = 140 km/hr

B.2 DAF Variation along the Length of the Middle Span for Different Span Length for Vehicle Position along Centerline of Box Girder Bridge

B.2.1 Variation along the Length of the Middle Span in Terms of Stress

B.2.1.1 Variation for Span Length = 50 m

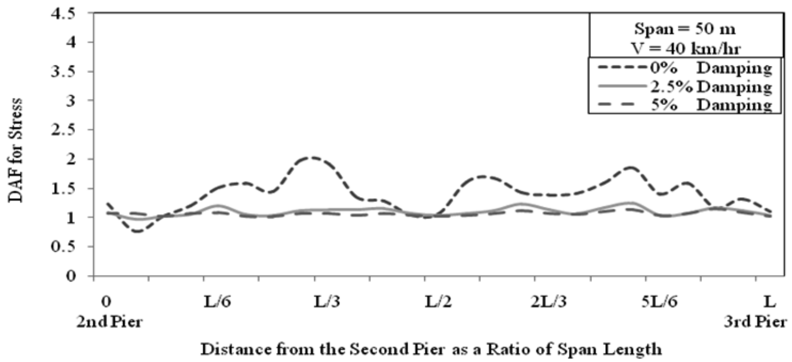

Fig B2.1 : DAF for 50 m Span Length and V = 40 km/hr

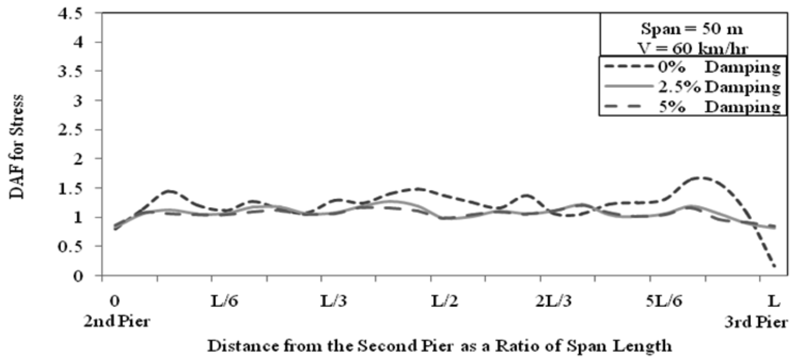

Fig B2.2 : DAF for Stress for 50 m Span Length and V = 60 km/hr

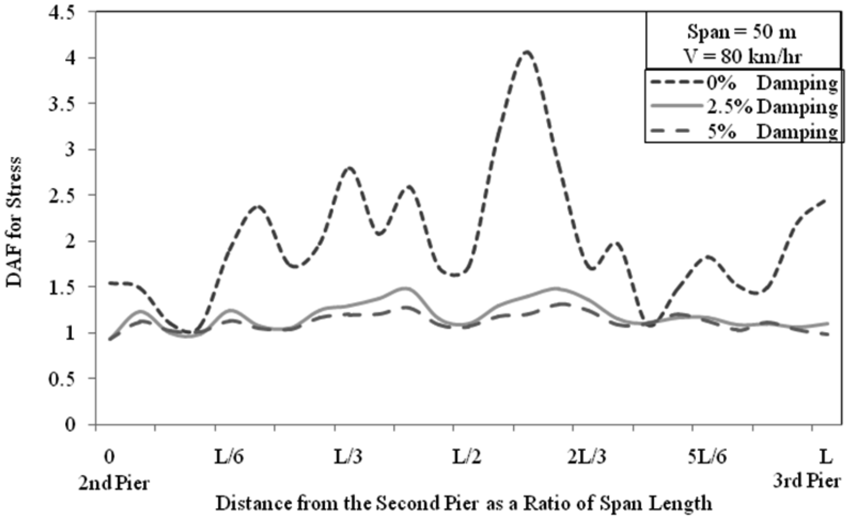

Fig B2.3 : DAF for Stress for 50 m Span Length and V = 80 km/hr

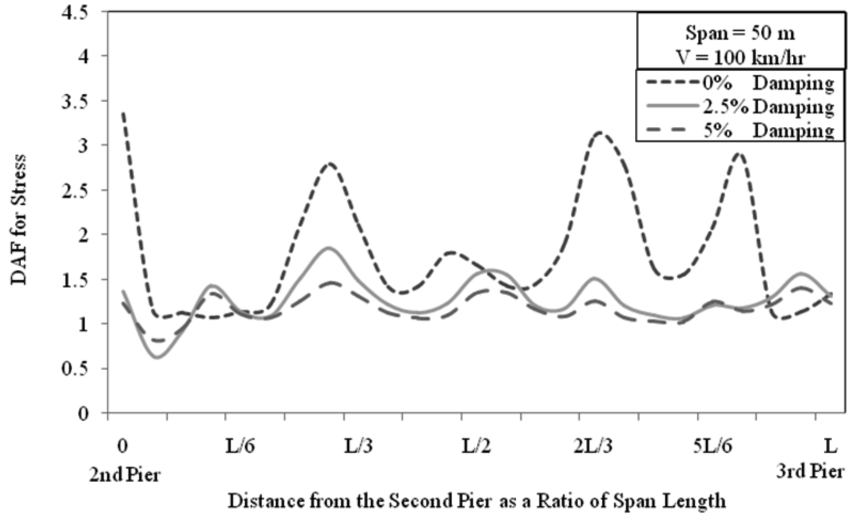

Fig B2.4 : DAF for Stress for 50 m Span Length and V = 100 km/hr

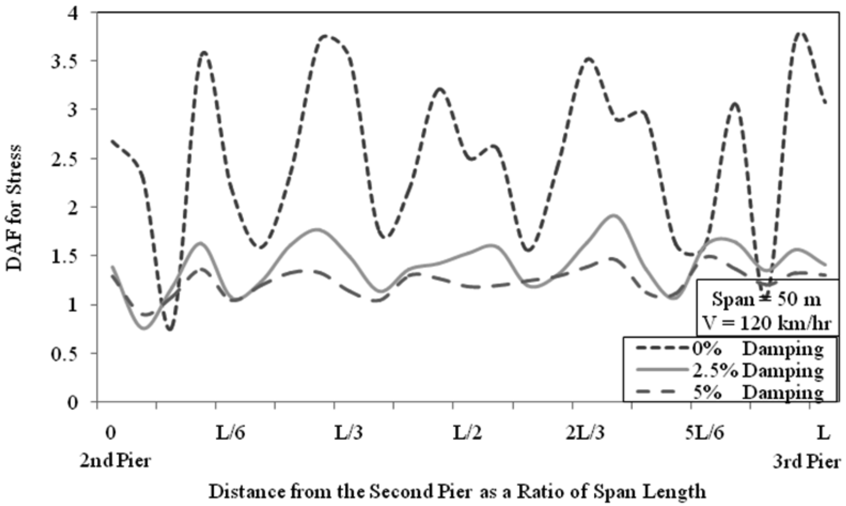

Fig B2.5: DAF for Stress for 50 m Span Length and V = 120 km/hr

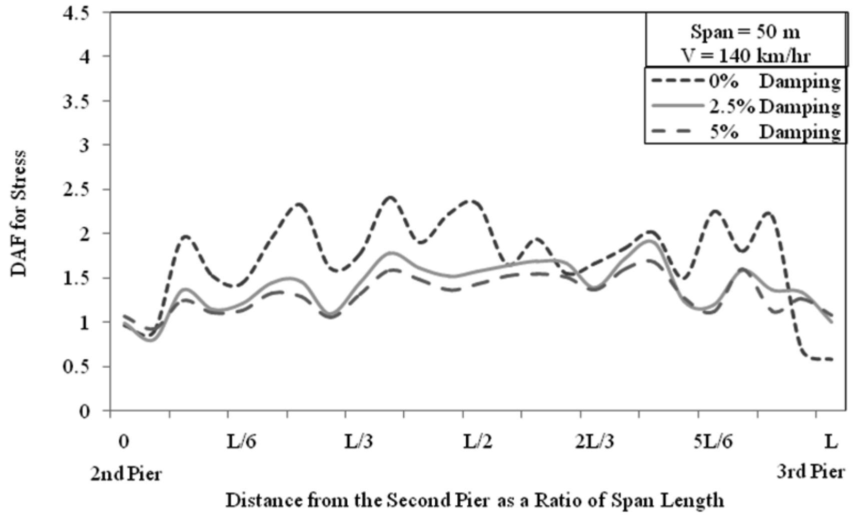

Fig B2.6 : DAF for Stress for 50 m Span Length and V = 140 km/hr

B.2.1.2 Variation for Span Length = 75 m

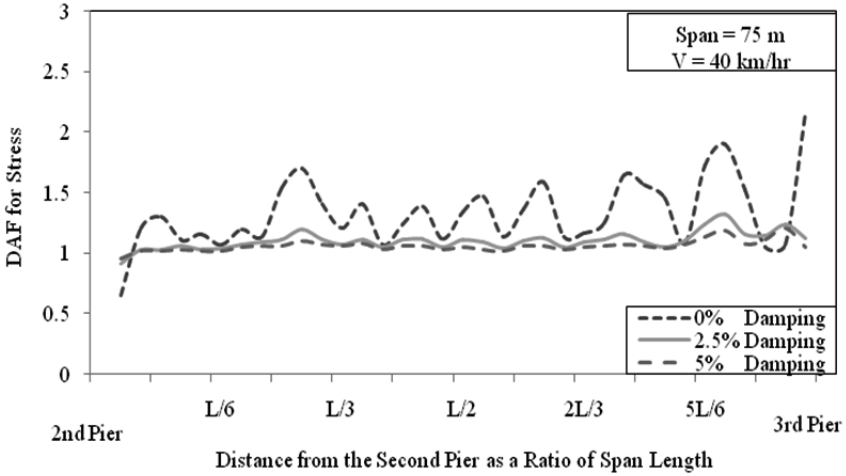

Fig B2.7 : DAF for Stress for 75 m Span Length and V = 40 km/hr

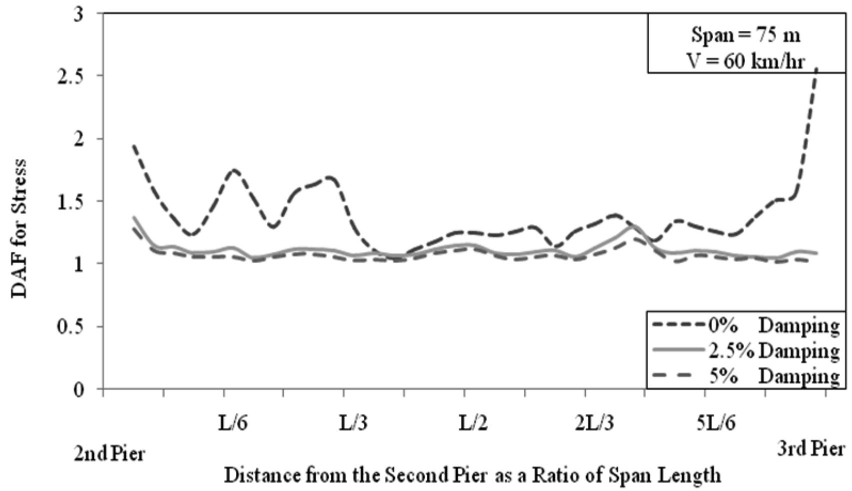

Fig B2.8 : DAF for Stress for 75 m Span Length and V = 60 km/hr

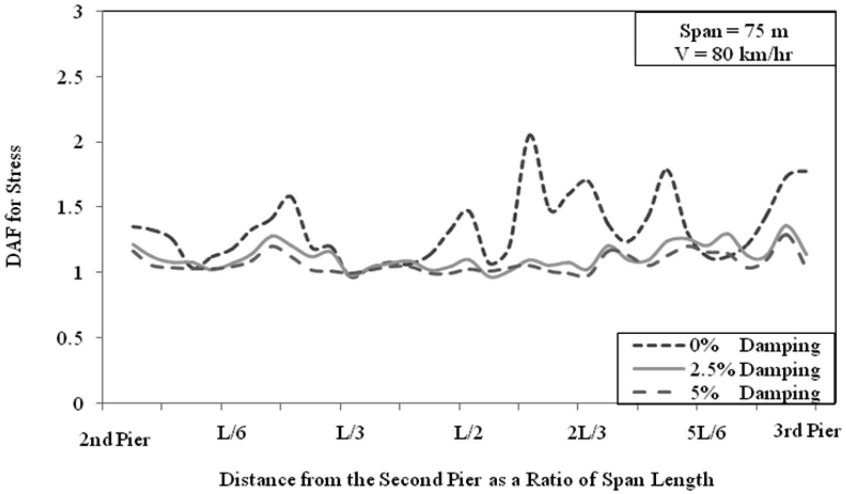

Fig B2.9 : DAF for Stress for 75 m Span Length and V = 80 km/hr

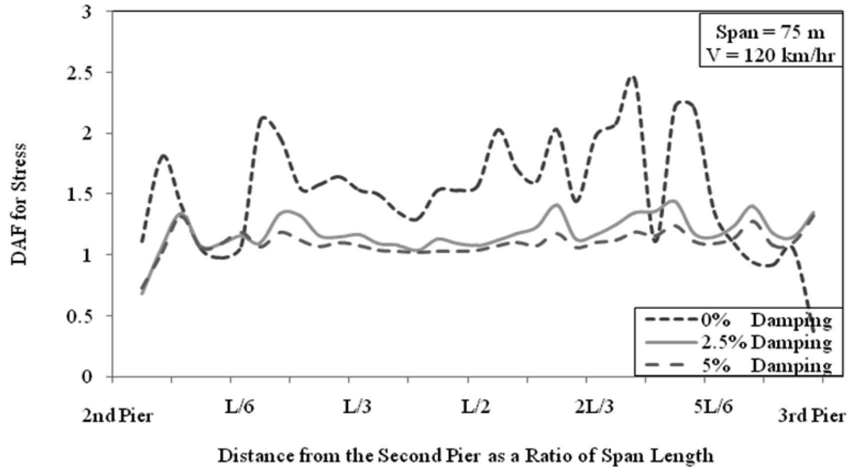

Fig B2.10: DAF for Stress for 75 m Span Length and V = 120 km/hr

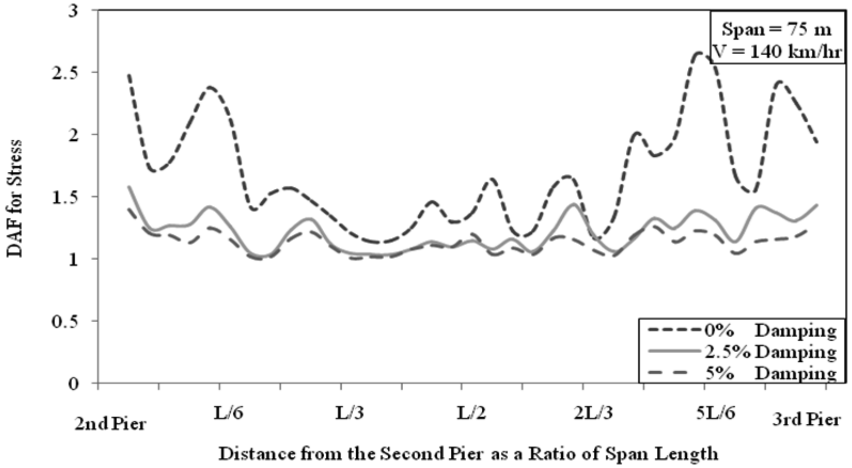

Fig B2.11 : DAF for Stress for 75 m Span Length and V = 140 km/hr

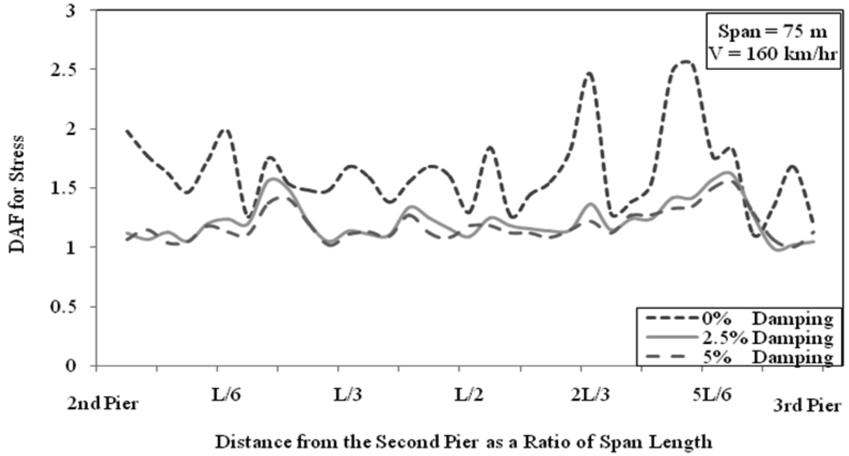

Fig B2.12 : DAF for Stress for 75 m Span Length and V = 160 km/hr

B.2.1.3 Variation for Span Length = 100 m

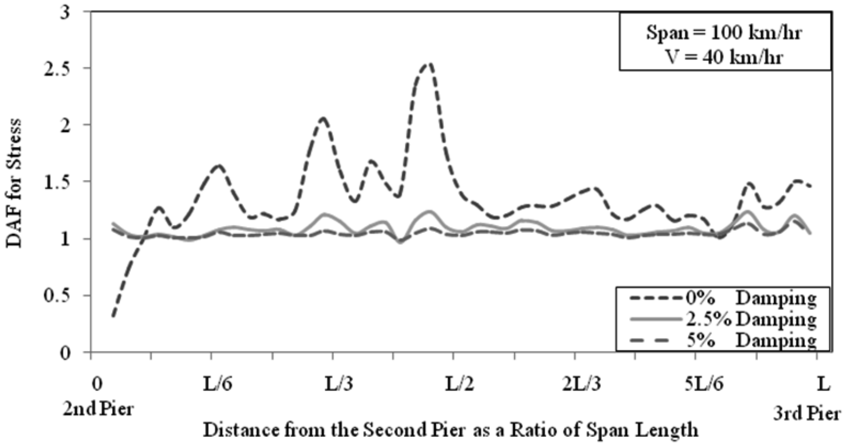

Fig B2.13 : DAF for Stress for 100 m Span Length and V = 40 km/hr

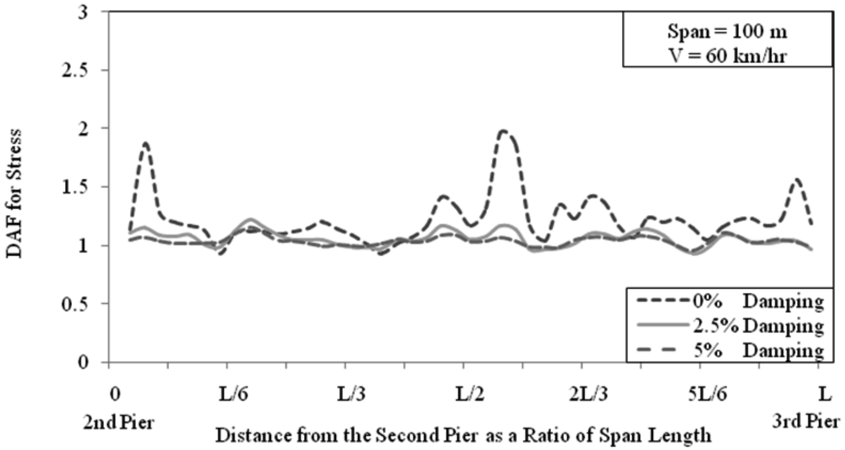

Fig B2.14 : DAF for Stress for 100 m Span Length and V = 60 km/hr

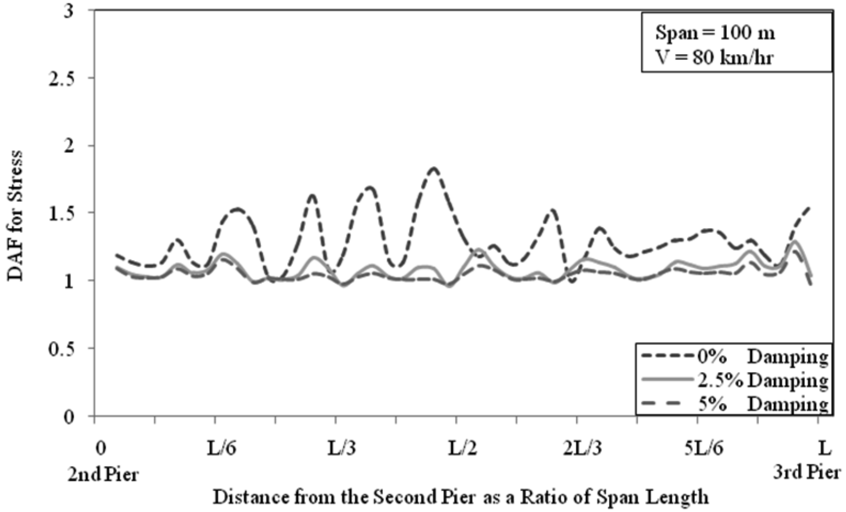

Fig B2.15 : DAF for Stress for 100 m Span Length and V = 80 km/hr

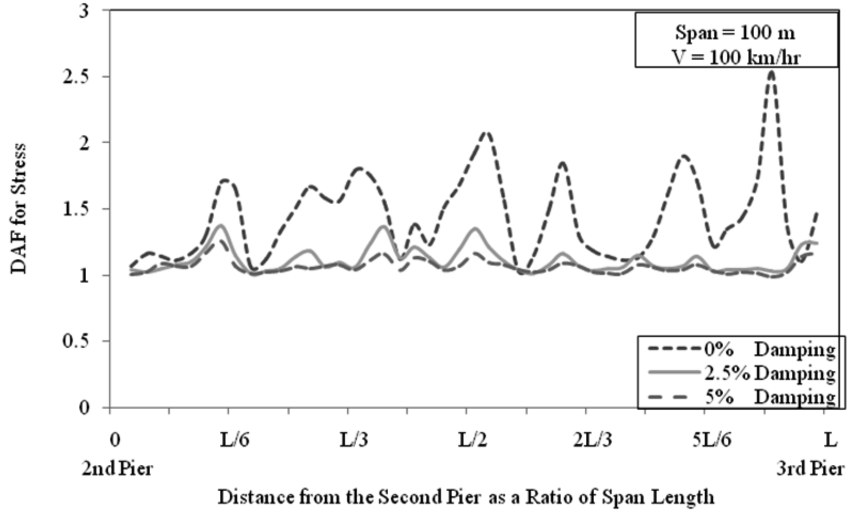

Fig B2.16 : DAF for Stress for 100 m Span Length and V = 100 km/hr

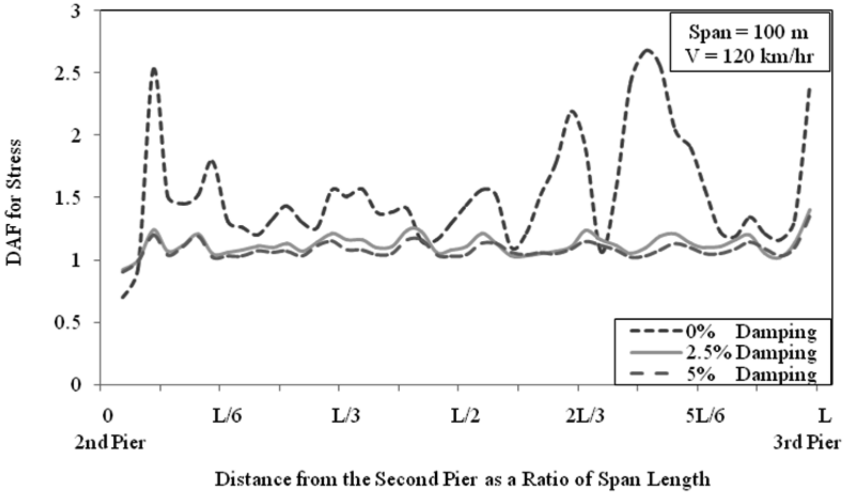

Fig B2.17 : DAF for Stress for 100 m Span Length and V = 120 km/hr

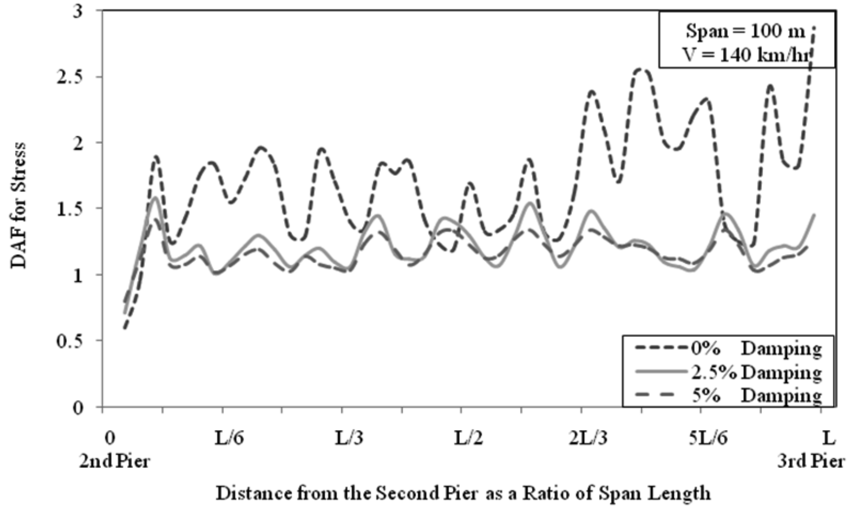

Fig B2.18 : DAF for Stress for 100 m Span Length and V = 140 km/hr

B.2.1.4 Variation for Span Length = 125 m

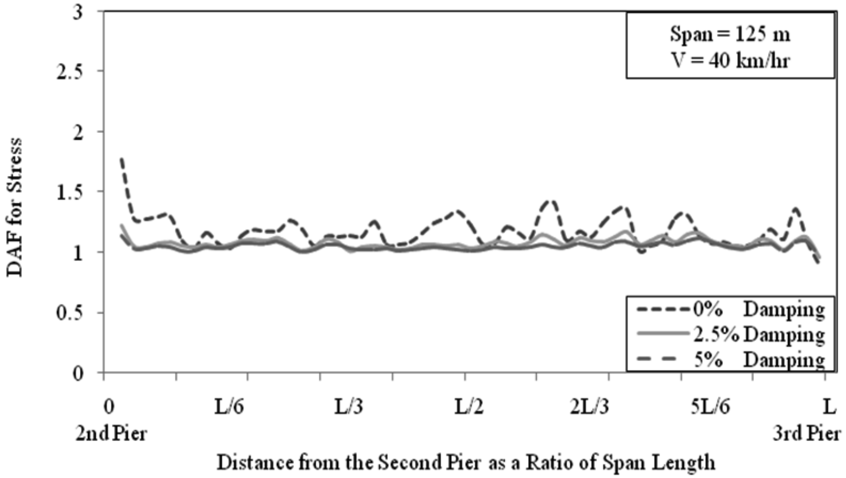

Fig B2.19 : DAF for Stress for 125 m Span Length and V = 40 km/hr

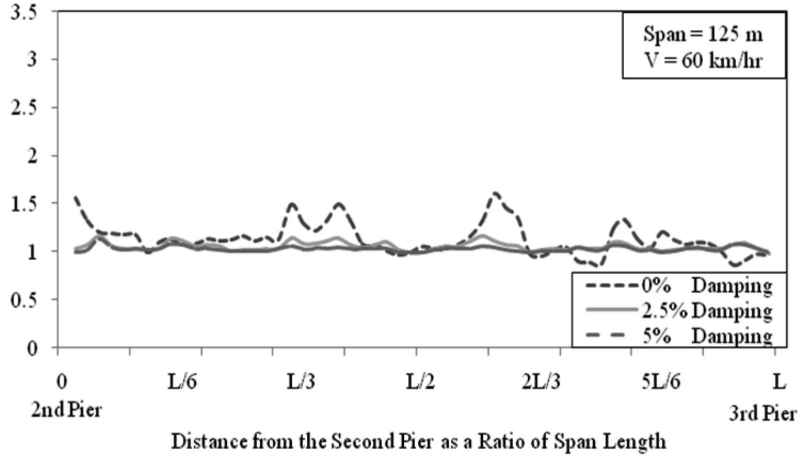

Fig B2.20 : DAF for Stress for 125 m Span Length and V = 60 km/hr

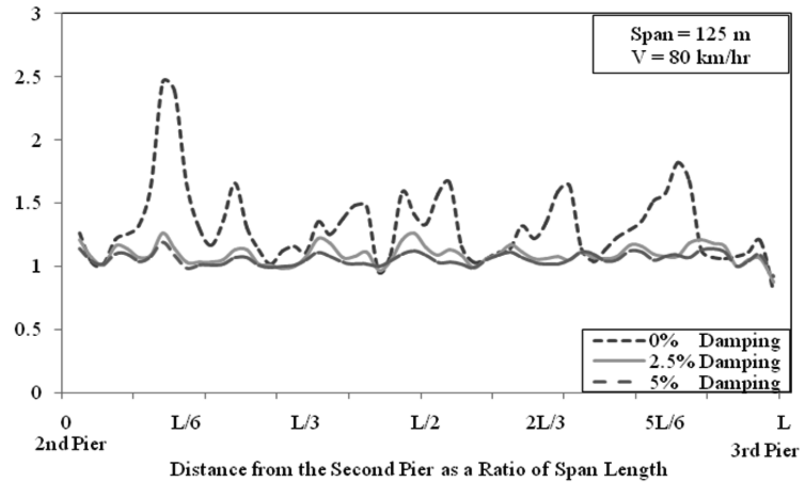

Fig B2.21: DAF for Stress for 125 m Span Length and V = 80 km/hr

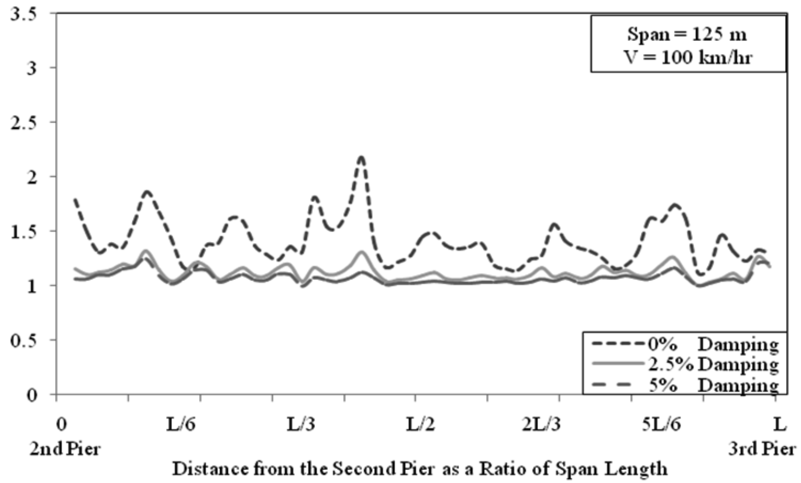

Fig B2.22 : DAF for Stress for 125 m Span Length and V = 100 km/hr

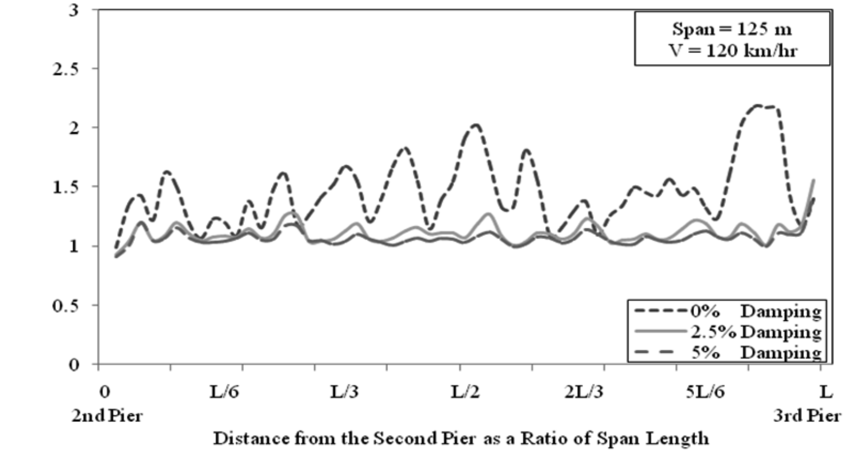

Fig B2.23 : DAF for Stress for 125 m Span Length and V = 120 km/hr

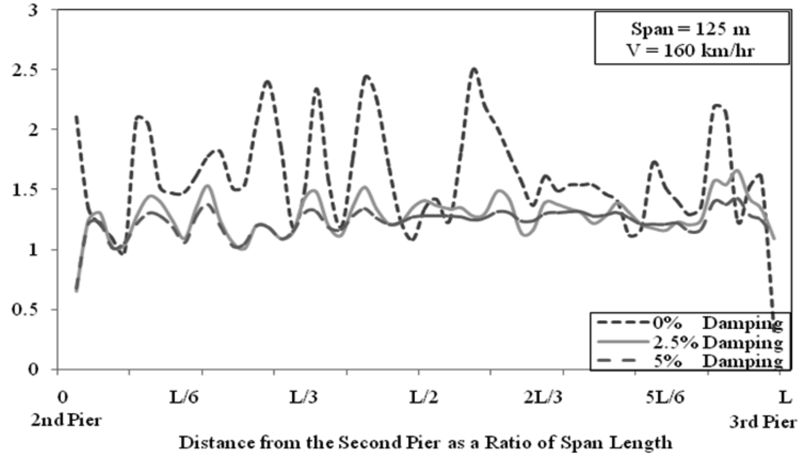

Fig B2.24 : DAF for Stress for 125 m Span Length and V = 160 km/hr

B.2.1.5 Variation for Span Length = 150 m

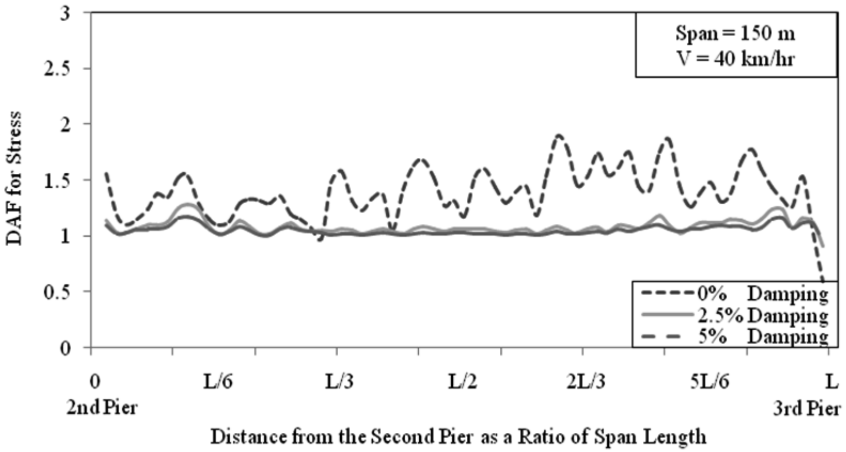

Fig B2.25 : DAF for Stress for 150 m Span Length and V = 40 km/hr

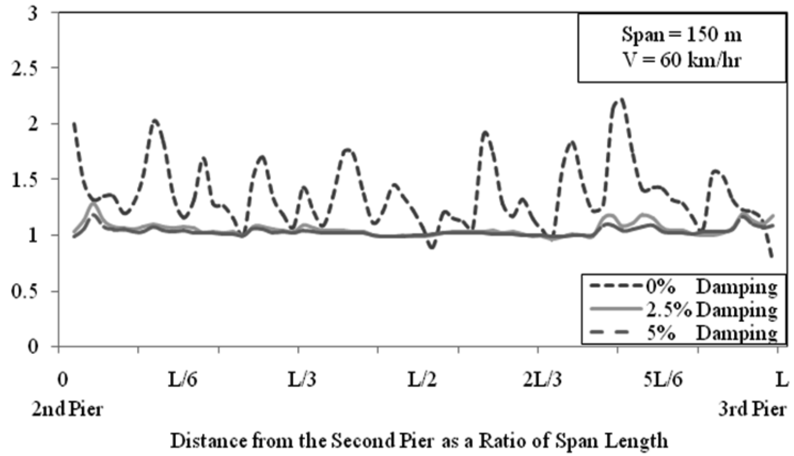

Fig B2.26 : DAF for Stress for 150 m Span Length and V = 60 km/hr

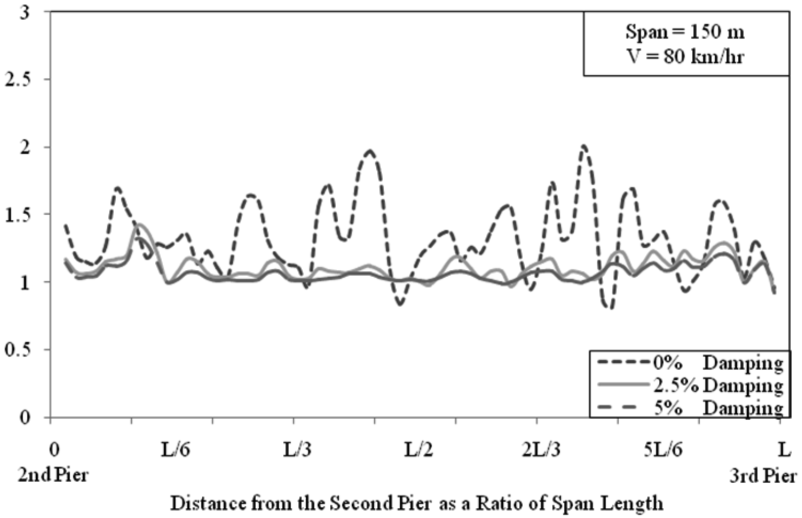

Fig B2.27 : DAF for Stress for 150 m Span Length and V = 80 km/hr

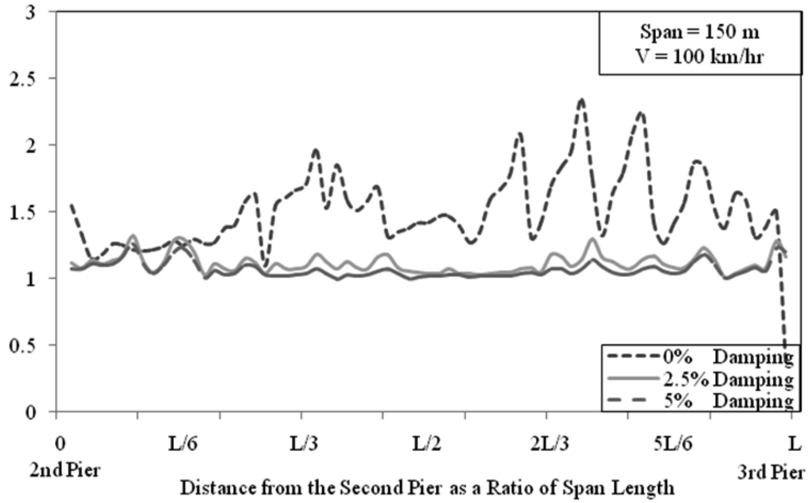

Fig B2.28 : DAF for Stress for 150 m Span Length and V = 100 km/hr

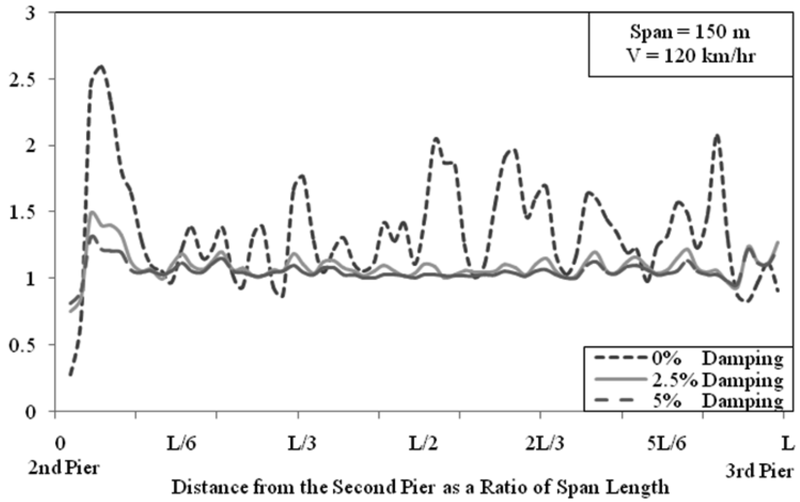

Fig B2.29 : DAF for Stress for 150 m Span Length and V = 120 km/hr

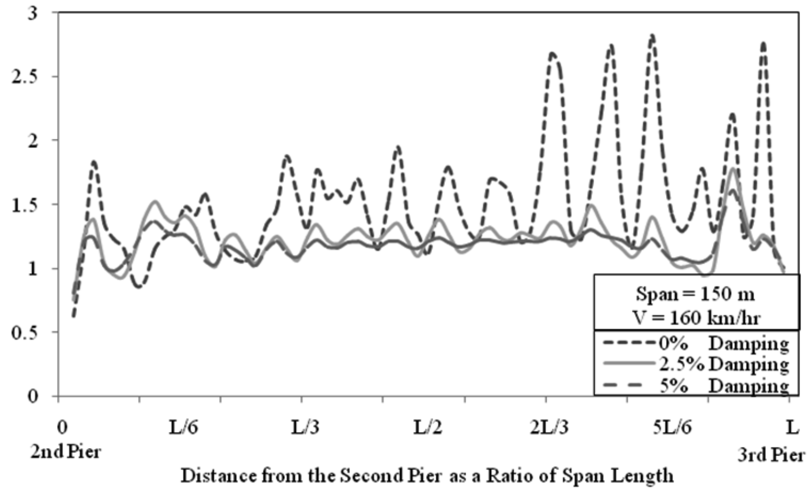

Fig B2.30 : DAF for Stress for 150 m Span Length and V = 160 km/hr

Appendix C

C.1 DAF Variation along the Length of the Middle Span for Different Cantilever Width for Vehicle Position along Cantilever Part of Box Girder Bridge

C.1.1 Variation along the Length of the Middle Span in Terms of Vertical Deflections

C.1.1.1 Variation for Cantilever Width = 3 m

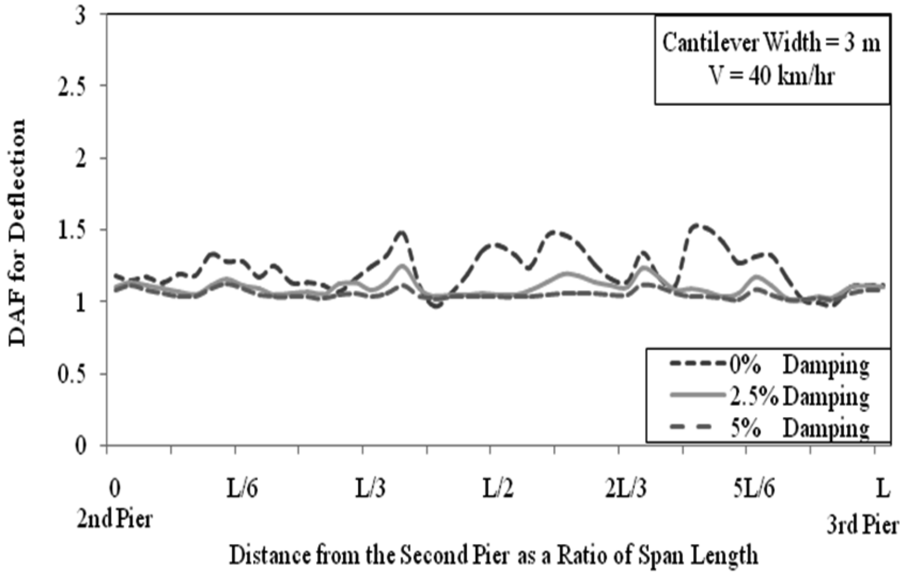

Fig C1.1 : DAF for Deflection for 3m Cantilever Width and V = 40 km/hr

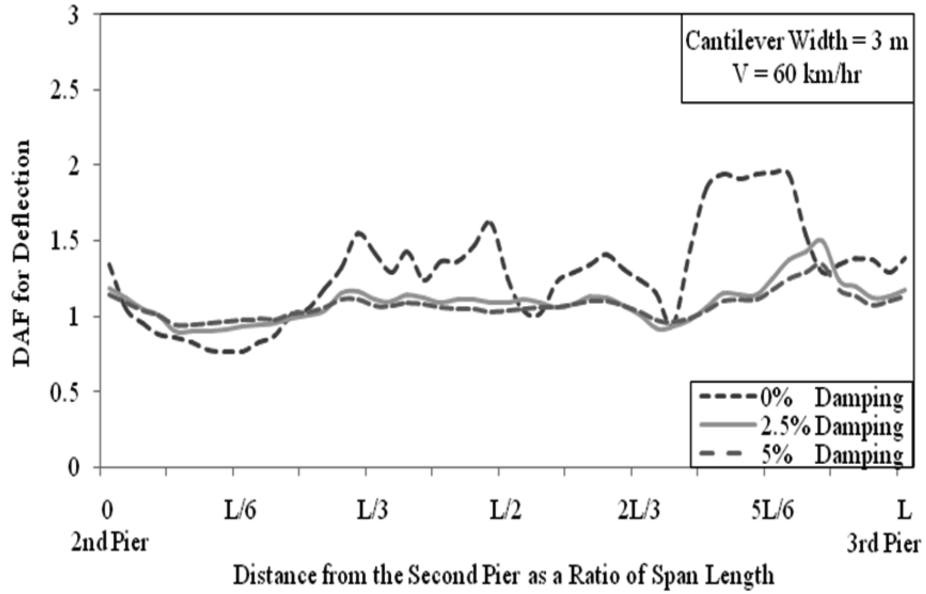

Fig C1.2 : DAF for Deflection for 3m Cantilever Width and V = 60 km/hr

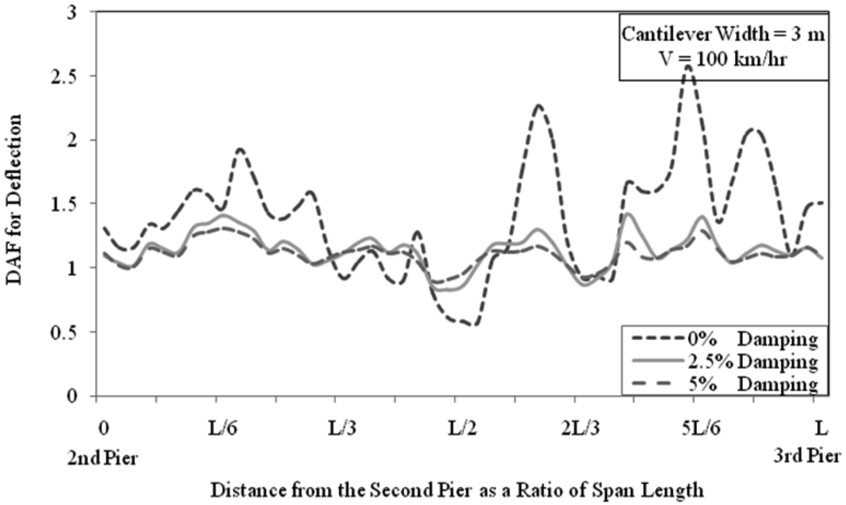

Fig C1.3 : DAF for Deflection for 3m Cantilever Width and V = 100 km/hr

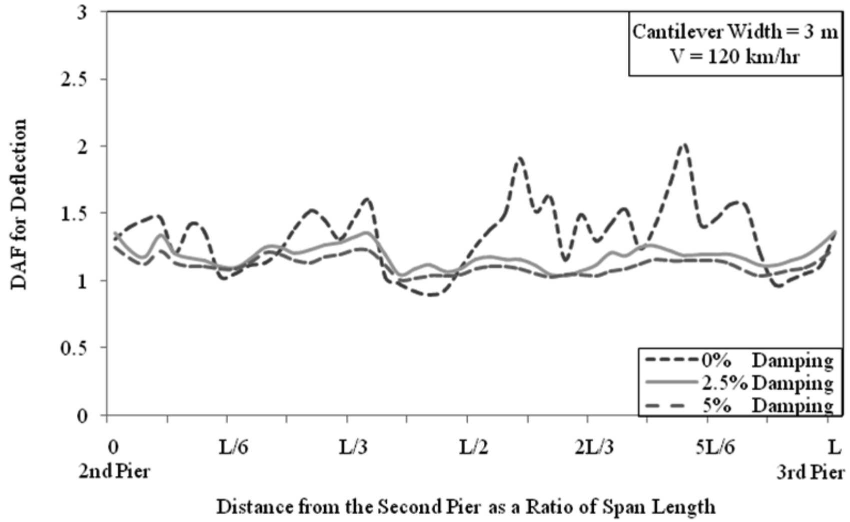

Fig C1.4 : DAF for Deflection for 3m Cantilever Width and V = 120 km/hr

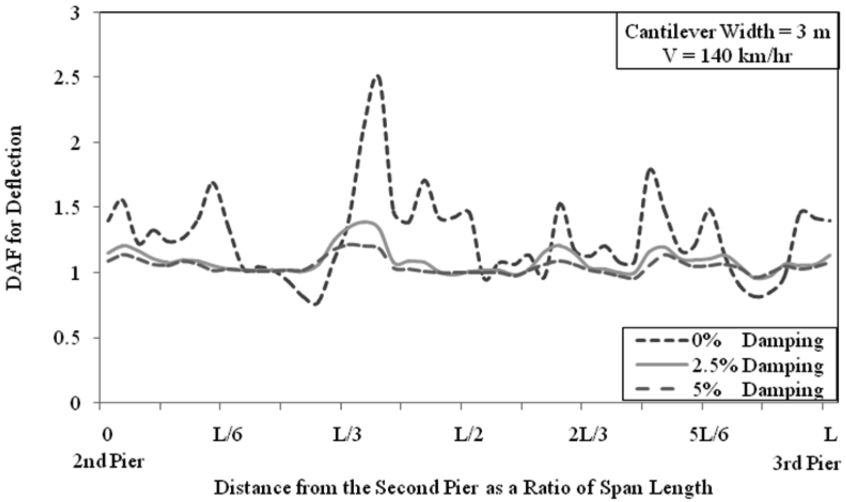

Fig C1.5: DAF for Deflection for 3m Cantilever Width and V = 140 km/hr

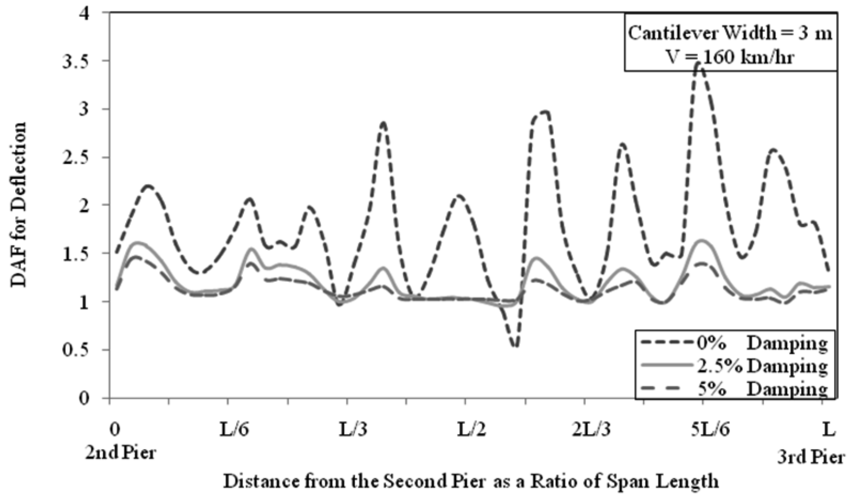

Fig C1.6 : DAF for Deflection for 3m Cantilever Width and V = 160 km/hr

C.1.1.2 Variation for Cantilever Width = 3.5 m

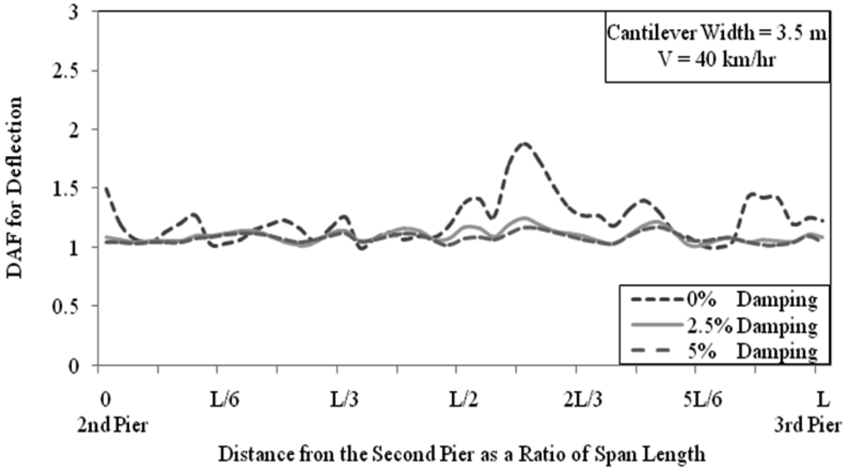

Fig C1.7 : DAF for Deflection for 3.5 m Cantilever Width and V = 40 km/hr

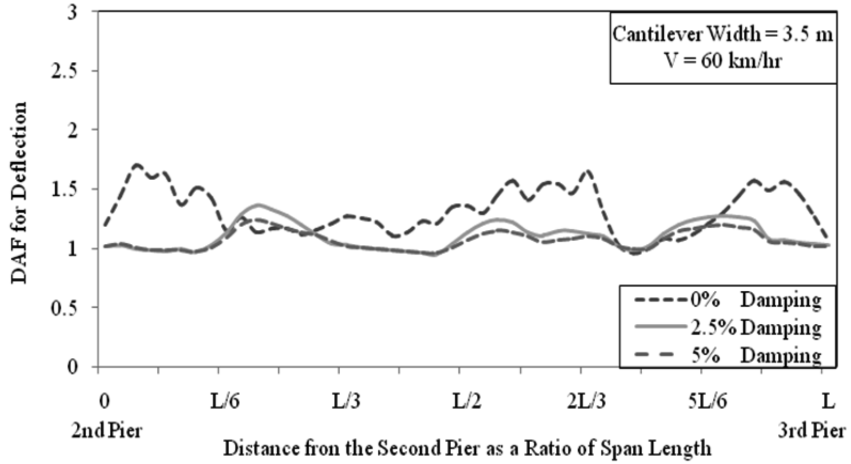

Fig C1.8 : DAF for Deflection for 3.5 m Cantilever Width and V = 60 km/hr

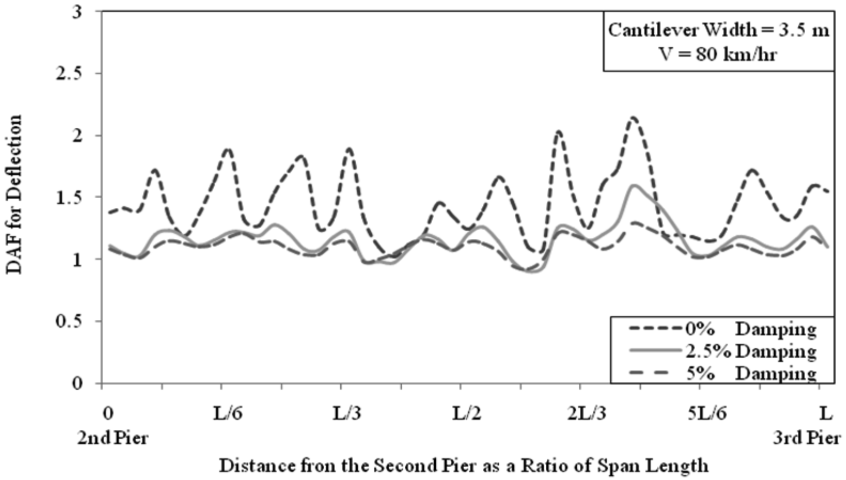

Fig C1.9 : DAF for Deflection for 3.5 m Cantilever Width and V = 80 km/hr

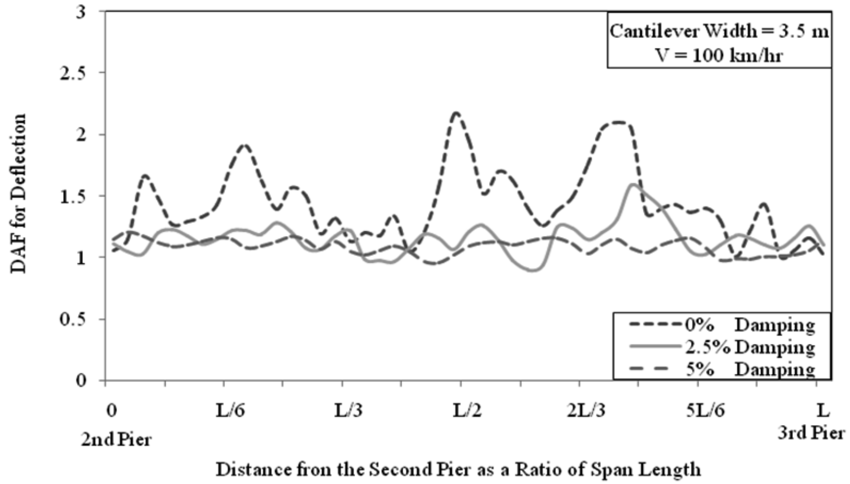

Fig C1.10 : DAF for Deflection for 3.5 m Cantilever Width and V = 100 km/hr

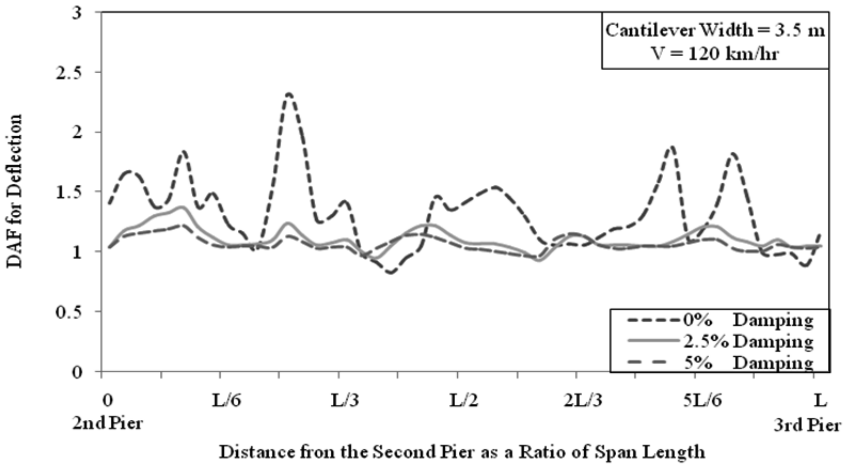

Fig C1.11 : DAF for Deflection for 3.5 m Cantilever Width and V = 120 km/hr

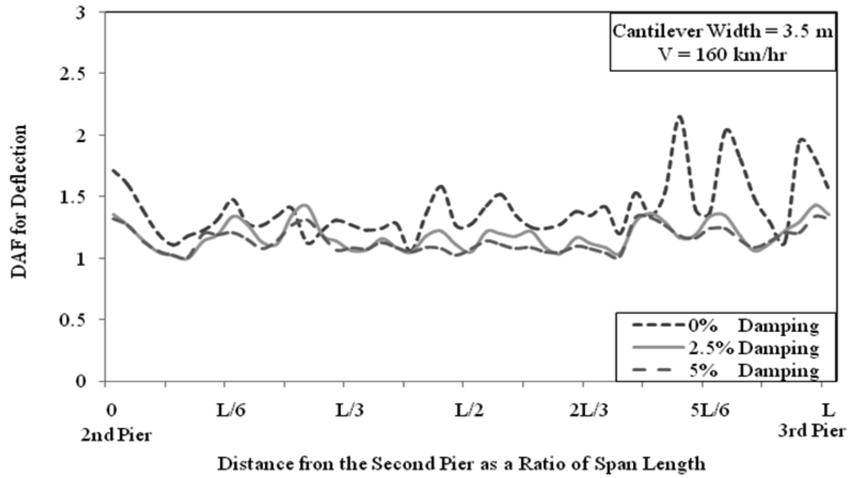

Fig C1.12 : DAF for Deflection for 3.5 m Cantilever Width and V = 160 km/hr

C.1.1.3 Variation for Cantilever Width = 4 m

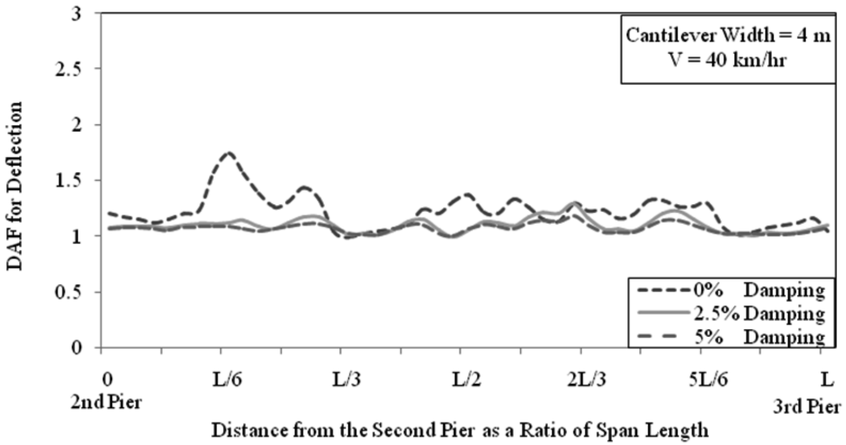

Fig C1.13 : DAF for Deflection for 4 m Cantilever Width and V = 40 km/hr

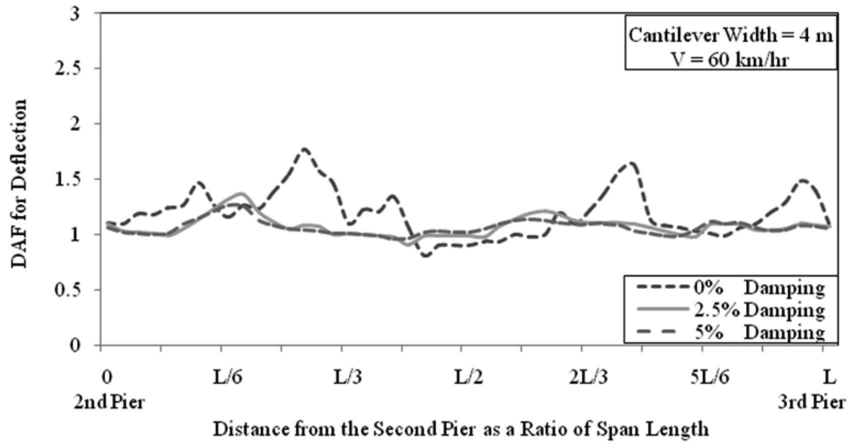

Fig C1.14 : DAF for Deflection for 4 m Cantilever Width and V = 60 km/hr

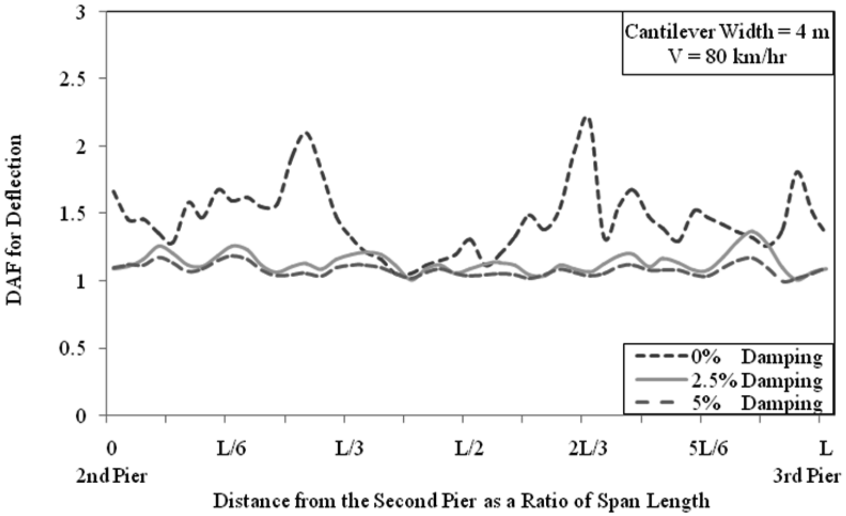

Fig C1.15 : DAF for Deflection for 4 m Cantilever Width and V = 80 km/hr

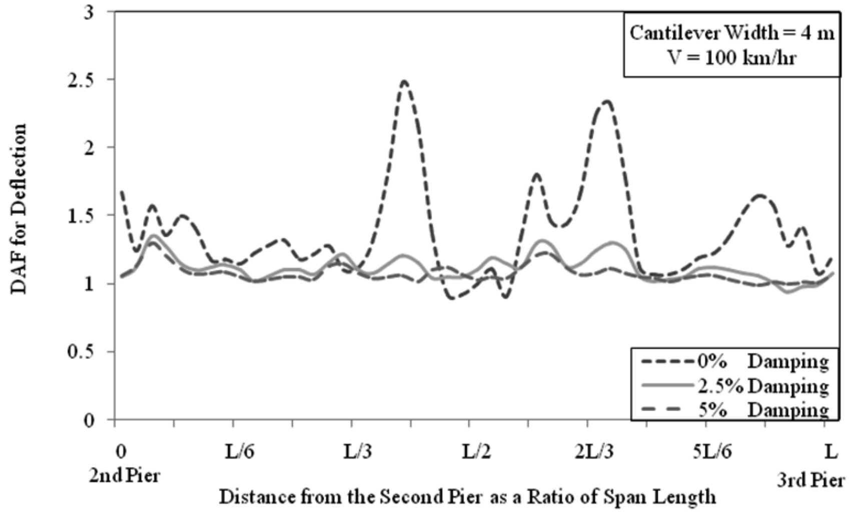

Fig C1.16 : DAF for Deflection for 4 m Cantilever Width and V = 100 km/hr

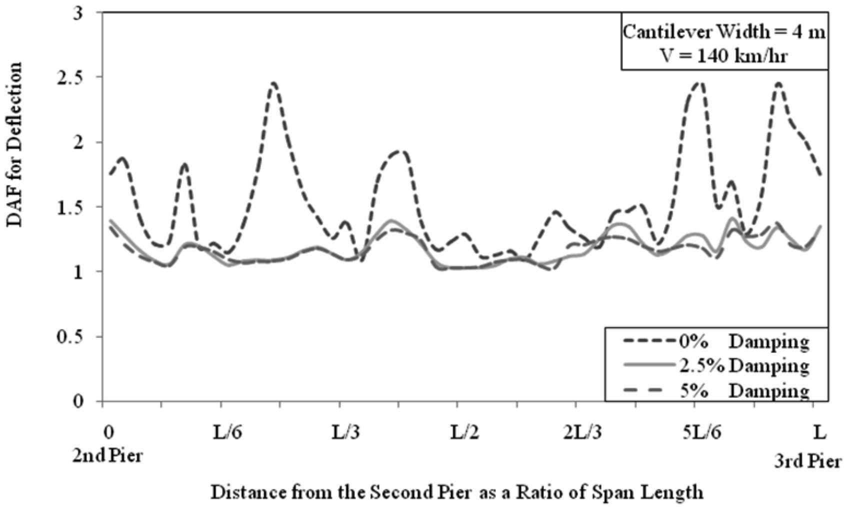

Fig C1.17 : DAF for Deflection for 4 m Cantilever Width and V = 140 km/hr

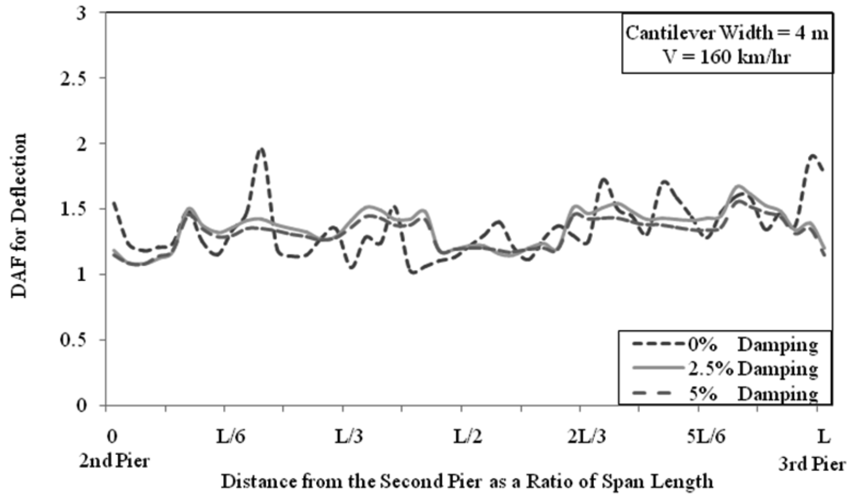

Fig C1.18 : DAF for Deflection for 4 m Cantilever Width and V = 160 km/hr

C.1.1.4 Variation for Cantilever Width = 4.5 m

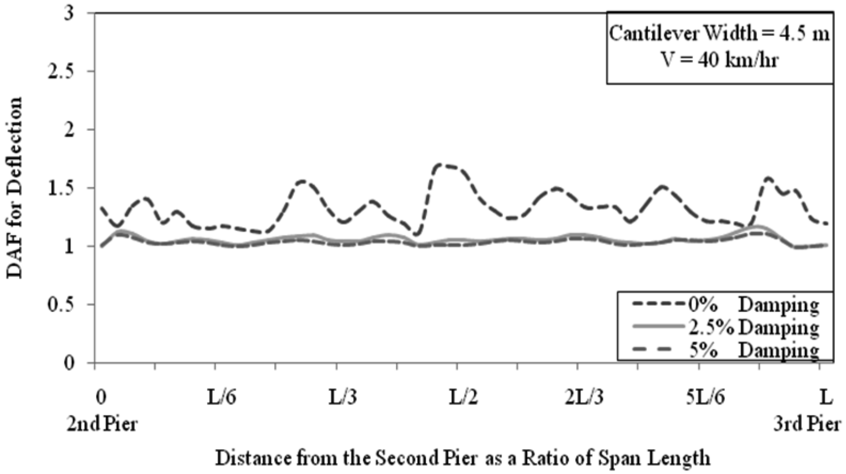

Fig C1.19 : DAF for Deflection for 4.5 m Cantilever Width and V = 40 km/hr

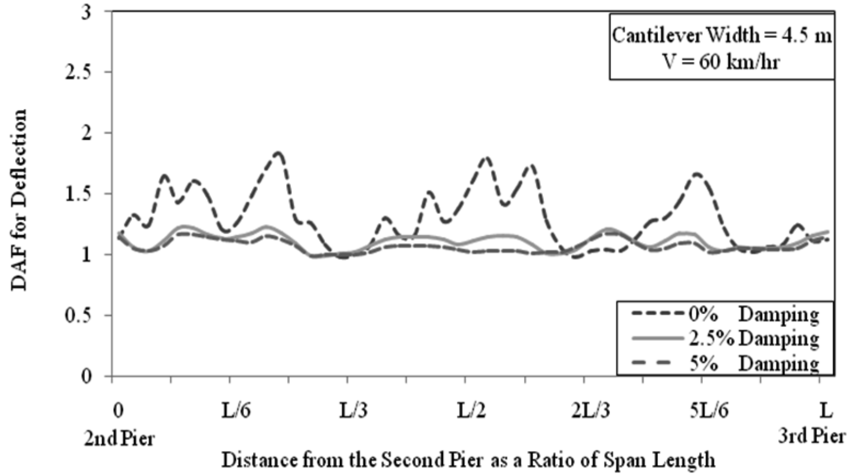

Fig C1.20 : DAF for Deflection for 4.5 m Cantilever Width and V = 60 km/hr

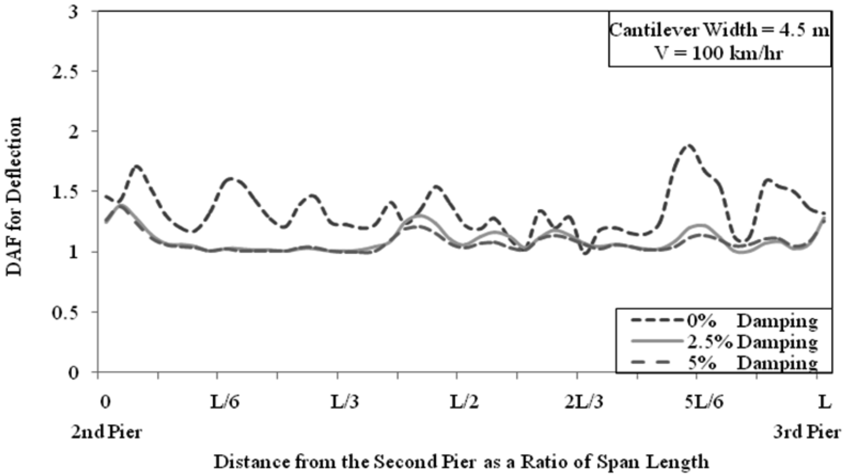

Fig C1.21 : DAF for Deflection for 4.5 m Cantilever Width and V = 100 km/hr

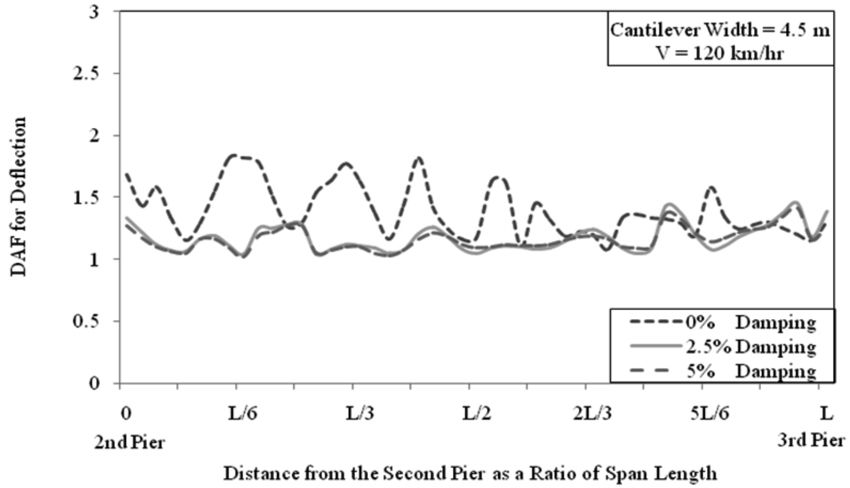

Fig C1.22 : DAF for Deflection for 4.5 m Cantilever Width and V = 120 km/hr

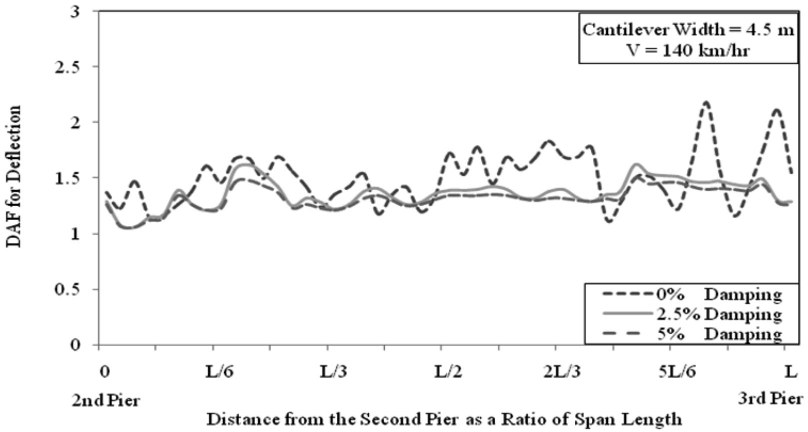

Fig C1.23 : DAF for Deflection for 4.5 m Cantilever Width and V = 140 km/hr

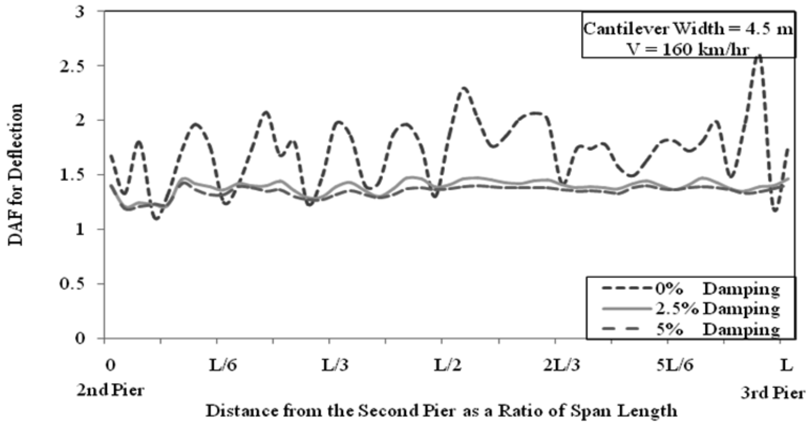

Fig C1.24 : DAF for Deflection for 4.5 m Cantilever Width and V = 160 km/hr

C.1.2 Variation along the Length of the Middle Span in Terms of Stress

C.1.2.1 Variation for Cantilever Width = 3 m

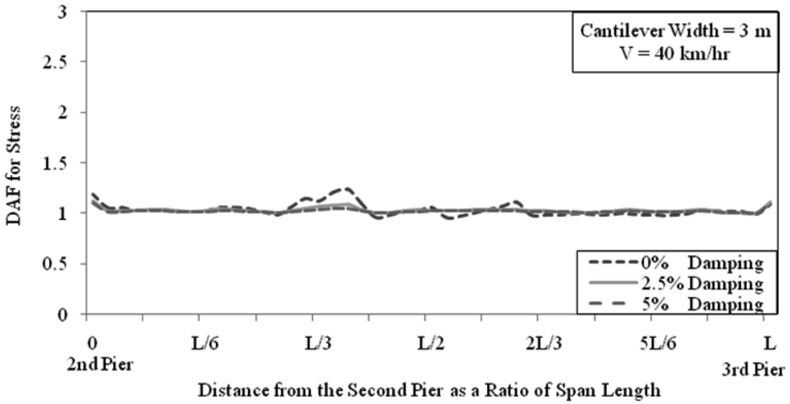

Fig C1.25 : DAF for Stress for 3m Cantilever Width and V = 40 km/hr

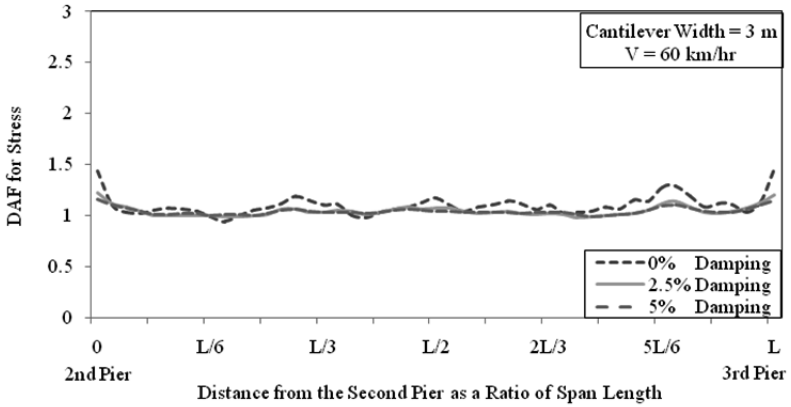

Fig C1.26: DAF for Stress for 3m Cantilever Width and V = 60 km/hr

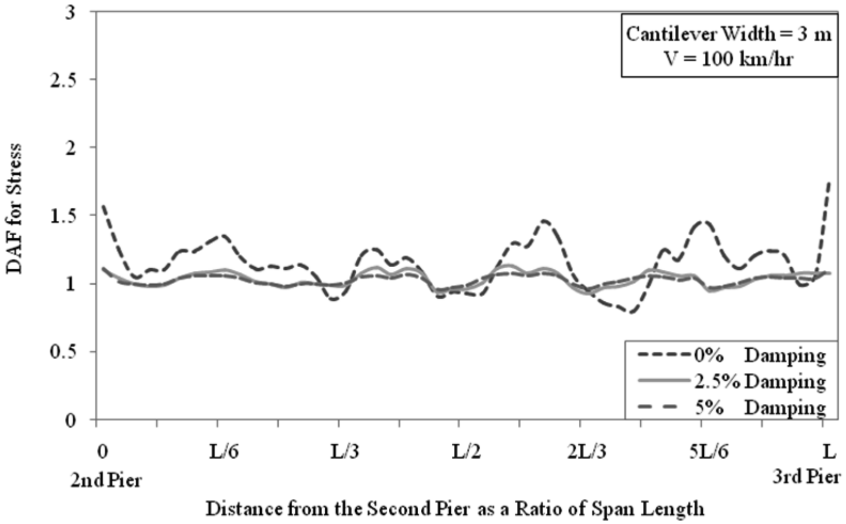

Fig C1.27 : DAF for Stress for 3m Cantilever Width and V = 100 km/hr

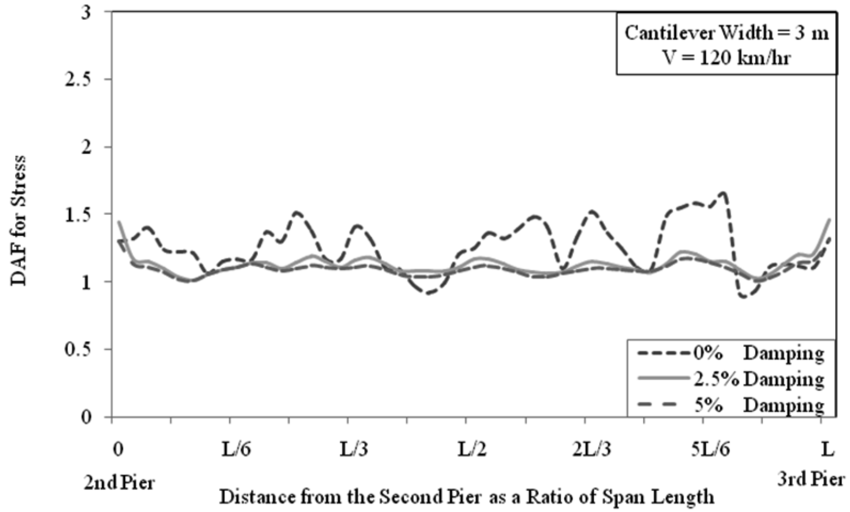

Fig C1.28 : DAF for Stress for 3m Cantilever Width and V = 120 km/hr

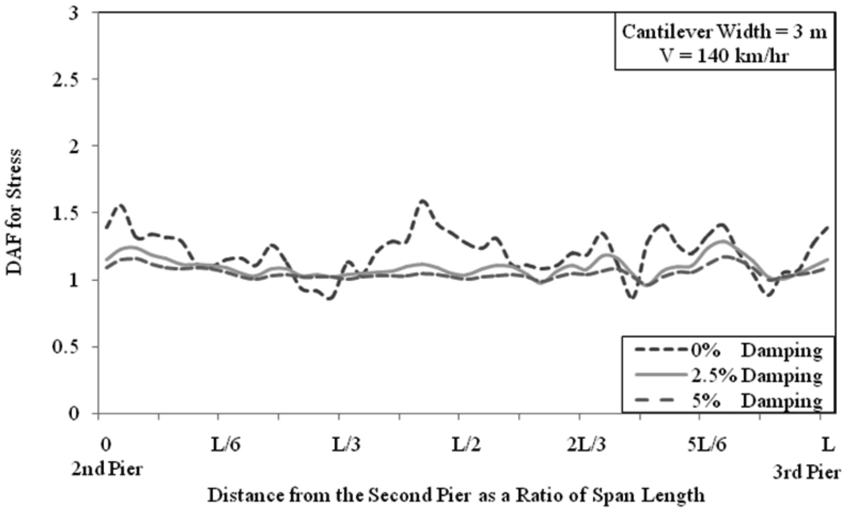

Fig C1.29 : DAF for Stress for 3m Cantilever Width and V = 140 km/hr

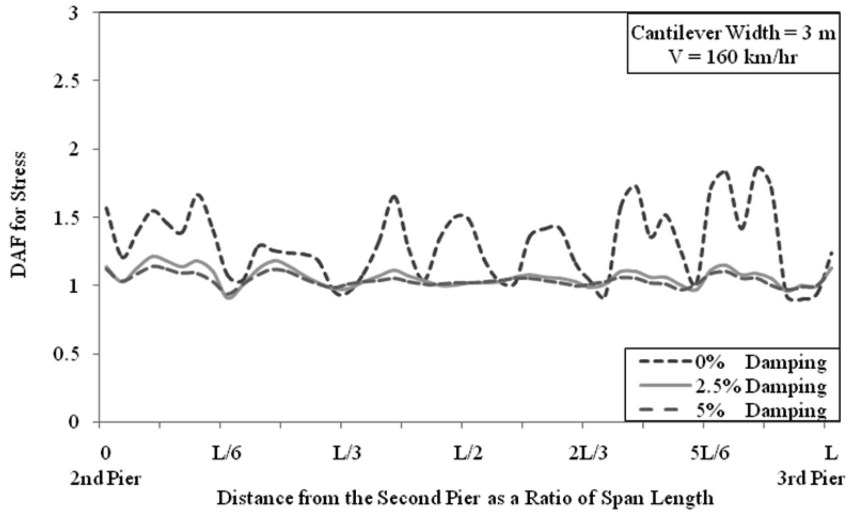

Fig C1.30 : DAF for Stress for 3m Cantilever Width and V = 160 km/hr

C.1.2.2 Variation for Cantilever Width = 3.5 m

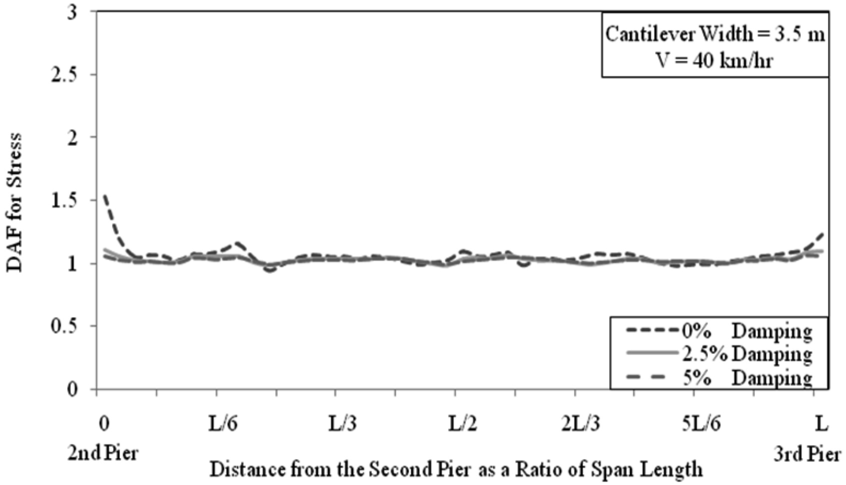

Fig C1.31 : DAF for Stress for 3.5 m Cantilever Width and V = 40 km/hr

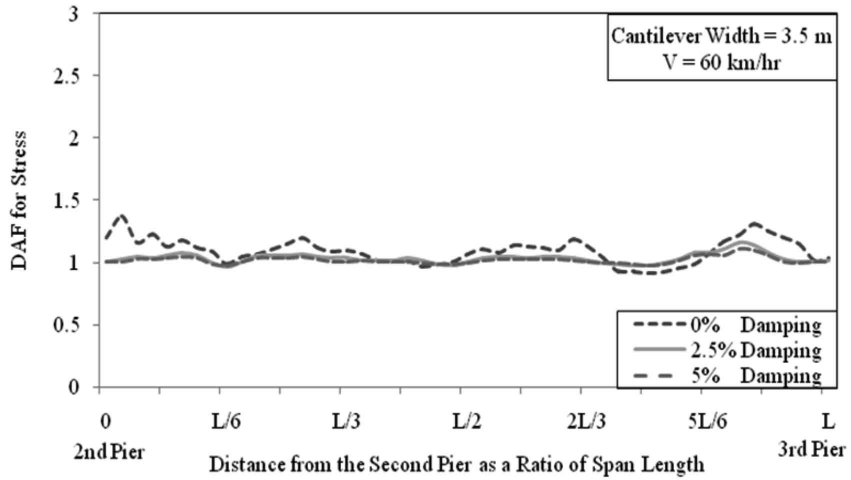

Fig C1.32 : DAF for Stress for 3.5 m Cantilever Width and V = 60 km/hr

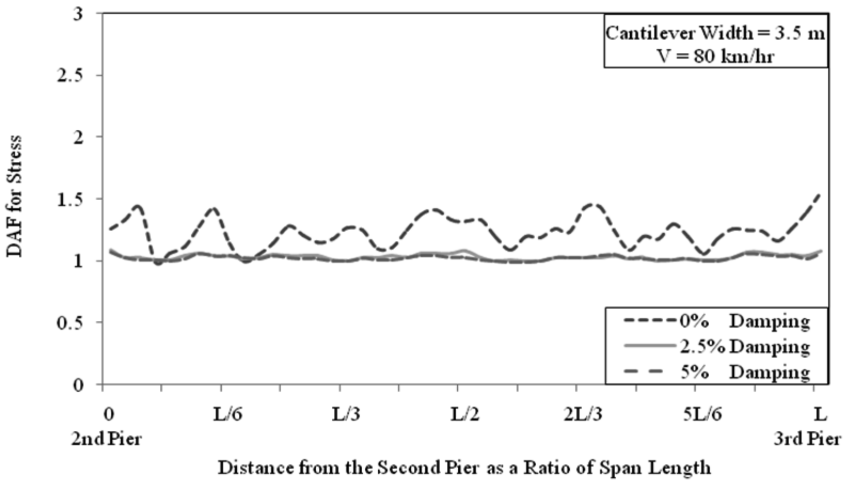

Fig C1.33 : DAF fo Stress for 3.5 m Cantilever Width and V = 80 km/hr

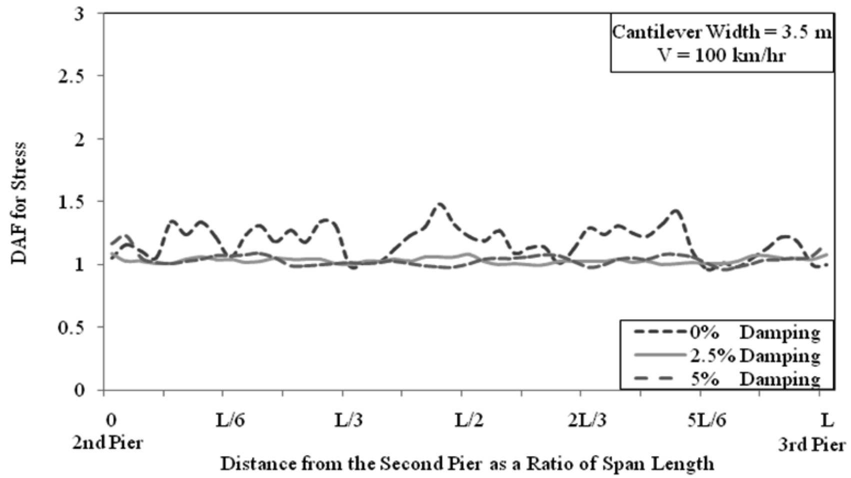

Fig C1.34 : DAF for Stress for 3.5 m Cantilever Width and V = 100 km/hr

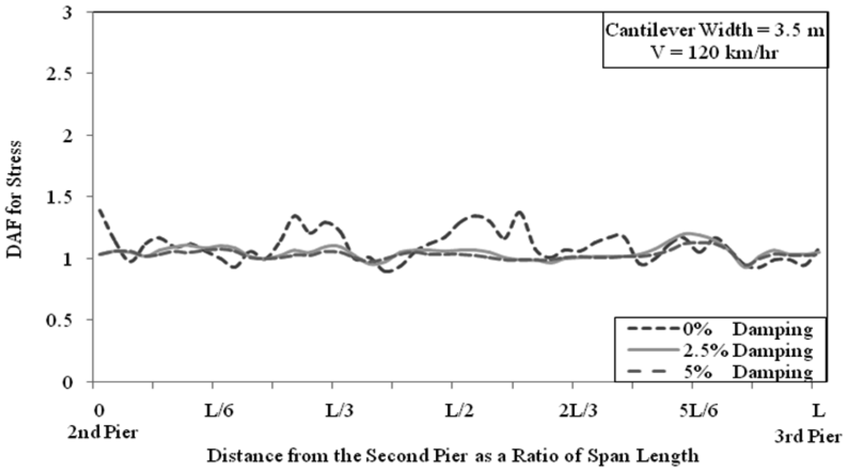

Fig C1.35 : DAF for Stress for 3.5 m Cantilever Width and V = 120 km/hr

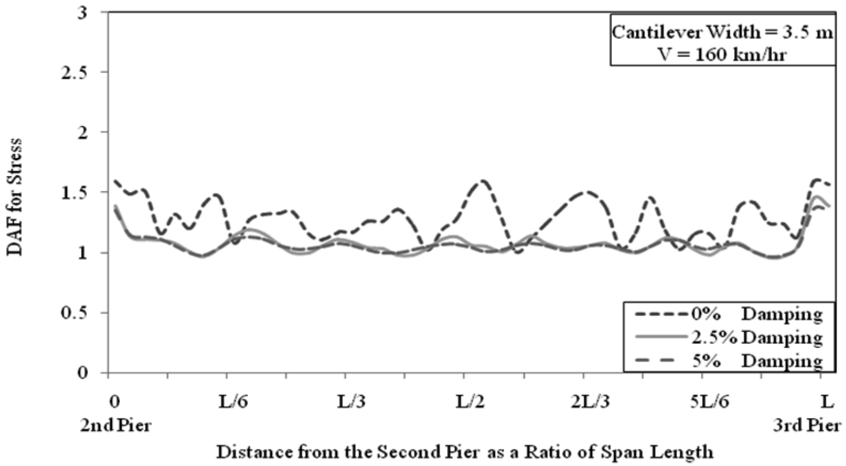

Fig C1.36 : DAF for Stress for 3.5 m Cantilever Width and V = 160 km/hr

C.1.2.3 Variation for Cantilever Width = 4 m

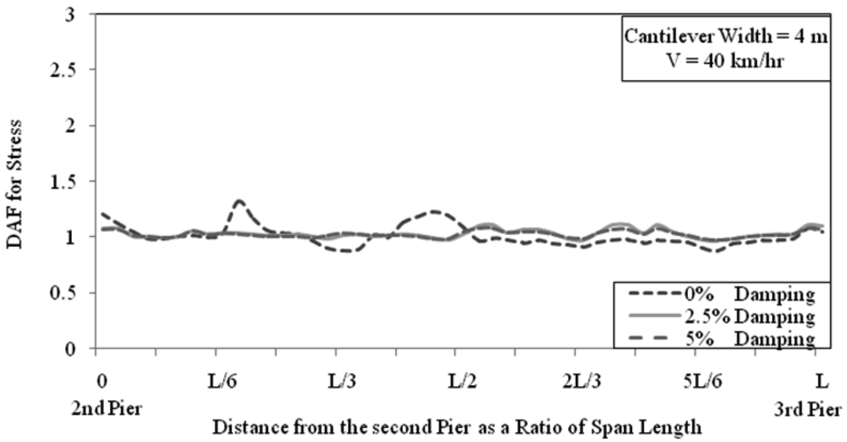

Fig C1.37 : DAF for Stress for 4 m Cantilever Width and V = 40 km/hr

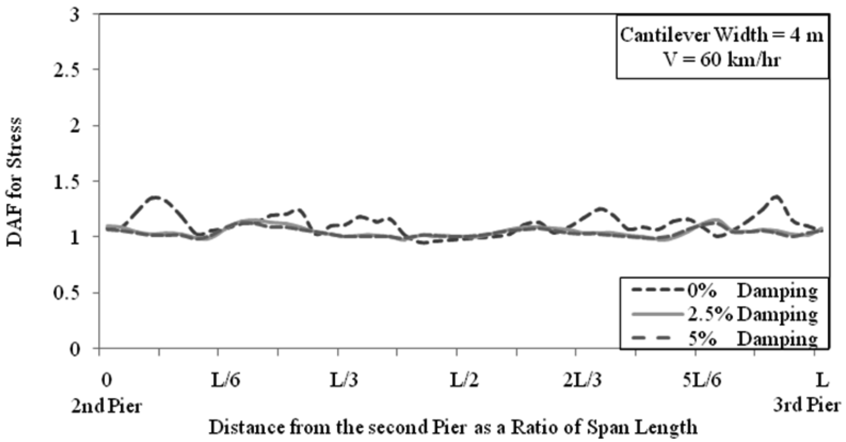

Fig C1.38 : DAF for Stress for 4 m Cantilever Width and V = 60 km/hr

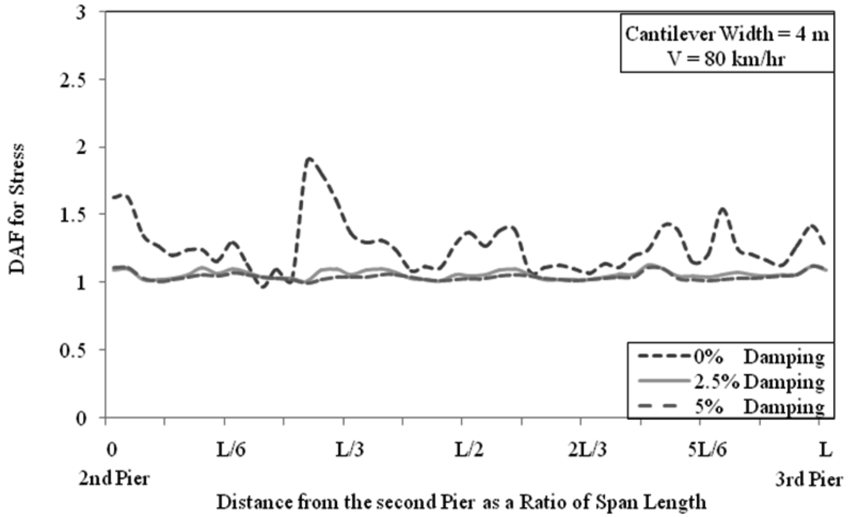

Fig C1.39 : DAF for Stress for 4 m Cantilever Width and V = 80 km/hr

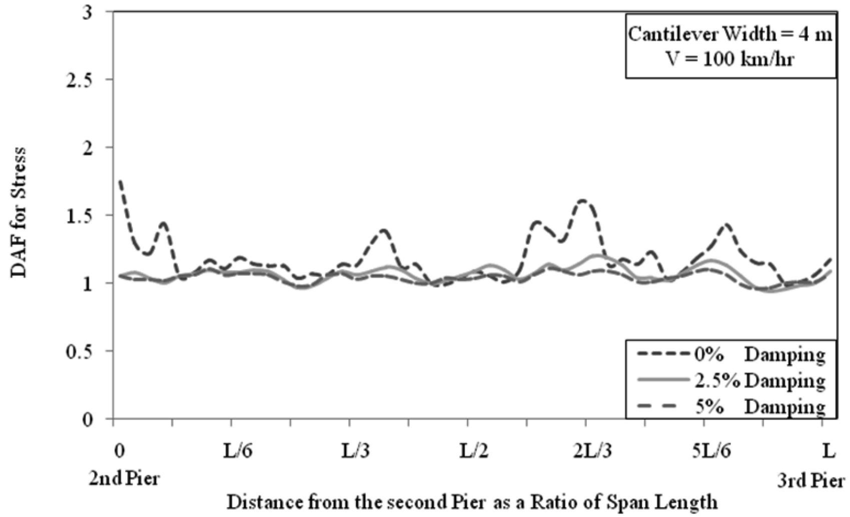

Fig C1.40 : DAF for Stress for 4 m Cantilever Width and V = 100 km/hr

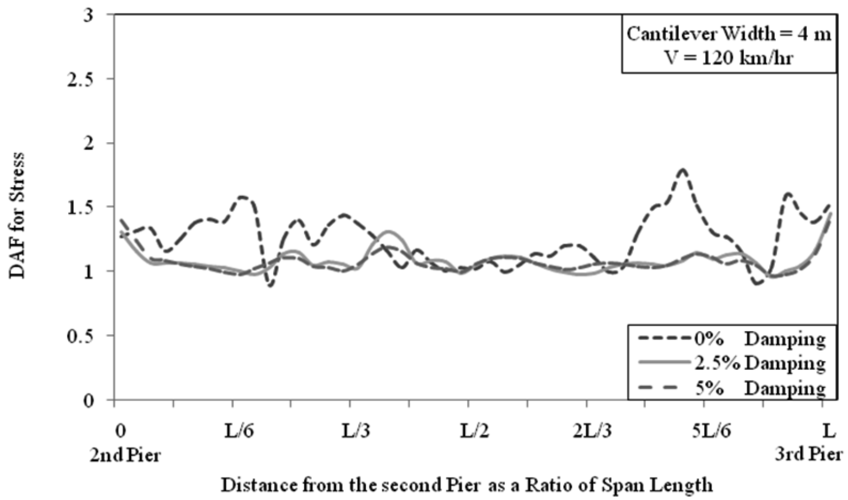

Fig C1.41 : DAF for Stress for 4 m Cantilever Width and V = 120 km/hr

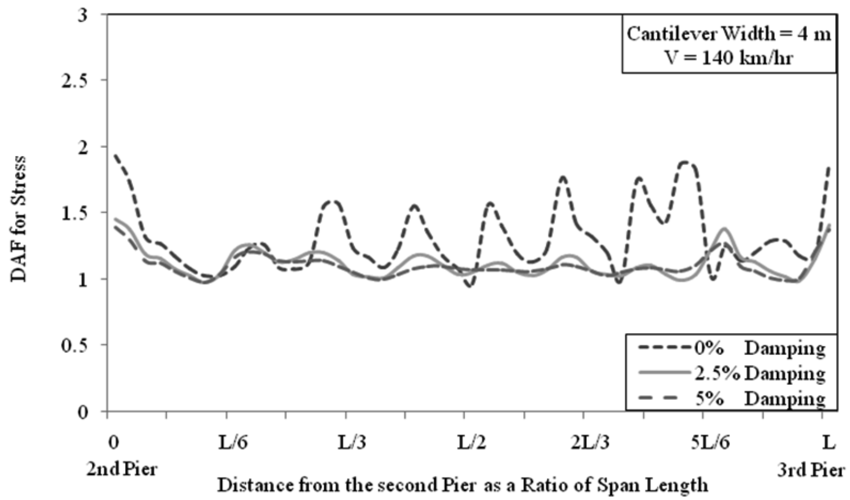

Fig C1.42 : DAF for Stress for 4 m Cantilever Width and V = 140 km/hr

C.1.2.4 Variation for Cantilever Width = 4.5 m

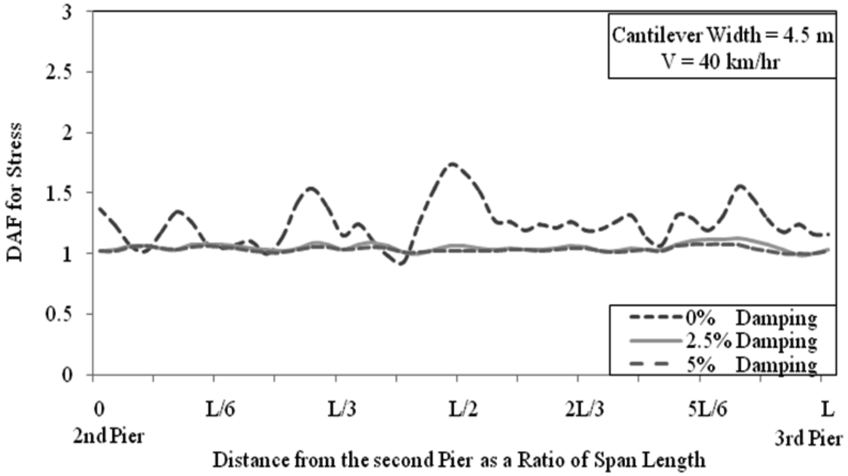

Fig C1.43 : DAF for Stress for 4.5 m Cantilever Width and V = 40 km/hr

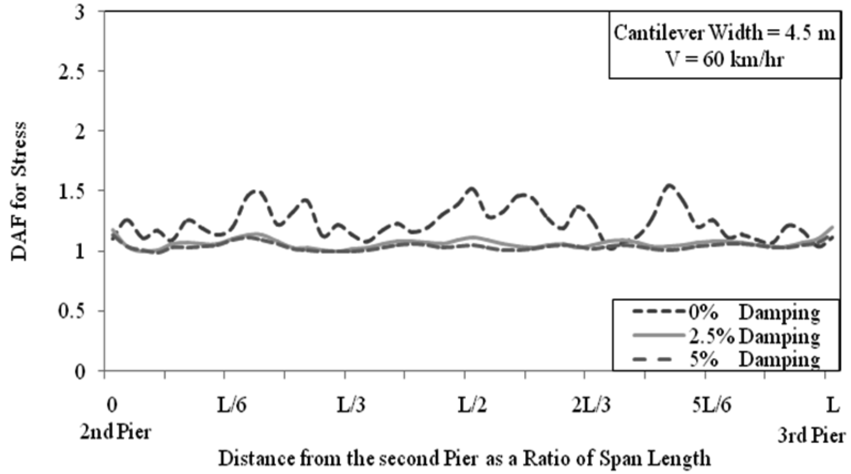

Fig C1.44 : DAF for Stress for 4.5 m Cantilever Width and V = 60 km/hr

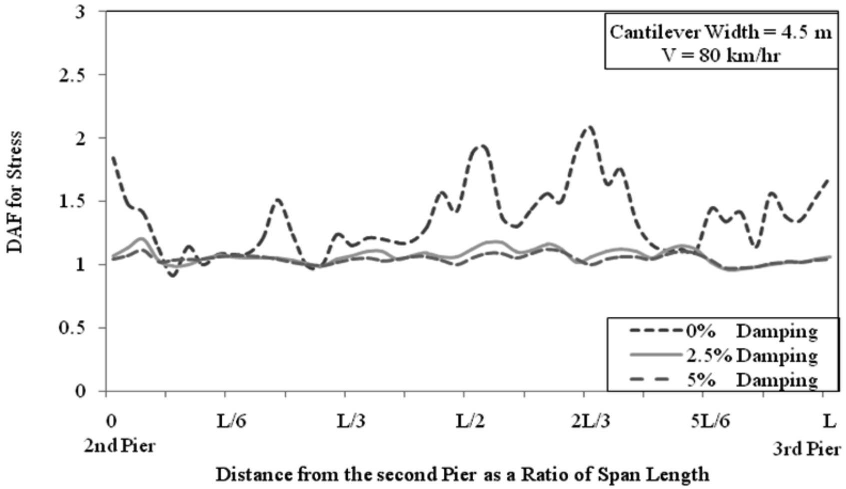

Fig C1.45 : DAF for Stress for 4.5 m Cantilever Width and V = 80 km/hr

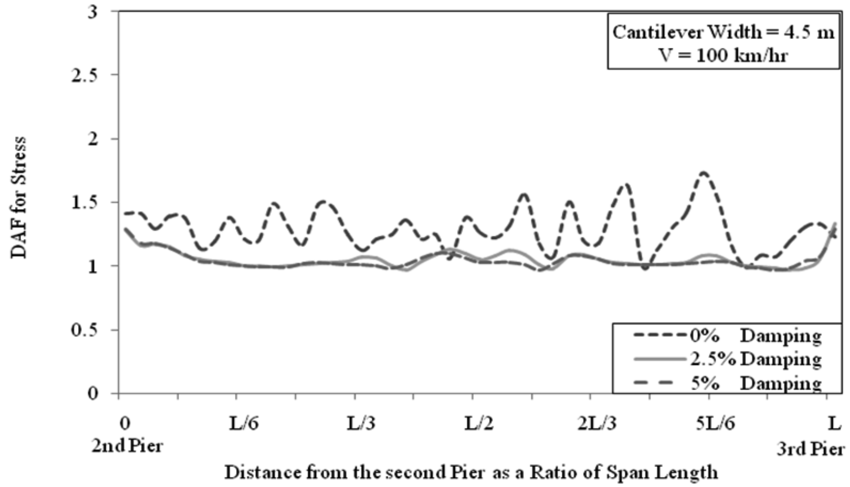

Fig C1.46: DAF for Stress for 4.5 m Cantilever Width and V = 100 km/hr

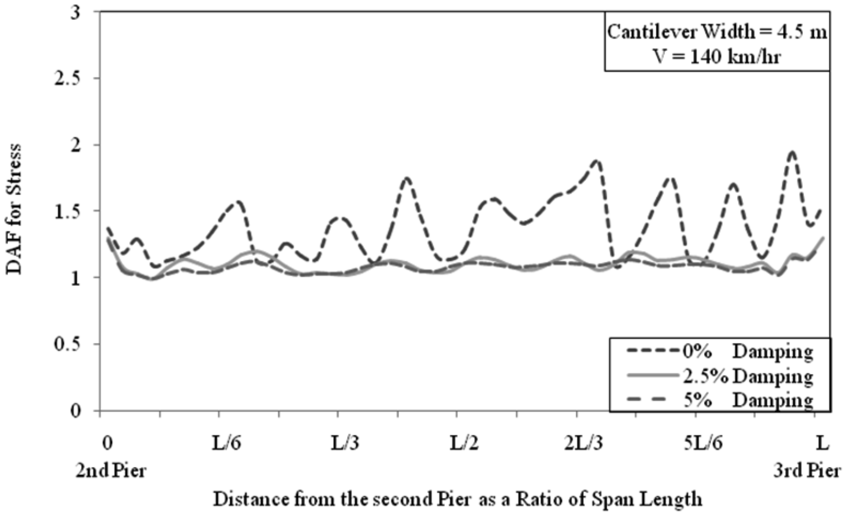

Fig C1.47 : DAF for Stress for 4.5 m Cantilever Width and V = 140 km/hr

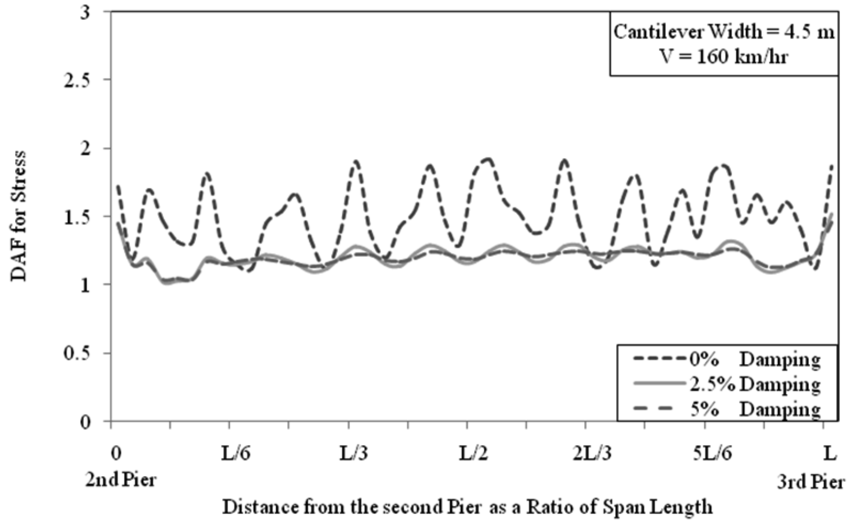

Fig C1.48 : DAF for Stress for 4.5 m Cantilever Width and V = 160 km/hr